

**Department of Chemical Engineering**

**Treatment of Oily and Dye Wastewater with Modified Barley Straw**

**Shariff Che Ibrahim**

**This thesis is presented for the Degree of  
Doctor of Philosophy  
of  
Curtin University of Technology**

**March 2010**

## DECLARATION

To the best of my knowledge and belief this thesis contains no material previously published by any other person except where due acknowledgment has been made.

This thesis contains no material which has been accepted for the award of any other degree or diploma in any university.

Signature: .....

Date: .....

## ACKNOWLEDGEMENT

All praises and glories to Almighty Allah (SWT) who had bestowed me courage and  
patience upholding this work.

Whenever I was down at the life wheel, this '**Don't Quit!**' poem always helped me  
undulate even stronger

### **Don't Quit!**

When things go wrong, as they sometimes will,  
When the road you're trudging seems all uphill,  
When the funds are low, and the debts are high,  
And you want to smile, but you have to sigh,  
When care is pressing you down a bit,  
Rest if you must, but don't you quit.

Life is queer with its twists and turns,  
As everyone of us sometimes learns,  
And many a failure turns about,  
when he might have won had he stuck it out;  
Don't give up though the pace seems slow,  
You may succeed with another blow.

Success is failure turned inside out,  
The silver tint of the clouds of doubt,  
And you never can tell how close you are,  
It may be near when it seems so far;  
So stick to the fight when you're hardest hit,  
It's when things seem worse, that...

### **You Must Not Quit.**

~C. W. Longenecker ~

This sweet achievement is truly indebted to these wonderful people;

*Research project supervisor*

Prof. Ming Ang and Dr Shaobin Wang

"A master can tell you what he expects of you.

A teacher, though,

Awakens your own expectations"

~Patricia Neal

*Parent and in law and siblings*

"Thank you so much for all you do;

You're truly a delight;

When my life overwhelms and does me in,

You make everything all right."

~Joanna Fuchs

*Beloved family who stick through thick and thin (mostly thick though!!)*

NurAziah and the superkids-Raeiqal, Wardah and Rania

"Your love and support will always be remembered,

fondly in good times, and as encouragement in bad ones.

Someday I hope to give to you a fraction of all you've given me"

~Christy Rakoczy

*Chemical Engineering Staff,*  
Prof Moses Tade, Jann, Naomi, Karen

"Kindness is the language which the deaf can hear  
and the blind can see."

~Mark Twain

*Research mates*  
Pradeep Shukla of Curtin and Megat Ahmad Kamal of UiTM

"A real friend is one who walks in when the rest of the world walks out."

~Walter Winchell

Malaysian friends who made life in Perth most memorable, blessed with cheers

"Unselfish and noble actions are the most radiant pages  
in the biography of souls."

~David Thomas

To those not mentioned here, but in my sincerest mind and heart

"I would thank you from the bottom of my heart,  
But for you my heart has no bottom"

~Unknown

Many Thanks to:  
Chemical Engineering Dept, Curtin University of Technology,  
Faculty of Applied Sciences, MARA University of Technology, Shah Alam and  
Ministry of Higher Education, Malaysia.

Also humbly dedicating this achievement to the most influential people in my life,  
even though they are physically no longer with us, but they are spiritually and will be  
forever remembered... Amin..

Tuan Hj Ibrahim b. Abd.Rahman ( father) and  
Sharzula b. Ibrahim( brother)

## **DEDICATIONS**

This work is dedicated to my family in appreciation of their loving support, understanding and encouragement during my study in wonderful Western Australia.

When you look at your life, the greatest happiness's are family happiness's.

~Joyce Brothers

## PUBLICATIONS

### Refereed journal publications

Broto Chandra Oei, **Shariff Ibrahim**, Ha-Ming Ang, Shaobin Wang., 2009. Surfactant modified barley straw for removal of acid and reactive dyes from aqueous solution, *Bioresource Technology*, 100(18): p. 4292-4295.

**Shariff Ibrahim**, Ha-Ming Ang, Shaobin Wang., 2009. Removal of emulsified food and mineral oils from wastewater using surfactant modified barley straw, *Bioresource Technology*, 2009. 100(23): p. 5744-5749.

**Shariff Ibrahim**, Shaobin Wang, Ha-Ming Ang. Removal of emulsified oil from wastewater using agricultural waste barley straw, *Biochemical Engineering Journal*, 2010. 49(1): p. 78-83.

**Shariff Ibrahim**, Ha-Ming Ang, Shaobin Wang. Adsorptive Separation of emulsified oil in wastewater using biosorbents, *Asia Pacific Journal of Chemical Engineering*. (Accepted for publication)

**Shariff Ibrahim**, Ha-Ming Ang, Shaobin Wang. Preparation of Bioadsorbents for Effective Adsorption of Reactive dye in Aqueous Solution, *Asia Pacific Journal of Chemical Engineering*. (Accepted for publication)

**Shariff Ibrahim**, Is Fatimah, Ha-Ming Ang, Shaobin Wang. Adsorption of anionic dyes in aqueous solution using chemically modified barley straw, *Water Science and Technology Journal*). (Accepted for publication)

## Peer reviewed Conference proceedings

**Shariff Ibrahim**, Ha-Ming Ang, Shaobin Wang. Utilisation of barley straw for removal of emulsified oil in wastewater. *12th Asia Pacific Confederation of Chemical Engineering Congress (APCChE 2008)*, 2008, Dalian, China. (Oral presentation and Conference Proceeding)

**Shariff Ibrahim**, Ha-Ming Ang, Shaobin Wang. Kinetics of emulsified oil removal in wastewater using barley straw. *CHEMECA 2008*, Newcastle City Hall, Newcastle, Australia. (Oral presentation and Conference Proceeding)

**Shariff Ibrahim**, Ha-Ming Ang, Shaobin Wang. Adsorption of reactive dye in solution using chemically modified barley straw. *CHEMECA 2009*, Perth, Western Australia, Australia. (Oral presentation and Conference Proceeding)

**Shariff Ibrahim**, Ha-Ming Ang, Shaobin Wang. Utilization of Barley Straw as a Biosorbent for Treatment of Emulsified Oily Wastewater. Sino-Australia Symposium of Biomass and Coal 2009, Wuhan, China. (Oral presentation and Conference Proceeding)

**Shariff Ibrahim**, Is Fatimah, Ha-Ming Ang, Shaobin Wang. Adsorption of anionic dyes in aqueous solution using chemically modified barley straw. Water 09, International Water Association (IWA), Palmerston North, New Zealand (Oral presentation and Conference Proceeding)

# TABLE OF CONTENTS

DECLARATION	
ACKNOWLEDGEMENT	
DEDICATIONS	
PUBLICATIONS	viii
TABLE OF CONTENTS	x
LIST OF TABLES	xv
LIST OF FIGURES	xvii
NOTATIONS	xxi
ABSTRACT	xxiii

## CHAPTER 1 BACKGROUND

1.1 Introduction	1
1.2 Research objectives	3

## CHAPTER 2 REVIEW OF LITERATURE

2.1 Introduction	5
2.2 Oils	6
2.3 Oily Wastewater	6
2.4 Emulsified Oily Wastewater for Environmental Concern	8
2.5 Dyes	9
2.6 Dye Wastewater	12
2.7 Dye Wastewater for Environmental Concern	12
2.8 Remediation of Oily and Dyes Wastewater	16
2.8.1 Mechanical/physical separation	16
2.8.1.1 Air flotation	16
2.8.1.2 Filtration	18
2.8.1.3 Sorption	19
2.8.2 Chemical methods	20
2.8.2.1 Chemical coagulation	20
2.8.2.2 Ozonation	21
2.8.3 Biological methods	23

2.9	Adsorption	25
2.10	Agricultural Waste as an Adsorbents	26
2.11	Modification of Agricultural Waste	27
2.12	Chemistry of Cationic Surfactant	28
2.13	Modification of Solid Surface with Cationic Surfactant	31
2.13.1	Binding mechanism	31
2.14	Surfactant Modified Adsorbent for Environmental Concern	32
2.15	Cationic Surfactant Selection	36
2.15.1	Influence of surfactant chain length	36
2.15.2	Influence of polar head group	38
2.15.3	Influence of cationic surfactant concentration	39
2.16	Section Summary	40

### **CHAPTER 3      EXPERIMENTAL**

3.1	Introduction	41
3.2	Adsorbent Preparation	42
3.2.1	Materials	42
3.2.2	Treatment with base solution	42
3.2.3	Modification with cationic surfactant	42
3.3	Characterization of Adsorbent	43
3.3.1	Carbon and Nitrogen percentage	43
3.3.2	Surface area	43
3.3.3	Microstructure and surface morphology	43
3.3.4	Water soluble minerals	44
3.3.5	Identification of functional group	44
3.3.6	Elemental analysis	44
3.3.7	Acidic and basic surface groups	44
3.3.8	Bulk density	44
3.3.9	Cellulose, hemicelluloses and lignin	45
3.4	Stability/Desorption of CPC	45
3.5	Experimental Studies of Emulsified Oil Removal	45
3.5.1	Batch adsorption studies	45
3.5.2	Batch kinetic studies	46

3.5.3	Batch isotherm studies	46
3.5.4	Batch equilibrium studies	46
3.5.5	Batch experimental operational parameters	46
3.5.6	Leaching/desorption experiments	47
3.5.7	Fixed bed column breakthrough studies	47
3.5.8	Preparation of emulsified oil solutions	48
3.5.9	Measurement of oil in water	48
3.6	Experimental Studies of Dyes Wastewater	49
3.6.1	Batch adsorption preliminary studies	49
3.6.2	Batch kinetic studies	49
3.6.3	Batch Isotherm studies	49
3.6.4	Batch equilibrium studies	50
3.6.5	Leaching/desorption experiments	50
3.6.6	Batch experimental operational parameters	50
3.6.7	Fixed bed column breakthrough studies	50
3.6.8	Preparation of dyes wastewater	51
3.6.9	Measurement of dyes in wastewater	51
3.7	Batch Experimental Model	51
3.7.1	Kinetic models	51
3.7.2	Kinetic diffusion models	52
3.7.3	Isotherm models	53
3.8	Fixed Bed Column Models	54
3.8.1	Thomas model	56
3.8.2	Yoon-Nelson model	56
3.9	Best Fitting Model Estimation	57
3.10	Standard Error of The Measurement	57

## **CHAPTER 4      MODIFICATION AND CHARACTERIZATION OF STRAW SURFACE**

4.1	Introduction	58
4.2	Treatment with Base Solution	59
4.3	Modification with Cationic Surfactant	60
4.4	Physicochemical Characteristics of Raw and Modified Barley	64

Straw	
4.5 Morphology of Raw and Modified Barley Straw	68
4.6 Spectroscopy Study of The Raw and Modified Straw	71
4.7 Desorption of Cationic Surfactant	73
4.8 Section Summary	75

## **CHAPTER 5 REMOVAL OF EMULSIFIED OILS**

5.1 Introduction	77
5.2 Preliminary Experiments	78
5.3 Dynamics Adsorption of Oils	81
5.3.1 Kinetic models	83
5.3.2 Kinetic diffusion models	87
5.4 Isotherm Models	90
5.5 Comparison with other Adsorbents	93
5.6 Effect of Oil Solution Temperature	95
5.7 Effect of Initial pH of Oil Solution	96
5.8 Effect of Adsorbent Size	98
5.9 Desorption	99
5.10 Column Breakthrough Studies	101
5.11 Modelling of Fixed Bed Column Breakthrough	105
5.11.1 Thomas model	105
5.11.2 Yoon-Nelson model	107
5.12 Section Summary	109

## **CHAPTER 6 REMOVAL OF ANIONIC DYES**

6.1 Introduction	111
6.2 Preliminary Experiments	112
6.3 Dynamic Adsorption	116
6.3.1 Kinetic models	118
6.3.2 Kinetic diffusion models	123
6.4 Isotherm Models	127
6.5 Comparison with other Adsorbents	131
6.6 Effect of Dye Solution pH	133

6.7	Effect of Dye Solution Experimental Temperature	135
6.8	Dye Desorption	137
6.9	Column Breakthrough Studies	138
6.10	Modelling of Fixed Bed Column Breakthrough	141
6.10.1	Thomas model	142
6.10.2	Yoon-Nelson model	144
6.11	Section Summary	146

## **CHAPTER 7 CONCLUSIONS AND FUTURE DIRECTIONS**

7.1	Introduction	148
7.2	Conclusion	149
7.3	Future Directions	156

<b>REFERENCES</b>	158
-------------------	-----

## **APPENDICES**

## LIST OF TABLES

Table 2.1	Concentration of oil in different sources	7
Table 2.2	Classification dyes according to the chemical structure	10
Table 2.3	Application classes of dyes and their chemical types	11
Table 2.4	Estimated degree of fixation for different dyes	12
Table 2.5	Some of the information of the dyes used in this work	15
Table 2.6	Typical characteristics of membrane processes	18
Table 2.7	Characteristic of some cationic surfactant	30
Table 2.8	Sorption capacity for some of the surfactant modified adsorbent for low polarity compounds	34
Table 2.9	Sorption capacity for some of the surfactant modified adsorbent for anionic dyes	35
Table 4.1	Characteristics of raw and modified straw	65
Table 5.1	Kinetics models constants and error analysis for adsorption of oil on SMBS and BMBS	86
Table 5.2	Effective diffusion constants ( $D_i$ ) for adsorption of oil on SMBS and BMBS	90
Table 5.3	Freundlich and Langmuir isotherm constants and error analysis for adsorption of oil on SMBS and BMBS	92
Table 5.4	Oil sorption capacities of some sorbents reported in literature	94
Table 5.5	Adsorption breakthrough data for column experiments for the adsorption of CO and SMO on SMBS and BMBS	104
Table 5.6	Thomas model parameters for fixed-bed adsorption of CO and SMO	107
Table 5.7	Yoon-Nelsons model parameters for fixed-bed adsorption of CO and SMO	109
Table 6.1	Kinetics models constants and error analysis for adsorption of anionic dyes on SMBS and BMBS.	122
Table 6.2	Effective diffusion constants ( $D_i$ ) for adsorption of anionic dyes on SMBS and BMBS	127
Table 6.3	Freundlich and Langmuir isotherm constants and error analysis for adsorption of anionic dyes on SMBS and BMBS	130

Table 6.4	Anionic dyes sorption capacities of some sorbents reported in literature	132
Table 6.5	Adsorption breakthrough data for column experiments for the adsorption of AB40 and RB5 on SMBS and BMBS	141
Table 6.6	Thomas model parameters for fixed-bed adsorption of AB40 and RB5	144
Table 6.7	Yoon-Nelsons model parameters for fixed-bed adsorption of AB40 and RB5	146

## LIST OF FIGURES

Figure 2.1	Schematic illustration of a surfactant monomer and a micelle structure in aqueous solution	29
Figure 2.2	Adsorption of cationic surfactants onto perlite samples: (a) at low surface coverage, (b) of the point of zeta potential reversal, (c) at monolayer coverage, (d) at high surface concentration	32
Figure 2.3	Effect of the surfactants (1.0 CEC used for each of the different surfactant types) on adsorption capacity of surfactant-modified MMT for CR.	37
Figure 3.1.	Schematic diagram of fixed bed column study	48
Figure 3.2.	Examples of breakthrough curves: (a) poor adsorption (b) normal adsorption and (c) strong adsorption	55
Figure 4.1	Effectiveness of NaOH treated raw barley straw for methylene blue 1 removal	60
Figure 4.2	Sorption of CPC on RBS and RBS-N surface	61
Figure 4.3a	Log - log scale SMBS	62
Figure 4.3b	Log - log scale BMBS	62
Figure 4.4a	Schematic illustration of ion exchange mechanism of the cationic surfactants at straw water interface	63
Figure 4.4b	Incomplete bilayer formation of CPC onto straw surface	63
Figure 4.4c	Complete bilayer formation of CPC onto straw surface	64
Figure 4.5	SEM micrograph of (a) RBS (b) RBS-N (c) SMBS and (d) BMBS showing the irregular shape	69
Figure 4.6	SEM micrograph showing the fiber like structure	69
Figure 4.7	SEM micrograph of BMBS indicate (a) removal a thin wax layer (b) creating a perforation	70
Figure 4.8	SEM micrograph of straw indicating the deposition of organic molecules (a) before CPC treatment (b) after CPC treatment	70
Figure 4.9	FT-IR spectra of RBS, RBS-N, SMBS, BMBS and CPC	72
Figure 4.10a	Desorption of CPC from SMBS in various liquid media	73
Figure 4.10b	Desorption of CPC from BMBS in various liquid media	74
Figure 5.1	Adsorption of CO and SMO using unmodified and surfactant modified straw	78
Figure 5.2a	FT-IR spectra of SMBS and oil loaded SMBS	79
Figure 5.2b	FT-IR spectra of BMBS and oil loaded BMBS	80

Figure 5.3	Schematic diagram showing adsolubilization/partitioning of oils (represented by black round dots) in surfactant modified straw	80
Figure 5.4a	Effect of contact time on adsorption of CO onto SMBS and BMBS	82
Figure 5.4b	Effect of contact time on adsorption of SMO onto SMBS and BMBS	82
Figure 5.5a	Nonlinear kinetic models for adsorption of CO onto SMBS	83
Figure 5.5b	Nonlinear kinetic models for adsorption of CO onto BMBS	84
Figure 5.5c	Nonlinear kinetic models for adsorption of SMO onto SMBS	84
Figure 5.5d	Nonlinear kinetic models for adsorption of SMO onto BMBS	85
Figure 5.6a	Boyd plot for the sorption of CO onto SMBS	87
Figure 5.6b	Boyd plot for the sorption of CO onto BMBS	88
Figure 5.7a	Boyd plot for the sorption of SMO onto SMBS	88
Figure 5.7b	Boyd plot for the sorption of SMO onto BMBS	89
Figure 5.8a	Nonlinear adsorption isotherms for adsorption of CO onto SMBS and BMBS	91
Figure 5.8b	Nonlinear adsorption isotherms for adsorption of SMO onto SMBS and BMBS	91
Figure 5.9a	Effect of temperature on adsorption of CO and SMO onto SMBS	95
Figure 5.9b	Effect of temperature on adsorption of CO and SMO onto BMBS	96
Figure 5.10a	Effect of solution pH on adsorption of CO and SMO onto SMBS	97
Figure 5.10b	Effect of solution pH on adsorption of CO and SMO onto BMBS	97
Figure 5.11a	Effect of adsorbent size on adsorption of CO and SMO onto SMBS	98
Figure 5.11b	Effect of adsorbent size on adsorption of CO and SMO onto BMBS	99
Figure 5.12a	Desorption of oil loaded SMBS in deionized water	100
Figure 5.12b	Desorption of oil loaded BMBS in deionized water	100
Figure 5.13a	Breakthrough plot of CO adsorption on RBS and RBS-N	101

Figure 5.13b	Breakthrough plot of SMO adsorption on RBS and RBS-N	102
Figure 5.13c	Breakthrough plot of CO adsorption on SMBS and BMBS	102
Figure 5.13d	Breakthrough plot of SMO adsorption on SMBS and BMBS	103
Figure 5.14a	Nonlinear Thomas plots for adsorption of CO onto SMBS and BMBS	106
Figure 5.14b	Nonlinear Thomas plots for adsorption of SMO onto SMBS and BMBS	106
Figure 5.15a	Non linear Yoon-Nelson plots for adsorption of CO onto SMBS and BMBS	108
Figure 5.15b	Non linear Yoon-Nelson plots for adsorption of SMO onto SMBS and BMBS	108
Figure 6.1	Adsorption of AB40, RB4 and RB5 using unmodified and surfactant modified straw	112
Figure 6.2a	FT-IR spectra of SMBS and dyes loaded SMBS	114
Figure 6.2b	FT-IR spectra of BMBS and dyes loaded BMBS	115
Figure 6.3	Schematic diagram showing anionic dyes (represented by black round dots) attracted onto opposite charge on modified straw	115
Figure 6.4a	Effect of contact time on adsorption of AB40 onto SMBS and BMBS	116
Figure 6.4b	Effect of contact time on adsorption of RB4 onto SMBS and BMBS	117
Figure 6.4c	Effect of contact time on adsorption of RB5 onto SMBS and BMBS	117
Figure 6.5a	Nonlinear kinetic models for adsorption of AB40 onto SMBS	119
Figure 6.5b	Nonlinear kinetic models for adsorption of AB40 onto BMBS	119
Figure 6.6a	Nonlinear kinetic models for adsorption of RB4 onto SMBS	120
Figure 6.6b	Nonlinear kinetic models for adsorption of RB4 onto BMBS	120
Figure 6.7a	Nonlinear kinetic models for adsorption of RB5 onto SMBS	121
Figure 6.7b	Nonlinear kinetic models for adsorption of RB5 onto BMBS	121
Figure 6.8a	Boyd plot for the sorption of AB40 onto SMBS	124
Figure 6.8b	Boyd plot for the sorption of AB40 onto BMBS	124
Figure 6.9a	Boyd plot for the sorption of RB4 onto SMBS	125

Figure 6.9b	Boyd plot for the sorption of RB4 onto BMBS	125
Figure 6.10a	Boyd plot for the sorption of RB5 onto SMBS	126
Figure 6.10b	Boyd plot for the sorption of RB5 onto BMBS	126
Figure 6.11a	Nonlinear adsorption isotherms for adsorption of AB40 onto SMBS and BMBS.	128
Figure 6.11b	Nonlinear adsorption isotherms for adsorption of RB4 onto SMBS and BMBS	128
Figure 6.11c	Nonlinear adsorption isotherms for adsorption of RB5 onto SMBS and BMBS	129
Figure 6.12a	Effect of solution pH on adsorption of AB40, RB4 and RB5 onto SMBS	134
Figure 6.12b	Effect of solution pH on adsorption of AB40, RB4 and RB5 onto BMBS	134
Figure 6.13a	Effect temperature on adsorption of AB40, RB4 and RB5 onto SMBS	136
Figure 6.13b	Effect of temperature on adsorption of AB40, RB4 and RB5 onto BMBS	136
Figure 6.14a	Desorption of SMBS loaded AB40, RB4 and RB5 at different pH solution	137
Figure 6.14b	Desorption of BMBS loaded AB40, RB4 and RB5 at different pH solution	138
Figure 6.15a	Breakthrough plot of AB40 adsorption for RBS and RBS-N	139
Figure 6.15b	Breakthrough plot of RB5 adsorption for RBS and RBS-N	139
Figure 6.15c	Breakthrough plot of AB40 adsorption for SMBS and BMBS	140
Figure 6.15d	Breakthrough plot of RB5 adsorption for SMBS and BMBS	140
Figure 6.16a	Nonlinear Thomas plots for adsorption of AB40 onto SMBS and BMBS	142
Figure 6.16b	Nonlinear Thomas plots for adsorption of RB5 onto SMBS and BMBS	143
Figure 6.17a	Nonlinear Yoon-Nelson plots for adsorption of AB40 onto SMBS and BMBS	145
Figure 6.17b	Nonlinear Yoon-Nelson plots for adsorption of RB5 onto SMBS and BMBS	145

## NOTATIONS

$C_e$	Concentration at equilibrium
$C_{ex}$	Column exhaustion concentration
$C_i$	Concentration at initial
cm	Centimeter
$C_o$	Concentration at time zero
$C_t$	Concentration at time t
CEC	Cation exchange capacity
$D_i$	Effective diffusion coefficient
F	Fraction of adsorbate adsorbed at time t
g	Gram
h	Hour
HRT	Hydraulic residence time
$K_1$	Rate constant pseudo-first-order
$K_2$	Rate constant pseudo-second-order
$K_F$	Freundlich equilibrium constant
kg	Kilogram
$k_{TH}$	Thomas rate constant
$K_{YN}$	Yoon-Nelson rate constant
L	Litre
M	Molar
m	Weight
mg	Milligram
Min.	Minute
mL	Milliliter
mm	Millimeter
mM	Millimolar
N	Normality
$\mu\text{m}$	Micrometer
nm	Nanometre
$^{\circ}\text{C}$	Degree Celsius

$p$	Number of experimental data
ppm	Part per million
$Q$	Column volumetric flowrate
$q_e$	Adsorption capacity at equilibrium
$q_{e, \text{calc}}$	Adsorption capacity of calculated value
$q_{e, \text{meas}}$	Adsorption capacity of experimental value
$Q_{\text{max}}$	Langmuir maximum adsorption capacity
$q_o$	Column adsorption capacity
$q_t$	Adsorption capacity at time $t$
$q_{\infty}$	Adsorption capacity at infinite time
rpm	Revolutions per minute
$s$	Second
$t$	Time
$t_b$	Column breakthrough time
$\tau$	Time at 50% column breakthrough
$t_{\text{exh}}$	Column exhaustion time
$V$	Volume
$V_b$	Column breakthrough volume
$V_{\text{exh}}$	Column exhaustion volume
$\sigma_m$	Standard error measurement

## ABSTRACT

Barley straw, an agricultural byproduct, was identified as a potential adsorbent material for wastewater treatment as it offers various advantages such as abundant availability at no or very low cost, little processing cost and ability to biodegradation. The raw barley straw, however, needs to be modified as a preliminary study showed less favorability of the raw barley straw in removing oil and anionic dyes. Barley straw was chemically pretreated with sodium hydroxide and modified using a cationic surfactant, hexadecylpyridinium chloride monohydrate (CPC). Generally, the treatment with NaOH increases the negatively charged sites on straw surface and the cationic surfactant introduced forms a hydrophobic layer on the straw surface and changes the surface potential charge from negative to positive. From this exercise, four different adsorbents have been prepared, viz; raw barley straw (RBS), raw barley straw pretreated with sodium hydroxide (RBS-N), and the modification of RBS and RBS-N with the cationic surfactant CPC, which were labelled as surfactant modified barley straw (SMBS) and base pretreated surfactant modified barley straw (BMBS).

Several physical and chemical techniques were employed to characterize barley straw samples to understand the properties of raw and modified straws as well as to study the effects of modification on the textural and surface properties of the raw barley straw. Chemical compositional analyses showed that the amounts of potassium, sodium, arsenic and cadmium existing in RBS, RBS-N were generally low. The availability of cellulose, hemicellulose and lignin in RBS offers the great potential of using the barley straw as a biosorbent material. Surface group measurement by the Boehm titration showed higher acid groups in the base-treated straw (RBS-N) than raw straw due to the base hydrolyzation of lignocellulosic material, which is responsible for the increase in surface acidic sites such as carboxylic and hydroxyl groups. The percentages of carbon and nitrogen for SMBS and BMBS were greater compared to RBS and RBS-N, due to loading of CPC. Based on carbon and nitrogen values, the impregnated CPC on SMBS and BMBS was calculated as 0.086 and 0.109 mmol g<sup>-1</sup>, respectively. For the surfactant modified straw, lower BET surface area was observed and could be explained by the attachment of the surfactant moieties to the

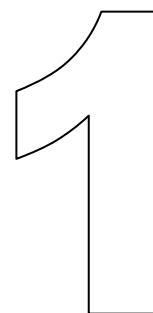
internal framework of raw adsorbents causing the constriction of pore channels. The electrical conductivity was found much lower in surfactant modified straw due to significant reduction in water soluble mineral after the surfactant modification. Higher bulk density of SMBS and BMBS was due to the addition of CPC onto the straw surface. SEM microphotos of all the prepared adsorbents showed the highly irregular shapes and sizes. The treatment with alkaline solution partly removed the protective thin wax on straw surface. The surfactant modified surface appeared to be rough, indicating that the surface had been covered with organic molecules. FT-IR spectra of RBS and RBS-N did not show any radical changes indicating that the treatment with mild base solution did not significantly alter the chemical properties of the straw. Two new bands lying at about 2920, 2850  $\text{cm}^{-1}$  referred as asymmetric and symmetric stretching vibration of methylene (C-H) adsorption bands originated from the alkyl chain of CPC were observed on SMBS and BMBS, proving the existence of CPC on straw surface. Desorption of CPC from the surfactant modified straw was observed to increase with increasing acid solution concentration. The increasing desorption of CPC (with increased in acid solution) describes that ion exchange is the major binding mechanism. The sorption of CPC generally showed that the sorption capacity of CPC increases with increasing CPC equilibrium concentration for both RBS and RBS-N. The surfactant sorption was at the maximum when the equilibrium surfactant concentrations reached the critical micelle concentration, CMC.

Preliminary experiments found the effectiveness of the prepared adsorbents, namely; RBS, RBS-N, SMBS and BMBS in removing different types of emulsified oil from wastewater such as canola oil (CO) and standard mineral oil (SMO). Comparing to SMBS and BMBS, RBS and RBS-N showed low removal efficiency of the emulsified oil. This provided a sensible justification in using SMBS and BMBS as adsorbent materials. The adsorption tests were performed using SMBS and BMBS on CO and SMO by batch adsorption. For the sorption of CO and SMO on SMBS and BMBS, the adsorption was less favorable at high acidic condition and the maximum adsorption capacity was observed at about neutrality. Larger particle size would result in lower adsorption while adsorption temperature would not affect adsorption significantly. The kinetic study revealed that equilibrium time was short and pseudo first order model provided the best correlation for the kinetic adsorption data of CO

and SMO on both SMBS and BMBS. The film diffusion was observed as the rate limiting in the sorption of CO and SMO on SMBS and BMBS. The isotherm data for sorption of CO and SMO on SMBS and BMBS indicated that the adsorption was fitted well by the Langmuir model. The Langmuir adsorption capacities of CO and SMO on SMBS were 576.00 and 518.63 mg g<sup>-1</sup>; and 613.29 and 584.22 mg g<sup>-1</sup> on BMBS, respectively. Desorption experiments also showed the stability of the oil loaded on straw. The adsorbent was later evaluated in a fixed bed column. The breakthrough curves indicated the favorable performance of SMBS and BMBS for both CO and SMO; however, less success was observed for RBS and RBS-N. The modeling of column tests showed a good agreement of experimental data of oil adsorption on SMBS and BMBS with the Thomas and Yoon-Nelson models. The column adsorption capacities from the Thomas model for SMBS and BMBS were 368.82 and 440.74 mg g<sup>-1</sup> for CO; and 310.16 and 336.31 mg g<sup>-1</sup> for SMO, respectively.

The applicability of the prepared adsorbents was also evaluated for treating dye containing wastewater. The adsorption tests were performed using SMBS and BMBS on anionic dyes of Acid Blue 40(AB40), Reactive Blue 4(RB4) and Reactive Black 5(RB5) as the preliminary batch adsorption experiments showed low removal percentage of dyes on RBS and RBS-N. The batch study also revealed that the adsorption was a function of dye concentration, pH and temperature. Adsorption capacity was found higher at pH about neutrality for AB40, and at acidic condition (pH 3) for the other dyes. Adsorption capacity of AB40 increased at increasing experimental temperature whereas no significant change was observed for RB4 and RB5. The kinetic experiment revealed that adsorption of dyes was rapid at initial stage followed by a slower phase where equilibrium uptake was achieved. Based on batch kinetic study of adsorption of AB40, RB4 and RB5 on SMBS and BMBS, the pseudo-second-order model fitted well with the kinetic data other than the pseudo first order model. The film diffusion was observed as the rate limiting in the sorption of AB40, RB4 and RB5 on SMBS and BMBS. The isotherm data of dye adsorption on SMBS and BMBS indicated that the adsorption was fitted well by the Langmuir model. The Langmuir adsorption capacities of AB40, RB4 and RB5 were 45.4, 29.16 and 24.92 mg g<sup>-1</sup> for SMBS and 51.95, 31.50 and 39.88 mg g<sup>-1</sup> for BMBS, respectively.

Desorption experiments also showed that the dye loaded straw was stable at acidic condition but desorption increased as the pH increased (i.e pH 11). The applicability of the adsorbents for AB40 and RB5 removal was also tested in a fixed bed column study. Similar to the column system for CO and SMO, the breakthrough curves on RBS and RBS-N was also poor, however, favorable column breakthrough performance was observed on SMBS and BMBS. The column breakthrough modeling showed the better fit of the experimental data of SMBS and BMBS with the Thomas and Yoon-Nelson breakthrough models. The adsorption capacities from the Thomas model for SMBS and BMBS were estimated as 53.39 and 77.29 mg g<sup>-1</sup> for AB40; and 24.57 and 33.46 mg g<sup>-1</sup> for RB5, respectively.



# BACKGROUND

## 1.1 Introduction

Rapid increase in world population, industrialization and urbanization has led to an increase in ecological problems. Water is particularly vulnerable to the contamination from discharge of wastes from various industrial activities. The indiscriminate discharge of untreated or partially treated effluents into the natural environment creates a major ecological problem throughout the world. Organic pollutants such as oil and organic dyes have left an undesired impact on the environment. It is estimated that between 1.7 and 8.8 million metric tons of oil are released into the world's water every year [1], of which more than 90% are directly related to human activities including deliberate waste disposal. Meanwhile, roughly 10,000 of different commercial dyes and pigments exist, most of which are difficult to biodegrade due to the complex aromatic structure and synthetic origin [2, 3]. Over  $7 \times 10^5$  tonnes are produced annually worldwide [3] while 10-15% of the dyes were estimated to be lost in the effluent during dyeing process [4].

Oils in wastewater especially petroleum origin have very low biodegradability and their presence not only produces aesthetically unpleasant, detrimental to aquatic life but also could cause serious problems for wastewater treatment plants [5, 6]. Synthetic dyes are considered to be dangerous organic compounds for the environment [7-9], thus the existence of dye pollutants in water system is undesirable due to their appearance and toxicity [10, 11]. Various methods for oily wastewater treatment including physical, biological, chemical, mechanical, physicochemical methods (i.e flotation), and membrane processes have been developed [12]. Meanwhile for dye wastewater, the methods developed include adsorption, anaerobic treatment, coagulation, electro coagulation, flotation, filtration, ion exchange, membrane separation, and advanced oxidation [3, 13-16]. However, there are many limitations for those treatments, such as low efficiency, high operation costs, corrosion and recontamination problems, incomplete removal of colored effluent (for dyes) and etc [5, 17].

Adsorption process is one of the interesting methods for removing organic and inorganic pollutants in waterway systems [18] and activated carbon is the widely used adsorbent material. However, it is uneconomical in using activated carbon especially for treatment of oily wastewater [19] and dye wastewater [20], hence the possibility of using alternative inexpensive materials has been actively explored by many researchers in the past years [6, 21, 22].

Development of low cost adsorbent materials based on agricultural waste/byproducts as an alternative to activated carbon had been studied in the past few decades [7, 23]. Agricultural wastes offer advantages such as cheap and abundantly available, simplicity in technology, relatively inexpensive in running cost and biodegradable. Due to these reasons, an agricultural waste, barley straw, has been chosen as an adsorbent in this work. Utilization of barley straw as an adsorbent/biosorbent material has been studied by some researchers, and it has demonstrated excellent efficiency in removing heavy metals [24, 25] and basic dyes [17, 26]. The existence of various functional groups such as carboxyl, hydroxyl, sulphate, phosphate, ether and amino groups on agricultural wastes, which act as binding sites [23, 27], makes a good reason for them to be employed as adsorbent materials. However, using raw untreated

agricultural waste did not give good account in removing certain types of oil and dye wastewater especially emulsified oil [17, 28] and anionic dyes [17]. Thus, it is necessary to modify the straw surface to enhance the sorption capacity towards emulsified oil and anionic contaminants. Modification with a cationic surfactant has been chosen for this study due to encouraging outcomes from previous investigations that reported the effectiveness of cationic surfactant modification on inorganic and organic materials for emulsified oil adsorption [21, 22, 29] and dye removal from wastewater [30-32]. However, most of the modification was performed on mineral surface [33-35] and only a few applications on agricultural waste/byproduct have been reported, i.e on coir pith [36] and wheat straw [29]. Hence, in this work, the potential of using cationic surfactants modified agricultural byproduct, barley straw was investigated.

## **1.2 Research Objectives**

The overall purpose of this study is to assess the feasibility of using raw and surfactant modified barley straws as potential adsorbents for the removal of the emulsified oil and dyes in wastewater in batch and continuous column studies. Two types of oil namely emulsified canola oil (CO) and standard mineral oil (SMO), and three types of dyes namely, Acid Blue (AB40), Reactive Blue (RB4) and Reactive Black (RB5), were chosen to represent the contaminants originated from oils and anionic dyes. The key outcome of this research is to provide a scientific basis for potentially new approaches to oily and colored wastewater treatment by utilizing cheap and abundantly available agricultural waste material.

This thesis is outlined in seven chapters, which begins with Background as Chapter 1 to introduce an overview of this thesis. Literature review in Chapter 2 can be best viewed in two segments; the first segment discusses the emulsified oils and dyes in wastewater including but not restricted to their classification, physicochemical properties, potential hazard and current available treatments. The second segment focuses on cationic surfactant and the usefulness in modifying the solid surface for environmental remediation. Mechanism of surfactant adsorption to solid surface and the potential of using surfactant modified adsorbents to remediate emulsified oil and dye wastewater were thoroughly reviewed in this part. Chapter 3 covers the

experimental methodology and is divided into three parts. Firstly, the preparation and characterization of adsorbent materials is described, secondly the procedure of batch and column adsorption for emulsified oils and anionic dye wastewater are described, and finally the appropriate models for simulate the batch and column test data are discussed. Overall, Chapter 3 describes research methodology, including materials, instrumentation, general experimental techniques and procedures.

Results, data analysis and discussion were presented into three chapters, Chapters 4-6. Chapter 4 can be best viewed in two segments. The first segment describes the modification of barley straw and the second segment establishes the characteristics of the prepared barley straw. Generally, two types of modification were applied; treatment with a base solution and treatment with a cationic surfactant. In this chapter, the effects of concentration of base and cationic surfactant were studied in order to ascertain the relationship between the base solution and the active site creation. The physical and chemical properties of raw and modified straw were established in order to ascertain the influence of various treatments applied to the straw properties as well as to prove the existing of cationic surfactant on the straw surface. Chapters 5 and 6 generally discuss the treatment of oily wastewater and dye wastewater, respectively, using the prepared adsorbents. The discussions include the findings in batch and column studies. The appropriate models were also employed to fit the experimental data. Finally, Chapter 7 presents the overall summary of the results and a concise account of conclusion drawn from this study. Recommendations as well as future research directions are also presented in Chapter 7 as well.

# 2

## REVIEW OF LITERATURE

### 2.1 Introduction

Overall discussion in this chapter could generally be divided into two main parts; the first part focuses on dye and oily wastewater including the classification, sources and impact of oil and dye wastewater on the environment and the possible remediation technologies. The second part discusses the applicability of cationic surfactant modified adsorbents for dye and oily wastewater treatment. The discussion includes the chemistry of cationic surfactant, mechanism of cationic surfactant adsorption to solid surface and the extensive review of previous work done on utilizing surfactant modified adsorbents for removal of low polarity contaminants and anionic dyes from aqueous solution.

## 2.2 Oils

Fats, oils, and waxes are naturally occurring esters of long straight-chain carboxylic acids [37] which are normally derived from animal and vegetable materials. Meanwhile, mineral oil usually consists of mixtures of high molecular paraffins, naphthene and aromatic hydrocarbons with a certain admixture of tar and asphaltene substances [38]. Oils derived from biological sources are normally polar and biodegradable, whereas the ones originated from petroleum or mineral, basically non polar forms are believed to be bioresistant [39]. Generally, oil can be classified into five types as below [21]:

**Mineral oil** is a viscous liquid that is insoluble in water but soluble in alcohol or ether and is flammable.

**Petroleum** is made up of gaseous, liquid and solid components and its viscosity varies according to the mixture composition.

**Animal oil** is also known as fatty acids or fixed oil. In solid form, animal oils are known as fats.

**Vegetable oil** is primarily derived from kernel or many other parts of plant materials.

**Essential oil** is a complex, volatile liquid derived from flowers, stems, etc.

## 2.3 Oily Wastewater

Oily wastewater can be described as the oil water mixture that is no longer useful. The type of oil may refer to oil of any kind and any form, such as petroleum and non-petroleum oils. The presence of oil in wastewater can be traced back to two main sources; industrial and municipal sources. For the industrial wastewater, Patterson [39] reported that major sources of oils in contaminated waters are petroleum, metals, food processing, textiles and cooling and heating industries. Petroleum industry was one of the principal industrial sources of oily waste. It may be resulted from producing, refining, storing or transportation operation [40, 41]. In metal industry, most of the oil generated from metal working or forming operation, where the oil is used to cool the instruments, lubricate the cutting/grinding process or to dissipate heats during the rolling of metals strip [40, 42]. Scouring of fiber especially wool in the textile processing industry was reported as the main process contributing to the

presence of oil in textile water [40]. In vegetable oil processing, main source of oil waste came from the cleaning, screening and crushing of fruits, nuts or seeds to extracted oil [43]. For municipal sources, oily waste is originated from food preparation, garbage disposal and cleaning [40, 44]. The oil concentration present in the various sources of wastewater is reported in Table 2.1. However, it is worth to note that the concentration of oil is highly dependent on various factors such as the size of the industry and the technology of manufacturing process employed. For the oil and grease existed in food outlet, the varieties of food served and the timing of sampling may influence the characteristics of the effluent.

Table 2.1. Concentration of oil in different sources

Source of wastewater	Concentration (ppm)	Reference
Palm oil Mill	4000–6000	[45]
Locomotive washing and maintenance	5066	[6]
Vegetable oil Processing	5000-10000	[43]
Pet food industries	52000-114000	[46]
Metal industries (Hot milling operation)	1080-3271	[42]
Poultry slaughterhouse	1500-1800	[47]
Chinese restaurant	120-172	[44]
Western restaurant	52.6-2100	
American fast-food	158-799	
Student canteen	415-1970	
Bistro	140-410	

It is crucial to identify the characteristics of oil existing in water as it may lead to the effectiveness of the treatment that needs to be undertaken. The physical existence of oil in wastewater could be classified into several modes as follows [48, 49]:

**Free oil** is termed as the oil which rapidly rises to the surface of the water under calm conditions and has a droplet size of 150 microns or more.

**Mechanical dispersion** consists of fine droplets ranging in size of 10-1000 microns. These droplets are electrostatically stabilized without the influence of emulsifying agents.

**Chemically stabilized emulsified oil** consists of fine droplets usually less than 20 microns and is stabilized in the presence of an emulsifying agent.

**Dissolved oil** consists of finely oil droplets less than 5 microns and usually refers to the light end of the oil spectrum such as benzene, toluene and xylene.

**Oil wet solids** refer to the oils that adhere to sediments such as metal chaffing that are common in industrial wastewater.

## **2.4 Emulsified Oily Wastewater for Environmental Concern**

Oily waste always poses a challenge not only in petroleum or petrochemical industry but in others as well, such as food, cosmetic and pharmaceutical production [50]. Even though the composition of oily wastes varies from one industry to another, but it is important to note that a significant part of oily waste always exists in the emulsified form which is often difficult to treat [49, 50]. For example, due to the open sea action, about 40% of oil spill can become an emulsion in a single day and rapidly jump to 80% just after 5 days [40]. This is certainly a real issue, as oil emulsion is known for its stability in aqueous phase [51] and can be possibly removed only by applying a chemical clarification method [45, 51]. Oil emulsion is described as a heterogeneous system in which the dispersion medium is water and dispersed phase is oil. It can be mineral oils, mineral oils with admixture and fats [38]. Stable oil emulsion can be formed once the oil comes into contact with water in the presence of an emulsifying agent [5]. The term 'stable' refers to the capacity of oil droplets to remain an independent entity within the dispersion [42]. This produces a milky white solution which is one of the characteristics of stable oil emulsion [49]. The existence of emulsified oil in wastewater leaves a very strong negative influence on the environment and the efficiency of wastewater treatment technology. It may reduce the effectiveness of membrane separation [50], blind the pores of adsorbent material (i.e activated carbon) in adsorption and filtration process [19, 52] and interfere microorganism in biological wastewater treatment units [6, 53]. Generally, the suitable method for oily wastewater treatment was depended on four wastewater parameters, which are oil droplet size distribution, droplet velocity, concentration of oil in wastewater, and emulsion [54]. As vegetable oil, fats and petroleum oil share common chemical and physical properties, they cause the similar environmental

effects. They can also contain toxic components and produce similar acute toxic effects, chronic toxicity, and carcinogenicity [55].

## **2.5 Dyes**

Dyes can be said to be colored, ionizing and aromatic organic compounds which show an affinity towards the substrate being applied. All commercial dyes are organic chemicals. Dye molecules consist of two key components; chromophore which is responsible for producing color and the auxochromes which supplement the chromophores as well as render the molecule soluble in water and enhance favorable bonding affinity [9]. Together, the dye molecule is often described as a chromogen. The absorption and reflection of visible and UV irradiation is ultimately responsible for the observed color of the dye [56].

There are several ways for classification of commercial colorants. It can be classified in terms of color, structure and application method [57]. However, due to the complexities of the dye nomenclature from the chemical structure system, the classification based on application is often favorable [9]. The classification based on chemical structure for the common class of the dyes is presented in Table 2.2 whereas Table 2.3 summarized the dye different application classes and chemical types [58]. Other than the above, dyes are also usually classified based on their particle charge upon dissolution in aqueous application medium (dye bath) [59, 60] as follows:

- i. Anionic (direct, acid, and reactive dyes)
- ii. Cationic (all basic dyes)
- iii. Nonionic (dispersed dyes)

Table 2.2. Classification of dyes according to the chemical structure

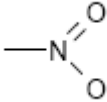
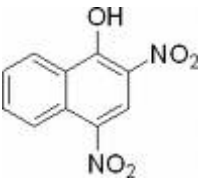
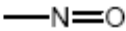
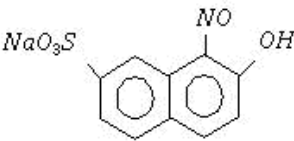

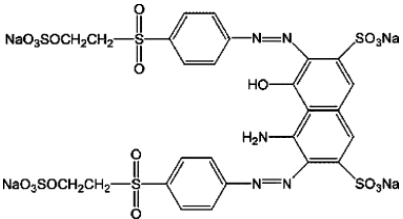
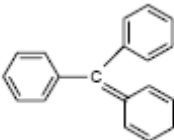
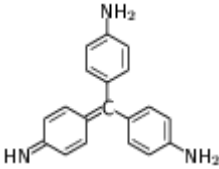
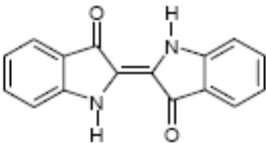
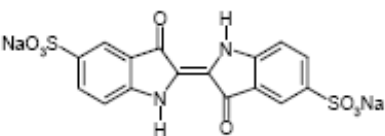
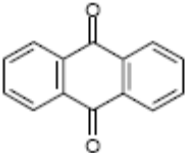
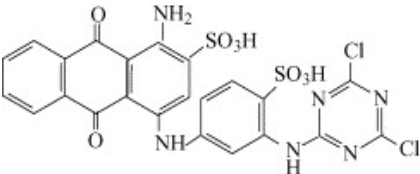
Class	Chromophore	Example
Nitro dyes		 Acid Yellow 24
Nitroso dyes		 Acid green 1
Azo dyes		 Reactive Black 5
Triarylmethane dyes		 Basic red 9
Indigoid dyes		 Acid Blue 71
Anthraquinone dyes		 Reactive Blue 4

Table 2.3. Application classes of dyes and their chemical types [58]

Class	Substrate	Method of application	Chemical types
Acid	Nylon, wool, silk, paper, inks and leather.	Usually from neutral to acidic bath.	Azo (including premetallized), anthraquinone, triphenylmethane, azine, xanthene, nitro and nitroso.
Basic	Paper, polyacrylonitrile, modified nylon, polyester and inks.	Applied from acidic dye baths.	cyanine, hemicyanine, diazahemicyanine, diphenylmethane, triarylmethane, azo, azine, xanthene, acridine, oxazine and anthraquinone.
Reactive	Cotton, wool, silk and nylon.	Reactive site on dye reacts with functional group on fibre to bind dye covalently under influence of heat and pH (alkaline).	Azo, anthraquinone, phthalocyanine, formazan, oxazine and basic.
Direct	Cotton, rayon, paper, leather and nylon.	Applied from neutral or slightly alkaline baths containing additional electrolyte.	Azo, phthalocyanine, stilbene, and oxazine.
Disperse	Polyester, polyamide, acetate, acrylic and plastics.	Fine aqueous dispersions often applied by high temperature/pressure or lower temperature carrier methods; dye maybe padded on cloth and baked on or thermo fixed.	Azo, anthraquinone, styryl, nitro and benzodifuranone.
Solvent	Plastics, gasoline, varnishes, lacquers, stains, inks, fats, oils, and waxes.	Dissolution in the substrate	Azo, triphenylmethane, anthraquinone, and phthalocyanine
Sulphur	Cotton and rayon	Aromatic substrate vatted with sodium sulfide and reoxidized to insoluble sulfur-containing products on fibre	Indeterminate structures
Vat	Cotton, rayon and wool	Water-insoluble dyes solubilised by reducing with sodium hydrogensulfite, then exhausted on fibre and reoxidized	Anthraquinone (including polycyclic quinines) and indigoids

## 2.6 Dye Wastewater

Wastewater is the major route where the dyes can enter the environment [61]. Huge amounts of dye contaminated water were generated as the result of substantial usage of dyes in quite processes. Many industries such as dyestuff, textile, paper, printing, carpet, plastic, food and cosmetic industry use dyes to provide color to their products [7, 62, 63]. These dyes are invariably left in industrial waste and consequently discharged mostly to the surface water resources [64]. In 1991, 668 million tonnes of dyestuff were sold annually, where 214 tonnes of them were acid and reactive dyes. This accounted over 30% of total sales [65]. The percentage fixation for each type of dye shown in Table 2.4 [66] indicates the relatively poor fixation of both acid and reactive dyes. The unfixed dyes of about 5-20 and 10-50% for acid and reactive dyes respectively may finally end up as an effluent. Factored with the overwhelming majority of acid and reactive dyes currently in use [63, 65], their impact to the environment should be seriously addressed.

Table 2.4. Estimated degree of fixation for different dyes [66]

Dye class	Fibre	Degree of fixation (%)
Acid	Polyamide	80-95
Basic	Acrylic	95-100
Direct	Cellulose	70-95
Disperse	Polyester	90-100
Reactive	Wool	50-90
Sulphur	Cellulose	60-90
Vat	Cellulose	80-95

## 2.7 Dye Wastewater for Environmental Concern

Colored wastewater no doubt will cause uneasiness to the public, as color wastewater was always presumed as hazardous and not safe. Due to highly visible, color is the easiest contaminant to be recognized in wastewater [67]. In fact the presence of very small amount of dyes in water, in some cases less than 1 ppm, is easily visible and enough to capture attention of both public and authorities [3]. These is alarming as typical discharge of textile processing effluent is about 10-200 mg L<sup>-1</sup> [68]. Put

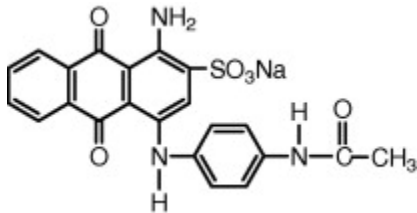
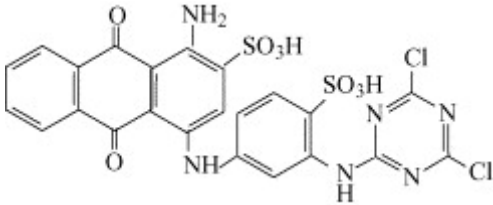
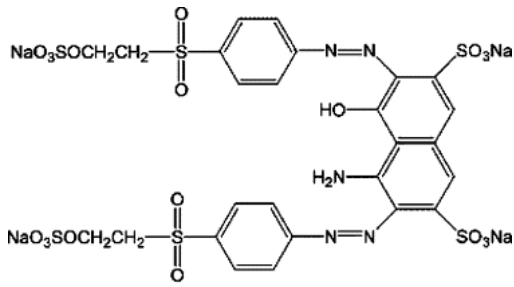
aesthetically unpleasant aside, the existence of dye wastewater actually causes greater damage. It can reduce the penetration of sunlight into the water body, thus affect the growth of bacteria that are responsible for biologically degrade the impurities in water and may hinder the photosynthesis activity in aquatic plants [69-71]. Moreover, large numbers of dyes are found to be toxic and carcinogenic thus pose a serious threat to the environment especially aquatic living organism [70].

In this work, acid and reactive dyes were chosen as these dyes are largely used, and their removal efficiency is still a major concern especially to the conventional treatment facilities [71]. This is partly because the dyes were designed to be resistant to degradation or fading by oxidizing agent, high temperature and enzyme degradation (especially from detergent washing) [72]. Acid dyes contain free acid groups, which are ionized in the aqueous application medium (dyebath). They are generally used to dye polyamine, wool, or silk and are primarily azo, anthraquinone, or triarylmethane structures [61]. Reactive dyes contain a reactive group that forms a covalent bond with a group on the substrate, usually hydroxyl or amine. Fiber reactive dyes are often of azo or anthraquinone type [61]. From acid and reactive dyes, Acid Blue 40 (AB40), Reactive Blue 4 (RB4) and Reactive Black 5 (RB5) were selected. According to basic chromophoric structures, RB5 is classified as an azo dye whereas AB40 and RB4 are anthraquinone dyes (Table 2.5). Both of these dyes have been popularly used especially in textile industries, where azo dye is the largest class of textile dyes used at about 60-70% followed by anthraquinone dyes (15-20%) [73, 74]. These groups of dyes are favorable as they offer a variety of color shades and easy of application [73].

The effect of azo and anthraquinone dyes on the environment deserves a special attention as they are widely used and show a low degree of fixation rate. Except for some of the dyes with free amino groups, azo dyes in purified forms seldom directly mutagenic or carcinogenic [75]. In spite of this, they could be degraded with bacteria under anaerobic and aerobic conditions and create toxic aromatic amines [76, 77] which are mutagens and carcinogens [77]. Compared to azo dyes, anthraquinone dyes own more stable structures, higher resistance to decolorization, and lower biodegradability [74, 78]. The low degradability of this dye is due to their fused

aromatic ring structure, thus allowing the color to remain longer in effluent [3]. Anthraquinone structures may be responsible for acute toxicity, mutagenic and carcinogenic effects when exposed to aquatic life [79]. Due to that, the release of anthraquinone dyes will considerably contribute to the environmental pollution.

Table 2.5. Some of the information of the dyes used in this work

Dye	Chemical formula	MW ( g mol <sup>-1</sup> )	$\lambda_{\text{max}}$ (nm)	Color Index (C.I)	Chemical Classification
Acid Blue 40 (AB40)		473.4	610	62125	Anthraquinone
Reactive Blue 4 (RB4)		637.4	595	61205	Anthraquinone
Reactive Black 5 (RB5)		991.8	591	20505	Azo

## **2.8 Remediation of Oily and Dye Wastewater**

Due to the detrimental effects of oily and dye wastewater on the environment, the treatment of oily and dye wastewater becomes highly necessary. Various techniques of removal of oily [12, 80, 81] and dye wastewater [7, 63] have been extensively reviewed by many authors. Treatment for oily and dye wastewater could be classified into several categories. Depending on the nature of wastewater, the treatment may involve more than one particular category. However, it is important to take note that the available technique is not restricted to the below mentioned only:

- i. Physical treatment
- ii. Chemical treatment
- iii. Biological treatment

### **2.8.1 Mechanical/Physical separation**

Mechanical/physical separation is a separation process in which a substance is removed from a mixture by physical means. A physical process usually treats suspended, rather than dissolved pollutants. It may be a passive process, such as simply allowing suspended pollutants to float to the top naturally or by allowing pollutants to pass through filtration medium [82]. Air flotation and filtration are among the techniques of physical separation.

#### **2.8.1.1 Air flotation**

The systems are operated by increasing the difference in specific gravity between the pollutants particles and water by blowing fine air bubble through the wastewater [54]. Air bubbles become attached to the suspended particles buoying them up to the surface of the water where they are removed by skimming. Flotation can be classified as follows: dispersed-air flotation (DispAF), dissolved-air flotation (DAF), and electroflotation depending on the method used to generate the bubbles [82]. In DispAF, compressed air is forced through the pores of sintered-glass disks in order to produce bubbles with diameters usually ranging from 75 to 655  $\mu\text{m}$  [83]. In DAF, wastewater is saturated under pressure with air. Upon released of pressure through needle valves into the flotation cell at atmospheric pressure, the bubbles of approximately 30-120  $\mu\text{m}$  in diameter was formed and rise to the surface of the liquid

[12]. Electroflotation involves the electrolysis of water. Bubbles of  $H_2$  are formed at the cathode and bubbles of  $O_2$  are formed at the anode. As for the electrical consumption, the hydrolysis of wastewater generally consumes significantly less electrical energy than tap water due to the existence of salts [12]. This method generates bubble diameters ranging from 22 to 50  $\mu m$ , depending on the experimental conditions [84].

For emulsified oil wastewater, air flotation was usually used after the oil emulsion had been destabilized. The usefulness of flotation in oily wastewater treatment has been extensively reported [85]. This method is usually employed for removing large quantities of fats, oil and grease (FOG), for example from dairy industry due to its capability in handling shock loads of oil [40]. Li et al. [86] applied this flotation principle in their work for removal of emulsified oil originated from an oil field. The separation study was performed in a long and narrow separation column in an effort to improve oil droplets and air bubble contact. By demulsification of the oil using a chemical treatment, a decent oil removal of 90% could be achieved.

For dye effluent, air flotation technique was usually applied after the particles had been destabilized. Due to the low density of color flocs formed after coagulation process, flotation was preferred as an alternative to sedimentation [87] where the hydrophobic dye flocs would adhere to the bubble surface and rise to the top of the liquid phase [82]. Recent work on applicability of air flotation in remediation of dye wastewater has been conducted [83, 88] showing the removal of dyes by flotation was closely related to the characteristics of wastewater such as pH, background electrolyte and surfactant concentration [88]. Dafnopatidou and Lazaridis [83] further observed that with assistance of chemical treatment, DAF could manage to remove more than 97% of dyeing mill effluent. However, surfactant rich dye wastewater could not be satisfactorily decolorized due to the exceptional foaming.

### 2.8.1.2 Filtration

The membrane separation process is based on the presence of semi permeable membranes consisting of either thin polymer or ceramics with pores in a certain range [82]. The membrane allows water to flow through while it blocks suspended solids and other substances. Membrane technique was applied on a number of applications mainly for the treatment of complex industrial wastewater [12]. Categories of typical membrane are presented in Table 2.6:

Table 2.6. Typical characteristics of membrane processes [82]

Process	Operating pressure (Bar)	Pore size (nm)	Molecular weight cut-off range(Dalton)	Size cut-off range (nm)
Microfiltration (MF)	<4	100–3000	>500,000	50–3000
Ultrafiltration (UF)	2–10	10–200	1,000–1,000,000	15–200
Nanofiltration (NF)	5–40	1–10	100–20,000	1–100
Reverse osmosis (RO)	15–150	<2	<200	<1

Micro filtration (MF) and ultra filtration (UF) are favorable for removal of larger particles, meanwhile for dissolved particle such as dissolved salts; nano filtration (NF) and reverse osmosis (RO) are usually applied. Unlike, MF and UF with separation being based on pressure to overcome the hydraulic resistance, separation in NF and RO will take place by diffusion via membrane based on the difference in potential side [89].

Some works on application of membrane filtration for treatment of oil emulsion have been reported. MF and UF is mostly reported, meanwhile less work on NF and RO [12]. The use of membrane separation for producing water which having a large percentage of emulsified oil was reviewed by Fakhru'l-Razi et al. [41]. Compared to other techniques for oil emulsion removal, membrane filtration has clear advantages as such no chemical is needed to destabilized the oil emulsion, high removal efficiencies and treatment facilities are quite compact and mostly fully automatic [90]. However, it is prone to failure. Most of the fouling/membrane failure was due to the oil adsorption on membrane walls, gel formation, pore blocking by oil droplets, salt presence, pH, temperature, shear stress and pressure [12, 91].

A number of pressure-driven membrane processes, including microfiltration, ultrafiltration, nanofiltration, and reverse osmosis, were thoroughly investigated for treatment of dye wastewater [92]. They offer the advantage to clarify, concentrate and separate dye simultaneously from effluent [59]. Even though, MF and UF are able to remove colored wastewater completely, however, the permeate can not reuse in the production plant as this type of membrane not efficiently block dissolved solids such as dissolved salt and surfactant [90]. NF and RO was found capable of removing dissolved solids, however low permeability of RO membrane requires high pressure thus consuming relatively high energy [93]. In general, the usage of membrane technique needs careful considerations as the membrane must own specific features such as resistant to temperature, chemical and microbial attack [3]. Other than that, the residue left after separation may pose problems such as disposal, possibility of clogging and replacement of membrane [59, 94]. In short, membrane fouling is the most significant problem with all membrane filters. This is due to [82, 89]:

- i. Build-up contaminants from the feed water deposit on the membrane surface
- ii. Formation of chemical precipitates due to chemistry of feed water
- iii. Damage of membrane due to reacting with chemical substances presence

The types and amounts of fouling are dependent on many different factors, such as feed water quality, membrane type, membrane materials and process design and control [89].

#### 2.8.1.3 Sorption

The research on the applicability of sorption technique to treat oil emulsion in wastewater had been demonstrated by many works [22, 95, 96]. Various sorbent materials including agricultural based material [29, 97], inorganic based [98, 99], and synthetic material [100] were tested. It was reported that the hydrophobicity of the adsorbent surface and others contributed to the sorption of oil onto the surface [97]. Out of various sorbent materials, activated carbon was reported as the most widely used material for emulsified oil removal [22, 101]. However, it lacks the efficiency as the oil will easily blind the pores [19].

For dye wastewater removal, sorption technique using activated carbon was also reported as the most widely used method [102]. However, using activated carbon as an adsorbent is not economical due to its cost and regeneration difficulties [20]. Thus, various types of material have been tested for removing dyes in wastewater. Large numbers of works utilizing an adsorbent material from various sources such as agricultural waste, mineral base and synthetic have been reviewed and some were found to give good potential on dye wastewater decolorization [7, 63, 103]. The dye molecules may attach to adsorbent surface either by physical or chemical forces [7, 8]. The color removal efficiency however, depends on many factors such as chemical structure of dyes, solubility, pH and temperature of dye effluent and other physicochemical parameters [103].

## 2.8.2 Chemical method

Chemical technique is a separation process that removes or separates a substance from a sample that involves differences in the chemical properties of the substances. This technique involves chemical coagulation, ozonation, Fenton reagent oxidation etc.

### 2.8.2.1 Chemical coagulation

Chemical coagulation is a process in which chemicals are added to an aqueous system for the purpose of creating rapid-settling aggregates out of finely divided, dispersed matter with slow or negligible setting velocities [104]. They are generally used to eliminate organic substances from wastewater. The principle function of chemical coagulation is known as destabilization, aggregation, and binding together of colloids. Alum, or aluminium sulphate, ( $\text{Al}_2(\text{SO}_4)_3 \cdot 18\text{H}_2\text{O}$ ) is one of the most common coagulants which may be added to a water system. The larger, heavier flocs particles settle, and can then be removed by subsequent settling and filtration [105]. Various inorganic coagulants are used, mostly lime, magnesium, iron and aluminium salts. Factors, which can promote the coagulation are the coagulant types, coagulant dosage, the solution pH, concentration and nature of organic compounds [106, 107].

For oily wastewater, this technique is usually employed when dealing with chemically stable emulsified oil [12]. From the various work done, it was easily observed that most of the researchers applied a combination of more than single method to get a desired result [108, 109]. Most of the work combines chemical and physical methods.

Chemicals are commonly used for the treatment of oily wastewater to enhance mechanical treatment. They are used to precipitate emulsifying agents, to affect the interfacial tension, to neutralize electrical charges and to adjust the pH [110]. The chemical method such as coagulation is used to promote the break up of the oil emulsion by reducing the superficial charge of the oil droplets, causing the coalescence of oil droplets [111] and the physical method such as flotation, flocculation and filtration is used to physically remove oils from wastewater.

Coagulation is often applied to dye wastewater either as a main treatment process [112] or as a post treatment to compliment other treatment processes [113, 114]. It was reported that, inorganic coagulant does not perform well for highly soluble dyes (i.e reactive dyes) [115]. However, polymer base organic coagulant was proven effective as a dye coagulant, including reactive dyes. High cost of the coagulants and the difficulty of disposing of the larger amount of the sludge produced by this process caused it to be abandoned [104].

#### 2.8.2.2 Ozonation

Ozone is a molecule that consists of three negatively charged oxygen atoms. The ozone molecule is very unstable and has a short half-life of 20 minutes, causing it to fall back into its original form after a while. Ozone can be artificially created through an ozonation process unit including an oxygen generator [105]. Ozone, a strong oxidizing gas, reacts with most organic and many inorganic molecules [105]. It is capable of degrading chlorinated hydrocarbons, phenols, pesticides and aromatic hydrocarbons [94] and also microorganisms such as viruses, bacteria and fungi [116]. Ozone is mainly applied in waste water and drinking water purification, for disinfection purpose as a replacement to chlorine in Europe [116]. The pH of effluent plays a major role as the decomposition of ozone requires high pH ( $>10$ ), therefore the treatment of organic molecules is favorable in alkaline solutions than at neutral or acidic [117, 118]. Ozone is extremely toxic and safety equipment capable of monitoring ozone in the atmosphere, as well as a ventilation system that prevents ozone levels higher than 0.1ppm, are required [105]

Like other treatment techniques, the oxidation of oily wastewater utilizing ozone was an attractive solution. It offers huge advantage as oils are directly destroyed in wastewater thus the limitation of oil loading are not an issue anymore [38]. Ozone attacks the organic compounds basically in two ways [119]:

- i. Direct attack by molecular ozone: Reaction of ozone with alkenes result in final products of aldehydes, carboxylic acids, ketones, and/or carbon dioxide
- ii. Indirect attack by free radicals: Decomposition of ozone in water leads to the formation of secondary oxidants such as hydroxyl ion.

Gunukula and Tittlebaum [120] observed that ozone treatment alone is capable of reducing oil and grease and petroleum hydrocarbon up to 86%, whereas 50% was achieved by utilizing only oxygen. They also observed the efficiency improvement if increasing ozone dosage rate [120]. However, in most oily wastewater treatment processes, the ozonation treatment was accomplished with another technique of treatment. Karageorgos et al. [121] conduct a study on the treatment of olive oil manufacturing waste (OMW) by utilizing ozone with another oxidation agent, UV. They found the treatment could substantially reduce the concentration of phenols exceeding 80% as well as decolorizing the effluent after relatively short treatment time. However, complete mineralization proved difficult even at reduced organic feed concentrations and increased oxidant doses. At the conditions employed in the study, COD removal varied from as little as 10% to about 60%. Andreozzi et al. [122] also observed the combination of O<sub>3</sub>/UV for mineral oil contaminated wastewater providing 80 to 90% removal of the inlet COD with reaction time less than 30 min. Meanwhile, Chang et al. [90] utilized ozone to compliment the ultrafiltration treatment to partially oxidized the surfactants in UF permeates in an effort to reuse the UF permeate as process water. Generally, the efficiency of oily wastewater remediation was influenced by many circumstances such as the origin of oily wastewater, dosage of the ozonation and the other accompanying treatment.

For dyes, ozonation process is preferable for soluble dyes (double bonded dyes molecule) as it normally attack dye double bonds which are responsible for coloration [123]. After this process, the effluent become colorless and suitable to directly discharge to waterways [94], as it has only oxidized substances, and byproduct

formation rarely occurs. Therefore, the significant advantage of ozone treatment was the fact that ozone is gas therefore no drastic increase in volume of wastewater and sludge was expected. Even though ozone was able to rapidly decolorize soluble dyes such as reactive and acid dyes, however, it reacts much slower for non soluble dyes (i.e vat dyes and dispersed dyes) [124]. Moreover, textile effluent may contain other pollutants/constituents, i.e inorganic salt, surfactant that have a possibility to react with ozone which may subsequently increase ozone consumption [64, 125]. Due to this, ozonation process is usually done at final stage/post treatment [126].

### 2.8.3 Biological method

Biological treatment, either aerobic or anaerobic, is generally considered to be the most effective means of removing bulk pollutants from complex and high-strength organic wastewater [14]. Most often, the degradable substances are organic in nature and may be present as suspended, colloidal or dissolved matters [127]. Even though, the biological treatment offers considerable advantages such as relatively inexpensive process, low running cost and non toxic end products [63]. The fact that this treatment required large land area, as well as less flexibility in design and operation, makes the application restricted [7]. Certain pretreatment may also be applied if toxic substances are present in influents, to lower the levels of these contaminants as microorganisms present in these processes can not tolerate to the certain level of the contaminants [127].

Biological treatment for oily wastewater is generally applicable for dissolved oils and other types of stabilized emulsions, which cannot be destabilized by chemical coagulants. Several works have found that biological technique had offered an attractive solution to remediation of oily wastewater [128, 129]. It was observed as effective in degrading fat, oil and grease into miscible molecules [128]. However, it faces several limitation such as blocking the oxygen transfer by the formation of a lipid coat around the floc [130, 131]. The agglomeration of fats in the activated sludge system may affect the sedimentation and reduce the efficiency of the treatment station [132]. Due to this, the need of pretreatment prior to the aerobic treatment is necessary. The use of alkaline/acid/enzymatic to hydrolyse the oil and grease prior to the biological treatment was reviewed [133] and was found capable improving the

biological degradation of fatty wastewaters, accelerating the process and improving time efficiency.

Compared to aerobic treatment, anaerobic treatment perhaps gets more attention as it produces less biomass and biogas(methane) [134]. However, the anaerobic treatment for oils and fats does have some problems as well and these have been reported by Petruy and Lettinga [135]. The disintegration of sludge due to the adsorption of fats, causes the granular sludge flotation of sludge and washout [136]. The overloads of fats and oils also greatly disturb the bacteria treatment efficiency [5, 6]. Recently, the application of Upflow Anaerobic Sludge Blanket(UASB) for oil and grease containing wastewater was favorable [137, 138] as the UASB has an advantage such as relatively lower hydraulic retention time compared to traditional anaerobic reactor. Due to this, the utilization of both anaerobic and aerobic treatment in remediate the oil and grease containing wastewater had been explored by many researchers [137, 138]. The good quality effluent for anaerobic and aerobic systems was observed in many works [137, 139]. Wahaab and El-Awady [138] for example found that the removal percentage of oil and grease was improved from 58% using UASB alone to 91% after integrating with aerobic treatment.

As dyes were designed to be stable and lasting, thus it is not easily biodegraded. So, the conventional biological wastewater treatment systems are inefficient in treating dye wastewater [76]. Majority of dyes were observed to be non biodegradable or non transformable under aerobic condition [14]. For degradability of the various dyes, 87 dyestuffs under aerobic condition were successfully conducted by Pagga and Brown [140]. By utilizing bacterial inoculate derived from an aerobic effluent treatment plant, they found that no dyestuffs show any significant biodegradation under these conditions [140]. This was because the majority of the dyes are chemically stable and resistant to microbial attacks [63]. Azo based dyes for example, are generally resistible to aerobic bacterial degradation [141, 142]. Works found that reduction under anaerobic conditions managed to breakdown the azo linkage and produced aromatic amines; colorless but potentially harmful compounds, however, can be biologically degradable under aerobic condition [143-145]. Unlike azo based dyes, anaerobic treatment was less efficient for anthraquinone [71] due to the stability of

structural characteristics and the ability of dyes to inhibit anaerobic microorganism [146]. Due to the prolong treatment time that may take a few days for decoloration, biological treatment was found incapable of removing dye effluent in continuous basis [7]. The potential of using combination of aerobic and anaerobic treatment seems sensible and was explored by several researchers [145, 147]. Higher removal and in several cases up to total removal was observed for this integration treatment system. However, the removal efficiency varies for each type of the azo dyes [145, 148, 149]. As for anthraquinone dyes, the removal was mainly due to the adsorption onto bacterial flocs materials rather than reduction degradation [150].

## **2.9 Adsorption**

Adsorption can be generally described as adhesion of extremely thin layer of gaseous molecules, dissolved substances, or liquid (referred as adsorbate) to the surface of solids (refer as adsorbents) which they are in contact [151]. Adsorption can be classified into two [152]; physical sorption and chemical sorption. Physical adsorption or physisorption is characterized by weak interparticle bonds (i.e van der Waals, hydrogen and dipole-dipole) exist between adsorbate and adsorbent [8] thus physical adsorption is often reversible [152]. Chemical adsorption or chemisorption meanwhile is characterized by the formation of strong chemical associations between ions or molecules of adsorbate to adsorbent surface, which is mainly due to the exchange of electrons [8] thus irreversible in most cases [152]. Factors that influence the adsorption efficiency include adsorbate adsorbent interaction, adsorbent surface area, adsorbent to adsorbate ratio, adsorbent particle size, temperature, pH and contact time [7, 8]. As for environmental remediation purpose, adsorption is widely used for equilibrium separation process and is an effective method for water decontamination applications [8, 153]. Adsorption has been found to be superior to other techniques for water re-use in terms of initial cost, flexibility and simplicity of design, ease of operation and insensitivity to toxic pollutants. Adsorption also does not result in the formation of harmful substances [7].

For packed column scenarios, adsorption could be depending on the effective contact of solute with packed adsorbent material. An adequate and good distribution of the solute in packed column is important to maximize the adsorbate to adsorbent contact.

The movements of solute in packed bed column could generally be described by dispersion and diffusion mechanism [154]. Dispersion is generally contributed by velocity variations in porous media. The factors that influence the dispersion efficiency may depend on the length of the packed column, viscosity and density of the fluid, ratio of column diameter to particle diameter, ratio of column length to particle diameter, particle size distribution, particle shape, fluid velocity and temperature [155]. Diffusion meanwhile is a molecular mass transport process in which solutes move from the areas of higher to lower concentration. Resistance due to the diffusion may be contributed by boundary layer that exists on particle surface and includes the intraparticle diffusion that describes the potential of solute to diffuse into the inner portion of particle via surface diffusion, pore diffusion, or both [156]. Solute will be distributed radially and axially by a variety of mechanisms in addition to molecular diffusion once it flows through the packed column material [157, 158]. Generally, the dispersion coefficient in axial direction is superior to the dispersion coefficient in radial direction for larger Reynolds number values ( i.e more than 10). Whereas, for lower values of the Reynolds number (i.e less than 1), the two dispersion coefficients are approximately the same and equal to molecular diffusion coefficient [155]. At very low flow rates, the dispersion process is usually dominated by molecular diffusion [158]. Dispersion effect could be minimized by ensuring the uniformly radial distribution of solute at column inlet which will help evenly distribute the liquid over a section of packing thus increasing the efficiency of the mass transfer [155].

## **2.10 Agricultural Waste as an Adsorbent**

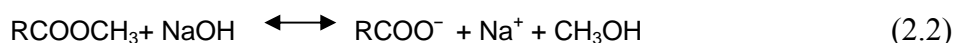
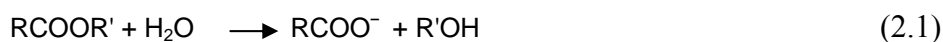
Development of low cost adsorbent materials based on agricultural waste/byproducts has been studied in the past few decades [7, 103]. Adsorption utilizing agricultural byproduct is exciting as it offers various advantages such as abundantly available at no or very low cost, simple technique, little processing cost and ability to biodegradation [103]. Due to their low cost, these materials can be disposed of without expensive regeneration [159, 160]. Bailey et al. [159] further added that the sorbent can be assumed as ‘low cost’ if it requires little processing, abundant in nature, or a by-product or waste material from another industry. As a lignocellulosic material, which is rich in cellulose, hemicellulose and lignin, agricultural waste has a

huge potential to be an efficient adsorbent as it consists of lots of polymeric material that posses a variety of functional groups [161]. Groups such as carboxyl, hydroxyl, sulphate, phosphate, ether and amino groups on agricultural wastes can act as binding sites [23, 27]. However, the application was limited as it performed poorly in some areas such as remediation of organic pollutants [29] and anionic contaminants [162]. Even though it works with other contaminants such as heavy metals and certain type of dyes, most of the works demonstrated that raw agricultural waste materials often exhibited low sorption capacity [163]. In addition, agricultural waste contributes to the release of soluble organic compounds in water [27, 164] bringing in secondary pollution. Due to this, it seems justified for agricultural waste to be modified for better application. Various options of modification either physically or chemically have been explored by a number of researchers in an effort to address the shortcoming of utilizing raw agricultural wastes [8, 165].

## 2.11 Modification of Agricultural Waste

Pretreatment of lignocelluloses materials such as agricultural waste utilizing a base solution has been demonstrated by many works to be efficient [165, 166] and has been a favorable method in improving the surface properties of plant waste [167, 168]. Washing with a base solution could help in improving sorption capacity of lignocellulosic material in many ways:

- i. Causes carboxylic groups on the cellulose surface bare to convert  $H^+$  type of functional groups into  $Na^+$  type allowing the cations to react more easily [169].
- ii. Breaks down the complex lignin structure thus allows more cellulose and hemicellulose available for binding activities [166].
- iii. Turns the less active ester groups into active carboxyl groups via hydrolization and saponification reaction. The simplified reaction of hydrolization [170] and saponification [171] could be describes in Eqs. 2.1 and 2.2 respectively, where R represents all the components in the biomass.



Apart from the above, base treatment of lignocellulosic material is also responsible for increasing a surface area, lowering the degree of polymerization, separation of structural linkages between lignin and carbohydrates and disruption of the lignin structure [170]. In addition, extraction with diluted caustic soda solutions at mild conditions may provide stability to the material by removing soluble substances with low molecular weight [168]. However, the concentration of base solution applied needs to be considered seriously as the marginally high concentration of the base solution used may damage the adsorbent structure thus reduce effectiveness [172].

Raw agricultural waste also proves to have less affinity to remove chemically stable emulsified oil in wastewater [29], thus modification of raw waste seems necessary to boost its performance. Some satisfactory findings made on applying cationic surfactant modified adsorbent for oil [19, 21, 22, 29] and dye removal [32, 162, 173] prompted us to consider the similar technique of treatment. Even though it may cause additional cost of processing, improving in sorption capacity and the versatility to work with different contaminants may compensate that. In an effort to better understand the concept of solid surface-cationic surfactant modification, the knowledge of surfactant chemistry and the adsorption mechanism of surfactant at liquid solid interface are greatly required

## **2.12 Chemistry of Cationic Surfactant**

Surfactant molecules are composed of a strongly hydrophobic group combined with a strongly hydrophilic group. The hydrophilic group is strongly polar or charged referred as the ‘heads’ meanwhile the hydrophobic group is a non polar group known as ‘tails’. Therefore, they are soluble in both organic solvents and water [174]. Surfactants are classified according to their head groups as anionic, cationic, nonionic, and zwitterionic(dual charge) [174, 175]. Surfactants are dissolved in water and exist as a monomer at lower concentration. As the surfactant concentration increases, the monomers will form self assembled aggregates which are known as micelles. The micelles vary in size and shape, but are commonly rough surfaced spheres with aggregation numbers at the order of 50-100. The surfactant concentration at which micelles begin to form is known as the critical micelle concentration or CMC. In short, a surfactant exists as a monomer at the concentration below CMC or as micelles

at the concentration above CMC [174, 176]. Cationic surfactants consist of positively charged head group and hydrophobic tails group thus allowing it to interact on negatively charged solid surface. Different types of cationic surfactants and their CMC are shown in Table 2.8 and a schematic diagram of cationic surfactant monomer and micelles is shown in Fig. 2.1 where the black circles represent the positively charged surfactant heads (hydrophilic moieties) and the black curved lines represent the surfactant tails (hydrophobic moieties).

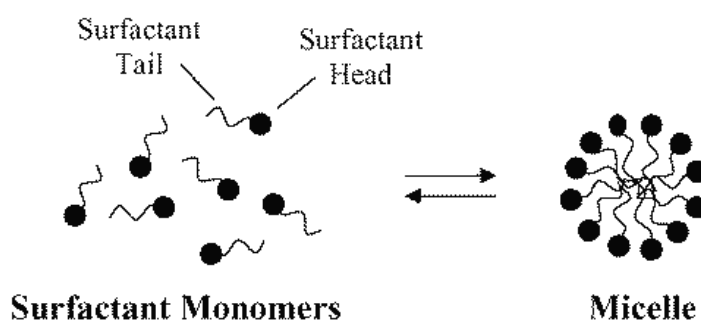


Figure 2.1. Schematic illustration of a surfactant monomer and a micelle structure in aqueous solution [177].

Table 2.7. Characteristic of some cationic surfactant [176]

Surfactant name	Structural formula	Acronym	cmc (mM)	cmc (mM) 10 mM salt
Cetyltrimethylammonium bromide	$\text{C}_{16}\text{H}_{33}\text{N}^+\text{Me}_3\text{Br}^-$	CTAB or HTAB	0.9	0.15
Cetyltrimethylammonium chloride	$\text{C}_{16}\text{H}_{33}\text{N}^+\text{Me}_3\text{Cl}^-$	CTAC	1.1	0.3
Cetylpyridinium bromide	$\text{C}_{16}\text{H}_{33}\text{N}^+(\text{C}_2\text{H}_5)_2\text{CHBr}^-$	CPBr	0.7	0.1
Cetylpyridinium chloride	$\text{C}_{16}\text{H}_{33}\text{N}^+(\text{C}_2\text{H}_5)_2\text{CHCl}^-$	CPC	0.8	0.15
Tetradecyltrimethylammonium bromide	$\text{C}_{14}\text{H}_{29}\text{N}^+\text{Me}_3\text{Br}^-$	MTAB, $\text{C}_{14}\text{TAB}$	3.6	2.1
Dodecyltrimethylammonium bromide	$\text{C}_{12}\text{H}_{25}\text{N}^+\text{Me}_3\text{Br}^-$	DTAB or $\text{C}_{12}\text{TAB}$	15.3	11
Dodecylpyridinium chloride	$\text{C}_{12}\text{H}_{25}\text{N}^+\text{Me}_3\text{Cl}^-$	DPC	14.7	10.5
Didodecyltrimethylammonium bromide	$(\text{C}_{12}\text{H}_{25})_2\text{N}^+\text{Me}_2\text{Br}^-$	DDAB	0.05	—
Benzyltrimethyloctylammonium bromide	$\text{C}_8\text{H}_{17}\text{N}^+\text{CH}_2\text{C}_6\text{H}_5\text{Me}_2\text{Br}^-$	BDOAB	—	—
Benzyltrimethyldodecylammonium bromide	$\text{C}_{12}\text{H}_{25}\text{N}^+\text{CH}_2\text{C}_6\text{H}_5\text{Me}_2\text{Br}^-$	BDDAB	5.6	—

Methyl groups ( $\text{CH}_3$ ) are abbreviated to M

## **2.13 Modification of Solid Surface with a Cationic Surfactant**

The adsorption of a surfactant at solid surface has been extensively studied by many researchers [176, 178-181] as the sorption of the surfactant will change the properties of the solid especially at the interface [182]. The orientation of a surfactant on the solid surface was largely depending on the concentration of the surfactant used [176, 179, 183].

### **2.13.1 Binding mechanism**

Understanding of cationic surfactant sorption mechanism on solid surface was crucial to study the interaction of modified surfactant with target pollutants. In general the sorption mechanisms of an ionic surfactant on solid surface involve both ion exchange and hydrophobic bonding [176, 178, 181]. As illustrated in Fig. 2.2, Alkan et al. [184] suggested that, at the concentration of ionic surfactant well below CMC, surfactant monomers are ion pairing with head-groups in contact with the surface to form incomplete monolayer and the surface excess can be determined by the surface charge. As the concentration of a surfactant increases, a complete monolayer has been formed and the surface charge has been neutralized. With further increasing of bulk concentration of monomers, surfactant monomers then formed hydrophobic bonding, where the monomers previously adsorbed act as an anchors (nucleation sites) for the formation of incomplete bilayer on the solid surface (admicelle). Above the CMC, the formation of fully formed aggregates and saturation level of surface coverage was observed. Further increasing the surfactant concentration resulted in the increase in concentration of surfactant micelles, thus insignificant change was observed in the adsorption density [185]. Besides surfactant concentration, there were other factors that influence the behavior of the cationic surfactant-solid interaction such as structure of adsorbent itself, (i.e. porosity, ion exchange capacity, hydrophobicity), the properties of surfactant used, i.e. type of surfactant, head group, hydrocarbon chain length and others. [176, 178, 183].

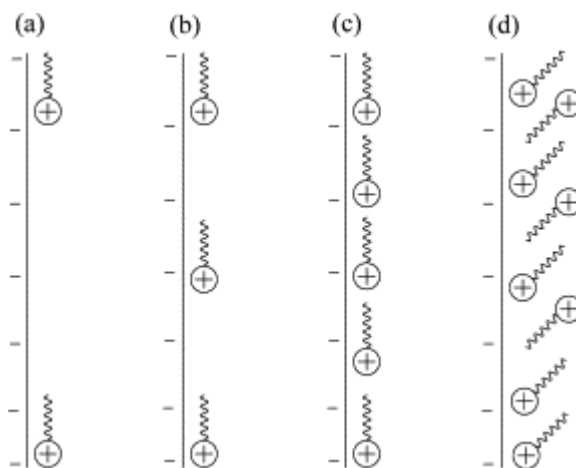


Figure 2.2. Adsorption of cationic surfactants onto perlite samples: (a) at low surface coverage, (b) of the point of zeta potential reversal, (c) at monolayer coverage, (d) at high surface concentration [184].

## 2.14 Surfactant Modified Adsorbent for Environmental Concern

The main reason for the modification of barley straw was that the raw agricultural waste possesses net negative surface charge [186] thus it has little ability to remove negatively charged anionic dye particles. In order to invert the surface charge, modification with a cationic surfactant was performed. Some earlier works found that the modification of adsorbents with cationic surfactants successfully reversed the surface properties of the adsorbents from negative charge to positive that is beneficial for removal of anionic contaminants [35, 36, 187]. Moreover, cationic surfactant modification also introduced alkyl chain hydrophobic medium, which may be partition/soluble low polarity contaminants into its layer [188, 189]. This was termed as adsolubilisation; a combination of adsorption and solubilisation [190]. Due to this, modification with a cationic surfactant was deemed as suitable for the raw adsorbent to be used for remediation of anions and organic pollutant contaminated wastewater.

Works on applicability of modified cationic surfactant for remediation of wastewater contaminated with emulsified oil and dyes were actively done, and some were reported in Table 2.8 and Table 2.9, respectively. From Tables 2.8 and 2.9, the summaries of some works on removal of emulsified oil and dyes could provide some brief ideas on the effectiveness of surfactant modified adsorbents. Overall, it can be concluded the effectiveness of utilizing surfactant modified adsorbents for emulsified

oil and anionic dyes wastewater remediation. The modification was largely performed on inorganic materials such as bentonite, zeolite and very little work on agricultural material and most of modification utilized the surfactant with long alkyl chain length. It is worth to mention that the reported adsorption efficiency has been achieved under specific experimental conditions and the extent of chemical modification made. Moreover, in the case of emulsified oil, the stability of emulsified oil (i.e either chemically or physically stabilized), the amount and type of emulsifier used will definitely influence the final removal performance. The reader is strongly encouraged to refer to the original articles for detailed information especially on experimental conditions.

Table 2.8. Sorption capacity for some of the surfactant modified adsorbent for low polarity compounds

Adsorbent	Base material	Cationic surfactant	Low polarity solution	Sorption Capacity (mg g <sup>-1</sup> )	Temp (°C)	Reference
HDTMA-Zeolite	zeolite	hexadecyltrimethylammonium bromide	phenol	0.76	20	[33]
				NA	40	
				NA	60	
			4-chlorophenol	12.71	20	
				9.40	40	
				7.03	60	
BDTA-Zeolite	zeolite	benzydimethylammonium bromide	phenol	1.30	20	[33]
				NA	40	
				NA	60	
			4-chlorophenol	6.41	20	
				6.55	40	
				8.12	60	
HDTMA-Bentonite	bentonite	hexadecyltrimethylammonium bromide	phenol	105	25	[188]
			p-chlorophenol	43.3		
			2,4-Dichlorophenol	44.3		
CTAB-Mont	Montmorillonite	cetyltrimethylammonium bromide	phenol	1.01	25	[191]
			m-NP	0.76		
			0-cresol	0.9		
Organoclay	Bentonite	quaternary amine	Valcool (Cutting oil)	0.14	21	[22]
Organoclay(30%) Anthracite (70%)	Bentonite	quaternary amine	Valcool (Cutting oil)	2.10 x10 <sup>-2</sup>	21	[19]
			Refinery Effluent	7.00 x10 <sup>-5</sup>		

Table 2.9. Sorption capacity for some of the surfactant modified adsorbent for anionic dyes

Adsorbent	Base material	Cationic surfactant	Dyes solution	Sorption Capacity (mg g <sup>-1</sup> )	Temp. ( °C )	Reference
MMT	Montmorillonite	no modification	Congo Red (CR)	10.2	30	[192]
OTAB-MMT		octyltrimethylammonium bromide		31.1		
DTAB-MMT		dodecyltrimethylammonium bromide		80		
CTAB-MMT		cetyltrimethylammonium bromide		229		
STAB-MMT		stealtrimethylammonium bromide		110		
CTAB- Bentonite	Bentonite	cetyltrimethylammonium bromide	Direct red	109.89	20	[31]
	Bentonite	cetyltrimethylammonium bromide		133.33	40	
				153.84	60	
Zeolite	Zeolite	no modification	Orange II	0.63	25	[193]
CPB- zeolite		cetylpyridinium bromide hexadecyl		3.62		
HDTMA - Zeolite		hexadecylammonium bromide		3.38		
MZ	clipnoptilolite	hexadecyltrimethylammonium bromide	Remazol Yellow	3.61	29.9	[194]
CPHDTMA	coir pith	hexadecyltrimethylammonium bromide	Acid brilliant blue	159	32	[195]
			procion orange	89		
CPHDTMA	coir pith	hexadecyltrimethylammonium bromide	Direct red 12	76.3	32	[162]
			Rhodamine B	14.9		
CPC-Carbon	Activated carbon (20-60 mesh)	cetylpyridinium chloride	Reactive black 5	99.2	20	[196]
	Activated carbon ( 8-20 mesh)	cetylpyridinium chloride	Reactive black 5	109.1		
	Activated carbon (4-8 mesh)	cetylpyridinium chloride	Reactive black 5	99.2		
DTMA-Bentonite	Bentonite	dodecyltrimethylammonium bromide	Acid Blue 193	1635.4	20	[197]
				2011.0	30	
				1732.0	40	
				4153.0	50	
HDTMA-Bentonite	Bentonite	hexadecyltrimethylammonium	Acid orange 10	143.06	25	[198]

## 2.15 Cationic Surfactant Selection

The selection of a cationic surfactant for modification is important as it will influence the properties of the modified adsorbent thus affecting the effectiveness. Due to that, it is necessary to gather enough information and have some ideas on the important characteristics of the cationic surfactant used and its implication toward the final application; as an adsorbent for removal of organic pollutants and anionic contaminants in wastewater. Among the properties of a cationic surfactant that may influence the characteristics of modified surfactant are discussed as follows:

### 2.15.1 Influence of surfactant chain length

The chain length of a cationic surfactant is important as the hydrocarbon chain does give an impact on the adsorption efficiency. Ersoy and Çelik [199] found that the surfactant chain length gave a significant effect on the ion exchange as well as hydrophobic interaction mechanism of surfactant adsorption on solid surface, where the sorption capacity was observed to increase with increasing the chain length. Hexadecyltrimethylammonium, HDTMA which having a relatively longer chain was found to adsorb more on solid surface than the shorter length of tridodecylmethylammonium, TDMA and dodecyltrimethylammonium bromide, DDTMA [199]. The surfactant with a longer hydrocarbon chain is also said to have more driving force for the aggregation thus dramatically reduce the solution CMC [178] which facilitates more surfactant adsorption.

A greater amount of surfactant adsorbed on the solid surface can be translated to the higher superiority of that particular adsorbent to remove organic contaminants. This was demonstrated by Wang and Wang [192] on removal of an anionic dye, congo red, (CR) by utilizing montmorillonite modified with a series of cationic surfactants which have different alkyl chain length, namely; octyltrimethylammonium bromide, OTAB (C8); dodecyltrimethylammonium bromide, DTAB (C12); cetyltrimethylammonium bromide CTAB (C16); stealtrimethylammonium bromide, STAB(C18). Fig.2.3 showed that the sorption capacity of CR generally increases with increased number of carbon atom of the surfactant from 8 to 16. However, the sorption capacity of CR on STAB was found decreasing; even though STAB has higher surfactant carbon atom

number of 18 and was suggested to be better suitability of CTAB to intercalate into montmorillonites galleries than STAB, hence increases the CR adsorption.

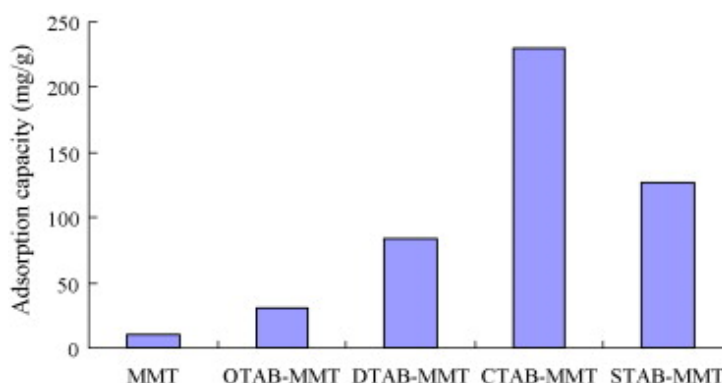


Figure 2.3. Effect of the surfactants (1.0 CEC used for each of the different surfactant types) on adsorption capacity of surfactant-modified MMT for CR [192].

The sorption study of nonanionic hydrophobic organic compounds; naphthalene and phenanthrene, using a clay modified with cationic surfactant of different alkyl chain length, such as hexadecyltrimethylammonium bromide, HDTMA (C16); tetramethylammonium bromide (TMA)(C4), and dodecyltrimethylammonium bromide, DTMA (C12); also showed the superiority of HDTMA-clay, where the sorption capacity was found to be higher than DTMA-clay and TMA-clay [200]. Gao et al. [201] also found the superiority of a longer alkyl chain in removing dichloromethane. In their work they found the different types of soil, black soil, yellow soil and red soil, modified with HDTMA showed a more tendency to remove chlorobenzene compared to modification of those soils with shorter alkyl chain cationic surfactant, TMA. A similar observation was reported by Akbal [202], who concluded that pumice modified with HDTMA (C16) exhibited better sorption of phenol and 4-chlorophenol in comparison with benzyldimethyltetradecylammonium chloride, BDTDA (C14).

Compared to shorter alkyl chain with the cationic cation in the interlamellar region isolated among each other, longer alkyl chain has an advantage of forming continuous organic phase on solid surface thus allowing more organic contaminants to be partition into the layer [200]. In terms of hydrophobicity, the longer chain was also

responsible for the contribution to the hydrophobic properties of the modified adsorbent [202]. Short hydrophobic tails cause hydrophilic heads to be composed of more than one similar charged ionic group, which restricts the occurrence of hydrophobic bonding between tails, thus preventing the formation of bilayer on the solid surface [203].

### 2.15.2 Influence of polar head group

The alkyl chain length of a cationic surfactant has a significant impact on its adsorption onto a solid surface and it is a great interest to evaluate the performance of different cationic surfactants which shared the same number of alkyl chain but with different polar head groups. Ghiaci et al. [204] reported that upon application of two modified zeolites for chromate removal, maximum adsorption capacity for CPB-Zeolite and HDTMA-Zeolite was reported at  $12.76 \text{ mmol kg}^{-1}$  and  $10.19 \text{ mmol kg}^{-1}$ , respectively. Higher removal of chromate for CPB-Zeolite than HDTMA-zeolite was due to the role of pyridinium group in the cationic surfactant adsorption. Jin et al. [193] also conducted an investigation comparing the effectiveness of the surfactant - zeolite with different types polar head in removing an anionic dye, Orange II. They found that the pyridinium head of cetylpyridinium bromide gave slightly better sorption capacity of  $3.62 \text{ mg g}^{-1}$  compared to  $3.38 \text{ mg g}^{-1}$  for hexadecylammonium bromide. The same trend was also shared by Widiastuti et al. [205], who found that CPC modified zeolite gave better removal of anionic contaminants, phosphate of  $45 \text{ mmol kg}^{-1}$  in greywater compared to  $42 \text{ mmol kg}^{-1}$  for HDTMA modified zeolite.

Praus et al. [179] found that cetylpyridinium (CP) was adsorbed more on montmorillonites (MMT) than cetyltrimethylammonium, CTA. CP was attached to the surface of MMT by electrostatic force and other interactions of pyridinium ring and  $\pi$ - $\pi$  interaction, whereas CTA was suggested to be adsorbed mainly by electrostatic force. This causes the CP to be more adsorbed on the solid surface. Size of hemimicelle aggregates also played a significant role. Bigger hemimicelle aggregates formed by planar polar head group of pyridinium ring were suggested to improve the hydrophobic interaction of cationic surfactant tail at the second layer compared to the smaller hemimicelle created by tetrahedral head group [204, 205].

### 2.15.3 Influence of cationic surfactant concentration

As discussed earlier, concentration of a cationic surfactant applied for modification of solid surface will greatly influence their characteristics. The cationic surfactant may retain on the solid surface as either incomplete monolayer, complete monolayer, patchy bilayer and bilayer, depending on the concentration of the cationic surfactant [203]. This is crucial as the effectiveness of targeted pollutant removal was very much related to the surfactant formation on the solid surface. Ghiaci et al. [204] studied the performance of zeolite modification at various concentrations of cationic surfactants; CPB and HDTMA for removal of chromate. At the concentration of the cationic surfactants of 0.5, 1.8 and 20 mmol kg<sup>-1</sup> the equivalent adsorption capacity of 3.44, 9.34 and 18.20 mmol kg<sup>-1</sup> (CPB loaded zeolite) and 3.72, 7.43 and 13.94 mmol kg<sup>-1</sup> for HDTMA loaded zeolite, respectively, was achieved. It can be seen that the adsorption capacity increases together with the increase in cationic surfactant concentration.

Widiastuti et al. [205] also observed that CPC and HDTMA loaded zeolites will generally result in the increase in phosphate removal at increasing surfactant loading. The concentration equivalent to 50, 100 and 200% of external cation exchange capacity (ECEC) produced the sorption capacity of 23, 45 and 12 mmol kg<sup>-1</sup> for CPC-zeolite and 11, 42 and 8 mmol kg<sup>-1</sup> for HDTMA-zeolite, respectively. The lower adsorption on surfactant loading at 200% ECEC was suggested to be due to the release of cationic surfactant into the aqueous solutions during the sorption experiment.

Cationic surfactant modification for adsorption is actually a complex system. Generally a common feature is the formation of monolayer at lower surfactant concentration and bilayer/admicelle at higher concentration (i.e. above CMC) [179, 185]. The creation of the bilayer is important as it creates a hydrophobic medium with less polar contaminant to partition [189]. Moreover, the net surface charge of solid changes to positive [36, 187] leading to favorable adsorption of anionic contaminants. Zhu and Zhu [206] observed the reduction of surface area as the loading of cationic surfactant (CTMA) on bentonite increases. The reduction in the surface area was due to the pores packed by CTMA. High density of the surfactant proved to be good as

contaminant partition was favorable at relatively high dense of hydrophobic layer [178, 207].

## **2.16 Section Summary**

This chapter demonstrates the environmental concern of the oily and dye wastewater. Several treatment methods used currently including physical, chemical and biological techniques provide some good results but each of them has shortcoming and there is always a room for improvement. The adsorption technique utilizing activated carbon was suggested as the best option available especially for dye wastewater treatment, but the cost of activated carbon and the difficulties in regeneration prompt the work to explore other low cost materials as a replacement of activated carbon. Agricultural waste seems a good candidate but exhibits lower affinity toward the emulsified oil and anionic dye removal. Hence, the modification of raw agricultural waste seems as necessary.

Literature to date has reported the successful story of using cationic surfactant modified adsorbents for low polar and anionic contaminant remediation. Various types of adsorbents ranging from inorganic material to synthetic material have been modified with various types of cationic surfactant. Nevertheless, the utilization of agricultural waste as a material was not extensively pursued. As far as the author is concerned, to date only a few agricultural waste materials were used, namely wheat straw and coconut coir pith. It was established that ion exchange and hydrophobic interaction are two main mechanisms taking place between solid surface and cationic surfactant. Agricultural waste was known as rich in negatively charged surface sites and the ability to biodegrade seems to suit nicely this purpose. The properties of a cationic surfactant used such as its alkyl chain length, the polar head properties and the concentration of surfactant applied were discussed by many works and have been found to significantly influence the characteristics of cationic surfactant retained on solid surface.

# 3

## EXPERIMENTAL

### 3.1 Introduction

This chapter describes the experimental procedures and analytical techniques that were used in this work. In general, this chapter can be split into three parts. The first part discusses the preparation of barley straw as an adsorbent material and its modification as well as physical and chemical characterization techniques. The second part explains the methodology of emulsified oil and dye removal in batch and continuous column modes. Batch experiments include the procedures for adsorbent selection, kinetics, isotherm and influences of physical and chemical parameters on oil and dye removal. Meanwhile the continuous column study describes column breakthrough. The method for preparation of emulsified oil and dye solution was also explained in detail here. The final part explains the theoretical aspect of batch adsorption and fixed bed column models. Batch adsorption models include kinetic and isotherm models. Meanwhile, some column models are introduced for breakthrough curve calculation. Error function technique was employed to evaluate the fitness of experimental data and proposed models. For the experiments that were repeated, standard error of the measurement was calculated to measure the deviation from the average value.

## 3.2 Adsorbent Preparation

**3.2.1 Materials** Barley straw, purchased from Stephen Bros Barley Straw Ltd., Australia, was repeatedly washed with water to remove dust and soluble impurities. Equal portions of straw and deionized water were ground in a blender (Breville Ikon 550, Italy) for about 15 min. Crushed straw was then separated from liquid and was again rinsed with distilled water until the washing was free of color. The straw was then dried overnight at about 65 °C and sieved using a sieve shaker (Retsch, AS 200. Germany) to obtain three different particle sizes, which were < 0.05 mm, 0.05 -1.18 mm and > 1.18 mm. The straw was then stored in a glass container and designated as raw barley straw (RBS) of respective sizes.

### 3.2.2 Treatment with base solution

Treating raw barley straw with an alkaline solution is important as the treatment is expected to increase the negatively charged active binding sites as well as to reduce the soluble organic compounds. In an effort to determine the optimum concentration of NaOH solution, 30 g of RBS was blended with 1 L of NaOH solution at various concentrations ranging from 0.001 M to 0.1 M and also with deionized water. The suspension was shaken by an orbital shaker at a speed of 170 rpm at 35 °C for 2 h and 4 h. The NaOH-treated straw was rinsed with distilled water until the washing was free from color. The straw samples were dried again in an oven at about 65 °C overnight. Then 0.2 g of the resulted straw from various concentrations of NaOH was mixed with 100 mL, 50 mg L<sup>-1</sup> of methylene blue, a cationic dye. The NaOH treated raw barley straw, which gave the highest removal of the cationic dye will be selected for further experiment and was labelled as RBS-N

### 3.2.3 Modification with cationic surfactant

The objective of treating straw with a cationic surfactant, hexadecylpyridinium chloride monohydrate (CPC) was to reverse its surface charge as well as to create a hydrophobic layer on the straw surface, which was vital in sorption of low polarity compounds as what has been thoroughly discussed in section 2.14 and 2.15. In brief, selection of long alkyl chain surfactant such as CPC is critical because short alkyl chain proves to be inferior in removing organic contaminants [199]. In addition, the planar polar head group in CPC can form bigger hemimicelle aggregates, allowing

them to be adsorbed more onto solid surface [204]. For adsorption of CPC onto straw surface, 30 g of RBS and RBS-N were blended with 1 L of CPC at various initial concentrations ranging from 0.08 to 5.30 mmol L<sup>-1</sup>. The suspension was shaken on an orbital shaker at 170 rpm at room temperature (25 °C) for 24 h. The CPC concentration was chosen in such a way as to represent the concentration well below and above the CPC critical micelle concentration (CMC). The treated barley straw was then separated from the liquid and washed with distilled water several times to remove surface retained surfactant. Finally, the treated barley straw was dried in an oven at 60 °C overnight. RBS and RBS-N modified with CPC were later labeled as surfactant modified barley straw, SMBS and base pretreated surfactant modified barley straw, BMBS, respectively.

### **3.3 Characterization of Adsorbent**

#### **3.3.1 Carbon and nitrogen content in straw**

The percentage of carbon and nitrogen content (C-N) of adsorbent sample was analyzed using a CHNS analyzer (Elementar, Vario Macro). The analysis was based on thermal conductivity detection for measuring carbon and nitrogen, after combustion and reduction. Glutamic acid and ASPAC44 were used as standard samples. The samples were analyzed twice under the similar conditions.

#### **3.3.2 Surface area**

The BET surface area of all samples was determined by N<sub>2</sub> adsorption at -196 °C using Autosorb (Quantachrome Corp. USA). All samples were degassed at 110-120 °C for 24 h, prior to the adsorption experiments. The BET surface area and pore volume were obtained by applying the BET equation and  $p/p_0=0.95$  to the adsorption data, respectively. The experiments were duplicated under the similar conditions.

#### **3.3.3 Microstructure and surface morphology**

Electron microscope images of adsorbent sample were taken using JEOL 6400 field emission scanning electron microscope (SEM) with an accelerating voltage 15.0 kV at various magnifications.

### 3.3.4 Water soluble minerals

The electrical conductivity (EC) method as suggested by Ahmedna et al. [208] was used to determine the content of water soluble minerals in the adsorbents. One percent (w/w) of straw in deionized water was mixed and stirred for 20 min and the electrical conductivity of the suspension was then measured using a Yokogawa SC82 conductivity meter (Yokogawa, Japan). The experiments were duplicated under the similar conditions.

### 3.3.5 Identification of functional groups

Fourier transform infrared (FT-IR) spectra were collected on a Perkin Elmer, Spectrum 100 spectrophotometer with an attenuated total reflectance (ATR) technique to identify the functional groups in the adsorbent sample. The spectrum was scanned four times from  $4000\text{ cm}^{-1}$  to  $650\text{ cm}^{-1}$  and corrected for background noise.

### 3.3.6 Elemental analysis

The amount of potassium, sodium, iron, arsenic and cadmium in adsorbent samples were analyzed by a commercial laboratory, A&A Scientific Resource, Shah Alam, Malaysia. For all the parameters, the sample was analyzed once based on the method described by APHA [209].

### 3.3.7 Acidic and basic surface groups

The Boehm titration method as described by Chen et al. [210] was used to measure the amount of acidic and basic surface groups. In each test, 0.5 g straw sample were suspended in 100 mL 0.05 N standard sodium hydroxide or hydrochloric acid solution. The suspensions were shaken in a closed container for 24 h, and then 5 ml of each filtrate was transferred and the excess of acid or base was titrated with HCl or NaOH. The experiments were conducted twice under the similar conditions.

### 3.3.8 Bulk density

The apparent (bulk) density was determined by the procedure described by Ahmedna et al.[208]. A 10 ml measuring tube was filled up with dry adsorbent sample and capped, tamped to a constant (minimum) volume by tapping on a table and weighed.

The experiments were duplicated under the similar conditions. The bulk density was calculated by:

$$\text{Bulk Density} = \frac{\text{weight of dry sample (g)}}{\text{volume of packed dry material (cm}^3\text{)}} \quad (3.1)$$

### 3.3.9 Cellulose, Hemicellulose and Lignin

The percentage of cellulose, hemicellulose and lignin in straw was determined by a series of experiments. Enzymatic Neutral Detergent Fiber (ENDF) was measured according to the method described by McQueen and Nicholson [211] and van Soest and Robinson [212]. Acid Detergent Fiber (ADF) according to the Association of Official Analytical Chemists (AOAC) method 973.18 [213] and the AOAC method 973.18C were used to determine the klason lignin [214]. Cellulose was computed as the difference between ADF and lignin, hemicellulose as the difference between ENDF and ADF and lignin is represented as klason lignin. The experiments were duplicated under the similar conditions and the analyses were performed at the Chemistry Centre, Perth, Western Australia.

## 3.4 Stability/Desorption of CPC

The stability and desorption of adsorbed CPC on raw straw was determined by dispersing 0.2 g SMBS in 100 mL of deionized water and other acid solutions, 0.01, 0.001 and 0.0001 M HCl for 6 h. The desorbed CPC was then measured using a UV/Vis spectrophotometer (Jasco V-670 spectrophotometer, Japan) at the maximum absorption of 257 nm.

## 3.5 Experimental Studies of Emulsified Oil Removal

### 3.5.1 Batch adsorption studies

Preliminary batch adsorption tests were conducted at room temperature (25 °C) by mixing RBS, RBS-N, SMBS and BMBS with emulsified CO at 10 g L<sup>-1</sup> for a period of 5 h. The rationale of conducting this experiment is to determine the suitability of the prepared adsorbents for removal of emulsified oil from aqueous solution. The adsorbent not giving a significant oil removal will be phased out. A similar batch adsorption experiment was repeated for emulsified SMO. A control test with no

adsorbent material was also carried out to determine the adsorption of emulsified oil effluent due to other factors.

### 3.5.2 Batch kinetic studies

As for batch kinetic study, it was conducted by agitating 10 g L<sup>-1</sup> of BMBS and synthetic CO or SMO emulsified oil at varying concentrations ranging from 1000 to 4500 mgL<sup>-1</sup>. A solution was withdrawn at preselected time for oil analysis.

### 3.5.3 Batch isotherm studies

An adsorption isotherm study was conducted to indicate the distribution of adsorbate molecules between liquid and solid phase. A batch isotherm study was performed by mixing adsorbent with the emulsified oil solution at five different dosages ranging from 0.1 to 1.3 g while keeping other parameters such as pH, concentration of emulsified oil solution, and stirring speed at constant. The sample was withdrawn for analysis once at equilibrium

### 3.5.4 Batch equilibrium studies

The effects of experimental parameters such as solution pH, adsorbent particle size and temperature were also investigated by varying one parameter above while keeping the others at constant values. The sample was withdrawn for analysis once at equilibrium

### 3.5.5 The parameters of batch experiment

Throughout the experiment (unless otherwise stated), an orbital shaker (B.Braun, Certomart, UK) was used to agitate the sample and pH of the solution was measured using Hanna HI 9811 pH meter (Hanna, Italy). As for the operating variables; original pH of CO solution at 7.5 and SMO at 7.3 was used. The volume of emulsified oil solution was set at 100 ml. Agitation speed, temperature, size and dosage of adsorbent were fixed at 170 rpm, 25 °C, 0.50-1.18 mm and 1.0 g, respectively, for all the experiments unless mentioned elsewhere. The experiments were repeated under the similar conditions and the average values were used in calculations.

### 3.5.6 Leaching/desorption experiments

In order to investigate the leaching/desorption of oil from the spent BMBS, The canola and mineral oil loaded BMBS was dried at about 45 °C for 5 h. One gram of the resulting straw was then dispersed into a flask that was filled with 100 mL deionized water. The suspension was then shaken at 170 rpm. Three samples were prepared and each water sample of the flasks was withdrawn at 1, 5 and 24 h, respectively. The sample was later measured for desorbed oil. The experiment was run twice under the same conditions and the mean/average of the results was presented.

### 3.5.7 Breakthrough studies of fixed bed column

Fixed bed column studies were conducted using Perspex columns of 2.9 and 12.5 cm in diameter and length, respectively. The experimental setup is shown in Fig. 3.1. In each run, 5 g of the prepared adsorbent, which was found to give 8 cm of bed height, was packed into the column. To support the adsorbent and to ensure the homogeneous distribution of the feed solution, top and bottom of the column was filled with 1.5 cm in bed height of glass beads (0.2 cm in diameter). The column was charged with emulsified CO wastewater in the up flow mode by a Cole Palmer Masterflex peristaltic pump with size 14 silicon tube to maintain a volumetric flow rate at 7.0 mL min<sup>-1</sup>. Samples of column effluent were collected at certain time intervals and were analyzed for remaining oil. The experiment was stopped when the adsorbent in the column were saturated with the oil, i.e the final oil effluent approaches the concentration as the same as influent (feeding solution). A similar fixed bed column experiment was repeated for emulsified SMO. The column study was conducted at room temperature of about 25 °C and original pH of CO solution at 7.5 and SMO at 7.3. The feeding concentration of emulsified CO and SMO was 1030 mg L<sup>-1</sup> and 990 mg L<sup>-1</sup>, respectively. Experimental control tests without addition of adsorbent material were also conducted to determine the possibility of emulsified oil removal due to the other factors. Only single experimental run was performed for all the straw-emulsified oil system.

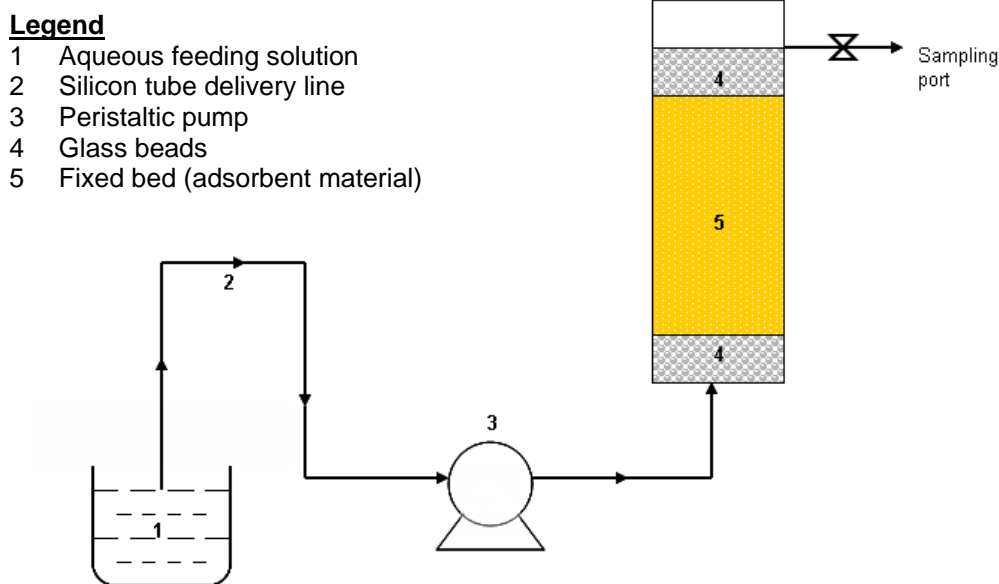


Figure 3.1. Schematic diagram of fixed bed column study

### 3.5.8 Preparation of emulsified oil solutions

Canola oil of unknown purity and standard mineral oil of 100% purity were obtained from Coles, Australia and Sigma-Aldrich, USA, respectively. A stock solution of emulsified canola oil wastewater (CO) was prepared by mixing 11.5 g of canola oil with 1 L of water and 12.5 g of non ionic emulsifier (Colgate-Palmolive, Australia). The mixture was then stabilized in a blender (Breville Ikon 550, Italy) at high speed for 15-20 min. The same procedure was repeated for the preparation of emulsified standard mineral oil (SMO). The resulted solution is milky white, which exhibits the characteristic of chemically stabilized solution [49].

### 3.5.9 Measurement of oil in water

The oil in water was measured using a partition–infrared method; InfraCal CVH, TOG/TPH Analyzer (WILKS Enterprise Inc, USA) and the emulsified oil from aqueous solution was extracted using an oil extraction solvent, S-316 (HORIBA Ltd, Japan). The partition infrared method was chosen due to its capability of measuring the low concentration of oil (i.e below 10 mg L<sup>-1</sup>) and ability to address the excessive evaporation of extraction solvent which subsequently reduces the losses of low

molecular weight compounds. The amount of emulsified oil adsorbed by the adsorbent at time  $t$ ,  $q_t$  ( $\text{mg g}^{-1}$ ), was computed using the following expression:

$$q_t = \frac{C_o - C_t}{m} V \quad (3.2)$$

where  $C_o$  and  $C_t$  are oil concentrations in  $\text{mg L}^{-1}$  initially and at time,  $t$ , respectively.  $V$  is the volume of emulsified oil solution in liter (L) and  $m$  is the weight of straw in gram (g).

### **3.6 Experimental Studies of Dye Wastewater**

#### **3.6.1 Preliminary batch adsorption studies**

Preliminary batch adsorption experiments were conducted at room temperature ( $25^\circ\text{C}$ ) by mixing  $2 \text{ g L}^{-1}$  of RBS, RBS-N, SMBS and BMBS with dye solution of Acid Blue, AB40; Reactive Blue 4, RB4; and Reactive Black 5, RB5, at a period of 8 h. The rationale of conducting these experiments is to determine the suitability of the prepared adsorbents for removal of dyes from aqueous solution. The adsorbent not giving a significant dye removal would be phased out. A batch control test with no adsorbent material was also performed to determine the adsorption of dye effluent due to other factors.

#### **3.6.2 Batch kinetic studies**

As for batch kinetic study, it was conducted by agitating  $2 \text{ g L}^{-1}$  of SMBS or BMBS with the studied dye solution at varying concentrations. Approximately 3 mL of the solution was drawn at preselected time for dye analysis. The concentration of dye in water was later analyzed.

#### **3.6.3 Batch isotherm studies**

Similar to the adsorption of oil, a batch isotherm study was performed by mixing the adsorbent with a 100 mL of dye solution at five different dosages ranging from 0.1 to 1.0 g while keeping other parameters such as pH, concentration of dye solution, and stirring speed constant. The sample was withdrawn for analysis once at equilibrium.

#### 3.6.4 Batch equilibrium studies

The effects of experimental parameters such as solution pH, adsorbent particle size were also investigated by varying one parameter above while keeping the other parameters unchanged. A batch isotherm study was performed by mixing adsorbents with the dye solutions at different dosages ranging from 0.4 to 1.6 g while keeping other parameters at constant values. The sample was withdrawn for analysis at 60 min. The equilibrium time chosen was based on the kinetic experiment.

#### 3.6.5 Leaching/desorption experiments

Desorption of AB40, RB4 and RB5 from spent SMBS and BMBS samples was conducted by dispersing the dye loaded straw at a dosage of 1 g L<sup>-1</sup> with deionized water in different pH of buffer solution at 3, 5, 8 and 11.

#### 3.6.6 Batch experimental operational parameters

Throughout the experiment (unless otherwise stated), an orbital shaker (B.Braun, Certomart, UK) was used to agitate the sample and the pH of solution was measured using a Hanna HI 9811 pH meter (Hanna, Italy). As for the operating variables; original pH of dye solution (AB40: 5.8, RB4: 5.6, RB5: 5.0) was used. The volume of dye solution was set at 50 ml. Agitation speed, temperature, size and dosage of adsorbent were fixed at 170 rpm, 25 °C, 0.50-1.18 mm and 0.1 g, respectively, for all the experiments unless mentioned elsewhere. For all the studies, a control with no adsorbent was also set up to determine the adsorption of dye due to other factors. Experiments were duplicated under the similar conditions and the average values were used in calculations.

#### 3.6.7 Breakthrough studies of fixed bed column

A same fixed bed column described in Fig.3.1 was also used for treatment of dye wastewater. In brief, 5 g adsorbents were packed into the Perspex column with glass beads placed at the top and bottom of the column. The dye wastewater of AB40 was feed in a up-flow mode at a volumetric flow rate of 10 mL min<sup>-1</sup>. The samples of column effluent were collected at certain time intervals and were analyzed for remaining dye in solution. The experiment was stopped when the dye concentration of column effluent approaches the feeding solution concentration, an indication of the

adsorbent in the column being exhausted. A similar set-up was repeated for RB5. The column study was conducted at room temperature of about 25 °C and original AB40 solution at pH 5.8 and RB5 at 5.0 were used. The initial concentration of feeding solution of both dyes was set at 50 mg L<sup>-1</sup>. Similar to the column experimental studies for emulsified oil, a control test was also conducted for dye effluent to determine the adsorption due to other factors. For each dye, single experimental run was conducted.

### 3.6.8 Preparation of dye wastewater

The stock solutions of dyes at 200 mg L<sup>-1</sup> of acid blue 40 (AB40, 473.0 g mol<sup>-1</sup>), reactive blue 4 (RB4, 637.4 g mol<sup>-1</sup>) and reactive black 5 (RB5, 991.8 g mol<sup>-1</sup>) were prepared by dissolving 0.2 g of respective dye with deionized water and making up to 1 L in volumetric flasks. The stock solution was later diluted with deionized water to the desired concentration. All the dyes used were obtained from Aldrich, USA.

### 3.6.9 Measurement of dyes in wastewater

Dye and adsorbent material were separated by filtering the dye solution–adsorbent suspension using a syringe filter with 25 mm filter disc (Acrodisc, USA). The concentrations of dye samples were measured using a UV/Vis spectrophotometer (Spectrometry 20 genesis). The measurement of AB40, RB4 and RB5 was performed at the maximum absorbance of 615 nm, 599 nm and 598 nm, respectively. The amount of dyes adsorbed by the adsorbent at time *t*, *q<sub>t</sub>* (mg g<sup>-1</sup>), was computed using the following expression:

$$q_t = \frac{C_o - C_t}{m} V \quad (3.3)$$

where *C<sub>o</sub>* and *C<sub>t</sub>* are dye concentrations in mg L<sup>-1</sup> initially and at time, *t*, respectively. *V* is the volume of dye solution in liter (L) and *m* is the weight of straw in gram (g).

## 3.7 Batch Experimental Model

### 3.7.1 Kinetic models

The dynamic dye or oil adsorption was simulated using pseudo-first order and pseudo-second-order models. The pseudo-first-order model is used to describe the reversibility of the equilibrium between the liquid and solid phases. The nonlinear

equation of the Lagergren pseudo-first-order model can be expressed by Eq. 3.4 [215].

$$q_t = q_e (1 - e^{-k_1 t}) \quad (3.4)$$

The pseudo-second-order equation assumes that rate limiting step might be due to the chemical adsorption and the non linear form of the equation can be expressed by Eq. 3.5 [216].

$$q_t = \frac{q_e^2 k_2 t}{(1 + q_e k_2 t)} \quad (3.5)$$

In Eqs.3.4 and 3.5,  $k_1$  and  $k_2$  represent the rate constant of the pseudo first order and second order, respectively, whereas  $q_e$  and  $q_t$  are the amount of dye or oil adsorbed at equilibrium and at time  $t$ , respectively.

### 3.7.2 Kinetic diffusion models

For a solid-liquid sorption, the resistance to mass transfer can be described by two processes, the resistance due to external mass transfer through the particle boundary layer/film diffusion and the resistance due to intraparticle diffusion [103] or a combination of more than one [156]. The diffusion study is significant as the pseudo first order and second order models failed to explain the diffusion mechanism during the adsorption process [217]. Although the kinetic studies help to identify the sorption process, predicting the mechanisms is required for design purposes [218]. For this, the Boyd kinetic diffusion model was employed to study the type of diffusion mechanism. The Boyd diffusion model [219] was applied to predict the actual slowest step involved in the adsorption process. The Boyd equation is expressed as follows:

$$F = 1 - \frac{6}{\pi^2} \sum_{n=1}^{\infty} \frac{e^{-n^2} B_t}{n^2} \quad (3.6)$$

and

$$F = \frac{q_t}{q_{\infty}} \quad (3.7)$$

where  $F$  represents the fraction of adsorbate adsorbed at any time  $t$  and is obtained by using Eq. (3.7),  $q_{\infty}$  is the amount of adsorbate adsorbed at infinite time ( $\text{mg g}^{-1}$ ),  $n$  is an integer and  $B_t$  is a mathematical function of  $F$ . The values of effective diffusion coefficients,  $D_i$  ( $\text{cm}^2 \text{s}^{-1}$ ) can be calculated using the following equation:

$$B = \frac{\pi^2 D_i}{r^2} \quad (3.8)$$

where  $r$  represents the radius of biosorbent (cm) by assuming spherical particles. Eq. (3.8) was proposed based on particle diffusion as the rate determining step. Substituting Eq. (3.6) in Eq. (3.7) simplifies to:

$$B_t = 6.28318 - 3.2899F - 6.28318(1 - 1.047F)^{1/2} \quad (3.9)$$

or

$$B_t = -0.4977 - \ln \left[ 1 - \frac{q_t}{q_{\infty}} \right] \quad (3.10)$$

Eqs 3.9 and 3.10 were used for the  $F$  value of 0 to 0.85 and 0.86 to 1, respectively [220]. The values of  $B$  can be obtained from the slopes of  $B_t$  versus time ( $t$ ). The linearity of the plots of  $B_t$  versus time ( $t$ ) could distinguish the type of diffusion controlled rate of sorption. A straight line passing through the origin suggests that the sorption processes are governed by particle-diffusion mechanisms; otherwise they are governed by film diffusion [221]. Beside, the effective diffusion coefficients ( $D_i$ ) could also be used, where  $D_i$  in the range of  $10^{-6} - 10^{-8} \text{ cm}^2 \text{s}^{-1}$ , film diffusion is said to be the rate determining step whereas  $D_i$  value in the range  $10^{-11} - 10^{-13} \text{ cm}^2 \text{s}^{-1}$  suggested pore diffusion as the rate determining step [222].

### 3.7.3 Isotherm models

The distribution of adsorbate between liquid and solid phases is generally described by the Langmuir [223] and Freundlich [224] adsorption isotherm models. Normally, an isotherm was obtained by measuring the changes in solution concentration after equilibrium has been reached at a constant temperature. The Langmuir isotherm model [223] is derived on the assumption of monolayer adsorption on a structurally

homogenous surface where there are no interactions between the molecules adsorbed on neighbouring sites, and is expressed as:

$$q = \frac{Q_{\max} bc_e}{1 + bc_e} \quad (3.11)$$

Where,  $Q_{\max}$  is referred to the maximum adsorption capacity and  $b$  is a constant related to energy of adsorption.  $C_e$  represents the concentration of dye or oil solution at equilibrium. The Freundlich isotherm model [224] is an empirical equation which represents the multilayer adsorption on heterogeneous surfaces where there are interactions between adsorbed molecules and is expressed as:

$$q = K_F c_e^{1/n} \quad (3.12)$$

Where,  $K_F$  is related to adsorption capacity and  $n$  is an empirical formula that varies with degree of heterogeneity.

### 3.8 Fixed Bed Column Models

The overall performance of a fixed bed column is judged through its service time, known as column breakthrough. The breakthrough curve is expressed as a column effluent concentration over time. The breakthrough time appearance and breakthrough curve shape are important characteristics for determining the operation and dynamic response of an adsorption column [225, 226]. A column is considered to be saturated and its operation can be stopped when it reaches breakthrough time and the breakthrough curve shape meanwhile indicates the performance of the column system. Generally, there are three types of breakthrough curves that can be observed as shown in Fig. 3.2 and they display: (a) poor adsorption, (b) normal adsorption and (c) strong adsorption. The breakthrough curve often observed in adsorption studies is the normal adsorption curve or the ‘S’ shape.

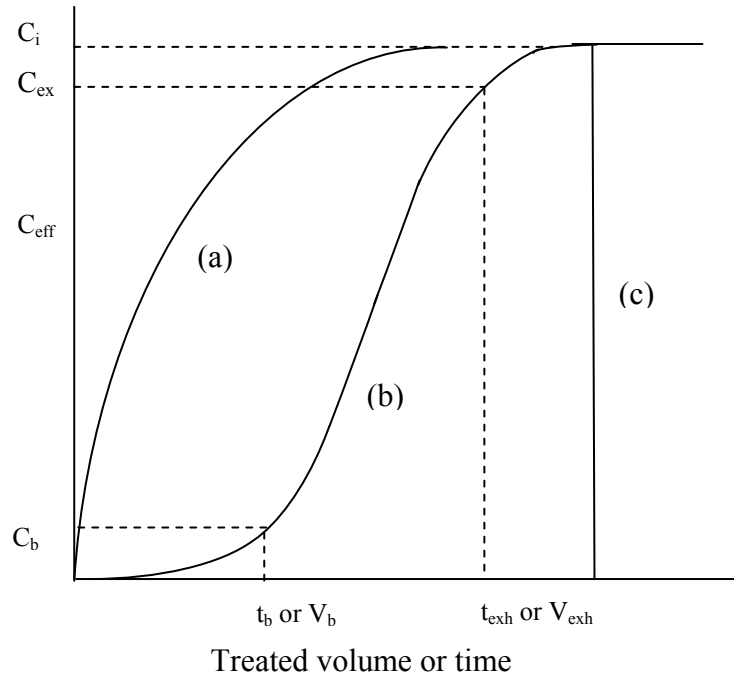


Figure 3.2. Examples of breakthrough curves: (a) poor adsorption (b) normal adsorption and (c) strong adsorption [227].

In Fig. 3.2,  $C_{\text{eff}}$  is representing the effluent concentration,  $t_b$  and  $V_b$  are referred as the breakthrough time and breakthrough volume, respectively; column exhaustion volume and column exhaustion time is denoted by  $V_{\text{exh}}$  or  $t_{\text{exh}}$  where  $C_{\text{ex}}$  is referred as corresponding column exhaustion concentration. Meanwhile,  $C_i$  is the initial concentration. In order to understand the behavior of adsorption of oils and dyes under column operation, the experimental data obtained were mathematically analyzed by using widely used column models of either the Thomas or Yoon-Nelson equations.

### 3.8.1 Thomas model

The Thomas solution [228] is one of the most general and widely used methods in column performance theory. The model assumes the Langmuir kinetics of adsorption-desorption and no axial dispersion derived with the adsorption and the driving force obeys the second order reversible reaction kinetics [229]. The expression by the Thomas model for an adsorption column is given as follows:

$$\frac{C_t}{C_i} = \frac{1}{1 + \exp\left[\frac{K_{Th}(q_o m - C_i V_{eff})}{Q}\right]} \quad (3.13)$$

where  $k_{Th}$  is the Thomas rate constant ( $\text{mL min}^{-1} \text{mg}^{-1}$ ),  $q_o$  is the equilibrium adsorbate uptake ( $\text{mg g}^{-1}$ ),  $Q$  is the volumetric flow rate ( $\text{mL min}^{-1}$ ),  $V_{eff}$  is the effluent volume ( $\text{mL}$ ) and  $m$  is the weight of adsorbent in the column ( $\text{g}$ ). A non linear plot of effluent concentration ( $\text{mg g}^{-1}$ ) versus sampling time ( $\text{min}$ ) was employed to determine the values of  $k_{Th}$  and  $q_o$  from the intercept and slope, respectively.

### 3.8.2 Yoon-Nelson model

The Yoon-Nelson model [230] is considered the less complicated column model as it requires no detailed data concerning the characteristics of adsorbate, the type of adsorbent, and the physical properties of adsorption bed. It was developed based on the assumption that the rate of decrease in the probability of adsorption for each adsorbate molecule is proportional to the probability of adsorbate adsorption and the probability of adsorbate breakthrough on the adsorbent [231]. The non linear form of the Yoon-Nelson model for a single component system is expressed by [232]:

$$\frac{C_t}{C_i} = \frac{1}{1 + \exp[k_{YN}(\tau - t)]} \quad (3.14)$$

where  $k_{YN}$  is the Yoon-Nelson rate constant ( $\text{L min}^{-1}$ ) and  $\tau$  is the time required for 50% adsorbate breakthrough ( $\text{min}$ ) based on the Yoon-Nelson model. A non linear plot of effluent concentration ( $\text{mg g}^{-1}$ ) versus sampling time ( $\text{min}$ ) was employed to determine the values of  $k_{YN}$  and  $\tau$ .

### 3.9 Best Fitting Model Estimation

There are many considerations being used to predict the best fit of models. In this work, the best fit of the equation to the experimental data was determined in two methods; regression correlation coefficient values ( $R^2$ ) and error estimation technique.  $R^2$  value closest to unity is assumed to provide the best fit meanwhile for the error function, the lesser value of the error indicates the better fit. The error estimation employed is Marquardt's percent standard deviation (MPSD) [233] and is given below:

$$\text{MPSD} = 100 \left( \sqrt{\frac{1}{p-n} \sum_{i=1}^p \left[ \frac{(q_{e,\text{meas}} - q_{e,\text{calc}})}{q_{e,\text{meas}}} \right]^2} \right) \quad (3.15)$$

Where  $p$  is the number of experimental data and  $n$  is the number of the parameters in the model equation.  $q_{e,\text{meas}}$  and  $q_{e,\text{calc}}$  are referring to the experimental and calculated values from the model equation, respectively.

### 3.10 Standard Error of The Measurement (SEM)

The error of measurement was calculated to express the confidence in mean value for the analysis that was repeated. For this, a standard error of the mean (SEM) was applied. The SEM estimates the amount that an obtained mean may be expected to differ by chance from the true mean. The SEM mean is designated as ( $\sigma_M$ ) and can be expressed by equation[234]:

$$\sigma_M = \frac{\sigma}{\sqrt{N}} \quad (3.16)$$

where  $\sigma$  represents the standard deviation of the original distribution and  $N$  is the sample size.

# 4

## MODIFICATION AND CHARACTERIZATION OF STRAW SURFACE

### 4.1 Introduction

This section describes the treatment of straw surface and the characterization of raw and modified straws. Two different types of treatments with base solution and cationic surfactant were used in this study. The aim of the base treatment was to increase acidic surface binding sites, which in our case is important as it is expected to increase cationic substance binding onto the surface. For this purpose, several sodium hydroxide solutions at different concentrations were used and the resulted straws were then tested with a cationic dye, methylene blue, to determine the effectiveness of the treatment. The treatment with a cationic surfactant was conducted on raw straw and base treated straw. Surfactant concentration below and above the critical micelle concentration, CMC, was used to determine the influence of the concentration on the sorption of CPC onto the straw surface. The sorption mechanism of the surfactant onto straw surface was thoroughly discussed in this chapter. Meanwhile the characteristics of raw and modified straws and the stability of the CPC adsorbed on the straw surface were discussed. The spectroscopic and various physicochemical properties of raw and modified straws were determined as adequate information of the prepared samples is significant to establish the

characteristics of the adsorbent and more important to study the influence of the modification to the straw properties for the sorption. Desorption of CPC from the modified straw was also tested in various types of solvents in an effort to determine the stability and the possible mechanism of sorbed CPC onto straw surface. For the experiments that were performed more than once, a standard error of the measurement for the analyses was calculated using equation 3.16 and the results were presented in appendix A.

## 4.2 Treatment with Base Solution

Base treatment of straw is expected to enhance the affinity towards the sorption of a cationic surfactant. Tan and Xiao [235] reported that the base hydrolyzation of a lignocellulosic material increased the formation of carboxyl group which is responsible for binding activities. Many works also shared the similar conclusion. It was found that the lignocellulosic based adsorbents treated with sodium hydroxide gave greater adsorption capacity than unmodified adsorbents [170, 236]. However, the usage of excessive concentration of base solution may damage the straw structure as reported by Xie et al. [172]. Hence, the suitable concentration must be determined.

The straws that was treated with various base solutions at varying concentrations were tested for a cationic dye, methylene blue, to find its effectiveness. Due to the nature of methylene blue with positively charge particle upon dissolution in aqueous solution, the straw that is able to remove more methylene blue is assumed to possess higher amount of negatively charged binding sites. From Figure 4.1, the removal capacity of methylene blue for the concentration of NaOH of 0.025, 0.05 and 0.1 N was 40.8, 50.3 and 40.0 mg g<sup>-1</sup>, respectively at a shaking time of 2 h. For shaking duration of 4 h, adsorption capacity of 43.4, 49.2 and 46.0 mg g<sup>-1</sup> were observed, respectively. For the straw that was only soaked in deionized water, adsorption capacity was found lower at 35.5 and 38.7 mg g<sup>-1</sup> for the shaking time of 2 and 4 h, respectively. In Fig. 4.1, it can be clearly observed that the adsorption capacity for methylene blue removal was the highest when the raw straw was treated with 0.05 N NaOH. It was also shown that the adsorption capacity for treatment duration of 2 and 4 h were about the same. Due to these factors, NaOH concentration of 0.05N and shaking time of 2 h were selected as treatment conditions for raw straw (RBS).

The lower adsorption capacity for the straw that was soaked with deionized water was further justified the necessity for base treatment. The base treated straw will later labelled as RBS-N and will be modified further with a cationic surfactant.

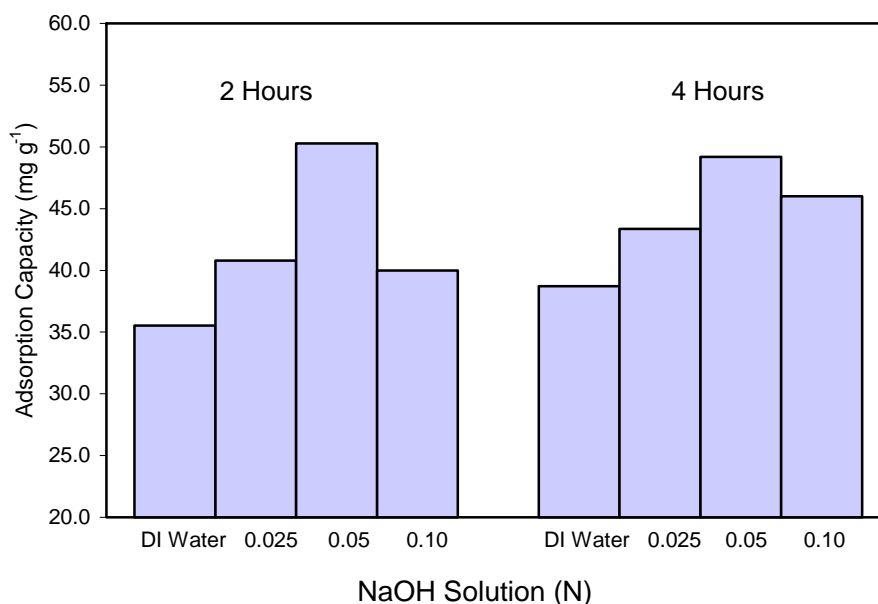


Figure 4.1. Effectiveness of NaOH treated raw barley straw for methylene blue 1 removal ([Dyes]:50 mgL<sup>-1</sup>; Shaking speed: 170 rpm; Dosage: 2 g L<sup>-1</sup>; 35 °C )

### 4.3 Modification with Cationic Surfactant

To understand the sorption mechanism and conformation of a surfactant to straw surface, the widely used surfactant depletion method was employed [183]. The result can be presented as the amount of surfactant adsorbed per gram of solid versus the equilibrium surfactant concentration at a constant temperature. The sorption of CPC presented in Fig. 4.2 generally showed that the sorption capacity of CPC increases with increasing equilibrium CPC concentration for both RBS and RBS-N. The dashed line in Fig. 4.2 represents the CMC for CPC in pure water in the range of 0.8 mmol L<sup>-1</sup> to 0.9 mmol L<sup>-1</sup> [176, 185]. It was observed that there are two main regimes on the adsorption isotherm; the first region of about 1.0 mmol CPC and below and the second region of 1.0 mmol and above. Fig. 4.2 shows that the surfactant sorption is at the maximum when the equilibrium surfactant concentration is equal to CMC. Generally, the region below CMC can be described as monolayer formation and admicelle or bilayer occurred at above the CMC level [178, 184, 203]. Higher adsorption capacity of RBS-N than RBS was

expected as the treatment with the base solution was observed to increase the affinity of straw surface for the binding of cation as discussed in the earlier section.

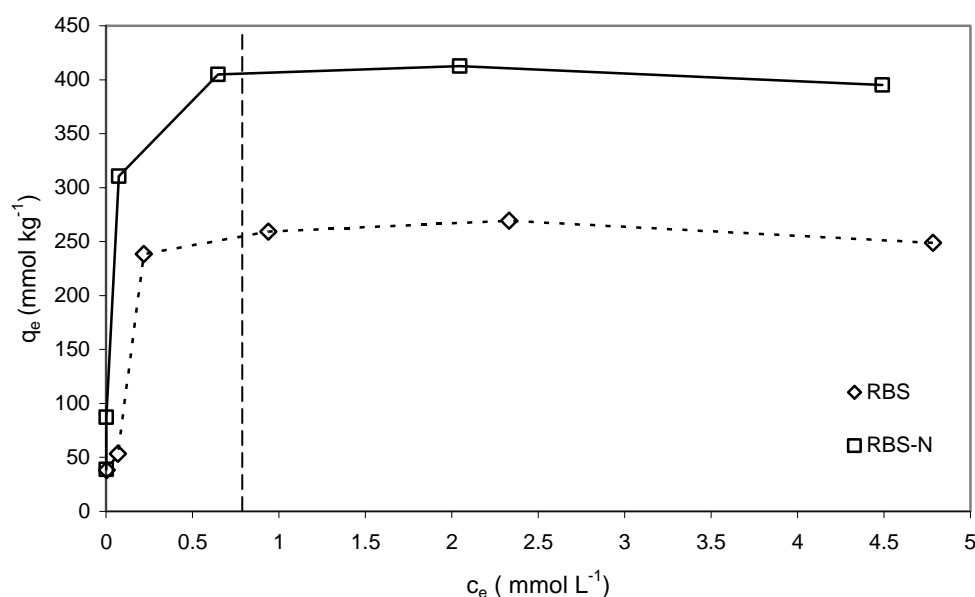


Figure 4.2. Sorption of CPC on RBS and RBS-N surface.

Dashed line indicates the CMC for CPC.

As discussed earlier in the literature review, due to the large polar group of the cationic surfactant, sorption generally occurs at the solid sorbent surface, with several possible mechanisms such as ion pairing and hydrophobic interactions [184]. To better explain the types of CPC formation on straw surface, the data from Fig. 4.2 could be reconstructed using log-log scale. This type of scale is favorable due to its applicability over a wider range of adsorption and surfactant concentration, and the plots generally have abrupt changes in slope with increasing surfactant concentration [176, 183]. Equilibrium adsorption data constructed on log-log scale was presented in Figs. 4.3a and 4.3b. Both log-log scale plots for SMBS and BMBS generally shown the similar trend, where the adsorption can be divided into four regions. The presence of four regions on the log-log scale plots was consistent with many other works done on surfactant adsorption over various types of solid surface [178, 183, 184, 203]. The four-region adsorption isotherm mainly occurs by adsorption of an ionic surfactant onto oppositely charged solid surface.

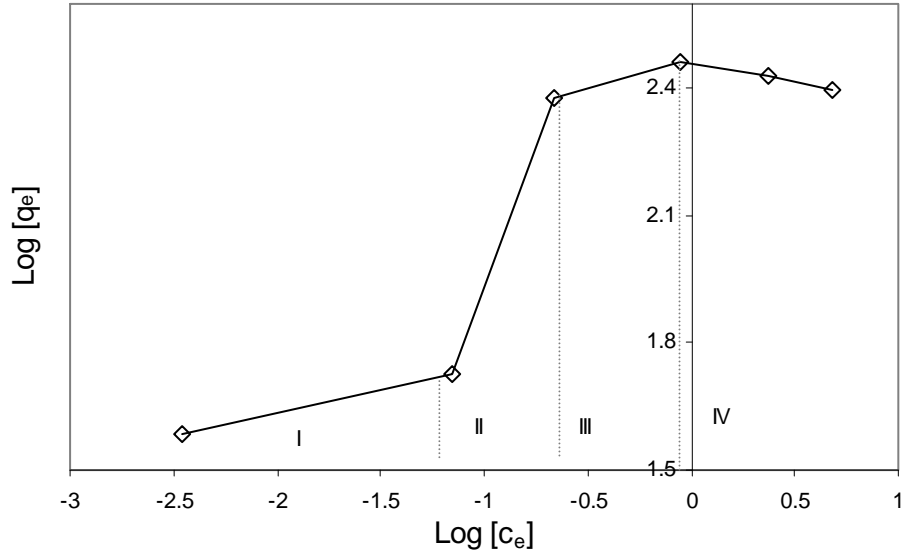


Figure 4.3a. Log - log scale SMBS

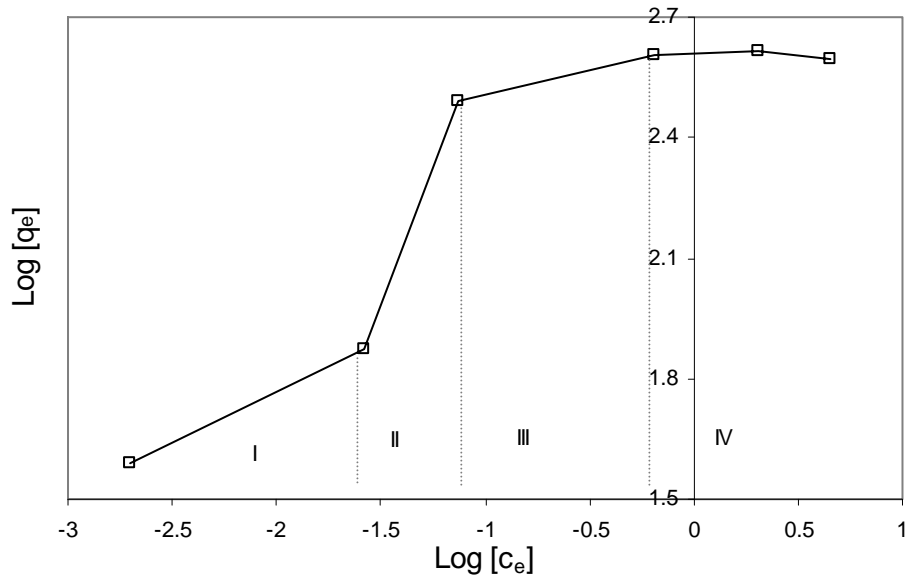


Figure 4.3b. Log - log scale BMBS

At low concentrations of CPC, region (I) generally represents the incomplete monolayer formation. The adsorption was observed to obey the Henry law [183, 203] where the sorption increases linearly with the increasing in CPC concentration. At the concentration of CPC well below CMC, the dominance sorption mechanism is ion exchange between surfactant monomers with the external cation of straw surface. Here the surfactant monomers were electrostatically adsorbed to the straw surface, with polar head-groups in contact with the surface. The same conclusion was also made by Ersoy and Çelik [199]

on adsorption of a cationic surfactant on clinoptilolite. The adsorption mechanism can be illustrated in Fig. 4.4, where  $M^+$  is exchangeable cation on the straw surface.

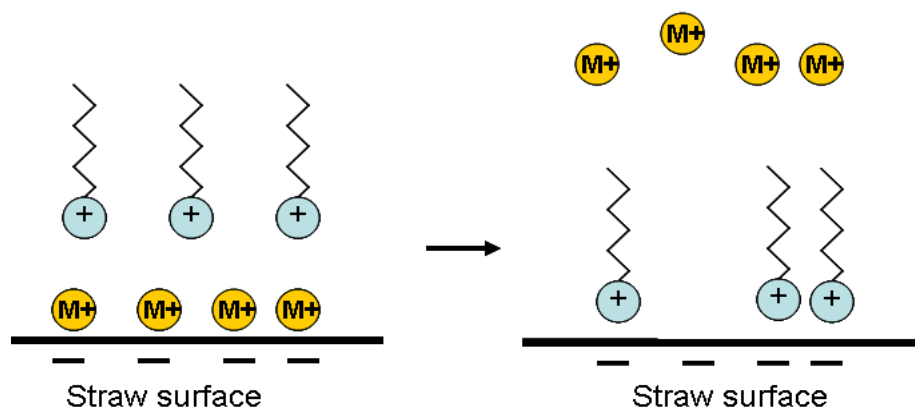


Fig.4.4a. Schematic illustration of ion exchange mechanism of the cationic surfactants at straw water interface

In region II, as surfactant concentration is increased, rapid increment of adsorption was observed. This was due to the strong lateral interaction between adsorbed monomers [176], resulting in the surface aggregation of the surfactant. In this region, the surfactant is formed as monolayer, bilayer or something in between [237], thus in some cases creating hydrophobic patches on the surface [238]. The formation of CPC on straw surface can be illustrated in Fig. 4.4b

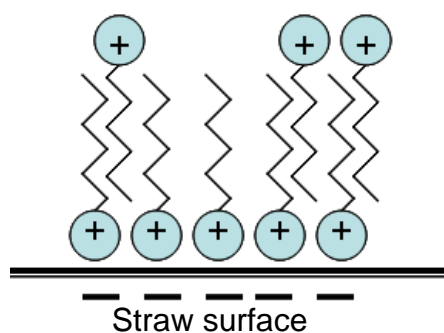


Fig.4.4b. Incomplete bilayer formation of CPC onto straw surface

Region III shows decreasing slope. The transition between regions II to III is thought to be due to neutralization of surface charge [176]. In region III, alkyl chain group that points towards the solution will form hydrophobic interaction with hydrocarbon group of

free surfactant monomers, thus resulting in the formation of aggregate cluster [183, 185, 203]. The adsorption mechanism can be illustrated in Fig. 4.4c

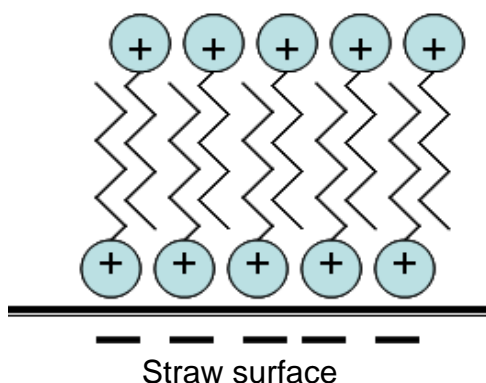


Figure 4.4c. A complete bilayer formation of CPC onto straw surface

Region IV is known as an plateau region where the increase in surfactant concentration only causes a marginal increase in adsorption. It can be observed that, the transition from region III to IV occurs at or near the CMC. At this stage, increase in the surfactant concentration does not give much impact as it only leads to increase in the concentration of surfactant micelles, thus little change will be observed in the adsorption density [185].

#### 4.4 Physicochemical Characteristics of Raw and Modified Barley Straw

The investigation of physical and chemical properties of raw and modified straws is important to establish the characteristics as well as to understand better the effect of modification made to the straw. Table 4.1 depicts some of the physical and chemical properties of RBS, RBS-N, SMBS and BMBS. Unless mentioned, all the analyses were performed for straw adsorbent size of 0.5-1.18 mm.

Table 4.1. Characteristics of raw and modified straw

Analysis	Unit	RBS	RBS-N	SMBS	BMBS
<sup>#</sup> Potassium	mg kg <sup>-1</sup>	ND<0.02	ND<0.02	-	-
<sup>#</sup> Sodium	mg kg <sup>-1</sup>	ND<0.01	29.24	-	-
<sup>#</sup> Iron	mg kg <sup>-1</sup>	45.8	20.55	-	-
<sup>#</sup> Arsenic	mg kg <sup>-1</sup>	ND<0.001	0.05	-	-
<sup>#</sup> Cadmium	mg kg <sup>-1</sup>	0.1	ND<0.005	-	-
<sup>#</sup> Mercury	mg kg <sup>-1</sup>	ND<0.002	1.47	-	-
<sup>#</sup> Nickel	mg kg <sup>-1</sup>	2.1	1.1	-	-
<sup>#</sup> Zink	mg kg <sup>-1</sup>	11.55	3.4	-	-
<sup>#</sup> Lead	mg kg <sup>-1</sup>	2.95	4.4	-	-
<sup>#</sup> Chromium	mg kg <sup>-1</sup>	ND<0.02	ND<0.02	-	-
Carbon	%	44.75	44.69	46.95	47.30
Nitrogen	%	0.24	0.17	0.36	0.33
<sup>‡</sup> Cellulose	%	51.31	56.88	-	-
<sup>‡</sup> Hemicellulose	%	30.80	28.70	-	-
<sup>‡</sup> Lignin	%	5.99	6.54	-	-
Acidic surface group	mmol g <sup>-1</sup>	3.35	3.95	3.18	3.18
Basic surface group	mmol g <sup>-1</sup>	0.45	0.33	0.47	0.50
Water soluble mineral content	μS cm <sup>-1</sup>	196.10	195.20	34.60	16.86
<i>S</i> <sub>BET</sub>	m <sup>2</sup> g <sup>-1</sup>	95.79	143.50	75.70	63.20
Pore volume	ml g <sup>-1</sup>	0.060	0.086	0.044	0.047
Bulk density	g ml <sup>-1</sup>	0.077	0.079	0.082	0.090
Particle size distribution					
Coarse (> 1.18 mm)	%	15	-	-	-
Medium (0.5-1.18 mm)	%	75	-	-	-
Fines (<0.5 mm)	%	10	-	-	-

<sup>#</sup> Analyzed at A&A Analytical Laboratory, Shah Alam, Malaysia

<sup>‡</sup> Analyzed at Chemistry Centre, Perth, Western Australia.

Chemical compositional analysis showed that the amount of potassium, sodium, arsenic and cadmium in RBS, RBS-N, was generally lower. Higher amount of sodium ions in RBS-N was found, due to the displacement of the external cation on the straw surface by  $\text{Na}^+$  from NaOH [169].

The content of cellulose, hemicellulose and lignin in RBS indicates the great potential of the barley straw as a biosorbent material due to the various functional groups in its structure [23, 27]. Generally, the percentage of cellulose, hemicellulose and lignin for RBS and RBS-N was observed to be different, which was due to the effect of base treatment to RBS. The percentages of cellulose and lignin in RBS-N were higher, while the percentage of hemicellulose was lower. It was early reported that base treatment would reduce lignin availability due to breakdown of its structure [166, 239]. The higher amount of lignin observed in RBS-N was probably due to the disassociation of lignocellulosic complex upon being treated with NaOH [240]. The higher percentage of cellulose of base treated straw was ascribed to the partial removal of hemicellulose upon treatment with the base solution [241] which can be reflected by the reduction of hemicellulose in RBS-N. Similar results were also observed in other investigations [240, 241]. The increase in cellulose percentage produced an advantage in providing more binding sites in hydroxyl groups [241]. Moreover, the base treatment caused the cellulose to be more denser and thermodynamically stable than the native cellulose [242]. The influence of the base treatment on agricultural waste by creating more active sites has been discussed in section 2.11.

The acidic group is the negatively charged functional group which is responsible for cation binding. In Table 4.1, surface acidic group of  $3.95 \text{ mmol g}^{-1}$  in base treated straw (RBS-N) was higher than raw straw, RBS ( $3.35 \text{ mmol g}^{-1}$ ). This was due to the hydrolyzation of lignocellulosic material resulting in the formation of surface acidic site such as carboxylic and hydroxyl which are responsible for binding activities [235]. Lower acidic surface group for SMBS and BMBS compared to RBS and RBS-N indicates the participation of these groups in  $\text{CPC}^+$  binding (hence at the same time increased the value of basic surface group). A similar observation was also reported by Namasivayam and Sureshkumar [36]. The reduction percentage of acidic group was calculated as 5.2% for RBS to SMBS and 19.6% for RBS-N to BMBS. The marginally

higher reduction percentage of the acid surface group observed in BMBS than SMBS suggested that the sorption of more CPC<sup>+</sup> on the acidic surface group of RBS-N than RBS.

It is interesting to determine the percentage of carbon and nitrogen in raw and surfactant modified adsorbents as the sorption of the cationic surfactant, CPC, was expected to increase the amount of carbon and nitrogen on the straw. It was found that, the percentage of carbon and nitrogen on SMBS and BMBS was greater comparing to those on RBS and RBS-N, respectively (Table 4.1). This was due to loading of CPC. Based on carbon and nitrogen values, the impregnated CPC on SMBS and BMBS was calculated as 0.086 mmol g<sup>-1</sup> and 0.109 mmol g<sup>-1</sup>, respectively. Higher amount of CPC in BMBS suggested more sorption of the CPC on RBS-N than RBS. This is consistent with the previous studies of treatment of lignocellulosic based adsorbents with sodium hydroxide [170, 236].

Surface area is also important as the greater surface area can increase the contact between the cationic surfactant and straw surface. In Table 5.1, BET surface area of 143.5 m<sup>2</sup> g<sup>-1</sup> for the base treated straw (RBS-N) was found higher than raw straw, RBS (95.79 m<sup>2</sup> g<sup>-1</sup>). Treatment with base may dissolve some of the low molecular weight organic matter thus creating more pores [170, 243]. For surfactant modified straws, lower BET surface area for BMBS of 63.2 m<sup>2</sup> g<sup>-1</sup> and 75.7 m<sup>2</sup> g<sup>-1</sup> for SMBS was observed and was ascribed to the attachment of surfactant moieties to the internal framework of raw adsorbent, causing the constriction of pore channels [36]. Similar findings were reported for other surfactant modified adsorbents such as coir pith [36] and montmorillonite [245]. The reduction in surface area for BMBS and SMBS was 56.0% and 21.0%. Higher reduction percentage of surface area observed in BMBS than SMBS indirectly suggested the existing of more CPC in BMBS than SMBS. The above conclusion was in agreement with the analysis of pore volume for BMBS and SMBS. The higher pore volume reduction percentage of 45.3% was calculated for BMBS compared to 26.7% reduction on SMBS.

The electrical conductivity was found much lower in SMBS and BMBS comparing to RBS and RBS-N respectively. This suggests the significant reduction in water soluble mineral after surfactant modification. The electrical conductivity was contributed mainly

by the leachable mineral contents on the adsorbent surface, such as the external cations upon exposed to the aqueous medium [208]. A lower value of electrical conductivity observed for BMBS than SMBS could be due to the less availability of the mineral ions on its surface, because a greater number of them had already been replaced by CPC ions during the cationic surfactant modification process.

Bulk density is not an intrinsic property of a material since it varies with the size distribution of the particles and their environment [246]. A higher bulk density for RBS-N than RBS was expected as the treatment with the base solution may dissolve some of the base soluble compounds in the straw. Whereas, a higher bulk density of SMBS and BMBS compared to RBS and RBS-N was suggested due to the addition of CPC onto straw surface. Higher bulk density in this case is favorable as it reflects the higher degree of compaction with less porosity which is good for holding aqueous solution [246]. This may subsequently improve the contact time between water contaminant and adsorbent.

#### **4.5 Morphology of Raw and Modified Barley Straw**

Raw and modified straw surface was investigated by scanning electron microscopy (SEM) as it provides the information of surface morphology. It offers detailed topographical and elemental information of solids with virtually large depth field, thus allowing different specimen to stay in focus at a time [247]. The SEM microphotos of all the prepared adsorbents showed the highly irregular shapes and size (Figs. 4.5a-d). The straws also consist of fiber like structure with longitudinal tissue and rough surface (Fig. 4.6). The surface morphology of untreated straw will be different from that of treated straw as the treatment may significantly alter the physicochemical properties and porosity of the materials. The treatment with alkaline was expected to partially remove protective thin wax on straw surface as what can be observed in Fig. 4.7a. SEM micrograph on existing of protective wax film on straw surface was extensively discussed by Wisniewska et al. [186]. Meanwhile, Fig. 4.7b shows the appearance of perforation probably due to the leaching of structural substances that might have exposed the active sites on RBS-N. This conclusion was also shared by Rocha et al. [160] in the modification of rice straw. The alkaline treated straw looks jagged and feels rough when physically touched indicating the substantial changes in its surface. Comparing the surfactant modified straw (Fig. 4.8b) with the unmodified one (Fig. 4.8a), it can be seen

that the surfactant modified surface appears to be rough, indicating that the surface had been covered with organic molecular layer. This was consistent with the observation made by Achak et al. [248] in their work related to modification of banana peel as a biosorbent.

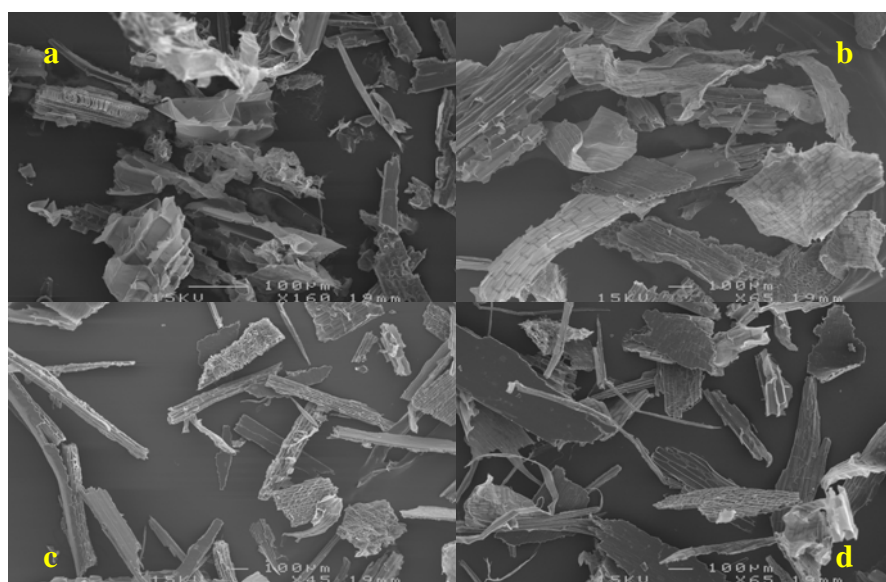


Figure 4.5. SEM micrograph of (a) RBS (b) RBS-N (c) SMBS and (d) BMBS showing the irregular shape

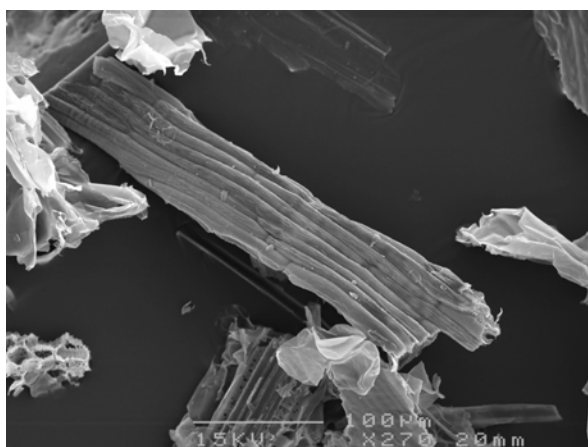


Figure 4.6. SEM micrograph showing the fiber like structure

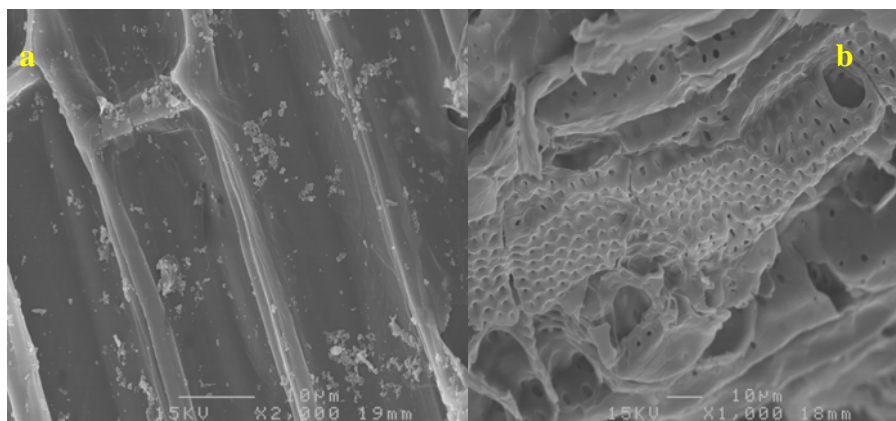


Figure 4.7. SEM micrograph of BMBS indicate (a) removal a thin wax layer (b) creating a perforation

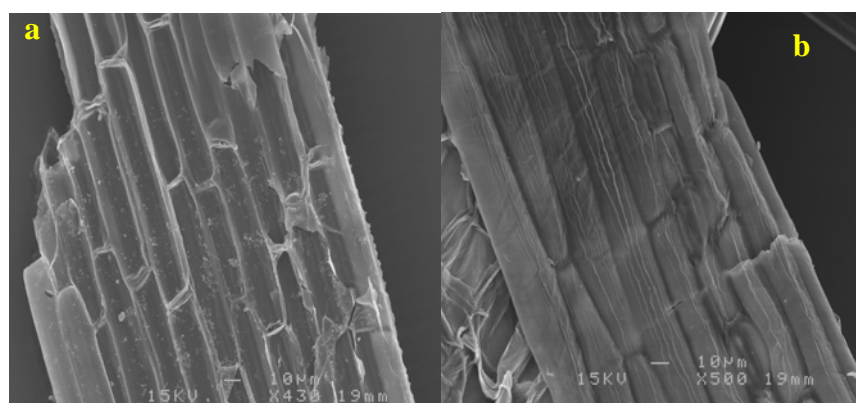


Figure 4.8. SEM micrograph of straw indicating the deposition of organic molecules (a) before CPC treatment (b) after CPC treatment

#### 4.6 Spectroscopic Study of Raw and Modified Straws

FT-IR provides information of the interaction of light and vibrational motion of the covalent chemical bonding of the molecules and lattice vibrations of ionic crystals [249]. Because each material is a unique combination of atoms, no two compounds produce the exact same infrared spectrum. Therefore, infrared spectroscopy can result in a positive identification (qualitative analysis) of different kinds of material [250].

Generally, FT-IR spectrum could be divided into two main regions; ID region (from 4000  $\text{cm}^{-1}$  to approximately 1500  $\text{cm}^{-1}$ ) which is useful for correlating peak location with bonds, and fingerprint region from 1500 to 600  $\text{cm}^{-1}$  which is typically complex band and is not as useful for such correlation [246]. Less meaningful information can be extracted from these fingerprint region [36]. Fig. 5.5 depicts the spectra of RBS, RBS-N, SMBS and BMBS. The spectra for RBS and RBS-N did not show any radical changes indicating that treatment with a mild base solution did not significantly alter the chemical properties of the straw. Spectrum of RBS and RBS-N contains several peaks, which can be assigned to: C=O groups stretching mainly of carboxylic and traces of ketones and esters (at 1712 $\text{cm}^{-1}$ ), OH stretching vibrations of H-bonded hydroxyl groups of phenol (at 3418  $\text{cm}^{-1}$ ), C-O stretching (at 1032  $\text{cm}^{-1}$ ), CH<sub>3</sub> weak stretching (at 2922  $\text{cm}^{-1}$ ), peaks of OH-stretching hydroxyl group (wide band at 416  $\text{cm}^{-1}$ ) and C-O (at 1041  $\text{cm}^{-1}$ ). To study the influence of cationic surfactant modification on straw surface, spectra of raw straw was compared against the spectra of CPC modified straw and pure CPC. In Fig. 4.9, two new bands lie at about 2920 and 2850  $\text{cm}^{-1}$  was observed for SMBS and BMBS, respectively. Interestingly, these matching bands also exist in CPC and was referred as asymmetric and symmetric stretching vibration of methylene C-H adsorption bands originated from the alkyl chain of CPC by Majdan et al. [251]. On the other hand, no such bands appear in RBS and RBS-N, thus confirms the existing of CPC in SMBS and BMBS.

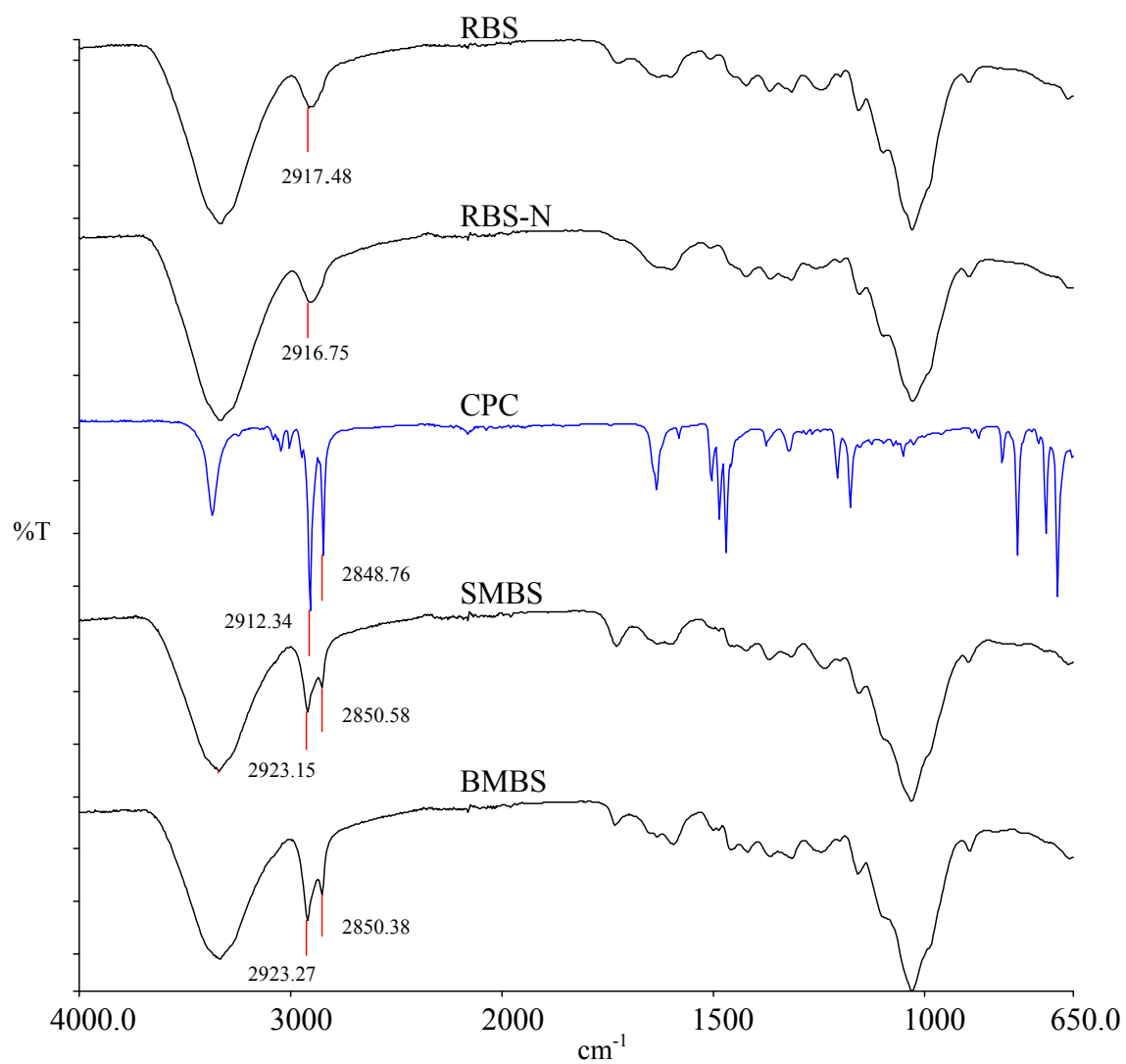


Figure 4.9. FT-IR spectra of RBS, RBS-N, SMBS, BMBS and CPC

## 4.7 Desorption of Cationic Surfactant

The retention of the cationic surfactant on straw surface is important, as the surfactant was responsible for retention of anionic pollutants and low polarity organic pollutants. Due to this, it is important to investigate the stability of CPC on straw surface being subjected to the various types of aqueous solution i.e, acidic, basic and organic solvent solution. Besides, the desorption study also could provide some insights about the possible mechanism of CPC-straw binding. Figs. 4.10a and 4.10b show the percentages of CPC desorption in various types of media.

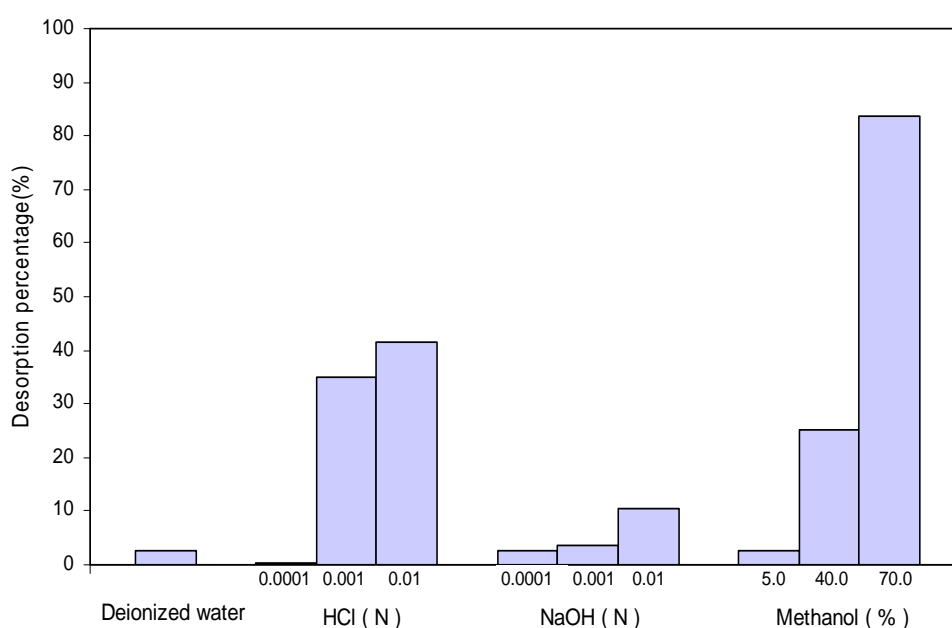


Figure 4.10a. Desorption of CPC from SMBS in various liquid media  
(Shaking speed: 170 rpm; dosage: 2 g L<sup>-1</sup>; Temperature: 25 °C; Shaking time: 6 h)

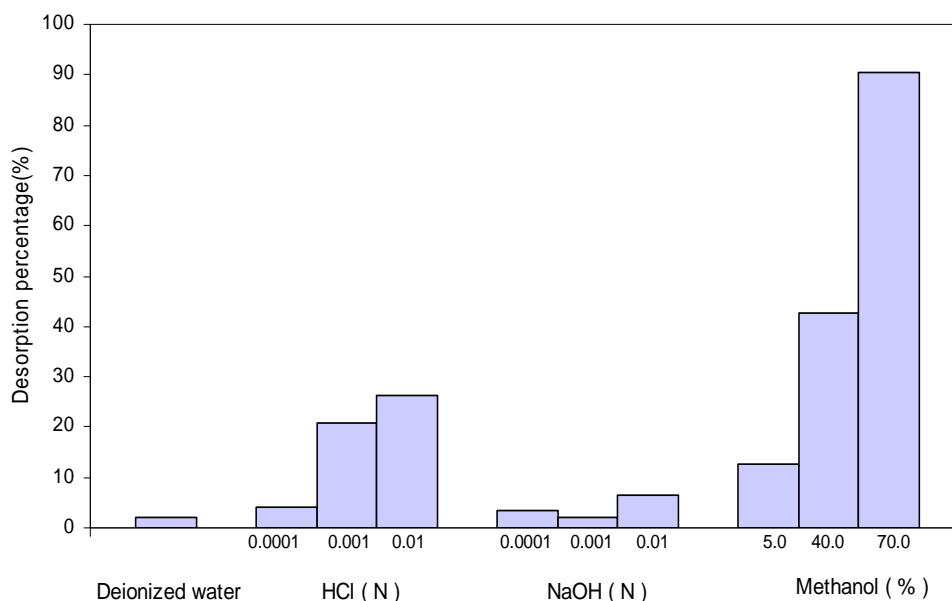


Figure 410b. Desorption of CPC from BMBS in various liquid media (Shaking speed: 170 rpm; dosage: 2 g L<sup>-1</sup>; Temperature: 25 °C; Shaking time: 6 h)

From Figs. 4.10a and 4.10b, desorption of CPC from SMBS and BMBS in deionized water was 2.67 and 1.94%, respectively. The relatively lower desorption of CPC from both SMBS and BMBS indicates a strong bonding between the CPC and straw surface. However, desorption of CPC was observed to increase with increasing acid solution concentration. The desorption percentages of CPC in 0.0001, 0.001 and 0.01 N HCl were 0.37, 34.97 and 41.45% for SMBS; and 4.15, 20.94 and 26.37 % for BMBS, respectively. Lower pH solution is believed to increase the positive charge on the adsorbent surface [2] thus promoting the desorption (due to the electrostatic repulsion) of positively charged CPC ions from adsorbent surface. The increasing desorption of CPC (as increasing in acid solution) also suggests ion exchange is the major binding mechanism [77].

As expected, the desorption was found lower in base solutions. At NaOH solution concentration of 0.0001, 0.001 and 0.01 N, CPC desorption was 2.60, 3.73 and 10.43% for SMBS; and 3.48, 2.13 and 6.41% for BMBS respectively. Unlike the desorption in acidic condition, electrostatic repulsion of CPC and straw surface at relatively basic solution does not expect to happen due to the high concentration of hydroxyl ion

contributed by NaOH solution. This reduces the possibility of electrostatic repulsion of straw surface to CPC ion, which subsequently results in the lower removal of CPC.

The behavior of surfactant CPC desorption in an organic solvent was conducted by exposing SMBS and BMBS to methanol-water solution. It was observed the significant increase in desorption of CPC at higher methanol concentration. The CPC desorption percentages on SMBS and BMBS were 2.50, 25.10 and 83.70% for SMBS; and 12.61, 42.72 and 90.37% for BMBS when they were soaked in aqueous methanol solution of 10, 40 and 70% v/v respectively. Leechart et al. [77] suggested that the high percentage of desorption of adsorbate in adsorbent-organic solvent system indicates chemisorption interaction of adsorbate and adsorbent.

The desorption study performed on both SMBS and BMBS indicated the different characteristic of CPC desorption in various types of aqueous solution. The lower desorption in deionized water suggests the physical sorption is not the major mechanism in CPC-straw binding, whereas the relatively high desorption in acid and organic solvent solution suggests the ion exchange and chemisorption as the binding mechanism.

#### **4.8 Section Summary**

Modification of barley straw was discussed in detail in this section. It was found that treatment of the straw with 0.05N NaOH solution greatly increased the sorption capacity. This would enhance the ability of the straw to retain a cationic surfactant. Adsorption of raw and treated straws with the surfactant revealed that the plateau was reached at about the critical micelle concentration of CPC. Due to that, the concentration of 2.5 mmol was chosen as a concentration for surfactant modification to ensure the formation of bilayer CPC. It is important to keep the CPC concentration at above CMC so as to create CPC admicelle/bilayer and at the same time render the positive charge on straw surface. The sorption system was observed to be four-region adsorption which was common for sorption of ionic surfactant onto oppositely charged solid surface. The characterization of the prepared adsorbents showed the existing of cellulose, hemicellulose lignin on barley straw. Analysis of C and N, acidic and basic surface groups, BET surface area of RBS, RBS-N, SMBS and BMBS proved the capability of base treated straw (RBS-N) to adsorb more CPC than raw straw (RBS). For both SMBS and BMBS, the desorption study

showed a strong bonding of CPC–straw in aqueous and base solution, however the desorption was found higher with increasing acid and organic solvent solution. The desorption study suggested that ion exchange and chemisorption are major binding mechanisms with less involvement of physisorption.

# 5

## REMOVAL OF EMULSIFIED OILS

### 5.1 Introduction

This chapter describes an investigation of barley straws as adsorbents for emulsified oil wastewater treatment in adsorption systems. Two types of investigations were performed; batch and fixed bed column studies. Preliminary batch studies were conducted to determine the effectiveness of the prepared adsorbents, namely; RBS, RBS-N, SMBS and BMBS in removing different types of emulsified oils such as canola oil (CO) and standard mineral oil (SMO). The influence of operation conditions in batch adsorption studies such as contact time, adsorption temperature, pH of solution, adsorbent particle size on oil uptake were investigated and discussed. The discussions for the fixed bed column studies mainly concentrated on column breakthrough. Stability of the oil adsorbed onto straw was evaluated by exposing to deionized water at various contact time. To provide better understanding of the adsorption process and mechanism, the data in batch experiments were analyzed with commonly used kinetic models; pseudo first order, pseudo second order, the Boyd diffusion model and also isotherm models namely, the Freundlich and Langmuir isotherm models. Meanwhile for fixed bed column breakthrough, the experimental data were fitted to some breakthrough models such as the Thomas and Yoon-Nelson. For some of the experiments that were run in duplicate, standard error of the measurement for the analyses were calculated using equation 3.16 and the results were shown in appendix B

## 5.2 Preliminary Experiments

The removal percentage of emulsified oils (CO and SMO) on RBS, RBS-N, SMBS and BMBS is shown in Fig. 5.1. The removal percentage of the emulsified oils using RBS and RBS-N was observed at 1.46 and 7.64% for CO; 2.82 and 2.56% for SMO, respectively. On the other hand, SMBS and BMBS demonstrated satisfactory removal of 89.10 and 90.91% for CO; 90.77 and 92.56% for SMO, respectively. A greater removal of both types of emulsified oils on surfactant modified adsorbents was consistent with what was suggested by Alther [49] and Hanna et al. [189], where they proposed that modification of solid surface with a surfactant created the hydrophobic, non-polar layer which allowed the partitioning of low polarity droplets. The lower removal of emulsified oils using RBS and RBS-N provided a sensible justification in using SMBS and BMBS as adsorbent materials for subsequent experiments. Control experiments also showed the removal of emulsified oil due to the other factors ( i.e inside wall of conical flask) was not significant at below 0.05%.

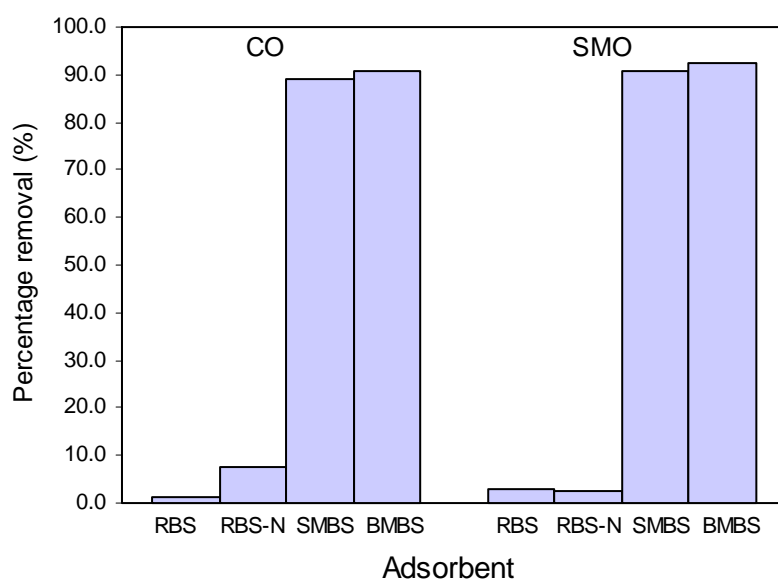


Figure 5.1. Adsorption of CO and SMO using unmodified and surfactant modified straw

([CO]: 2750 mgL<sup>-1</sup>, [SMO]: 3900 mgL<sup>-1</sup>, Contact time: 5 h, shaking speed: 170 rpm, dosage: 10 g L<sup>-1</sup>, Experimental temperature: 25 °C, Oil solution pH: CO: 7.5, SMO: 7.3 )

The participation of the cationic surfactant (existed on modified straw) on oil uptake was later confirmed by FT-IR spectra of the modified straw before and after the adsorption process. The spectra of oil-loaded SMBS and BMBS were shown in Figs. 5.2a and 5.2b. For the spectra of both CO and SMO loaded straws, it was observed that the carboxylic and carbonyl group bands at about  $2850\text{ cm}^{-1}$  originated from CPC on the straw surface marginally showed increased intensity compared to the fresh SMBS and BMBS (Figs. 5.2a and 5.2b). This suggests the involvement of hydrophobic bonding between SMBS and oil or BMBS and oil. As what have been reviewed in section 2.14, the adsorption of low polar organic compounds on surfactant modified adsorbents was reported to be due to partitioning or adsolubilization to the hydrophobic layer on the modified adsorbent surface. Based on this knowledge, the mechanism of oil adsorption on the modified straw surface in this study was proposed and illustrated in Fig. 5.3, which shows emulsified oil partition within the hydrophobic layer formed on the straw surface.

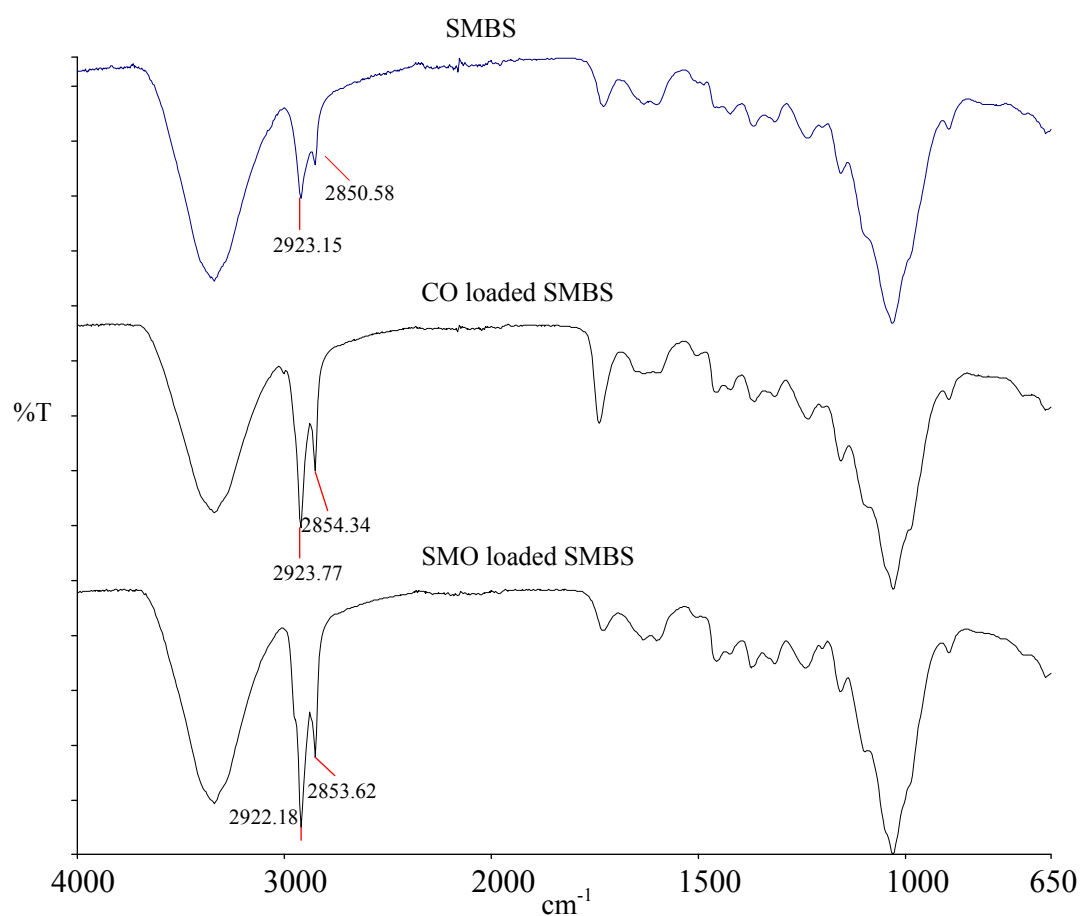


Figure 5.2a. FT-IR spectra of SMBS and oil loaded SMBS

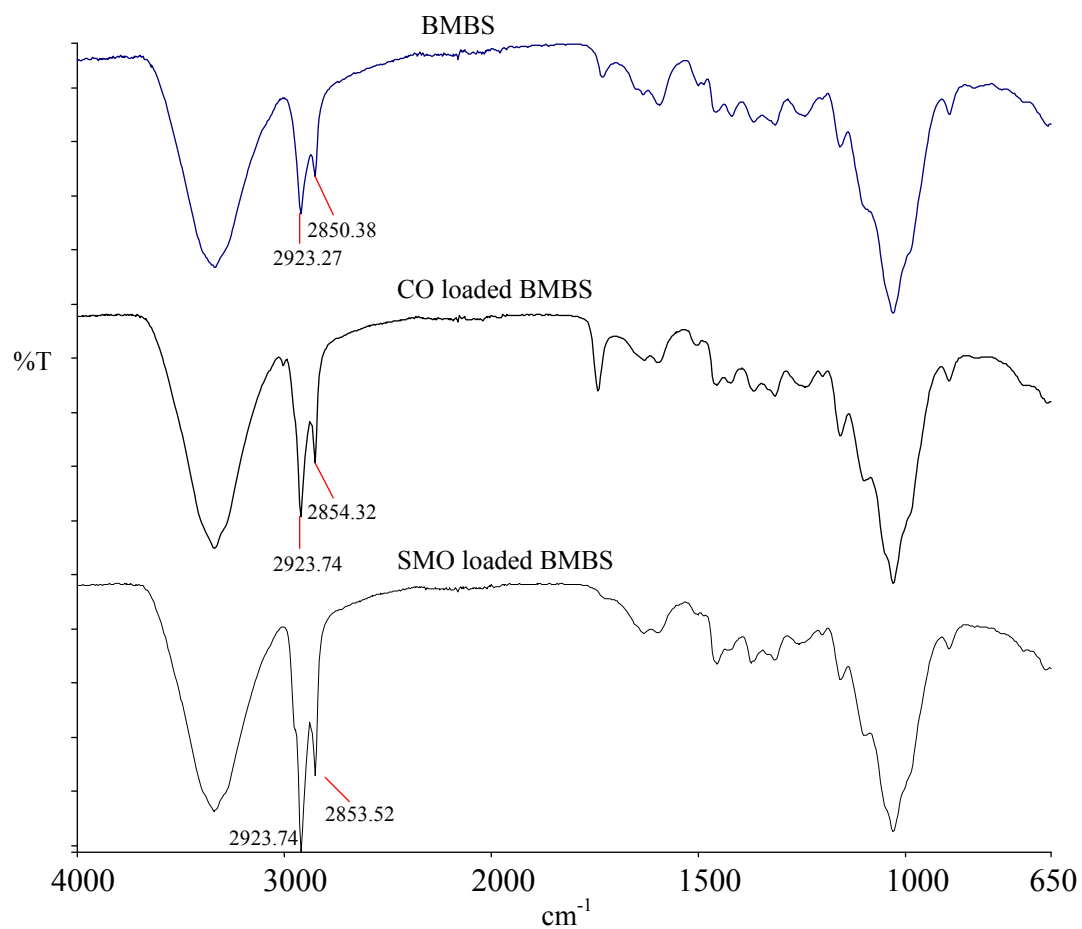


Figure 5.2b. FT-IR spectra of BMBS and oil loaded BMBS

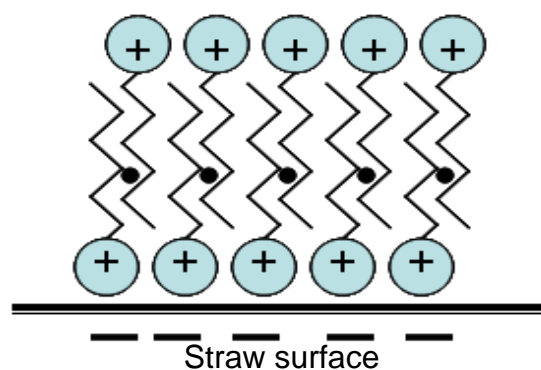


Figure 5.3. Schematic diagram showing adsolubilization/partitioning of oils (represented by black round dots) in surfactant modified straw.

### 5.3 Dynamic Adsorption of Oils

Dynamic sorption of emulsified oils on SMBS and BMBS are shown in Figs. 5.4a and 5.4b, respectively. Generally, for both adsorbents, the sorption was mainly consisting of two significant phases: a primary rapid phase and a slow phase. Most of oil uptake occurred at the initial rapid phase, while the second stage contributed to a relatively small uptake before the adsorption reached equilibrium. This initial high rate of oil uptake may be attributed to the greater bare surface existence for adsorption; however, as time increased, less adsorption sites were available hence a small amount of oil uptake occurred [252]. In Fig. 5.4a, for low concentration of CO at  $1040 \text{ mg L}^{-1}$ , the adsorption would reach equilibrium at 15 min for both SMBS and BMBS. Meanwhile the equilibrium would take a relatively longer at 45 and 35 min, for SMBS and BMBS, respectively, at higher concentration of  $3450 \text{ mg L}^{-1}$ . The similar trend was observed in Fig. 5.4b for SMO removal, where the equilibrium time for lower concentration of  $1680 \text{ mg L}^{-1}$  was 20 min for both SMBS and BMBS. At the higher concentration of  $4315 \text{ mg L}^{-1}$ , the equilibrium time was found to be 45 and 35 min for SMBS and BMBS, respectively. Therefore, it is determined that the equilibrium time can be set at 60 min for both CO and SMO, respectively, in order to ensure the equilibrium attained for both adsorbents and oil systems.

It was observed that, for both adsorbents, the adsorption capacity and equilibrium time is dependent on oil initial concentration. The increase in adsorption capacity with increasing initial oil concentration could be due to higher probability of collision between adsorbate and adsorbent surface [253]. The equilibrium time was also found to be quicker for lower oil concentration than the relatively higher initial oil concentration. It was reported that the optimum contact time was affected by the ratio of the number adsorption site to the number of adsorbate [254]. The relatively rapid kinetics observed in this study for both oil systems has significant practical importance, as it facilitates a smaller reactor volume thus ensuring high efficiency and economy [255]. The relatively higher removal for BMBS for both oils was due to the higher loading of CPC on BMBS than on SMBS as what had been discussed in section 4.3.

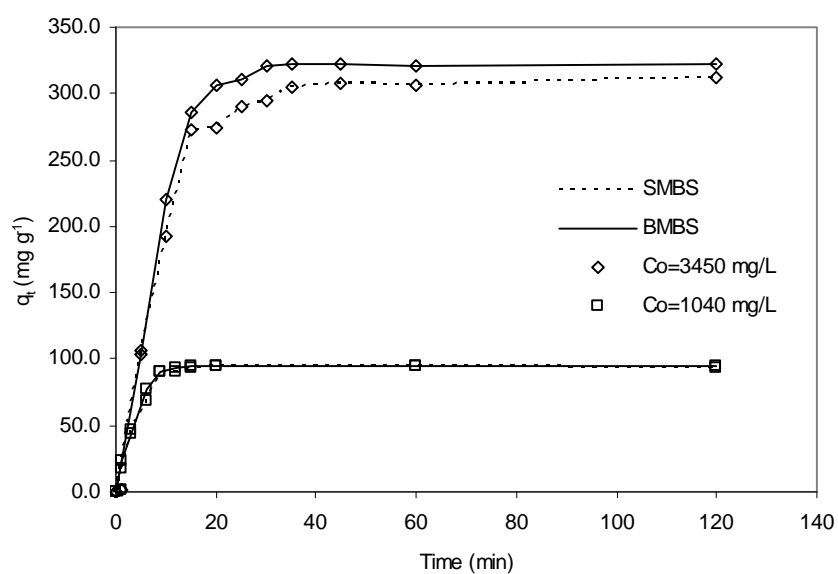


Figure 5.4a. Effect of contact time on adsorption of CO onto SMBS and BMBS. (CO solution pH: 7.5, shaking speed: 170 rpm, dosage: 10 g L<sup>-1</sup>, Experimental temperature: 25 °C)

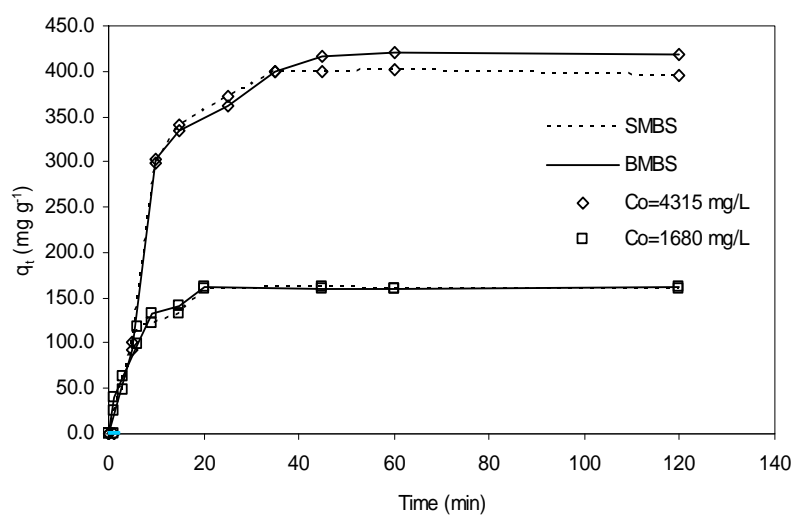


Figure 5.4b. Effect of contact time on adsorption of SMO onto SMBS and BMBS. (SMO solution pH: 7.3, shaking speed: 170 rpm, dosage: 10 g L<sup>-1</sup>, Experimental temperature: 25 °C)

### 5.3.1 Kinetic models

The transient behavior of oil adsorption was analyzed using two adsorption kinetic models, namely pseudo-first-order [215] and pseudo-second-order [216]. Non linear equations of the models (Eqs. 3.4 and 3.5) were curve fitted by employing a trial and error method using Polymath software, and the results are shown in Figs. 5.5a to 5.5d. To determine the best model fitted to the experimental data, a comparison of regression coefficient,  $R^2$  and error analysis values was performed. In Table 5.1,  $K_1$  and  $K_2$  represent the rate constant of the pseudo first order and second order, respectively, whereas  $q_e$  and  $q_t$  are the amount of oil adsorbed at equilibrium and time  $t$ , respectively. For both oils (Table 5.1),  $R^2$  of the pseudo first order was found higher than the pseudo second order model for SMBS and BMBS, indicating the suitability of the pseudo first order model. Moreover, the error function MPSTD values of the pseudo first order model for SMBS and BMBS were also found lower for both of CO and SMO thus confirming the fit of the pseudo first order kinetic model to the experimental data. Due to these, the sorption of CO and SMO on SMBS and BMBS can be concluded as the pseudo first order

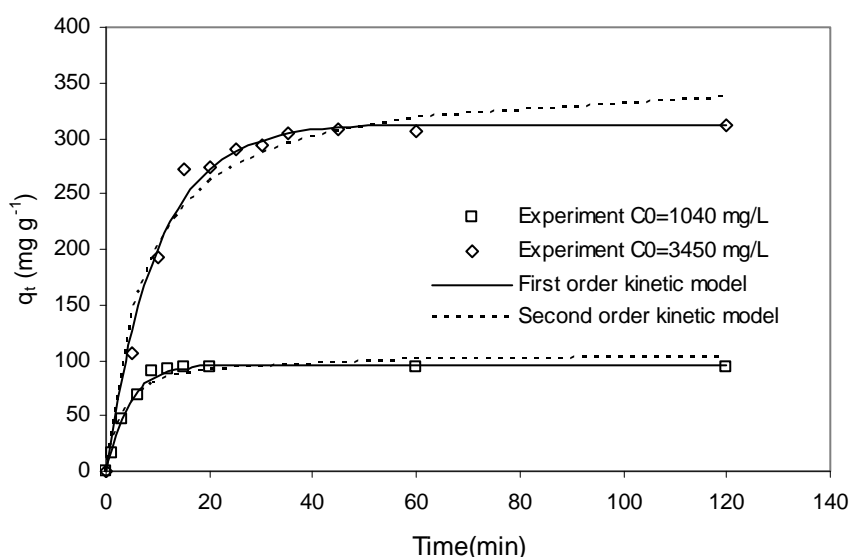


Figure 5.5a. Nonlinear kinetic models for adsorption of CO onto SMBS

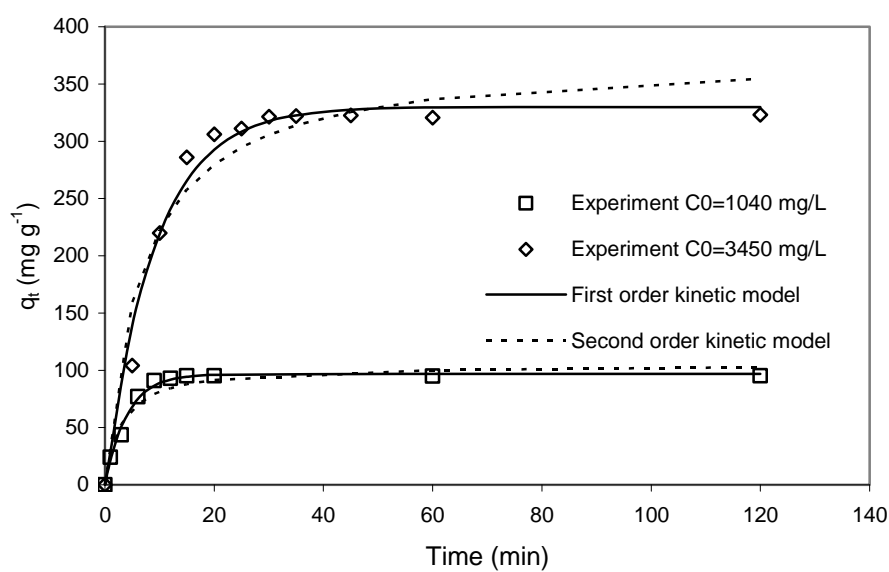


Figure 5.5b. Nonlinear kinetic models for adsorption of CO onto BMBS

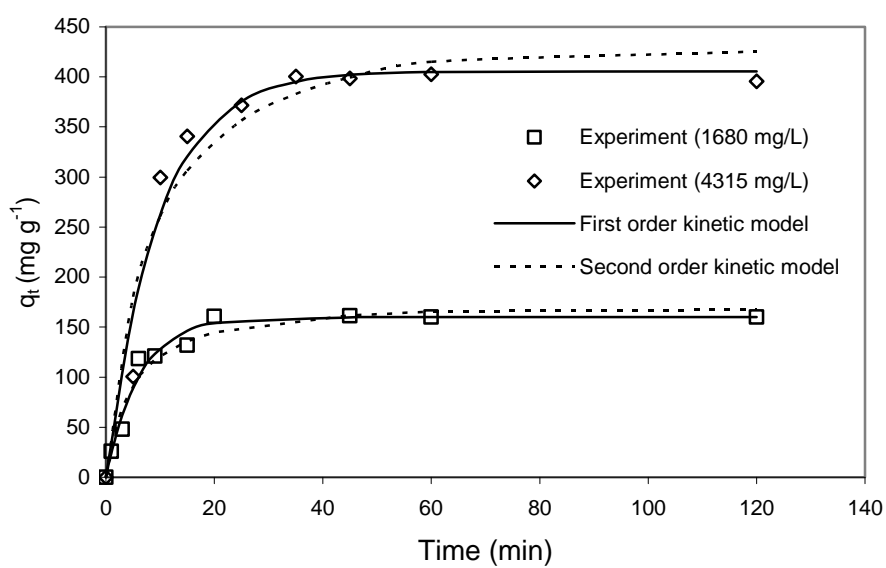


Figure 5.5c. Nonlinear kinetic models for adsorption of SMO onto SMBS

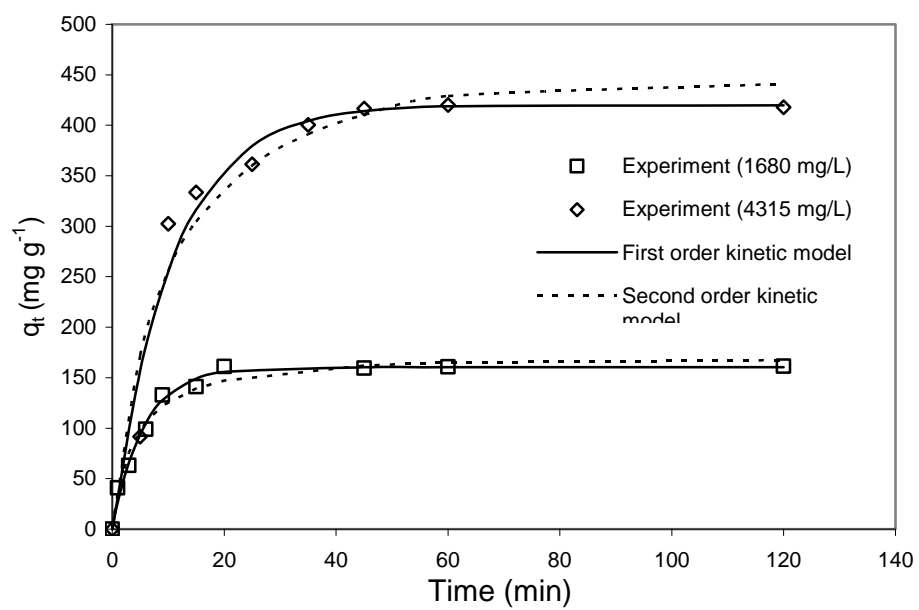


Figure 5.5d. Nonlinear kinetic models for adsorption of SMO onto BMBS

Table 5.1. Kinetics models constants and error analysis for adsorption of oil on SMBS and BMBS

Experimental				Kinetics Models				Error analysis			
Oil	Adsorbent	[55]	q <sub>e</sub>	Pseudo 1st order		Pseudo 2nd order		Pseudo first order		Pseudo 2nd order	
		mg L <sup>-1</sup>	mg g <sup>-1</sup>	k <sub>1</sub>	q <sub>e</sub> (mg g <sup>-1</sup> )	k <sub>2</sub>	q <sub>e</sub> (mg g <sup>-1</sup> )	R <sup>2</sup>	MPSD	R <sup>2</sup>	MPSD
CO	SMBS	1040	93.5	0.23	95.81	1.07 x 10 <sup>-2</sup>	105.09	0.99	6.86	0.96	22.88
		3450	310.0	0.10	312.39	3.79 x 10 <sup>-4</sup>	357.16	0.99	7.52	0.96	14.31
	BMBS	1040	95.2	0.25	96.66	3.50 x 10 <sup>-3</sup>	105.57	0.99	8.07	0.96	12.41
		3450	322.0	0.11	329.86	3.90 x 10 <sup>-4</sup>	375.04	0.98	12.22	0.95	19.68
SMO	SMBS	1680	160.6	0.16	159.92	1.21 x 10 <sup>-4</sup>	178.16	0.98	13.54	0.96	20.55
		4315	400.3	0.10	405.58	2.63 x 10 <sup>-4</sup>	471.23	0.97	26.66	0.94	33.28
	BMBS	1680	161.0	0.18	160.36	1.42 x 10 <sup>-3</sup>	176.28	0.99	14.46	0.98	42.04
		4315	416.7	0.09	420.26	2.13 x 10 <sup>-4</sup>	496.63	0.96	29.90	0.95	36.61

### 5.3.2 Kinetic diffusion models

The kinetic diffusion between liquid and solid phases were described using the Boyd diffusion model [219] to determine the participation of external diffusion or intraparticle diffusion as a controlling step in a solid liquid adsorption system.

The Boyd plots of  $B_t$  against time,  $t$  for all oil-straw systems were plotted and presented in Figs. 5.6a, 5.6b, 5.7a and 5.7b. El-Kamash et al, [221] suggested that a straight line passing through the origin showed sorption processes governed by particle-diffusion mechanisms; otherwise they are governed by film diffusion. Generally, the majority of the plots in Figs. 5.6a to 5.7b did not give a good straight line and none of them passed through the origin, in fact some of the points were really scattered with poor  $R^2$  (Table 5.2). This indicates that film diffusion mainly controlled the adsorption of oils on SMBS and BMBS

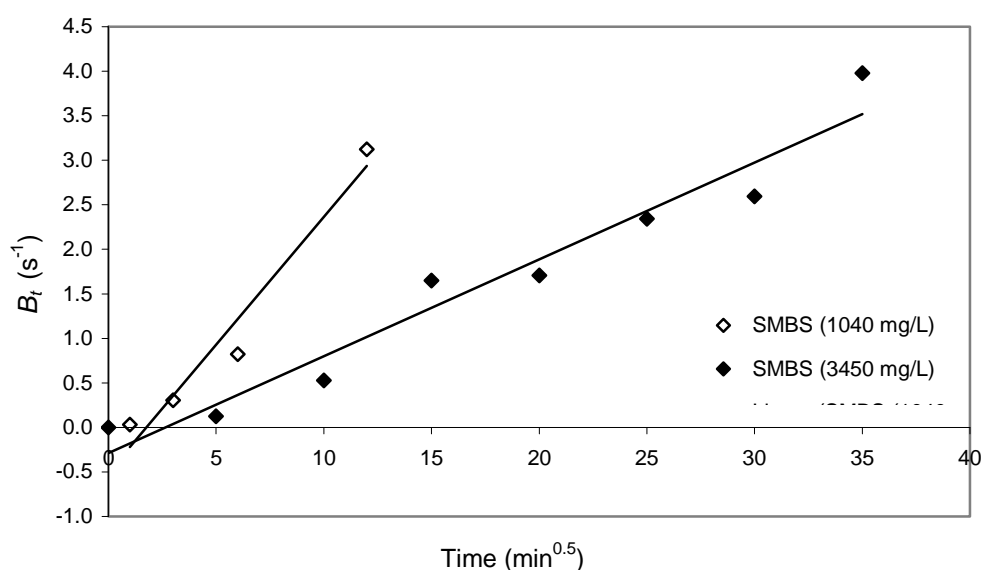


Figure 5.6a. Boyd plot for the sorption of CO onto SMBS

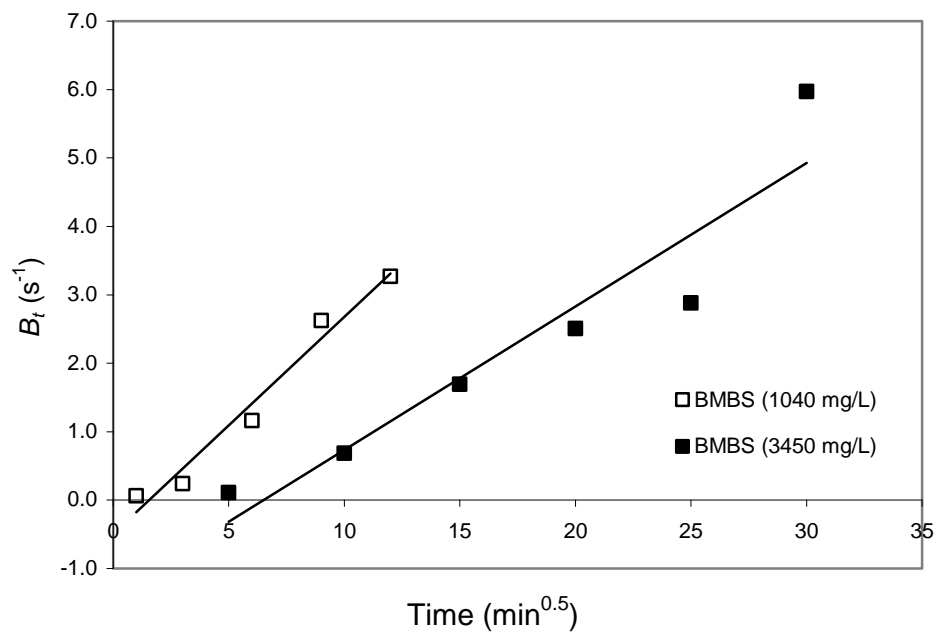


Figure 5.6b. Boyd plot for the sorption of CO onto BMBS

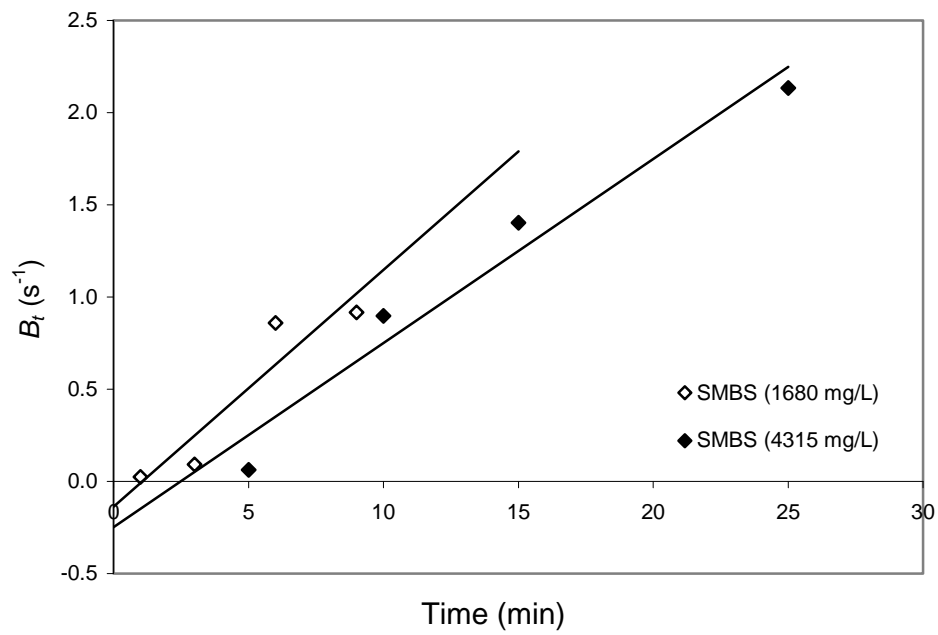


Figure 5.7a. Boyd plot for the sorption of SMO onto SMBS

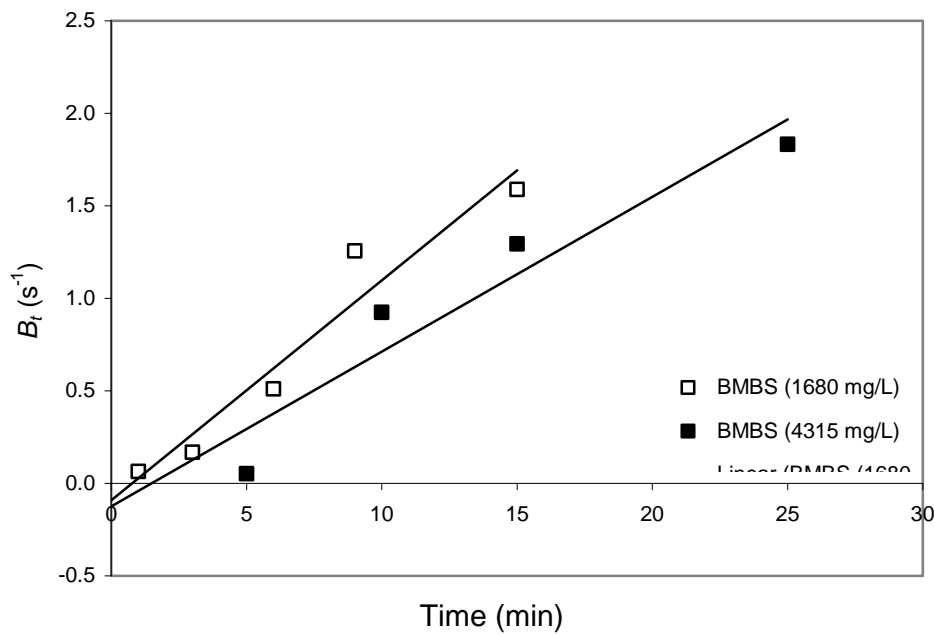


Figure 5.7b. Boyd plot for the sorption of SMO onto BMBS

The nature of diffusion process responsible for adsorption of oils onto straws could also be assessed by determining the effective diffusion rate,  $D_i$ . The effective diffusion rate was calculated based on Eq.3.8 and presented in Table 5.2. Due to the physical appearance of the straw that was not in spherical formed, the possible effective diffusion rate will be presented in range, based on straw particle size used.  $D_i$  in the range of  $10^{-6} - 10^{-8} \text{ cm}^2 \text{ s}^{-1}$  suggested film diffusion as the rate limiting step meanwhile the value in the range  $10^{-11} - 10^{-13} \text{ cm}^2 \text{ s}^{-1}$  suggests pore diffusion as the rate determining step [222]. It was found that  $D_i$  for all the oil-straw systems is in the range of  $10^{-6}$  to  $10^{-4} \text{ cm}^2 \text{ s}^{-1}$  (Table 5.2), which is a bit off from  $10^{-6} - 10^{-8} \text{ cm}^2 \text{ s}^{-1}$  range. For CO, the  $D_i$  values for the concentration of 1040 and 3450  $\text{mg L}^{-1}$  are  $6.89 \times 10^{-6}$  -  $3.84 \times 10^{-5}$  and  $1.82 \times 10^{-5}$  -  $1.01 \times 10^{-4} \text{ cm}^2 \text{ s}^{-1}$  (SMBS); and  $1.33 \times 10^{-5}$  -  $7.40 \times 10^{-5}$  and  $2.01 \times 10^{-5}$  -  $1.12 \times 10^{-4} \text{ cm}^2 \text{ s}^{-1}$  (BMBS), respectively.

Meanwhile for SMO,  $D_i$  values for the concentration of 1680 and 4315  $\text{mg L}^{-1}$  are  $6.33 \times 10^{-6}$  -  $3.52 \times 10^{-5}$  and  $8.13 \times 10^{-6}$  -  $4.53 \times 10^{-5} \text{ cm}^2 \text{ s}^{-1}$  (SMBS); and  $5.30 \times 10^{-6}$  -  $2.95 \times 10^{-5}$  and  $7.53 \times 10^{-6}$  -  $4.19 \times 10^{-5} \text{ cm}^2 \text{ s}^{-1}$  (BMBS), respectively. Based on the findings made earlier (on the straight line plot in Figs. 5.6a to 5.7b) it can be concluded that the film diffusion is a controlling step in oil-straw systems, even though the  $D_i$  value was

slightly over  $10^{-6} - 10^{-8} \text{ cm}^2 \text{ s}^{-1}$ . According to many scientists, the physical chemistry involved may be complex and no single theory of sorption has been put forward to explain the overall adsorptive removal process [218].

Table 5.2. Effective diffusion constants ( $D_i$ ) for adsorption of oil on SMBS and BMBS

Oil	Adsorbent	[Oil] (mg L <sup>-1</sup> )	Effective diffusion		R <sup>2</sup>
			$D_i$ (cm <sup>2</sup> s <sup>-1</sup> )		
CO	SMBS	1040	6.89 x 10 <sup>-6</sup> - 3.84 x 10 <sup>-5</sup>		0.96
		3450	1.82 x 10 <sup>-5</sup> - 1.01 x 10 <sup>-4</sup>		0.95
	BMBS	1040	1.33 x 10 <sup>-5</sup> - 7.40 x 10 <sup>-5</sup>		0.97
		3450	2.01 x 10 <sup>-5</sup> - 1.12 x 10 <sup>-4</sup>		0.89
SMO	SMBS	1680	6.33 x 10 <sup>-6</sup> - 3.52 x 10 <sup>-5</sup>		0.96
		4315	8.13 x 10 <sup>-6</sup> - 4.53 x 10 <sup>-5</sup>		0.88
	BMBS	1680	5.30 x 10 <sup>-6</sup> - 2.95 x 10 <sup>-5</sup>		0.91
		4315	7.53 x 10 <sup>-6</sup> - 4.19 x 10 <sup>-5</sup>		0.94

(Solution pH: CO= 7.5, SMO=7.3, shaking speed: 170 rpm, dosage: 10 g L<sup>-1</sup>, Straw size radius: 0.025-0.059 cm, Experimental temperature: 25 °C)

#### 5.4 Isotherm Models

The distribution of adsorbate between liquid and solid phases is described by several isotherms such as the Langmuir [223] and Freundlich [224]. The nonlinear equations of the respective isotherm models are listed in Eqs. 3.11 and 3.12 in Section 3.9. The nonlinear isotherms of SMBS and BMBS for adsorption of CO and SMO were curve fitted by employing a trial and error method using Polymath software and the plots are shown in Figs. 5.8a and 5.8b respectively. In Table 5.3,  $Q_{\max}$  is referred to the maximum adsorption capacity and  $b$  is a constant related to energy of adsorption, which quantitatively reflects the affinity between the adsorbent and adsorbate.  $K_F$  is related to adsorption capacity and  $n$  is an empirical formula that varies with degree of heterogeneity.

To determine the isotherm model that best fitted to the experimental data, a comparison of regression coefficient,  $R^2$  and error analysis values were performed. Even though all the plots gave relatively good  $R^2$  above 0.97 (Table 5.3), however, upon comparing the

MPSD error functions, the error value for the Langmuir isotherm of SMBS and BMBS was lower for both emulsified oils. Due to this, the Langmuir model could best describe the isotherm model for adsorption of emulsified oil on modified barley straw. The values of  $Q_{\max}$  calculated from the Langmuir model for SMBS and BMBS were 576.00 and 613.29  $\text{mg g}^{-1}$  for CO; 518.63 and 584.22  $\text{mg g}^{-1}$  for SMO respectively.

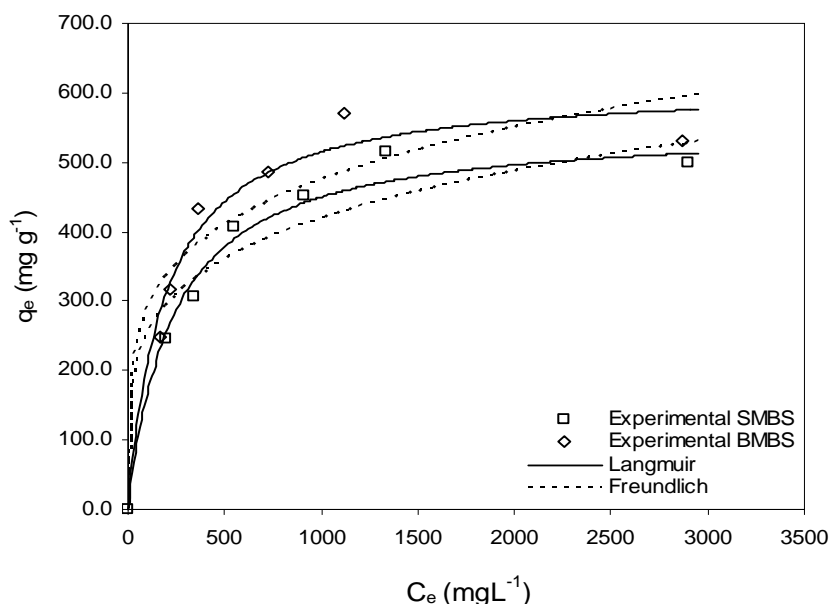


Figure 5.8a. Nonlinear adsorption isotherms for adsorption of CO onto SMBS and BMBS.

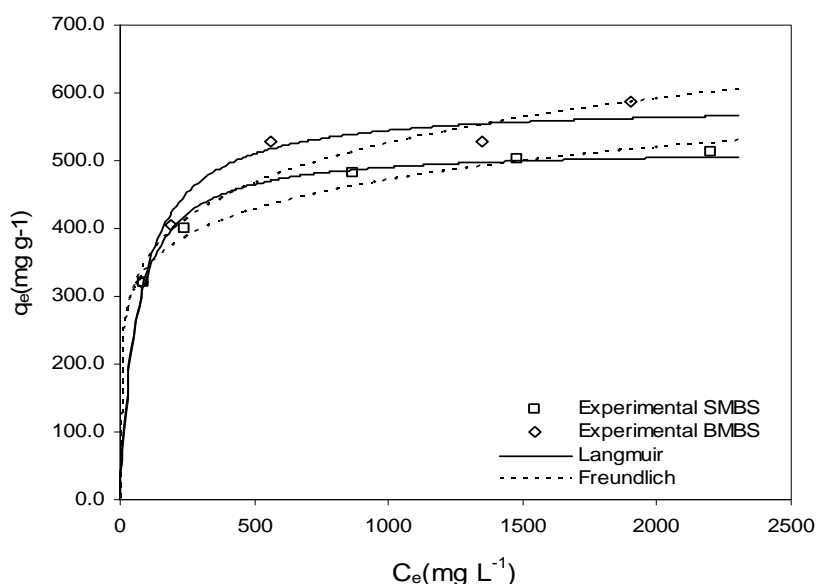


Figure 5.8b. Nonlinear adsorption isotherms for adsorption of SMO onto SMBS and BMBS

Table 5.3. Freundlich and Langmuir isotherm constants and error analysis for adsorption of oil on SMBS and BMBS

Experimental		Isotherm Models Constant				Error Analysis			
Oil	Adsorbent	Langmuir		Freundlich		Langmuir		Freundlich	
		$Q_{\max}$ (mg g <sup>-1</sup> )	b (L mg <sup>-1</sup> )	$K_F$ (mg g <sup>-1</sup> )	n	$R^2$	MPSD	$R^2$	MPSD
CO	SBS	576.00	$3.87 \times 10^{-2}$	84.39	4.25	0.99	6.60	0.95	13.02
	BBS	613.29	$5.20 \times 10^{-3}$	112.11	4.76	0.97	9.09	0.91	20.23
SMO	SBS	518.63	$1.74 \times 10^{-2}$	182.31	7.23	0.98	3.35	0.96	4.47
	BBS	584.22	$1.38 \times 10^{-2}$	165.03	5.94	0.96	5.32	0.92	7.65

## 5.5 Comparison with Other Adsorbents

Table 5.4 presents a comparison of the effectiveness of SMBS and BMBS as potential adsorbents for treatment of emulsified oil wastewater in terms of maximum adsorption capacity with other previously reported adsorbents. Higher adsorption capacity of BMBS than SMBS was expected due to the availability of more CPC in BMBS as what have been discussed in section 4.3. The adsorption capacity for CO was higher than SMO, consistent with the finding reported by Mysore et al [98] in the applicability of expanded vermiculite in sorption of emulsified CO and SMO. Srinivasan and Viraraghavan [256] suggested different interfacial tension of CO and SMO. The interfacial tension of the emulsified CO and SMO was reported as 3.1 and 5.3 dynes cm<sup>-1</sup>, respectively [98]. Compared to other adsorbents, it was found that SMBS and BMBS exhibited higher adsorption capacity than other surfactant modified adsorbents such as organoclay but lower than chitosan and wool based adsorbents. Taking the removal of the emulsified oil of CO and SMO as the reference, SMBS and BMBS were found to exhibit much greater sorption capacity when compared to the expanded and hydrophobized vermiculite. However, it was noted that each of the reported adsorption capacity or removal percentage has been achieved under specific experimental conditions and the extent of chemical modification made.

Table 5.4. Oil sorption capacities of some sorbents reported in literature

Adsorbent	Emulsified oil studied	Sorption capacity (g g <sup>-1</sup> )	Reference
Chitosan powder	Palm Oil Mills Effluent (POME)	3.42	[45]
Chitosan flake	Palm Oil Mills Effluent (POME)	1.97	[45]
Bentonite Organoclay	Valcool (Cutting oil)	0.14	[22]
Organoclay/anthracite	Valcool (Cutting oil)	2.10 x10 <sup>-2</sup>	[19]
	Refinery Effluent	7.00 x10 <sup>-5</sup>	
Acetylated rice straw	Machine oil	24.0	[257]
Acetylated Sugarcane bagasse	Machine oil	18.8	[258]
Natural wool fibers (NWF)	Real oily wastewater (motor oils)	5.56	[6]
Recycled wool-based nonwoven material (RWNM)	Real oily wastewater (motor oils)	5.48	[6]
Sepiolite	Real oily wastewater (motor oils)	0.19	[6]
Expanded vermiculite	Standard Mineral Oil (SMO)	1.50 x10 <sup>-2</sup>	[98]
	Canola oil (CO)	4.63 x10 <sup>-2</sup>	
	Kutwell 45	1.10 x10 <sup>-2</sup>	
	Refinery Effluent(RE)	8.09 x10 <sup>-3</sup>	
Hydrophobized vermiculite	Standard Mineral Oil (SMO)	2.30 x10 <sup>-2</sup>	[98]
	Canola oil (CO)	6.12 x10 <sup>-3</sup>	
	Kutwell 45	6.70 x10 <sup>-3</sup>	
	Refinery Effluent(RE)	2.70 x10 <sup>-3</sup>	
Modified barley straw (SMBS)	Canola oil (CO)	0.576	<i>This study</i>
	Standard Mineral Oil (SMO)	0.519	
Modified barley straw (BMBS)	Canola oil (CO)	0.613	<i>This study</i>
	Standard Mineral Oil (SMO)	0.584	

## 5.6 Effect of the Oil Solution Temperature

The effect of temperature on adsorption of CO and SMO was conducted at different temperatures of 23, 33 and 43 °C for both SMBS and BMBS and are shown in Figs. 5.9a and 5.9b, respectively. For CO, generally, the adsorption capacities of SMBS at the temperatures of 23 and 33 °C were about the same at 101.8 and 100.8 mg g<sup>-1</sup> for SMBS; and 107.2 and 105.89 mg g<sup>-1</sup> for BMBS, respectively. A similar trend was observed for SMO, where the adsorption capacities of SMBS at the temperatures of 23 and 33 °C were 98.0 and 99.0 mg g<sup>-1</sup> for SMBS; and 99.5 and 98.0 mg g<sup>-1</sup> for BMBS, respectively. This indicated a small effect of temperature at lower range on the adsorption capacities. However, at relatively higher temperature (43°C), adsorption capacity of SMBS and BMBS, increased slightly to 109.2 and 101.8 mg g<sup>-1</sup> for CO; and to 195.6 and 107.2 mg g<sup>-1</sup> for SMO respectively. It was reported that at elevated temperature, the movement of molecules increased (motion is higher) and the interactions between sorbent and molecules were more intense [259] thus increasing the diffusion rate of adsorbate molecules across the adsorbent surface [260].

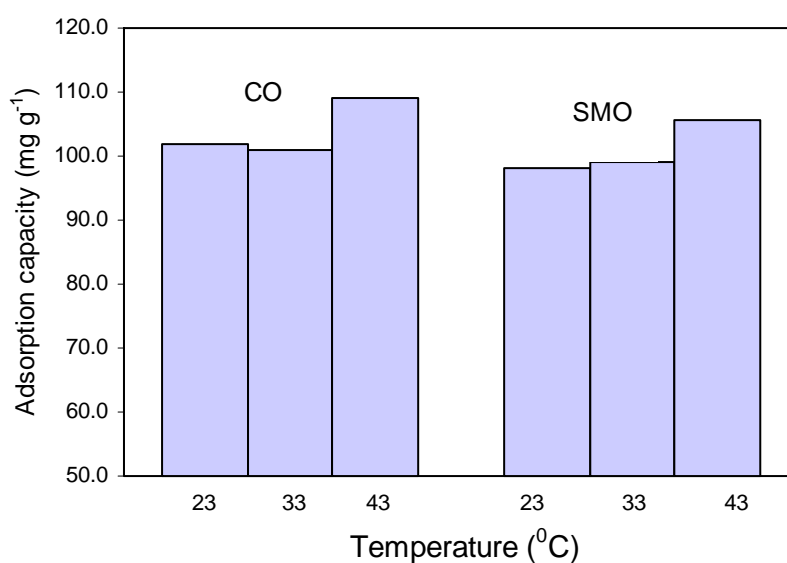


Figure 5.9a. Effect of temperature on adsorption of CO and SMO onto SMBS ([CO]: 1183 mgL<sup>-1</sup>, [SMO]: 1170 mgL<sup>-1</sup>, Contact time: 60 min, shaking speed: 170 rpm, dosage: 10 g L<sup>-1</sup>, Oil solution pH: CO: 7.5, SMO: 7.3 )

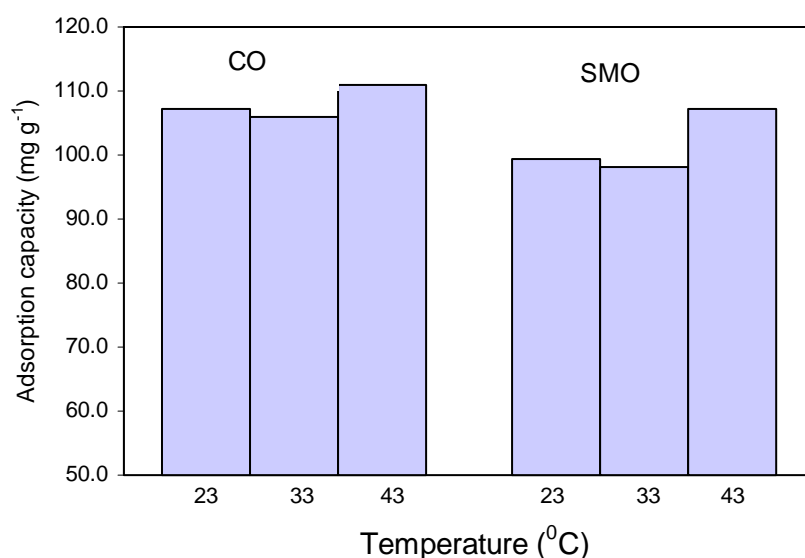


Figure 5.9b. Effect of temperature on adsorption of CO and SMO onto BMBS ([CO]: 1183 mgL<sup>-1</sup>, [SMO]: 1170 mgL<sup>-1</sup>, Contact time: 60 min, shaking speed: 170 rpm, dosage: 10 g L<sup>-1</sup>, Oil solution pH: CO: 7.5, SMO: 7.3)

## 5.7 Effect of Initial pH of Oil Solution

The effect of pH on oil adsorption on SMBS and BMBS is presented in Figs. 5.10a and 5.10b, respectively. pH of solution is an important parameter in the adsorption process due to its influence on the surface properties of adsorbent and surface binding sites [72]. For SMBS, the adsorption capacity of emulsified oil at pH 2 to 6 increased rapidly from 18.0 to 72.4 mg g<sup>-1</sup> (CO) and 15.4 to 77.4 mg g<sup>-1</sup> for SMO. A similar trend was observed for BMBS where adsorption capacity of the emulsified oil at pH 2 to 6 was increased from 26.0 to 77.4 mg g<sup>-1</sup> and 14.2 to 79.1 mg g<sup>-1</sup> for CO and SMO respectively. For the both oils, a maximum removal was observed at the pH around neutrality and higher pH of 8 and 10 did not improve the adsorption further. At lower pH, huge amount of protons are available and may saturate the adsorbent sites, thus increasing the cationic properties of adsorbent surface [100], which will greatly reduce the hydrophobic properties of the adsorbent. As for the stability of oil emulsion solution, strong acidic condition will induce oil emulsion to form unstable flocs [45], which could cause coalescence and subsequently increases the size of oil droplets. The oil droplets partition at the hydrophobic layer of surfactant [96] were expected to experience severe stress due to existence of larger (and heavier) oil

droplets. The increase in oil uptake with increasing pH solution was due to the reduced number of protons, hence maintaining the hydrophobicity level of adsorbent surface.

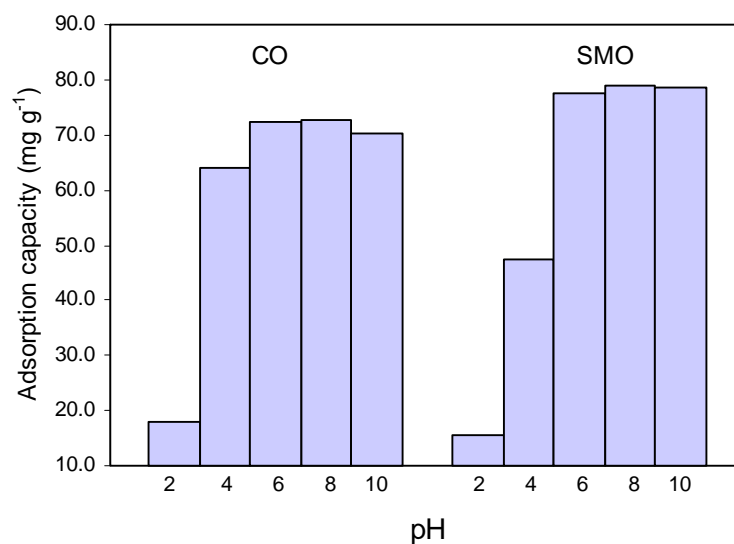


Figure 5.10a. Effect of solution pH on adsorption of CO and SMO onto SMBS ([CO]: 860 mgL<sup>-1</sup>, [SMO]: 821 mgL<sup>-1</sup>, Contact time: 60 min, shaking speed: 170 rpm, dosage: 10 g L<sup>-1</sup>, Experimental temperature: 25°C)

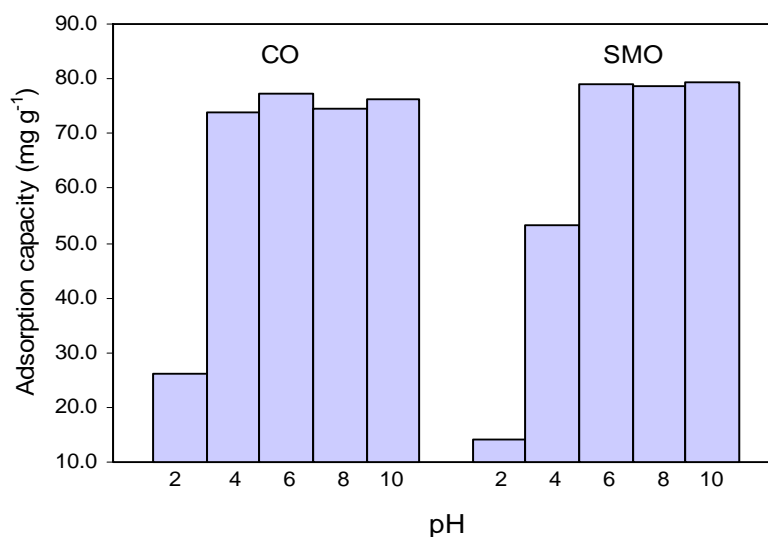


Figure 5.10b. Effect of solution pH on adsorption of CO and SMO onto BMBS ([CO]: 860 mgL<sup>-1</sup>, [SMO]: 821 mgL<sup>-1</sup>, Contact time: 60 min, shaking speed: 170 rpm, dosage: 10 g L<sup>-1</sup>, Experimental temperature: 25°C)

## 5.8 Effect of Adsorbent Size

The influence of particle size of adsorbent on CO and SMO sorption are shown in Figs. 5.11a and 5.11b, respectively. It was observed that the adsorption of oil on SMBS and BMBS was highly particle size dependent. The CO and SMO removal was increased with decreasing particle size for both adsorbents. For SMBS, the particles at the size of <0.50, 0.50 - 1.18, and 1.18 - 1.4 mm gave the correspondent adsorption capacities of 92.0, 83.2 and 80.6 mg g<sup>-1</sup> for CO and 93.1, 88.7 and 87.5 mg g<sup>-1</sup> for SMO, respectively. Meanwhile, For BMBS, straw particles at the size of <0.50, 0.50 - 1.18, and 1.18 - 1.4 mm showed adsorption capacities of 111.0, 108.5 and 102.0 mg g<sup>-1</sup> for CO and 110.5, 109.7 and 104.0 mg g<sup>-1</sup> for SMO, respectively. From the results, it is seen that adsorption capacity was the highest at the smallest adsorbent size. It was widely reported that decreased adsorbent size would increase the effective contact area [244]. This would eventually make more binding sites available hence increasing the adsorption capacity. However, a relatively small increase in adsorption capacity (for all the emulsified oil-straw system) did commensurate with marginally increased surface area, which was due to the unsaturation of the adsorption sites during the adsorption process. It was also likely due to the blockage of some of adsorbent sites as well increasing mass transfer resistance[261].

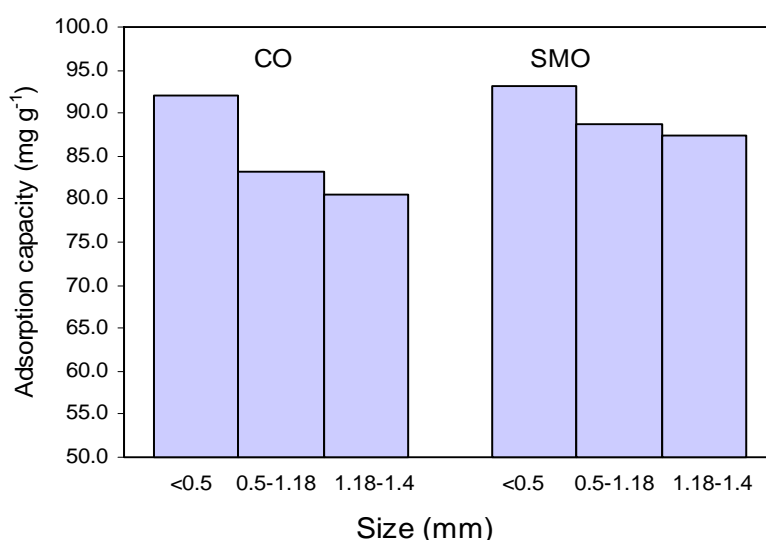


Figure 5.11a. Effect of adsorbent size on adsorption of CO and SMO onto SMBS ( [CO]: 1020 mgL<sup>-1</sup>, [SMO]: 1180 mgL<sup>-1</sup>, Contact time: 60 min, shaking speed: 170 rpm, dosage: 10 g L<sup>-1</sup>, Experimental temperature: 25°C, Oil solution pH: CO: 7.5, SMO: 7.3 )

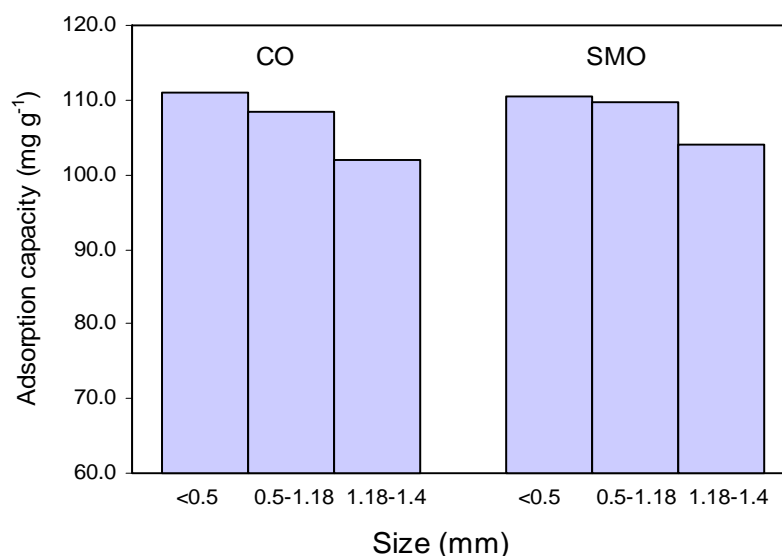


Figure 5.11b. Effect of adsorbent size on adsorption of CO and SMO onto BMBS ([CO]: 1020 mgL<sup>-1</sup>, [SMO]: 1180 mgL<sup>-1</sup>, Contact time: 60 min, shaking speed: 170 rpm, dosage: 10 g L<sup>-1</sup>, Experimental temperature: 25°C, Oil solution pH: CO: 7.5, SMO: 7.3 )

## 5.9 Desorption

A desorption study is important for the determination of the amount of oil that will be probably washed out when it is exposed to the natural erosion agent such as water (i.e raining, flood etc). The desorption percentages of oil loaded on SMBS and BMBS are shown in Figs. 5.12a and 5.12b, respectively. It was found that SMBS loaded with CO or SMO showed a lower percentage of desorption. The percentages of oil leached out at the exposure time of 1, 5 and 24 h were 4.13, 3.67 and 3.67% for CO and 1.50, 2.80 and 2.20% for SMO, respectively. Meanwhile, for BMBS the percentages of oil leached out at the exposure time of 1, 5 and 24 h were 2.30, 2.30 and 1.84% for CO and 1.70, 1.95 and 2.10% for SMO, respectively. It is apparent that the percentage of desorption is small and does not change with time. This suggests a strong bonding of oil with adsorbent surface and high stability of oil adsorbed on SMBS and BMBS thus making the arrangement/storage of the oil loaded straw much easier and simple.

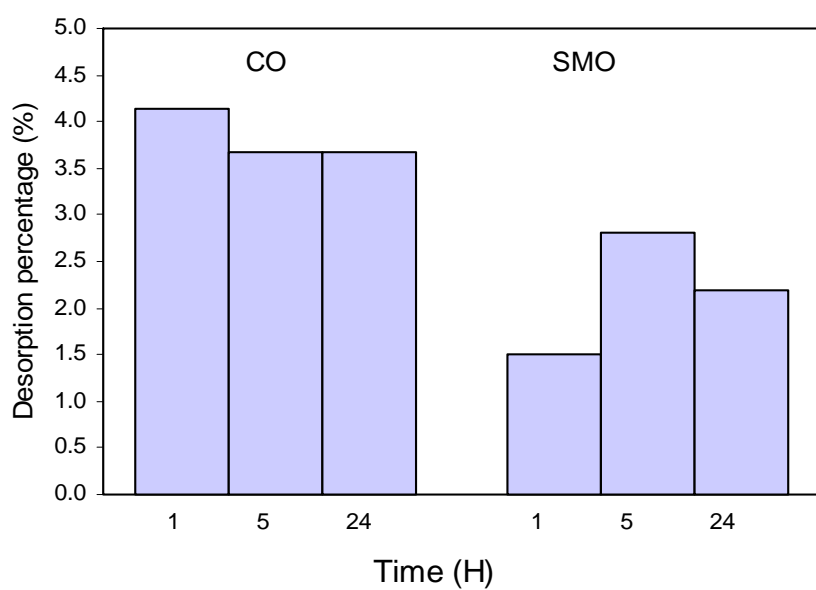


Figure 5.12a. Desorption of oil loaded SMBS in deionized water (Shaking speed: 170 rpm; dosage: 10 g L<sup>-1</sup>; Experimental temperature: 25 °C)

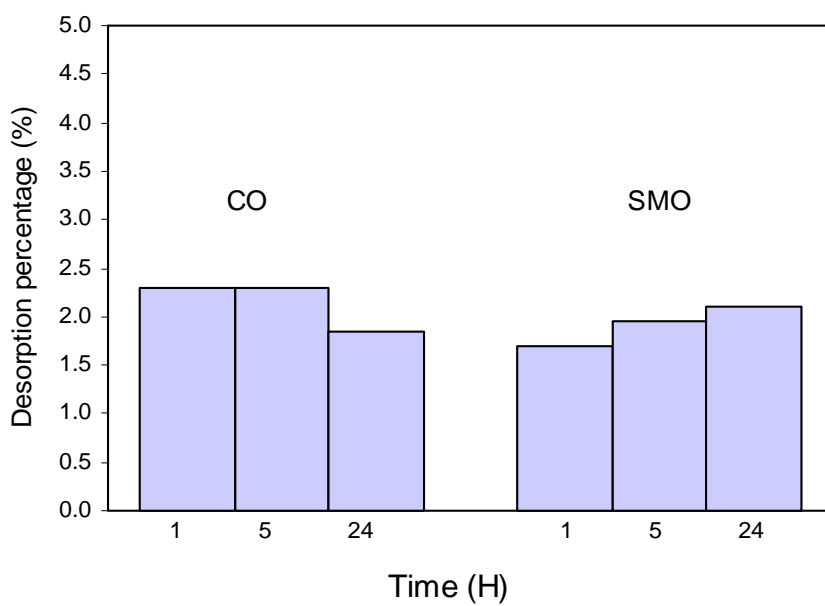


Figure 5.12b. Desorption of oil loaded BMBS in deionized water (Shaking speed: 170 rpm; dosage: 10 g L<sup>-1</sup>; Experimental temperature: 25 °C)

## 5.10 Column Breakthrough Studies

In practice, it was more sensible and efficient to remediate real wastewater using fixed bed columns [262] rather than batch operation. The overall performance of a column bed is usually described by the concept of breakthrough curve, which has been thoroughly discussed in section 3.8. The breakthrough curves for CO and SMO are shown in Figs. 5.13a to 5.13d. By comparing the breakthrough curves for RBS and RBS-N with the example of column breakthrough curves in Chapter 3, Fig. 3.2, it is evident that RBS and RBS-N gave poor adsorption performance for removal of both, CO and SMO. This is consistent with the results observed in batch operation (section 5.2). Whereas, for SMBS and BMBS, the favorable adsorption was observed, where all the curves have the ‘S’ shape, an indication of a favorable and normal column adsorption process (Figs. 5.13c and 5.13d). For CO and SMO, it was observed that there was a time where the oil concentration in the effluent remained zero until a certain period where the concentration started to increase gradually. For both CO and SMO, the oil concentration in effluent remained zero far much longer in BMBS than SMBS thus showing the superior performance of BMBS than SMBS in treating CO and SMO. As for the control experiments, the removal for both of the emulsified oil due the other factors especially the column set up such as glass beads, tubing etc was observed as low with removal percentage below 0.065%.

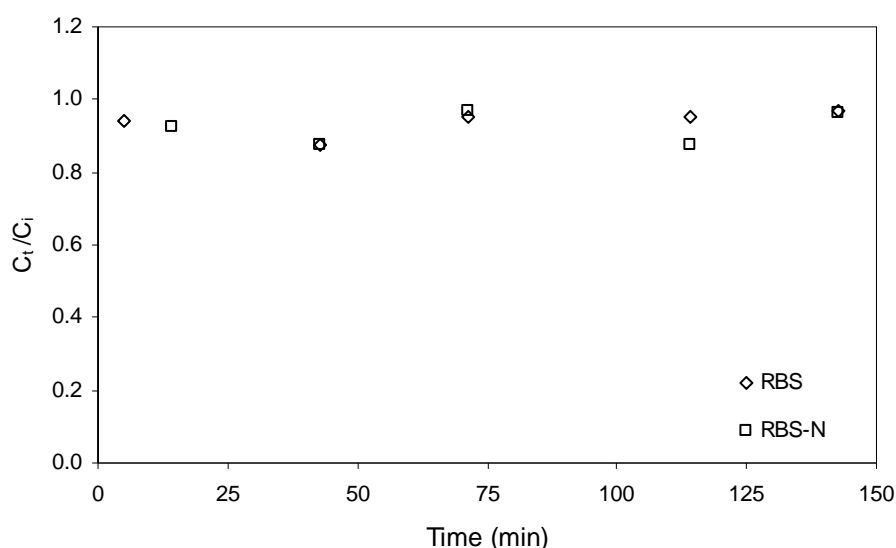


Figure 5.13a. Breakthrough plot of CO adsorption on RBS and RBS-N ([CO]: 1030 mgL<sup>-1</sup>, H = 8.0 cm; m = 5.0 g; Q = 7.0 mL min<sup>-1</sup>)

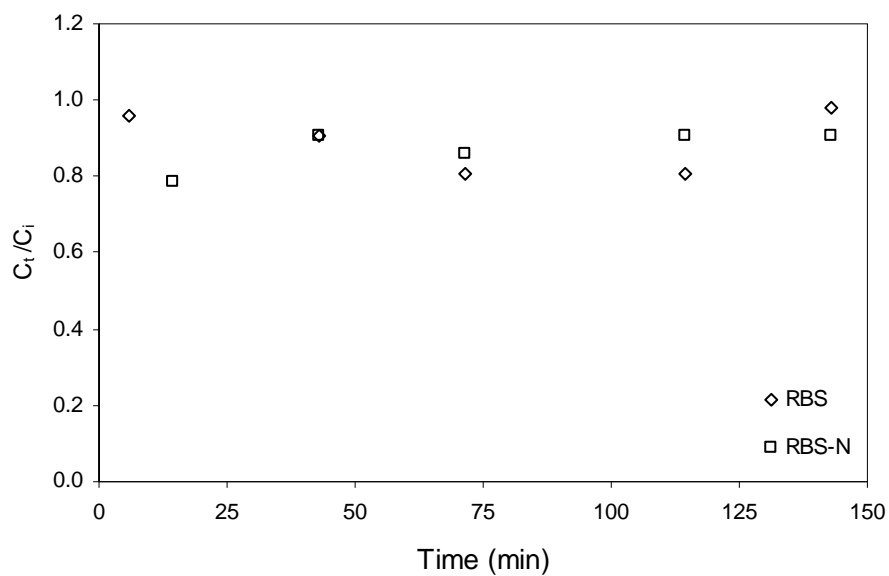


Figure 5.13b. Breakthrough plot of SMO adsorption on RBS and RBS-N ([SMO]:  $990 \text{ mgL}^{-1}$ ,  $H = 8.0 \text{ cm}$ ;  $m = 5.0 \text{ g}$ ;  $Q = 7.0 \text{ mL min}^{-1}$ )

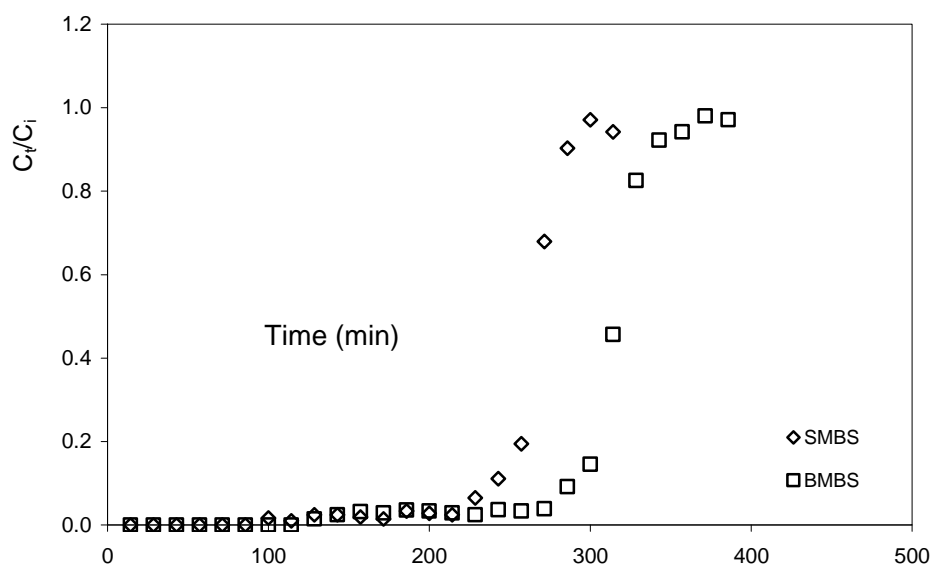


Figure 5.13c. Breakthrough plot of CO adsorption on SMBS and BMBS ([CO]:  $1030 \text{ mgL}^{-1}$ ,  $H = 8.0 \text{ cm}$ ;  $m = 5.0 \text{ g}$ ;  $Q = 7.0 \text{ mL min}^{-1}$ )

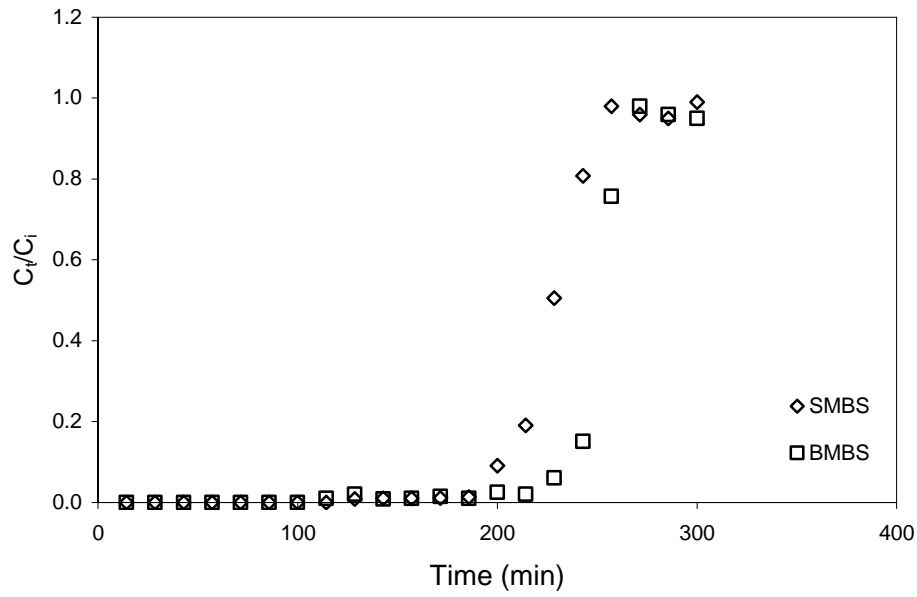


Figure 5.13d Breakthrough plot of SMO adsorption on SMBS and BMBS ([SMO]: 990 mgL<sup>-1</sup>, H = 8.0 cm; m = 5.0 g; Q = 7.0 mL min<sup>-1</sup>)

Table 5.5 summarizes the important data in the column studies. HRT is referred to column hydraulic residence time, meanwhile  $t_b$  and  $V_b$  are referred to breakthrough time and breakthrough volume, respectively.  $t_{exh}$  and  $V_{exh}$  are referred to column exhaustion time and column exhaustion volume, respectively,  $q_b$  is referred to breakthrough capacity. To facilitate the calculation of bed adsorption capacity, the breakthrough concentration is set at 5% of the inlet concentration. It is generally reported that the breakthrough concentration could be set at approximately 3-5% of the inlet concentration [263].

Hydraulic residence time (HRT) of effluent in the column is calculated as followed:

$$HRT = \frac{V_{cyl}}{Q} \quad (5.1)$$

where  $V_{cyl}$  and  $Q$  are volume of column (mL) and effluent volumetric flowrate ( mL min<sup>-1</sup>) respectively.

The total effluent volume ( $V_{\text{eff}}$ , mL) and breakthrough capacity ( $q_b$ , mg g<sup>-1</sup>) can be calculated from the following Eqs. 5.2 and 5.3, respectively:

$$V_{\text{eff}} = Qt \quad (5.2)$$

$$q_b = \frac{Qt_b C_i}{m} \quad (5.3)$$

where  $Q$  is the volumetric flow rate (mL min<sup>-1</sup>),  $t$  is the time (min),  $t_b$  is the breakthrough time (min) and  $m$  is the weight of adsorbent (g).

Data in Table 5.5 shows that SMBS gave shorter breakthrough time than BMBS for both CO and SMO. The breakthrough time of SMBS and BMBS was 223 and 274 min (CO); 192 and 225 min (SMO) respectively. At this point, 5 g of SMBS and BMBS manage to treat 1561 and 1918 L of CO; and 1344 and 1575 L of SMO respectively. These volumes correspond to column adsorption capacities ( $q_b$ ) of 321.57 and 395.11 mg g<sup>-1</sup> for CO; 266.11 and 311.85 mg g<sup>-1</sup> for SMO respectively. Generally, BMBS showed a greater efficiency compared to SMBS in treating the emulsified oil (of CO and SMO) as it exhibits longer column breakthrough time, higher amount of oil that could be treated at breakthrough time and greater adsorption capacity. This, however, was expected and consistent with the findings made in batch adsorption studies of CO and SMO (section 5.3)

Table 5.5. Adsorption breakthrough data for column experiments for the adsorption of CO and SMO on SMBS and BMBS

Oils	Adsorbent	HRT (min)	$t_b$ (min)	$V_b$ (mL)	$q_b$ (mg g <sup>-1</sup> )	$t_{\text{exh}}$ (min)	$V_{\text{exh}}$ (mL)
CO	SMBS	7.55	223	1561	321.57	296	2072
	BMBS	7.55	274	1918	395.11	360	2520
SMO	SMBS	7.55	192	1344	266.11	255	1785
	BMBS	7.55	225	1575	311.85	270	1890

([CO]: 1030 mgL<sup>-1</sup>, [SMO]: 990 mgL<sup>-1</sup>,  $H = 8.0$  cm;  $m = 5.0$  g;  $Q = 7.0$  mL min<sup>-1</sup>)

## 5.11 Modelling of Breakthrough Curves of Fixed Bed Column

It was rather difficult to understand the dynamic behavior of the fixed bed column as it did not occur at a steady state while the influent still passed through the bed. To describe the column adsorption behavior better, fixed bed column data were fitted to the models such as the Thomas and Yoon-Nelson models. The nonlinear equations of the Thomas and Yoon-Nelson models listed in Eqs. 3.13 and 3.14 (section 3.8) respectively were curve fitted for adsorption of CO and SMO by employing a trial and error method using Polymath software.

### 5.11.1 Thomas model

The Thomas model, which was formulated by Thomas [20], determines the maximum solid phase concentration of solute on the adsorbent and the adsorption rate constant for an adsorption column [264]. The Thomas plots for adsorption of CO and SMO are shown in Figs. 5.14a and 5.14b, respectively. At a glance, it can be observed that the simulation of whole breakthrough curve was predicted well by the Thomas model for all the plots. Higher  $R^2$  values of 0.99 for all the column tests (Table 5.6) indeed support this assumption. The packing of column with glass beads did help to evenly distribute the solute throughout the adsorbent packing thus minimize the occurrence of axial dispersion as what has been discussed in section 2.9. This was consistent with the hypothesis made to the Thomas model, which assumes no axial dispersion exists in the model.

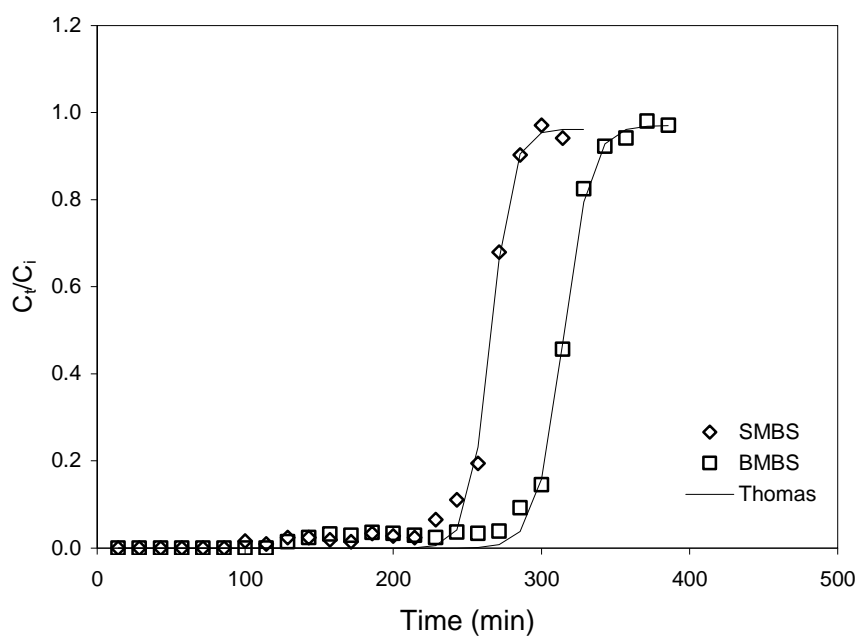


Figure 5.14a. Nonlinear Thomas plots for adsorption of CO onto SMBS and BMBS

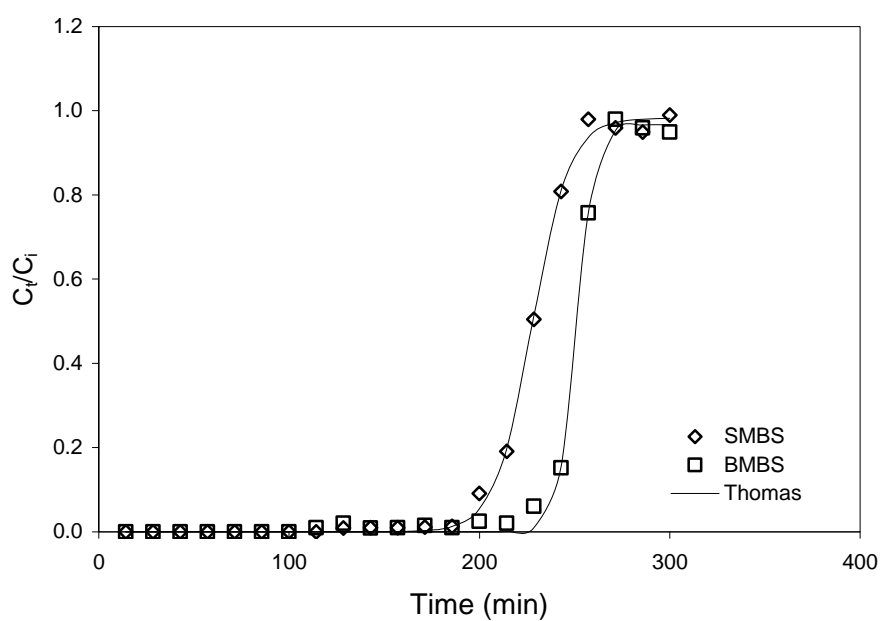


Figure 5.14b. Nonlinear Thomas plots for adsorption of SMO onto SMBS and BMBS

Table 5.6 summarizes the parameter values in the column studies where  $k_{Th}$  is the Thomas rate constant and  $q_0$  is the equilibrium oil uptake. The values of column

adsorption capacity,  $q_0$  calculated from the Thomas model for SMBS and BMBS were 368.82 and 440.74  $\text{mg g}^{-1}$  for CO; 310.16 and 336.31  $\text{mg g}^{-1}$  for SMO respectively. Higher adsorption capacity of BMBS than SMBS for both CO and SMO column system was consistent with the finding obtained in batch study (section 5.4) and was expected due to more CPC on BMBS. Generally, the adsorption capacities calculated from the Thomas model were lower than the values obtained in batch study, where the batch adsorption capacity was 576.00 and 613.29  $\text{mg g}^{-1}$  for CO; and 518.63 and 584.22  $\text{mg g}^{-1}$  for SMO respectively. The relatively lower adsorption capacity observed in fixed bed column than batch adsorption study was due to the liquid channelling as suggested by Amarasinghe and Williams [265], which results in poor interaction of adsorbate-adsorbent, poor adsorbate residence time and the failure of the column system to reach equilibrium. This was evidenced as contact time of straw with emulsified oil in column test was only 7.55 min and this is below the equilibrium time of about 35 min obtained from batch dynamic experiments ( section 5.3)

Table 5.6. Thomas model parameters for fixed-bed adsorption of CO and SMO

Oil	Adsorbent	$k_{\text{Th}}$ $\text{mL mg}^{-1} \text{min}^{-1}$	$q_0$ $(\text{mg g}^{-1})$	$R^2$
CO	SMBS	0.137	368.82	0.99
	BMBS	0.109	440.74	0.99
SMO	SMBS	0.105	310.16	0.99
	BMBS	0.210	336.31	0.99

#### 5.11.2 Yoon-Nelson model

The Yoon-Nelson model is the simplest theoretical model developed by Yoon-Nelson to investigate the column breakthrough behavior. Similar to the Thomas model, the Yoon-Nelson model also gave good fit to the experimental data as this model also predicts the same uptake capacity and  $C_t/C_i$  values for a particular data set, thus it'll be expected to produce the same  $R^2$  values [225]. This was indeed true in non linear plots of the Yoon-Nelson model in Figs. 5.15a to 5.15b, where a good fit with  $R^2$  of 0.99 for all column systems was obtained, similar to the  $R^2$  obtained in the Thomas model ( Table 5.7).

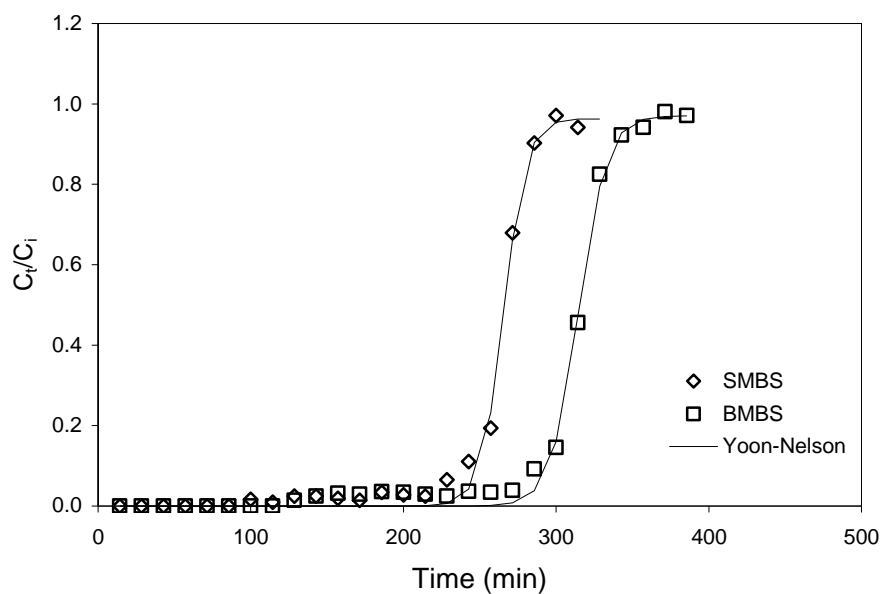


Figure 5.15a. Non linear Yoon-Nelson plots for adsorption of CO onto SMBS and BMBS

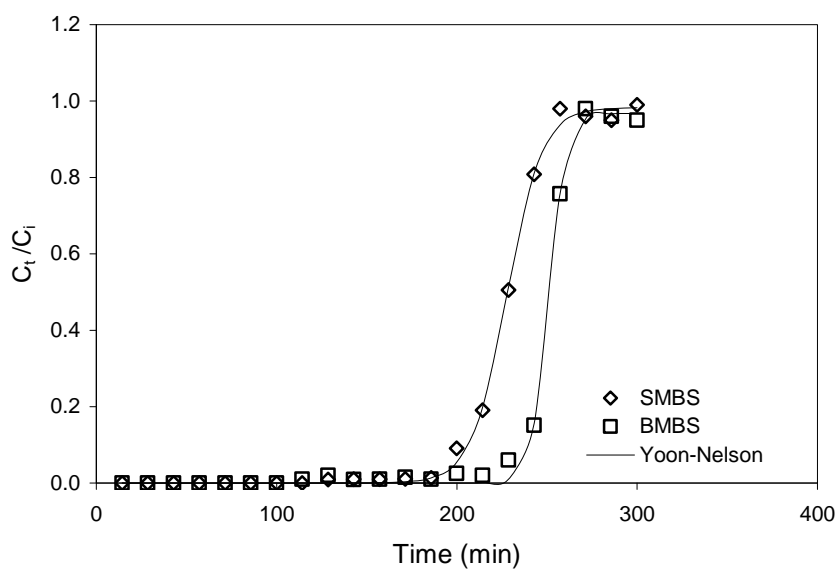


Figure 5.15b. Non linear Yoon-Nelson plots for adsorption of SMO onto SMBS and BMBS

In Table 5.7,  $k_{YN}$  is referred to the Yoon-Nelson rate constant and  $\tau$  is the time required for 50% adsorbate breakthrough. The time required to achieve 50% of adsorbate breakthrough ( $\tau$ ) for SMBS and BMBS was 265 and 314.7 min for CO; and 227.7 and 250.9 min for SMO respectively. The relatively longer ' $\tau$ ' for BMBS for

the column system compared to SMBS showed the superiority of BMBS. It could be observed in Table 5.6 also that the time required to achieve 50% of adsorbate breakthrough ( $\tau$ ) from the Yoon-Nelson model seemed in agreement with the experimental data ( $t_{50\%,\text{exp}}$ ) in all column adsorption tests. This indicated a good applicability of this model in column operations.

Table 5.7. Yoon-Nelsons model parameters for fixed-bed adsorption of CO and SMO

Dye	Adsorbent	$k_{YN}$ ( $\text{min}^{-1}$ )	$\tau$ (min)	$t_{50\%,\text{exp}}$ (min)	$R^2$
CO	SMBS	0.136	265.6	266	0.99
	BMBS	0.109	314.7	316	0.99
SMO	SMBS	0.103	227.7	228	0.99
	BMBS	0.205	250.9	251	0.99

## 5.12 Section Summary

Preliminary experimental study showed the effectiveness of cationic surfactant modified straws (SMBS and BMBS) in emulsified oil removal compared to unmodified straw. FT-IR spectra also indicated the involvement of surfactant on the straw surface to adsorb emulsified oil. The effectiveness of the surfactant modified barley straw, SMBS and BMBS for removal of emulsified CO and SMO was further evaluated under various experimental conditions. In batch study, the kinetic experiment revealed that adsorption of oil was rapid at initial stage followed by a slower phase where equilibrium uptake was achieved. The equilibrium time at lower concentration of CO ( $1040 \text{ mg L}^{-1}$ ) was 15 min for both SMBS and BMBS while the equilibrium would take a relatively longer time at 45 and 35 min, for SMBS and BMBS, respectively, at higher concentration of CO ( $3450 \text{ mg L}^{-1}$ ). For SMO, the equilibrium time for both SMBS and BMBS at lower concentration of  $1580 \text{ mg L}^{-1}$  was 20 min and the equilibrium time increased to 45 and 35 min for SMBS and BMBS, respectively at relatively higher concentration of  $4315 \text{ mg L}^{-1}$ . The equilibrium time was quicker for lower oil concentration. The pseudo first order model provided the best correlation for the kinetic adsorption data of CO and SMO for both SMBS and BMBS. Kinetic diffusion study identified that film diffusion

controls the adsorption of CO and SMO onto SMBS and BMBS. The Langmuir isotherm provided the best correlation for the equilibrium adsorption data of CO and SMO for both SMBS and BMBS. The Langmuir adsorption capacities of CO and SMO were 576.00 and 518.63 mg g<sup>-1</sup> for SMB; 613.29 and 584.22 mg g<sup>-1</sup> for BMBS respectively. Desorption experiments also showed good stability of the oil loaded on straw while being exposed to deionized water. The batch study also revealed that the adsorption was a function of oil concentration, pH, temperature of oil solution and adsorbent particle size. The adsorption capacity of SMBS and BMBS for both CO and SMO was very low when the oil solution was in strong acidic condition (i.e pH 2) and reached the maximum at pH around neutral (pH 6 and 8). For both CO and SMO, temperature at 23 and 33 °C could not produce a significant effect on the adsorption. However, oil uptake was found to increase at relatively higher temperature (43 °C). Adsorption capacity was observed to be closely related to size of adsorbent where adsorption capacity was the highest at the smallest adsorbent size.

In fixed bed column tests, RBS and RBS-N revealed the low efficiency in removing CO and SMO. SMBS and BMBS were observed to favorably treat both oils and the breakthrough curves exhibited the 'S' shape, an indication of a favorable and normal column adsorption process. Compared to SMBS, the effluent concentration remains longer at zero for BMBS for both oils, thus giving an indication of superiority of BMBS compared to SMBS. The breakthrough column models such as the Thomas and Yoon-Nelson models showed the suitability to the column experimental data of SMBS and BMBS with R<sup>2</sup> of 0.99 for all the plots. The Thomas column adsorption capacities of CO and SMO were 368.82 and 310.16 mg g<sup>-1</sup> for SMBS; and 440.74 and 336.31 mg g<sup>-1</sup> for BMBS respectively. Meanwhile Yoon-Nelson prediction of time required to achieve 50% of adsorbate breakthrough( $\tau$ ) seemed to agree well with the time ( $t_{50\%,\text{exp}}$ ) obtained from experimental data. The time required to achieve 50% of adsorbate breakthrough( $\tau$ ) for CO and SMO were 265 and 227.7 min for SMBS; and 314.7 and 250.9 min for BMBS respectively.

## REMOVAL OF ANIONIC DYES

### 6.1 Introduction

This section describes the tests of various barley straws as adsorbents for anionic dye wastewater cleaning. Two types of studies were conducted and would be discussed, batch and fixed bed column results. Preliminary experiments were conducted in batch wise mode to determine the effectiveness of the prepared adsorbents, RBS, RBS-N, SMBS and BMBS in removing different types of anionic dyes such as Acid Blue (AB40), Reactive Blue (RB4) and Reactive Black (RB5). The influences of physicochemical parameters such as contact time, adsorption temperature and pH of the solution on dye uptake were investigated and discussed. Leaching of dyes from spent straws was also tested at different initial pHs to determine the stability and applicability of the adsorbents at various conditions and the possible mechanism of sorbed dyes onto straw surface. The fixed bed column tests mainly showed column breakthrough curves. To understand the adsorption process and mechanism, the experimental data were analyzed with commonly used kinetic models; pseudo first order, pseudo second order and the Boyd diffusion model; Isotherm was described by fitting isotherm data to the Freundlich and Langmuir models. For fixed bed column breakthrough, the experimental data were fitted to the models such as the Thomas and Yoon-Nelson equations. Standard error of the measurement for the analyses that was run duplicated were calculated using equation 3.16 and the results were shown in appendix C

## 6.2 Preliminary Experiments

The removal percentages of various dyes on RBS, RBS-N, SMBS and BMBS are shown in Fig. 6.1. Unlike SMBS and BMBS, the removal percentage of anionic dyes using RBS and RBS-N was low at 7.61 and 12.57% for AB40; 1.51 and 1.34% for RB4; and 0.92 and 0.80% for RB5, respectively. SMBS and BMBS demonstrated satisfactory removal of 95.63 and 97.44% for AB40; 55.05 and 62.41% for RB4; and 55.24 and 64.68% for RB5 respectively. This was consistent with what was reviewed in section 2.14, where the modification of straw with a cationic surfactant renders the sorbent surface to a positive potential, which is conducive for the removal of anionic contaminants. The results also agree well with the findings made in section 5.2 for preliminary experiments of oil-straw system, thus justified SMBS and BMBS as effective adsorbents for subsequent studies. Insignificant removal below 0.005% of dye solution was observed in experiments that were run without the participation of an adsorbent material thus eliminating the dye removal due to the other factors.

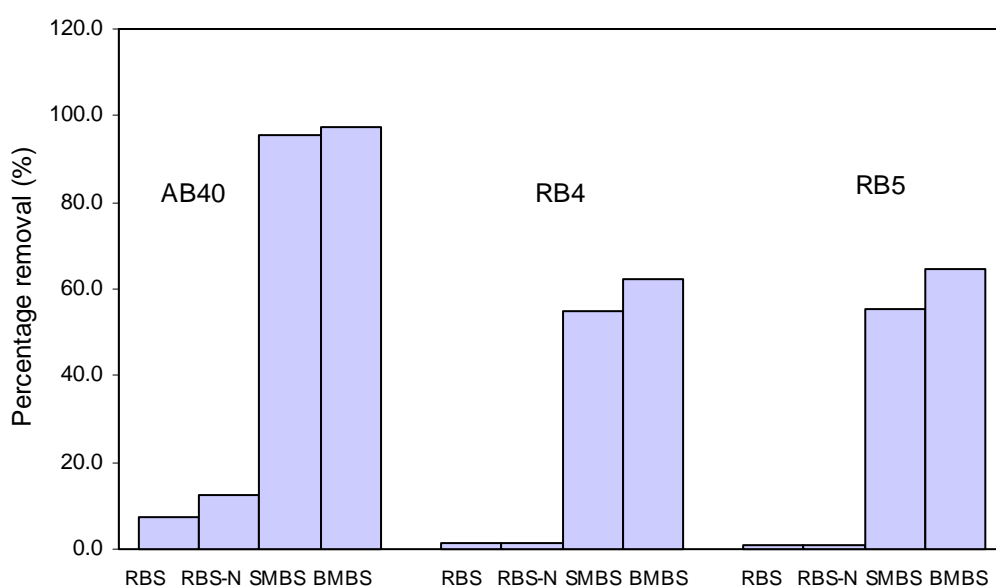


Figure 6.1. Adsorption of AB40, RB4 and RB5 using unmodified and surfactant modified straw

( [Dyes]: 100 mgL<sup>-1</sup>; Contact time: 8 hrs; shaking speed: 170 rpm; dosage: 2 g L<sup>-1</sup>; Temperature: 25 °C; Dye solution pH: AB40: 5.8, RB4: 5.6, RB5: 5.0 )

The participation of a cationic surfactant on dye uptake was confirmed by the FT-IR spectra of fresh and dye loaded adsorbents. The comparison of the spectra of fresh and dye loaded of SMBS and BMBS are shown in Figs. 6.2a and 6.2b. It was observed that the carboxylic and carbonyl group bands at about  $2850\text{ cm}^{-1}$  originated from CPC on the straw surface, as discussed in section 4.6, were almost diminished compared to the fresh SMBS and BMBS (Figs. 6.2a and 6.2b). Thus, it suggests the involvement of chemical bonding between the modified straw and anionic dyes, AB40, RB4 and RB5. Similar conclusions were made by Sureshkumar and Namasivayam [162] in their work pertaining to the removal of Rhodamine B by a surfactant modified coir pith. It was revealed in section 2.14, that modification with a cationic surfactant resulted in reversing the surface potential of straw from negative to positive. This made the surfactant modified straw surface capable of removing anionic contaminants, as it will attract the opposite electron charged surface. Based on this information, the mechanism of anionic dyes adsorbed on the modified straw surface was suggested and illustrated in Fig. 6.3.

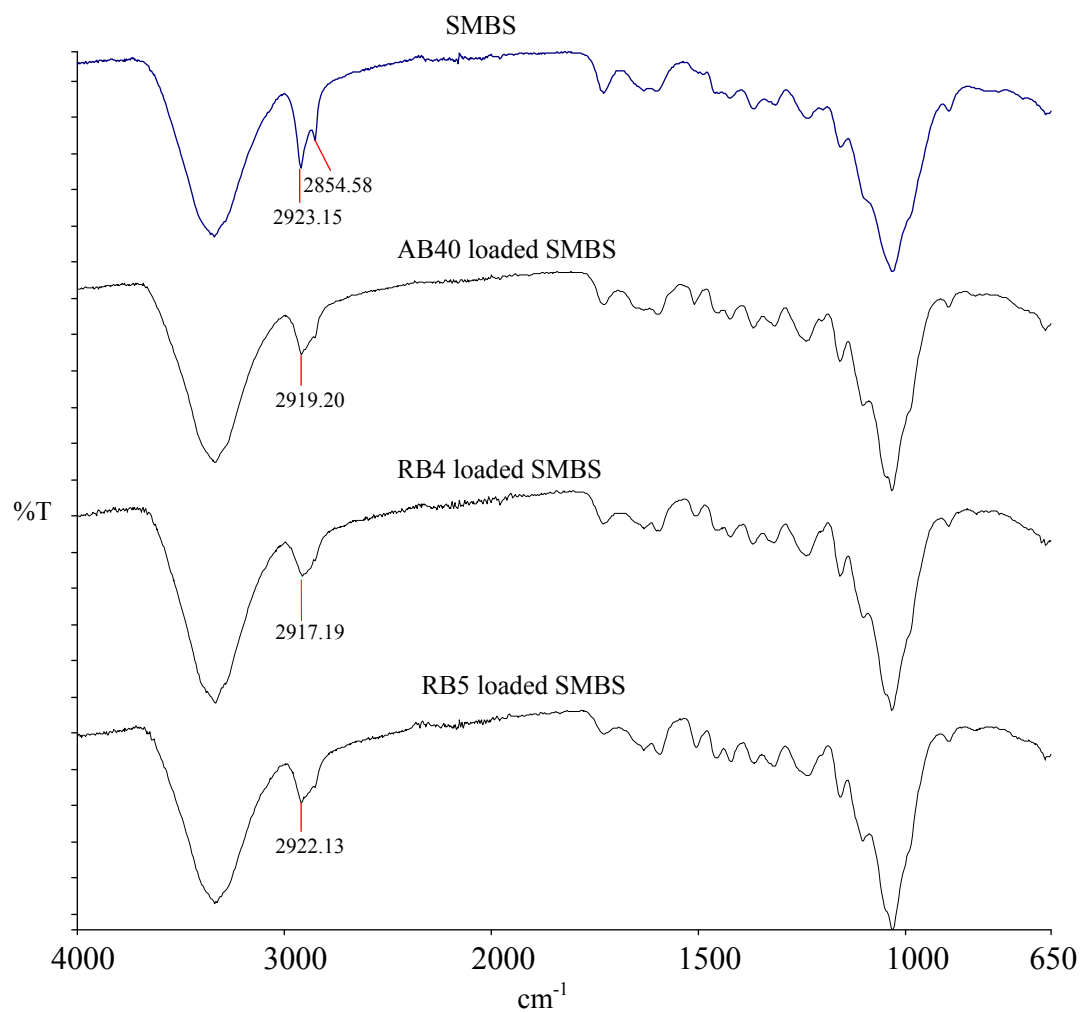


Figure 6.2a. FT-IR spectra of SMBS and dyes loaded SMBS

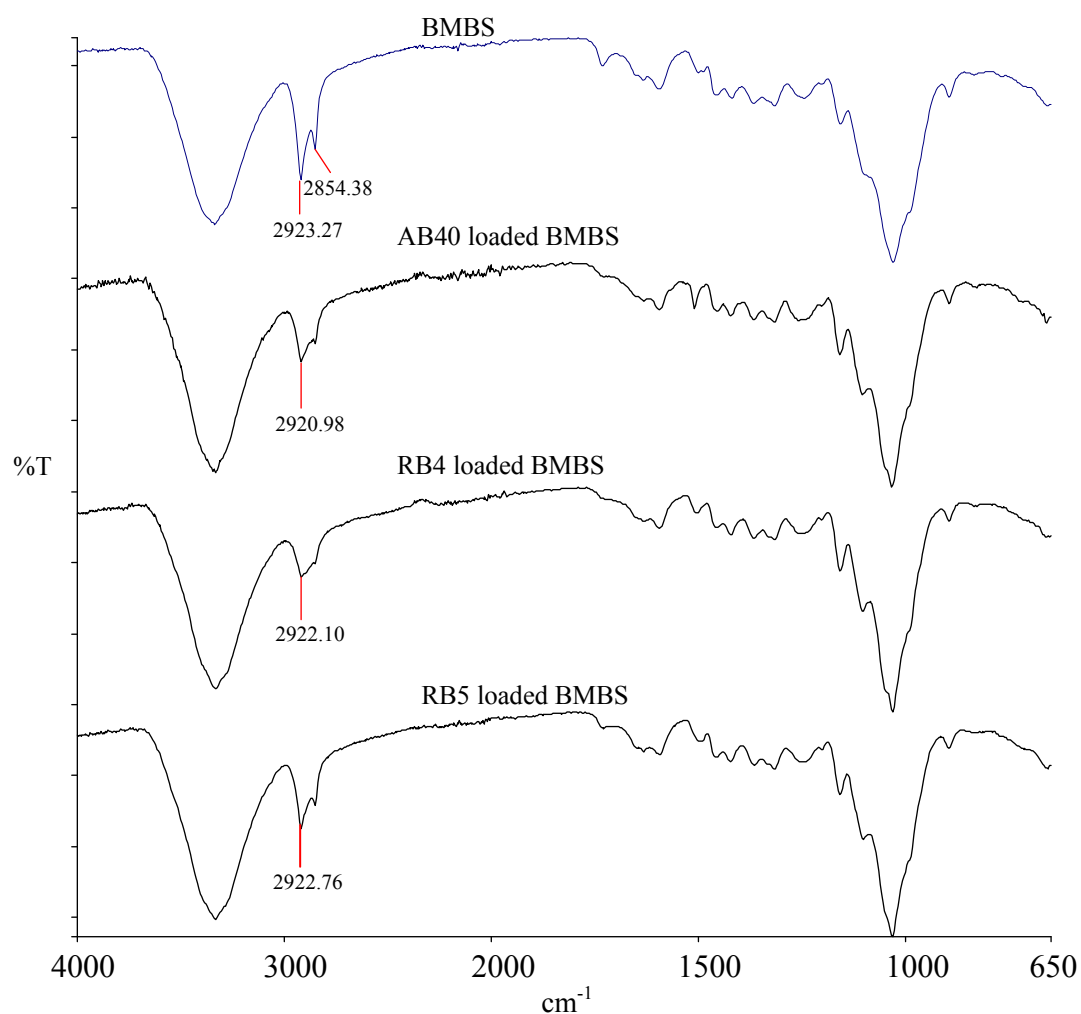


Figure 6.2b. FT-IR spectra of BMBS and dyes loaded BMBS

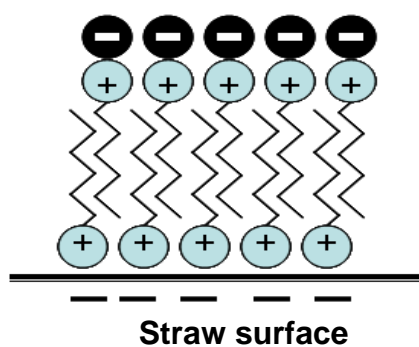


Figure 6.3. Schematic diagram showing anionic dyes (represented by black round dots) attracted onto opposite charge on modified straw

### 6.3 Dynamic Adsorption

Dynamic sorption of dyes on SMBS and BMBS are shown in Figs. 6.4a to 6.4c. As presented, most of dye uptake on SMBS and BMBS occurred at the primary rapid phase, followed by a relatively small uptake before it reached equilibrium. It was pointed out in section 5.3 that greater amounts of binding sites that are available at earlier stage of adsorption process may contribute to this rapid stage. However, as the time was increased a small amount of dye uptake was observed due to less adsorption sites available [252]. Generally, the equilibrium time of dye sorption was observed to increase with increasing initial dye concentration. For lower concentration of dye solution of  $50 \text{ mg L}^{-1}$ , the equilibrium time on SMBS and BMBS was 90 and 60 min for AB40; 90 and 60 min for RB4; 180 and 210 min for RB5, respectively. For a higher concentration of dye solution of  $100 \text{ mg L}^{-1}$ , the equilibrium time on SMBS and BMBS was 120 and 90 min for AB40; and 120 and 240 min for RB4 and RB5 for both SMBS and BMBS. Due to the variation of equilibrium time at different initial concentrations of each dye, therefore, it is determined that the batch adsorption time can be set at 300 min for all the dyes to ensure the equilibrium attained as well as to ease of handling and sampling scheduling during the experimental work.

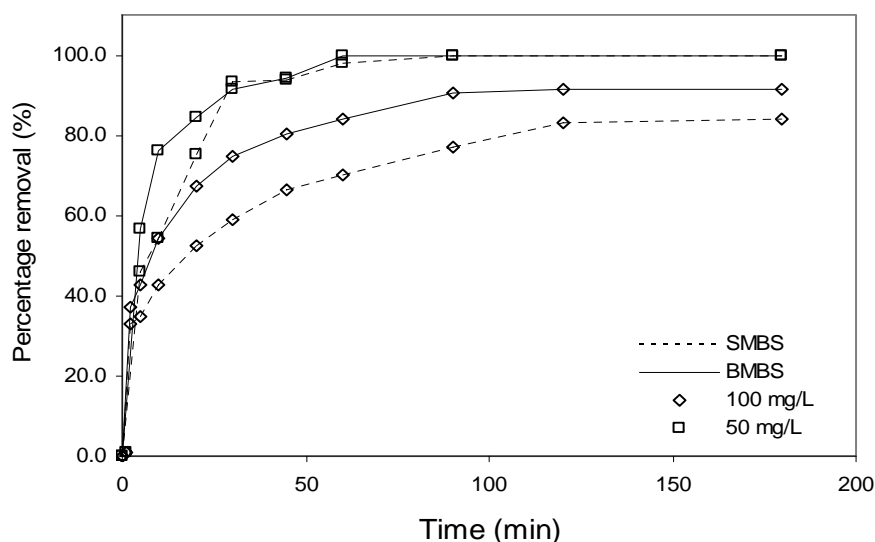


Figure 6.4a. Effect of contact time on adsorption of AB40 onto SMBS and BMBS. (Shaking speed: 170 rpm; dosage:  $2 \text{ g L}^{-1}$ ; Temperature:  $25^\circ\text{C}$ ; Dye solution pH: AB40: 5.8, RB4: 5.6, RB5: 5.0)

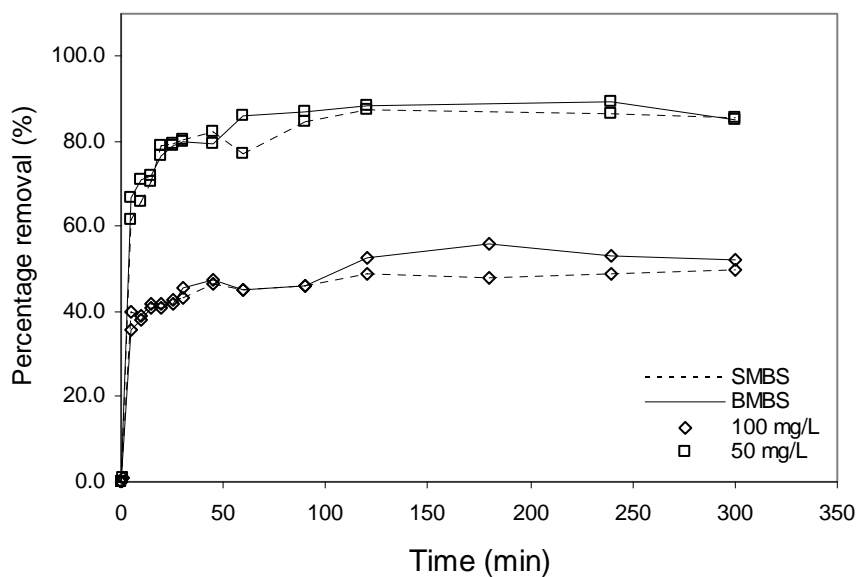


Figure 6.4b. Effect of contact time on adsorption of RB4 onto SMBS and BMBS. (Shaking speed: 170 rpm; dosage: 2 g L<sup>-1</sup>; Temperature: 25 °C; Dye solution pH: AB40: 5.8, RB4: 5.6, RB5: 5.0)

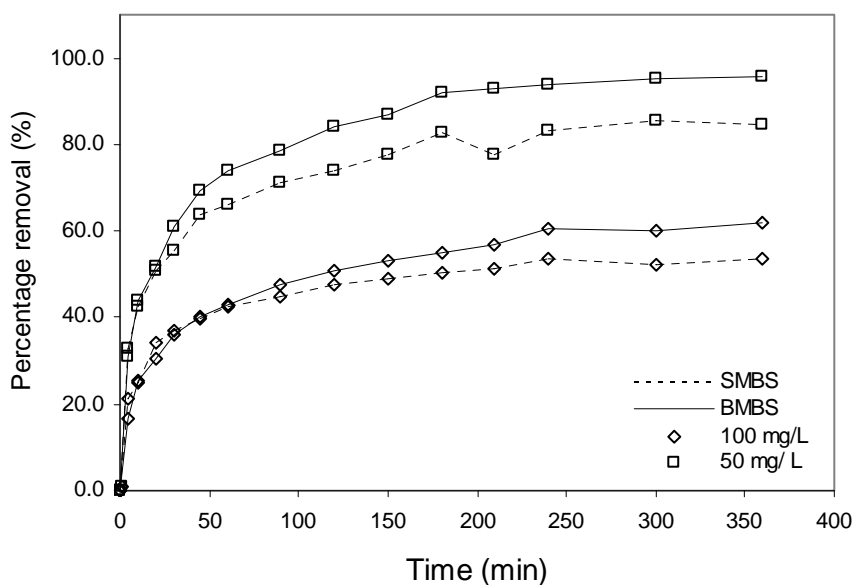


Figure 6.4c. Effect of contact time on adsorption of RB5 onto SMBS and BMBS. (Shaking speed: 170 rpm; dosage: 2 g L<sup>-1</sup>; Temperature: 25 °C; Dye solution pH: AB40: 5.8, RB4: 5.6, RB5: 5.0)

### 6.3.1 Kinetic Models

The dynamic dye adsorption was simulated using pseudo-first order and pseudo-second-order models. Non linear equations of the pseudo-first order (Eq. 3.4) and pseudo-second-order models (Eq. 3.5) were curve fitted by employing the trial and error method using Polymath software and the plots are shown in Figs. 6.5a to 6.7b. The best fit of the experimental data to the kinetic models was determined by the regression coefficient,  $R^2$  and error values of the modelling. In Table 6.1,  $K_1$  and  $K_2$  represent the rate constants of the pseudo first order and second order, respectively, whereas  $q_e$  and  $q_t$  are the amount of dye adsorbed at equilibrium and time  $t$ , respectively.

At a glance, the equilibrium adsorption from the pseudo second order model seems to be better in modelling the kinetics for the whole adsorption process. This was further confirmed by performing the regression and error function analysis on experimental data. For Table 6.1, the  $R^2$  of the pseudo second order for AB40, RB4 and RB5 was either the same or higher than that of the pseudo first order model, suggesting the suitability of the pseudo second order to the experimental data. The error function values, MPSD, of the pseudo second order model for SMBS and BMBS were lower (than those of the pseudo-first order model) for all the dye adsorption, which further validates the better fit of the pseudo second order to the experimental data. The experimental adsorption capacities ( $q_{e, \text{exp}}$ ) much closer to the calculated adsorption capacities ( $q_{e, \text{cal}}$ ) in Table 6.1 indeed suggests the better fit of the second order model to the kinetics.

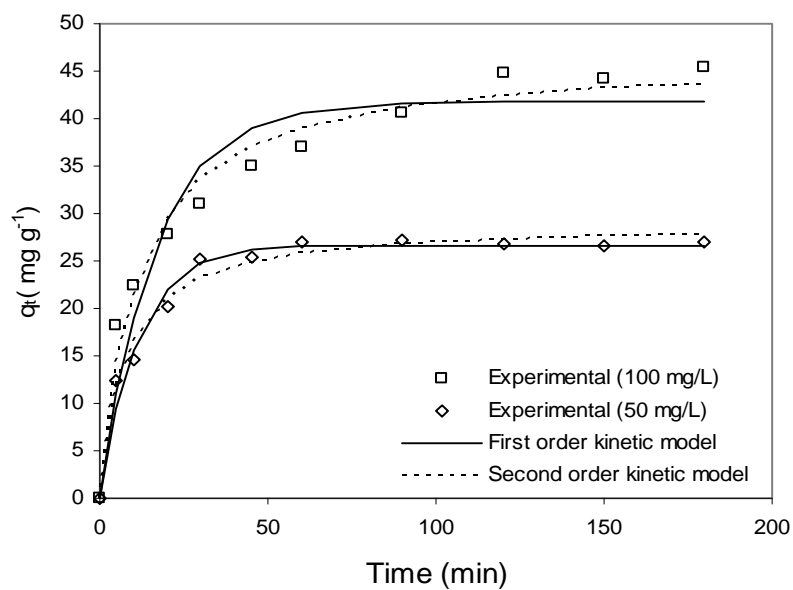


Figure 6.5a. Nonlinear kinetic models for adsorption of AB40 onto SMBS

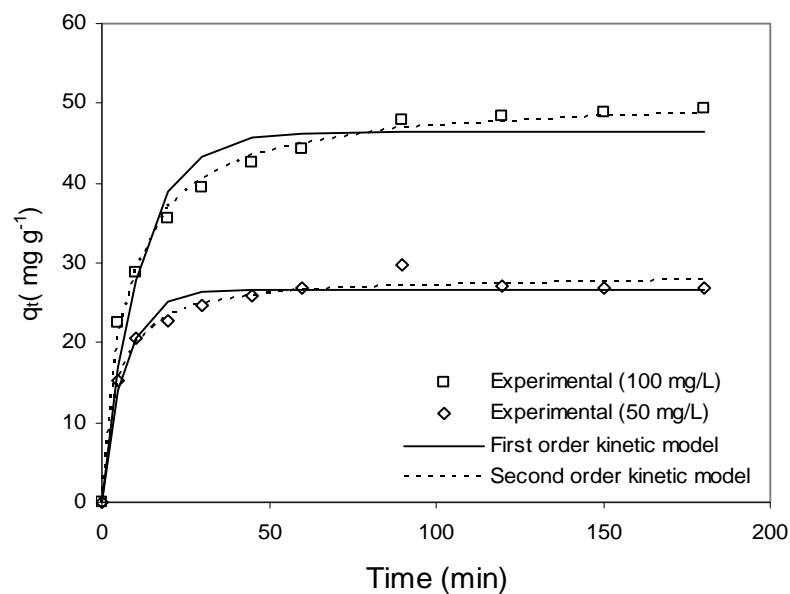


Figure 6.5b. Nonlinear kinetic models for adsorption of AB40 onto BMBS

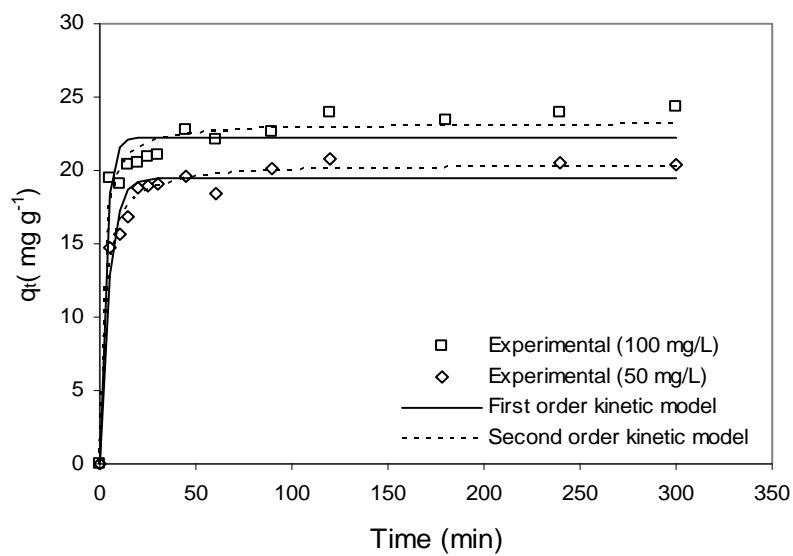


Figure 6.6a. Nonlinear kinetic models for adsorption of RB4 onto SMBS

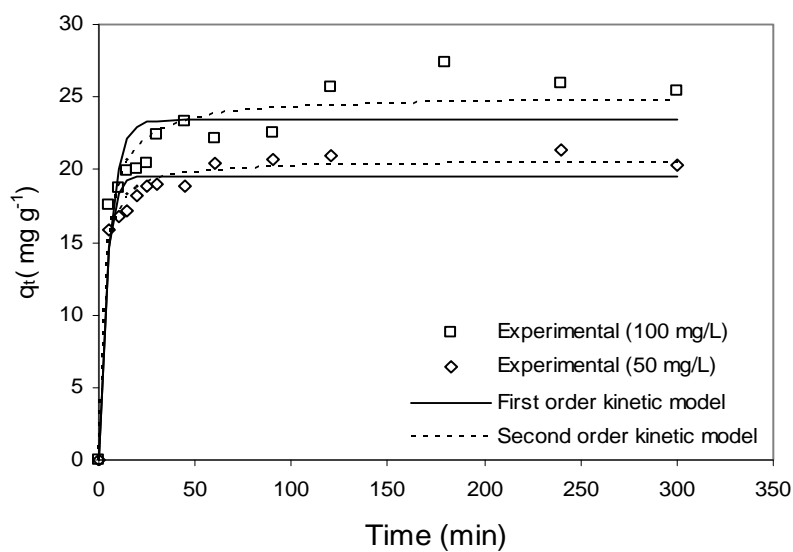


Figure 6.6b. Nonlinear kinetic models for adsorption of RB4 onto BMBS

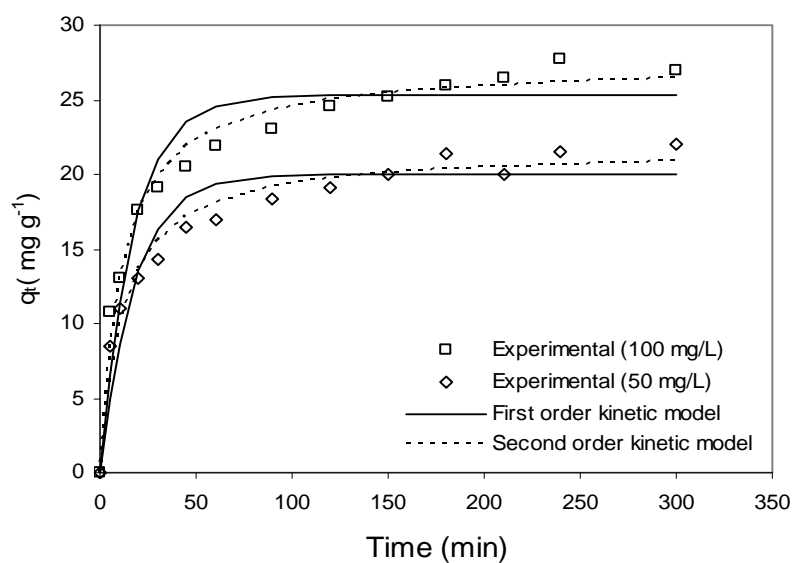


Figure 6.7a. Nonlinear kinetic models for adsorption of RB5 onto SMBS

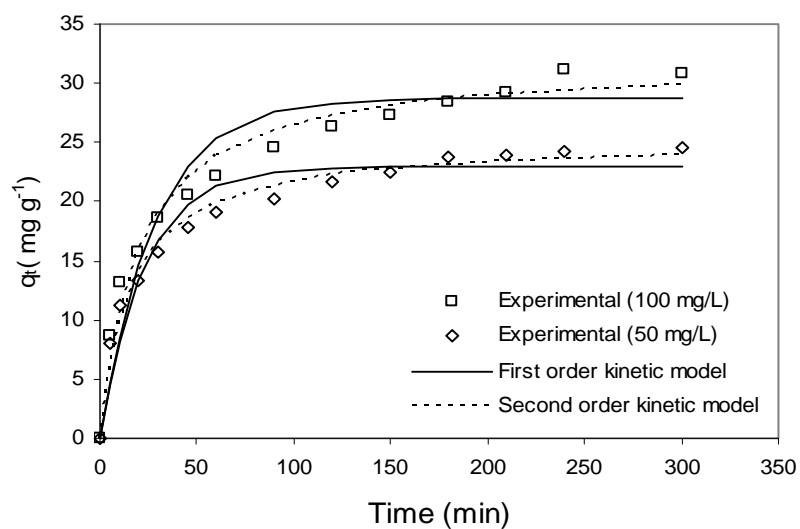


Figure 6.7b. Nonlinear kinetic models for adsorption of RB5 onto BMBS

Table 6.1. Kinetics models constants and error analysis for adsorption of anionic dyes on SMBS and BMBS

Dyes	Experimental		Kinetics Models Constant					Error Analysis			
	Adsorbent	[Dye]	Exp.	Pseudo first order		Pseudo second order		Pseudo first order		Pseudo second order	
		(mg L <sup>-1</sup> )	q <sub>e</sub> (mg g <sup>-1</sup> )	k <sub>1</sub> (min <sup>-1</sup> )	q <sub>e</sub> (mg g <sup>-1</sup> )	k <sub>2</sub> (min <sup>-1</sup> )	q <sub>e</sub> (mg g <sup>-1</sup> )	R <sup>2</sup>	MPSD	R <sup>2</sup>	MPSD
AB40	SBS	50	27.01	0.09	26.51	4.30 x 10 <sup>-3</sup>	29.38	0.98	10.69	0.98	7.31
		100	43.82	0.09	39.28	2.90 x 10 <sup>-3</sup>	43.19	0.86	26.53	0.93	19.06
	BBS	50	27.01	0.16	25.97	9.00 x 10 <sup>-3</sup>	28.04	0.98	5.76	0.99	2.09
		100	47.83	0.12	44.72	4.00 x 10 <sup>-3</sup>	48.63	0.92	20.15	0.97	13.04
RB4	SBS	50	20.1	0.22	19.43	1.07 x 10 <sup>-1</sup>	20.47	0.96	7.22	0.98	4.00
		100	23.9	0.36	22.23	2.75 x 10 <sup>-2</sup>	23.24	0.94	7.50	0.98	4.85
	BBS	50	20.4	0.28	19.57	2.41 x 10 <sup>-2</sup>	20.62	0.95	7.51	0.98	4.18
		100	25.7	0.19	23.44	1.22 x 10 <sup>-2</sup>	25.07	0.88	11.30	0.95	7.44
RB5	SBS	50	21.4	0.06	20.02	3.90 x 10 <sup>-3</sup>	21.68	0.93	16.86	0.97	9.22
		100	27.7	0.06	25.30	3.20 x 10 <sup>-3</sup>	27.40	0.91	15.10	0.98	7.83
	BBS	50	24	0.04	22.97	3.00 x 10 <sup>-3</sup>	25.15	0.94	17.25	0.98	9.10
		100	31.2	0.04	28.73	1.00 x 10 <sup>-3</sup>	31.92	0.93	19.41	0.98	11.04

### 6.3.2 Kinetic diffusion models

Similar to the oil-straw system, the Boyd diffusion model was also employed to predict the controlling diffusion step in dye-straw systems. The theory regarding this model has been thoroughly discussed in section 3.7.2. In brief, film diffusion is identified as a controlling step if the straight line in the Boyd plots does not pass through the origin and the effective diffusion,  $D_i$  values calculated from the Boyd model fall within  $10^{-6} - 10^{-8} \text{ cm}^2 \text{ s}^{-1}$  range.

The Boyd plots of  $B_t$  against time derived from Eqs.3.9 and 3.10 (section 3.7) for all the dye-straw systems were constructed and presented in Figs. 6.8a to 6.10b. Unlike the Boyd plots for CO and SMO (section 5.3.2), the plots for AB40 and RB5 produce relatively decent linear lines with  $R^2$  of about 0.9 and higher for all the plots (Table 6.2). However, AB40 and RB5 linear line was not passing through the origin, even though RB5 was so close (to pass the origin) (Figs. 6.8a to 6.10b). This indicates the film diffusion mainly governed the AB40 and RB5 sorption onto SMBS and BMBS. As for RB4, the plots however did not produce a good straight line where some of the points were scattered with a low  $R^2$ . Due to this, it could also be concluded that film diffusion played a role as a controlling step similar to AB40 and RB5.

To further justify the above conclusion, the kinetic data were also evaluated in the form of effective diffusion rate,  $D_i$ . Due to the straw that was not spherical shape, in Table 6.2,  $D_i$  was presented in a range of values according to radius range of straw particle size used.  $D_i$  values for all the plots are presented in Table 6.2 and were observed to be within the range of  $10^{-6} - 10^{-8} \text{ cm}^2 \text{ s}^{-1}$ , thus further confirming our earlier conclusion that the slowest step sorption of AB40, RB4 and RB5 on SMBS and BMBS was film diffusion. For AB40,  $D_i$  for the concentration of 50 and 100  $\text{mg L}^{-1}$  are  $3.72 \times 10^{-6}$ - $2.07 \times 10^{-5}$  and  $1.40 \times 10^{-6} - 7.79 \times 10^{-6}$  (SMBS); and  $2.04 \times 10^{-6} - 1.14 \times 10^{-5} \text{ cm}^2 \text{ s}^{-1}$  (BMBS), respectively.

For RB4 the  $D_i$  for the concentration of 50 and 100  $\text{mg L}^{-1}$  are  $4.00 \times 10^{-6} - 2.23 \times 10^{-5}$  and  $1.04 \times 10^{-6} - 5.82 \times 10^{-6} \text{ cm}^2 \text{ s}^{-1}$  (SMBS); and  $3.06 \times 10^{-6} - 1.71 \times 10^{-6}$  and  $6.90 \times 10^{-7} - 3.84 \times 10^{-6} \text{ cm}^2 \text{ s}^{-1}$  (BMBS), respectively. Meanwhile, for RB5, the  $D_i$  for the concentration of 50 and 100  $\text{mg L}^{-1}$  are  $8.36 \times 10^{-7} - 4.66 \times 10^{-6}$  and  $6.90 \times 10^{-7} - 3.84 \times$

$10^{-6} \text{ cm}^2 \text{ s}^{-1}$  (SMBS); and  $9.56 \times 10^{-7} - 5.33 \times 10^{-6}$  and  $6.40 \times 10^{-7} - 3.56 \times 10^{-6} \text{ cm}^2 \text{ s}^{-1}$  (BMBS), respectively.

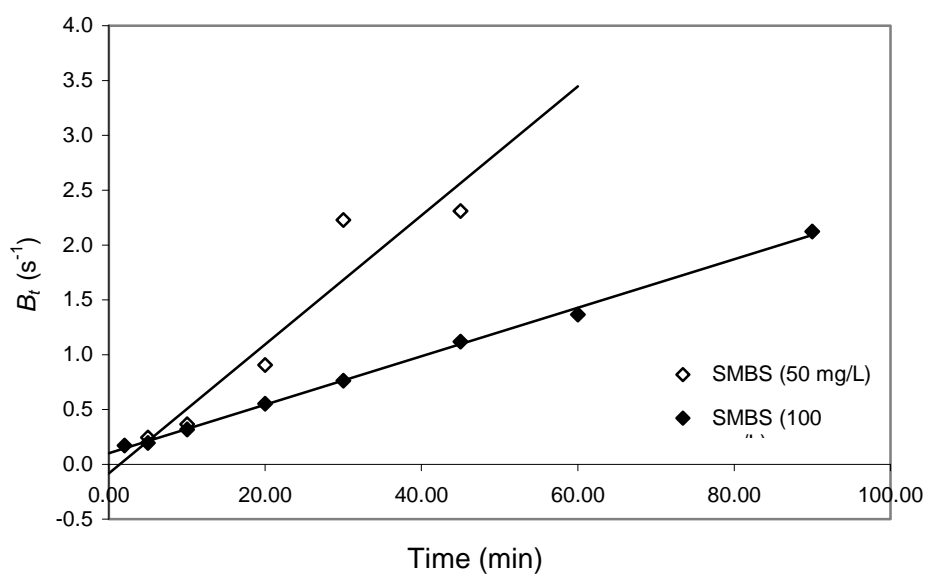


Figure 6.8a. Boyd plot for the sorption of AB40 onto SMBS

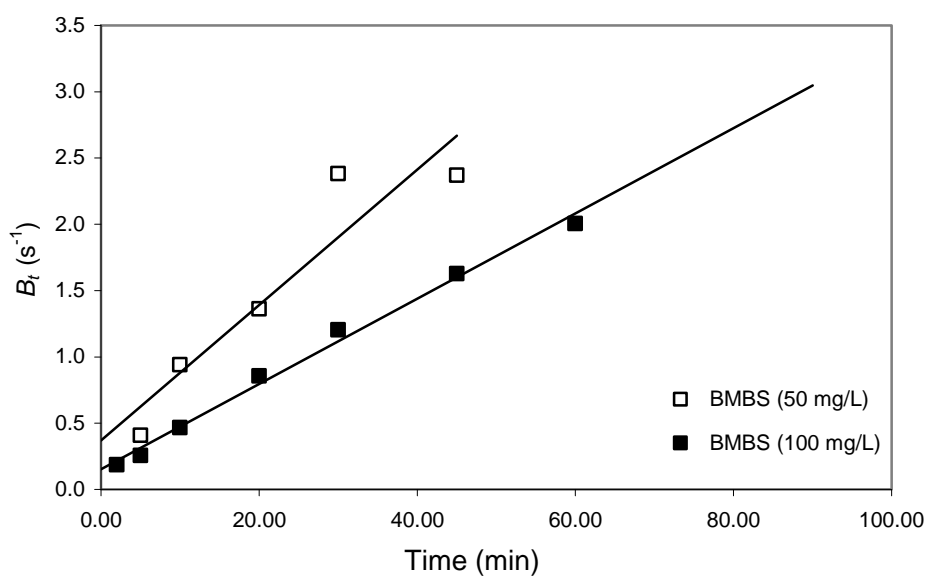


Figure 6.8b. Boyd plot for the sorption of AB40 onto BMBS

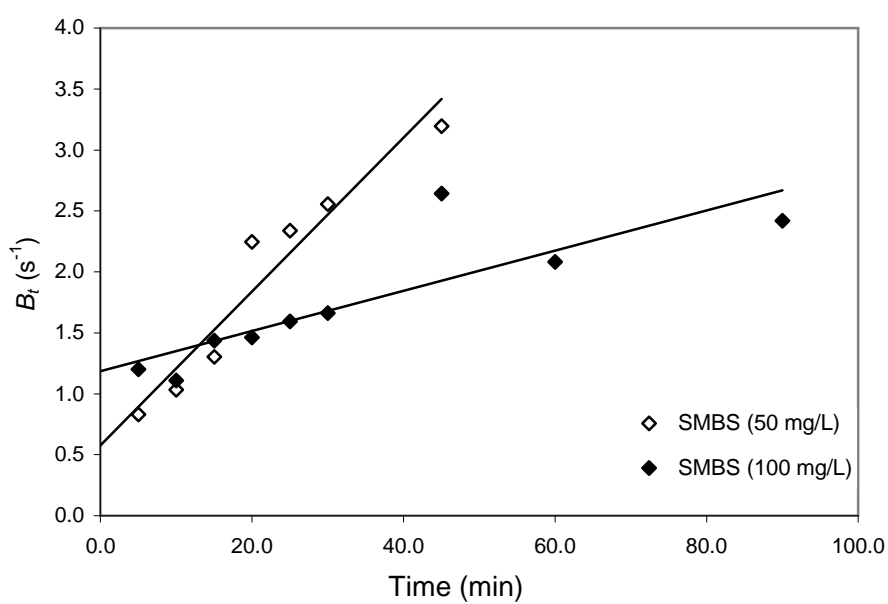


Figure 6.9a. Boyd plot for the sorption of RB4 onto SMBS

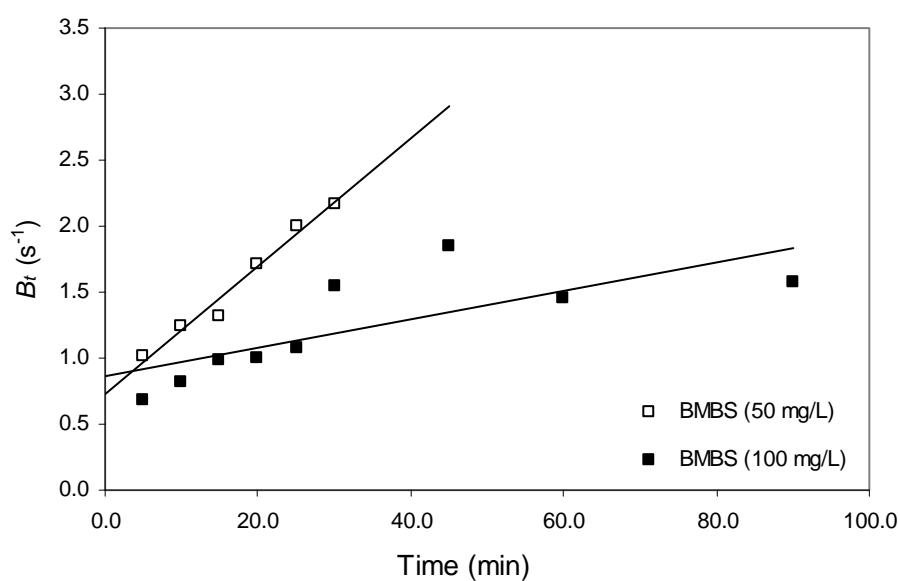


Figure 6.9b. Boyd plot for the sorption of RB4 onto BMBS

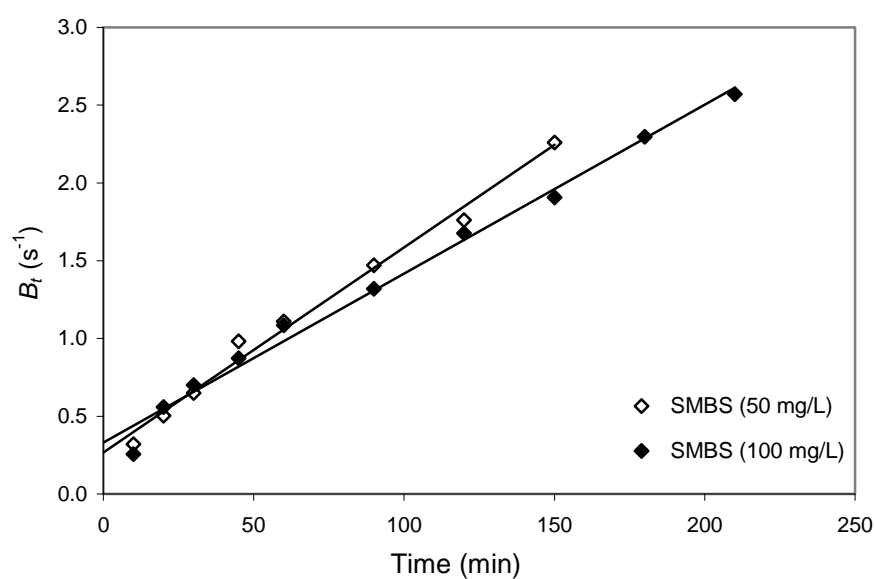


Figure 6.10a. Boyd plot for the sorption of RB5 onto SMBS

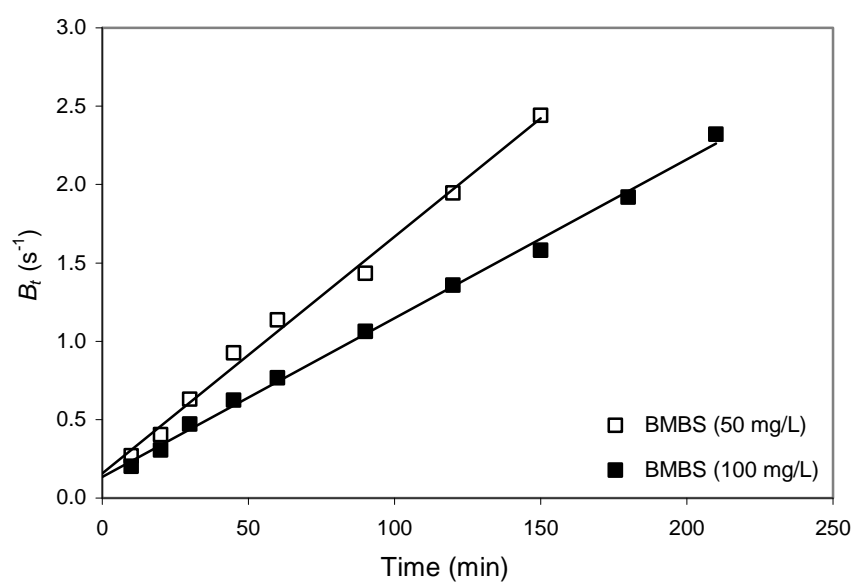


Figure 6.10b. Boyd plot for the sorption of RB5 onto BMBS

Table 6.2. Effective diffusion constants ( $D_i$ ) for adsorption of dye on SMBS and BMBS

Oil	Adsorbent	[Dye] (mg L <sup>-1</sup> )	Effective diffusion	
			$D_i$ (cm <sup>2</sup> s <sup>-1</sup> )	R <sup>2</sup>
AB40	SMBS	50	3.72 x 10 <sup>-6</sup> - 2.07 x 10 <sup>-5</sup>	0.99
		100	1.40 x 10 <sup>-6</sup> - 7.79 x 10 <sup>-6</sup>	0.99
	BMBS	50	3.23 x 10 <sup>-6</sup> - 1.80 x 10 <sup>-5</sup>	0.99
		100	2.04 x 10 <sup>-6</sup> - 1.14 x 10 <sup>-5</sup>	0.99
RB4	SMBS	50	4.00 x 10 <sup>-6</sup> - 2.23 x 10 <sup>-5</sup>	0.93
		100	1.04 x 10 <sup>-6</sup> - 5.82 x 10 <sup>-6</sup>	0.72
	BMBS	50	3.06 x 10 <sup>-6</sup> - 1.71 x 10 <sup>-6</sup>	0.98
		100	6.90 x 10 <sup>-7</sup> - 3.84 x 10 <sup>-6</sup>	0.57
RB5	SMBS	50	8.36 x 10 <sup>-7</sup> - 4.66 x 10 <sup>-6</sup>	0.9
		100	6.90 x 10 <sup>-7</sup> - 3.84 x 10 <sup>-6</sup>	0.99
	BMBS	50	9.56 x 10 <sup>-7</sup> - 5.33 x 10 <sup>-6</sup>	0.88
		100	6.40 x 10 <sup>-7</sup> - 3.56 x 10 <sup>-6</sup>	0.99

(Solution pH: AB40= 5.8, RB4=5.6, RB5.0; shaking speed: 170 rpm, dosage: 2 g L<sup>-1</sup>, Straw size radius: 0.025-0.059 cm, Experimental temperature: 25 °C)

#### 6.4 Isotherm Models

The adsorption isotherms that relate the adsorbate concentration in the bulk and the adsorbed amount on the interface at equilibrium were evaluated using the Langmuir and Freundlich models. The isotherm models shown in Figs. 6.11a to 6.11c were constructed using the Polymath software based on nonlinear equations of the isotherm models, listed in Eqs. 3.11 and 3.12. The best fit of experimental data to the isotherm model can be evaluated by regression coefficient, R<sup>2</sup> and error analysis values. Generally, all the plots produced a decent fit to the equilibrium data as shown in Table 6.3 with R<sup>2</sup> of above 0.94 for all the plots. However, the error function, MPSD, showed that the Langmuir model gave lower error values for all the dyes; AB40, RB4 and RB5. This indicated the better fit of the Langmuir model to the experimental adsorption isotherm of dyes on SMBS and BMBS. The maximum Langmuir adsorption capacities, Q<sub>max</sub> for adsorption of AB40, RB4 and RB5 were 45.44, 29.16 and 24.92 mg g<sup>-1</sup> for SMBS; and 51.95, 31.50 and 39.88 mg g<sup>-1</sup> for BMBS, respectively.

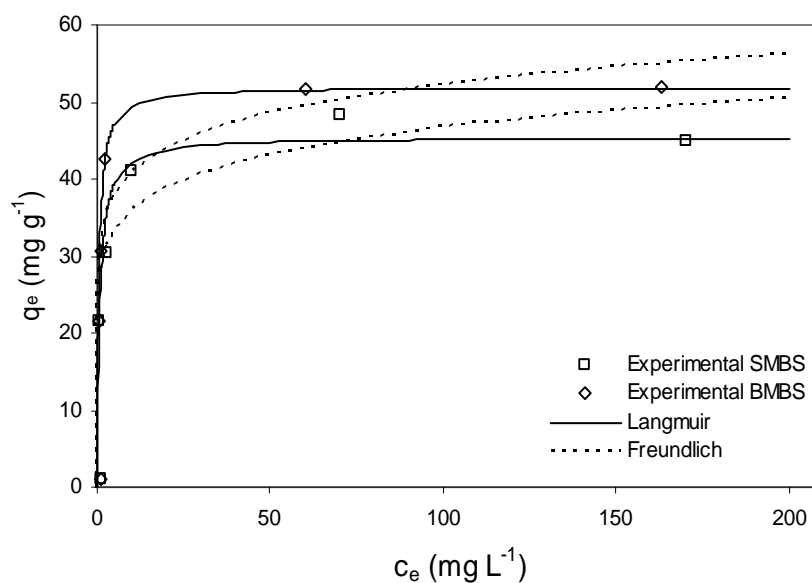


Fig. 6.11a. Nonlinear adsorption isotherms for adsorption of AB40 onto SMBS and BMBS.

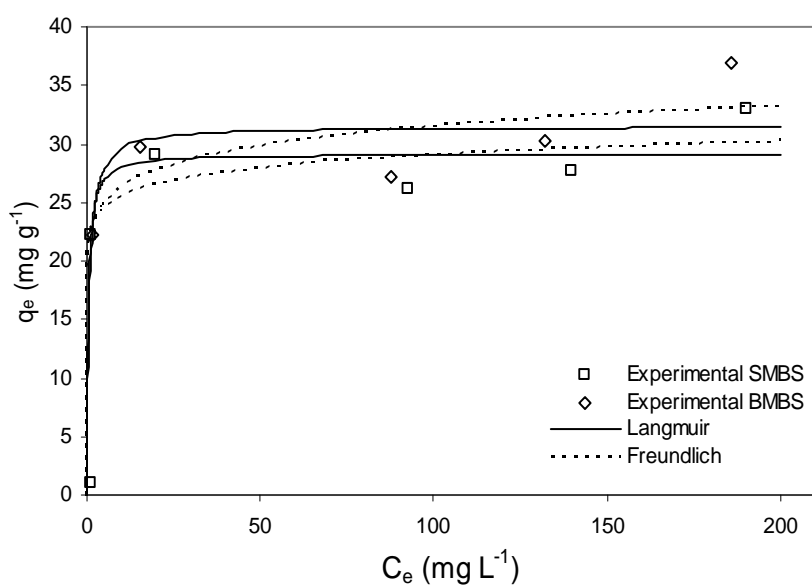


Figure 6.11b. Nonlinear adsorption isotherms for adsorption of RB4 onto SMBS and BMBS.

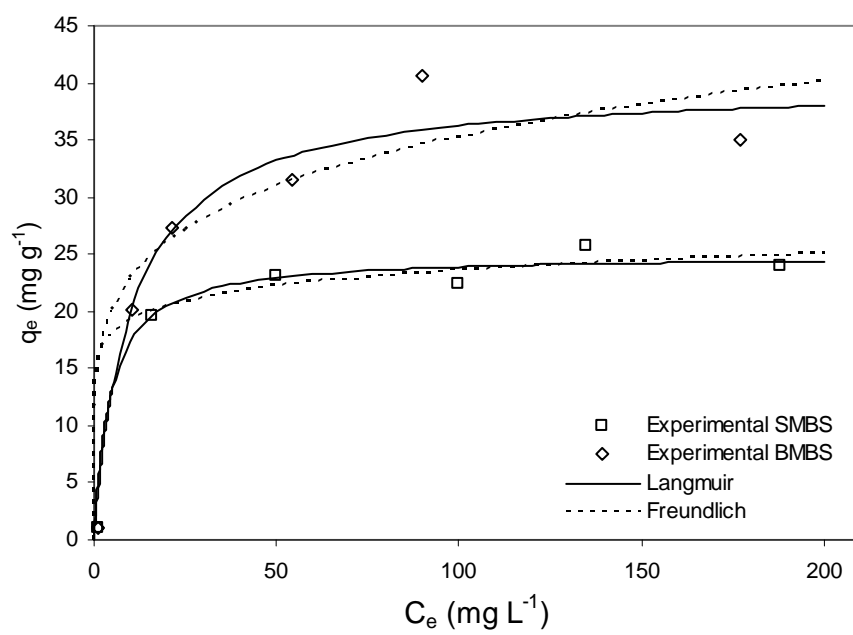


Fig. 6.11c. Nonlinear adsorption isotherms for adsorption of RB5 onto SMBS and BMBS

Table 6.3. Freundlich and Langmuir isotherm constants and error analysis for adsorption of anionic dyes on SMBS and BMBS.

Experimental		Isotherm Models Constant				Error Analysis			
Oil	Adsorbent	Langmuir		Freundlich		Langmuir		Freundlich	
		$Q_{\max}$	b	$K_F$	n	$R^2$	MPSD	$R^2$	MPSD
		(mg g <sup>-1</sup> )	(L mg <sup>-1</sup> )	(mg g <sup>-1</sup> )					
AB40	SMBS	45.44	1.31	27.66	8.81	0.97	13.39	0.95	15.04
	BMBS	51.95	1.94	31.92	8.81	0.99	9.30	0.94	21.58
RB4	SMBS	29.16	2.44	22.46	17.93	0.96	9.91	0.96	10.35
	BMBS	31.50	1.54	21.94	12.75	0.94	12.69	0.95	12.30
RB5	SMBS	24.92	0.23	15.78	11.49	0.99	5.05	0.98	5.57
	BMBS	39.88	0.10	14.87	5.33	0.97	9.06	0.94	14.23

## 6.5 Comparison with Other Adsorbents

Table 6.4 presents some previous investigations of AB40, RB4 and RB5 adsorption on various materials. Between SMBS and BMBS, BMBS was observed to give higher adsorption capacity for all the dyes. This was expected due to the availability of more CPC on BMBS. Among the dyes, the highest adsorption of AB40 was found. This was due to the smaller molecular size of AB40 at  $473.43 \text{ g mol}^{-1}$  thus facilitating it accessible to the small pores on the adsorbent compared to the  $673.4 \text{ g mol}^{-1}$  for RB4 and  $991.8 \text{ g mol}^{-1}$  for RB5.

Compared with other adsorbents, SMBS and BMBS were found to give a moderate adsorption capacity. For AB40, sorption capacity of SMBS and BMBS was about half of that on cone biomass of *Thuja orientalis*. Calcine alunite was observed to give the highest sorption capacity, about four times higher than BMBS and SMBS. The only work on adsorption of RB4 was conducted by Bayramoglu et al. [266] using various modification fungal biomass. Heat treated fungal biomass was observed to give the highest removal of  $156.9 \text{ mg g}^{-1}$  which was about five times higher than SMBS and BMBS. For RB5, SMBS and BMBS show better adsorption than some other biomass adsorbents such as sunflower seed, mandarin peeling and peat but lower than other adsorbents such bamboo derived carbon material, bone char and etc. It was noted that the reported adsorption capacity or removal percentage was achieved under specific experimental conditions as well as the varying extent of modification.

Table 6.4. Anionic dye sorption capacities of some sorbents reported in literature.

Adsorbent	Sorption capacity (mg g <sup>-1</sup> )	Reference
	AB40	
Calcined alunite	212.8	[267]
Cone biomass of <i>Thuja orientalis</i>	97.1	[268]
Activated carbon	57.5	[267]
Activated carbon	53.6	[269]
Modified straw BMBS	52.0	<i>This study</i>
Modified straw SMBS	45.4	<i>This study</i>
Titania	23.7	[270]
	RB4	
Fungal Biomass ( <i>p. chrysosporium</i> ):		
heat-treated	156.9	[266]
acid treated	147.7	[266]
native(no treatment)	134.5	[266]
base-treated	81.1	[266]
Modified straw BMBS	31.5	<i>This study</i>
Modified straw SMBS	29.2	<i>This study</i>
	RB5	
Bamboo carbon (1400 m <sup>2</sup> g <sup>-1</sup> )	545	[271]
Bamboo carbon (2123 m <sup>2</sup> g <sup>-1</sup> )	447	[271]
Active carbon F400	176	[271]
<i>Corynebacterium glutamicum</i>	169.5	[272]
Bone char	157	[271]
Sepiolite with hexadecyltrimethylammonium bromide	120.5	[273]
Modified basic oxygen furnace slag (BTA)	109.5	[274]
<i>Aspergillus foetidus</i>	106	[275]
Brown seaweed	101.5	[276]
Activated carbon using cetylpyridinium chloride	99.2	[196]
Modified basic oxygen furnace slag (BTM)	74.4	[274]
Zeolite with hexadecyltrimethylammonium bromide	60.6	[273]
Activated carbon	58.8	[277]
Modified straw BMBS	39.9	<i>This study</i>

Modified straw SMBS	24.9	<i>This study</i>
Natural zeolite with cetyltrimethylammonium bromide	12.9	[278]
Coal Fly ash	7.9	[277]
Coal Fly ash (High Lime)	7.2	[278]
Peat	7.0	[271]
Biomass fly ash	4.38	[279]
Sunflower seed shells	0.87	[280]
Mandarin peelings	0.75	[280]

## 6.6 Effect of Dye Solution pH

The results of the pH effect on the adsorption of dyes are presented in Figs. 6.12a and 6.12b. In general, pH of solution is an important parameter due to its influence on the surface properties of adsorbent and surface binding sites [244]. In this work the influence of pH on the removal of AB40, RB4 and RB5 was analyzed by varying the initial pH of dye solution in the range of 3-11. Generally, the adsorption of dyes on SMBS and BMBS is highly pH dependent. For RB4 and RB5, percentage removal was generally found to decrease with increasing initial pH. A complete removal of RB4 and RB5 on SMBS and BMBS was equivalent to  $49.97 \text{ mg g}^{-1}$  at pH 3. However, a different trend was observed for AB40, where the maximum removal of 43.42 and  $48.74 \text{ mg g}^{-1}$  for SMBS and BMBS respectively was achieved at pH 5. The adsorption of AB40 and RB4 was also observed to give low removal at highly basic solution ( i.e pH 11)

Basically, lower pH solution was believed to increase the positive charge on the adsorbent surface, which would attract the negatively charged functional groups located on the reactive dyes [2]. As the initial solution pH increases, the amount of negatively charged sites on the adsorbent surface also increases thus may create the electrostatic repulsion between the adsorbent surface and RB4 and RB5 molecules. This observation is consistent with several reported works [281-283]. The relatively lower removal percentage of AB40 at high acidity (i.e pH 3) could be attributed to the decrease in the dissociation of acid dyes in the solution thus subsequently reducing the concentration of anionic species available to interact with positively charged

adsorbent sites [284]. A similar trend had also been observed by Atia et al. [285]. On the other hand, higher adsorption of RB5 at pH 11 was reported by Oei et al. [17], attributed to the presence of phenolic group in RB5 structure, thus increasing the chemical bonding between RB5 and modified straw at  $\text{pH} > 6$ , which subsequently increases the adsorption.

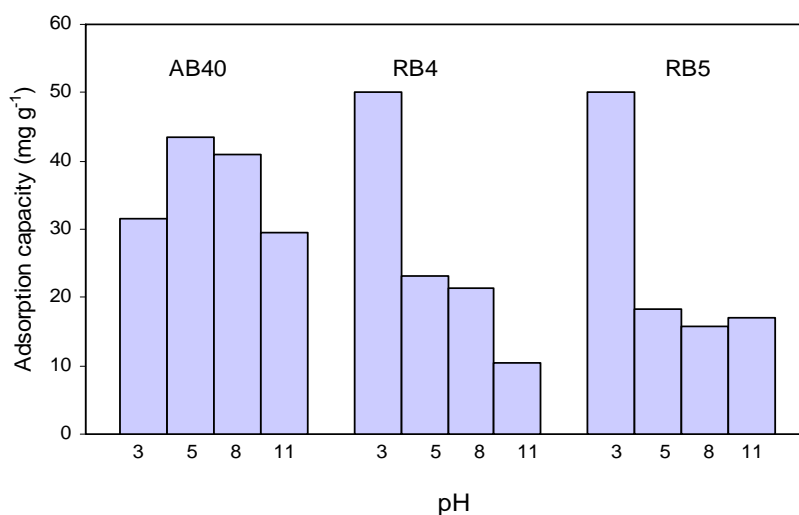


Figure 6.12a. Effect of solution pH on adsorption of AB40, RB4 and RB5 onto SMBS ([Dyes]:100 mgL<sup>-1</sup>; Shaking speed: 170 rpm; Contact time: 5 hrs; dosage: 2 g L<sup>-1</sup>; Temperature: 25 °C)

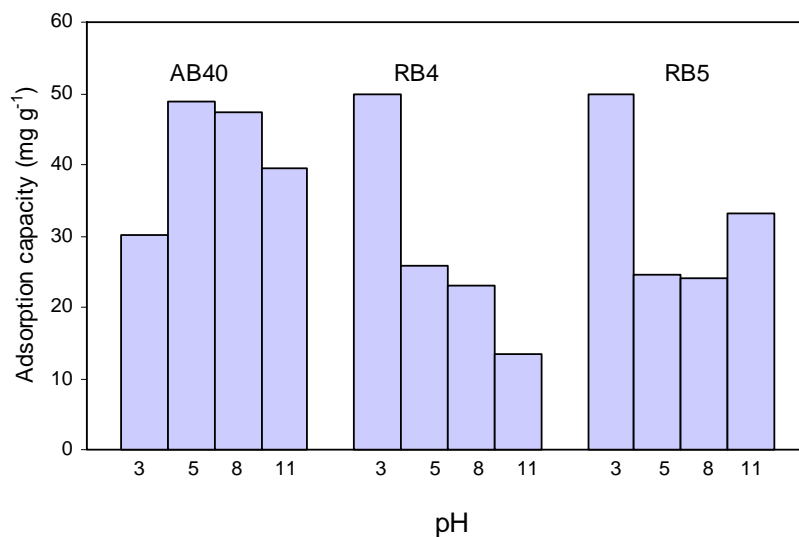


Figure 6.12b: Effect of solution pH on adsorption of AB40, RB4 and RB5 onto BMBS ([Dyes]:100 mgL<sup>-1</sup>; Shaking speed: 170 rpm; Contact time: 5 hrs; dosage: 2 g L<sup>-1</sup>; Temperature: 25 °C)

## 6.7 Effect of Experimental Temperature of Dye Solution

The effect of temperature on adsorption of AB40, RB4 and RB5 conducted at different temperatures of 30, 40 and 50 °C for both SMBS and BMBS are shown in Figs. 6.13a and 6.13b, respectively. Experimental temperature of the dye solution at high values is important because various textile and other dye effluents are discharged at relatively high temperatures of about 50 to 60 °C [286].

For AB40, generally, the temperature gives a significant influence. The adsorption capacity of SMBS and BMBS was observed to increase from 41.85 to 58.00 mg g<sup>-1</sup> on SMBS and 50.56 to 70.59 mg g<sup>-1</sup> on BMBS when the temperature increased from 30 to 50 °C. For RB4 and RB5, experimental temperature, however, did not produce a significant effect. Sorption capacity at the temperature of 30, 40 and 50 °C was 18.27, 22.07 and 20.52 mg g<sup>-1</sup> (RB4); and 22.50, 23.63 and 24.17 mg g<sup>-1</sup> (RB5), respectively. Meanwhile for BMBS, sorption capacity was 20.69, 24.05 and 21.90 mg g<sup>-1</sup> (RB4); and 26.40, 31.17 and 33.73 mg g<sup>-1</sup> (RB5) respectively. Even though there is a variation in sorption capacity for RB4 and RB5, generally the difference is not so significant.

Increase in experimental temperature was suggested to improve the mobility and dispersion of dyes thus increasing the significant attraction of dye molecules and adsorbent surface [77, 287] and may also enlarge the adsorbent pore size [288]. This seems to be true for AB40 where the sorption capacity was observed to tremendously increase at elevated temperature. However, a contrast trend was found for RB4 and RB5, the increase in temperature has little effect on sorption capacity. A similar result was also observed by Tunç et al. [289]. The increase of AB40 sorption with temperature was suggested to be physisorption where the relatively small molecular weight allows more AB40 to be retained at enlarged adsorbent pores [2]. RB4 and RB5 did not expected to experience this possibly due to the relatively high molecular size. The exceptionally higher sorption capacity of AB40 than RB4 and RB5 was attributed to the occurrence of both of the physisorption and chemisorption in sorption of AB40.

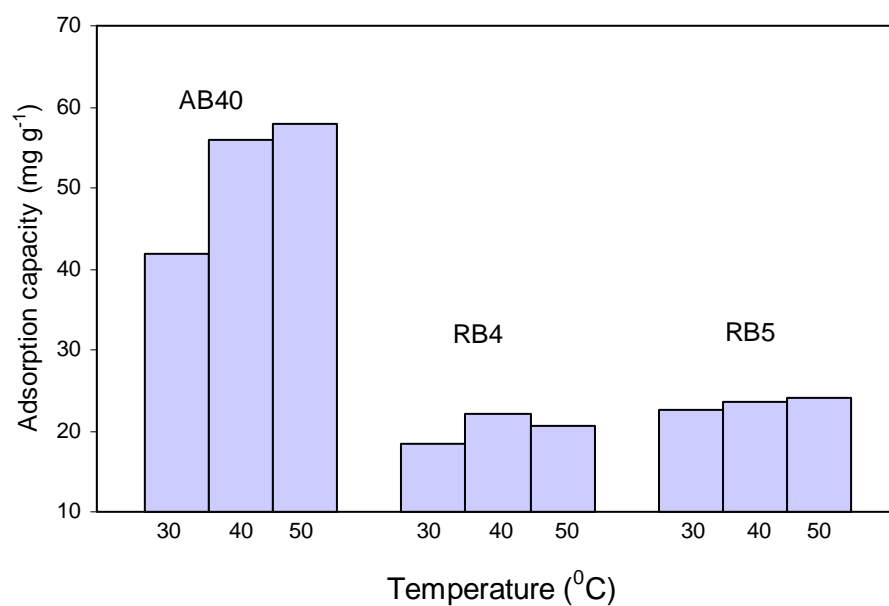


Figure 6.13a. Effect of solution pH on adsorption of AB40, RB4 and RB5 onto SMBS ([Dyes]: 100 mgL<sup>-1</sup>; Shaking speed: 170 rpm; Contact time: 5 hrs; dosage: 2 g L<sup>-1</sup>; Dye solution pH: AB40: 5.8, RB4: 5.6, RB5: 5.0)

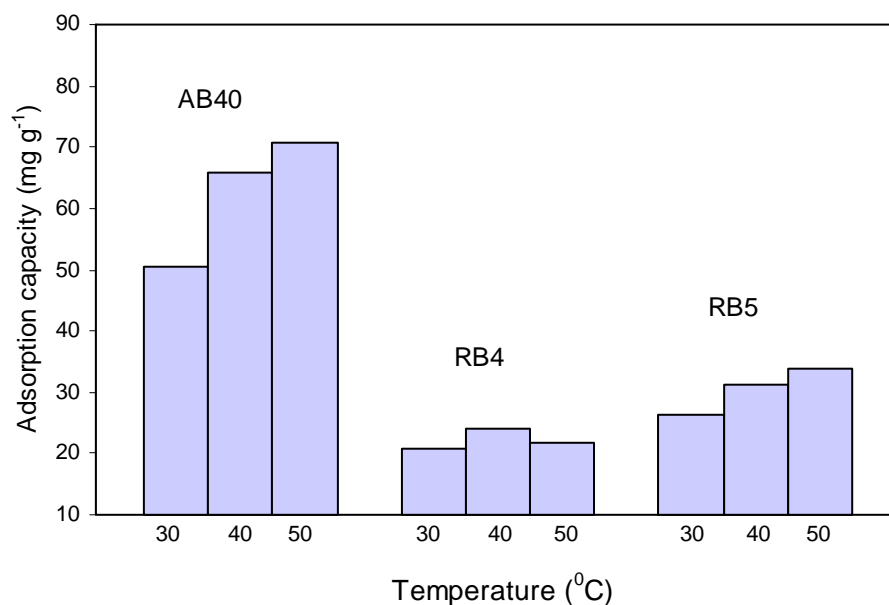


Figure 6.13b. Effect of solution pH on adsorption of AB40, RB4 and RB5 onto BMBS ([Dyes]: 100 mgL<sup>-1</sup>; Shaking speed: 170 rpm; Contact time: 5 hrs; dosage: 2 g L<sup>-1</sup>; Dye solution pH: AB40: 5.8, RB4: 5.6, RB5: 5.0)

## 6.8 Dye Desorption

The desorption behavior of AB40, RB4 and RB5 from the dye loaded SMBS and BMBS was evaluated at different aqueous pHs and is presented in Figs. 6.14a and 6.14b. Overall, the desorption pattern for the dye loaded SMBS and BMBS was observed to increase with increasing initial solution pH. The percentages of dyes leached out at pH of 3, 5, 8 and 11 for SMBS were 0, 13.86, 16.14 and 17.27% for AB40; 0, 10.09, 12.66 and 26.78% for RB4; 0, 16.85, 23.96, 26.80% for RB5. Meanwhile for BMBS the same series of solution resulted in the dye desorption of 0, 6.61, 8.82 and 13.84% for AB40; 0, 9.64, 15.07 and 27.77% for RB4; 0, 4.96, 13.51, 22.13% for RB5 respectively. As discussed in section 6.6, the net positive charge on adsorbent surface decreases as the pH of solution increases. The reduced amount of positively charge adsorbent sites (as pH of solution increases) indirectly promotes the desorption (due to the electrostatic repulsion) of negatively charged dye particle from adsorbent surface. This strongly suggests the role of ion exchange as one of the important binding mechanism in this particular system [77]. This observation agrees well with the work done by Li et al. [290].

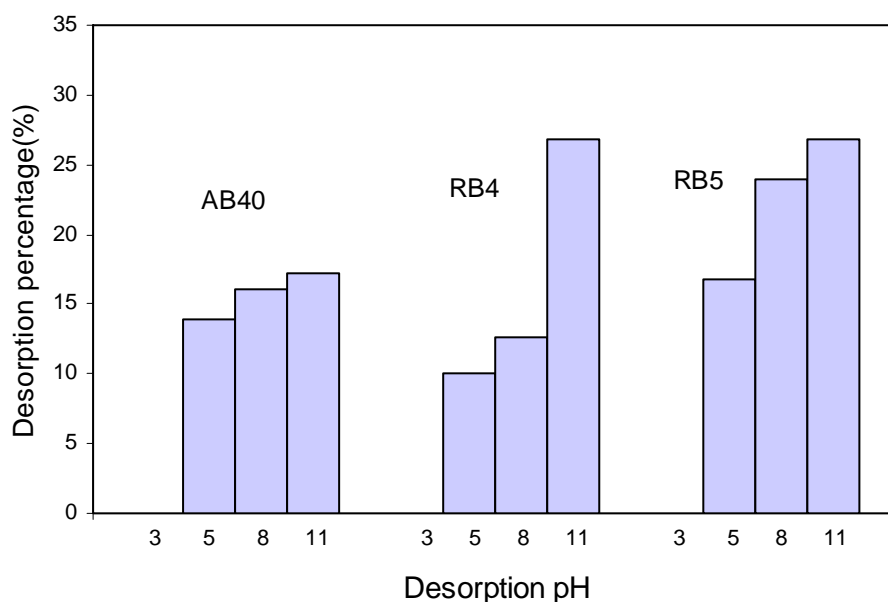


Figure 6.14a. Desorption of SMBS loaded AB40, RB4 and RB5 at different pH solution  
(Shaking speed: 170 rpm; Contact time: 6 hrs; dosage: 2 g L<sup>-1</sup>; Temperature: 25 °C)

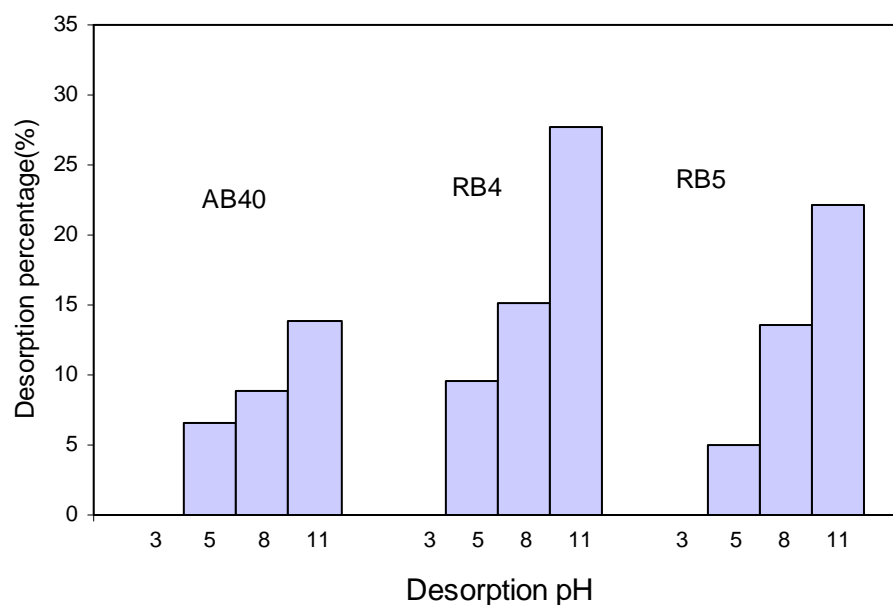


Figure 6.14b. Desorption of BMBS loaded AB40, RB4 and RB5 at different pH solution  
(Shaking speed: 170 rpm; Contact time: 6 hrs; dosage: 2 g L<sup>-1</sup>; Temperature: 25 °C)

## 6.9 Column Breakthrough Studies

The breakthrough curves for AB40 and RB5 are shown in Figs. 6.15a to 6.15d. Upon comparing with the example of column breakthrough curve (Fig. 3.2), RBS and RBS-N gave poor adsorption performance for removal of both AB40 and RB5. This poor performance was observed similarly in batch operation (section 6.2). For SMBS and BMBS, a favorable adsorption was observed, with all the curves exhibiting the ‘S’ shape. For both dyes, BMBS proved to be more superior as the effluent remained zero dye concentration longer than SMBS before the concentration of dye started to increase gradually. Consistent with the finding on emulsified oil (section 5.10), the removal for both of the dyes in a control run was observed not really significant with removal percentage below 0.0045%.

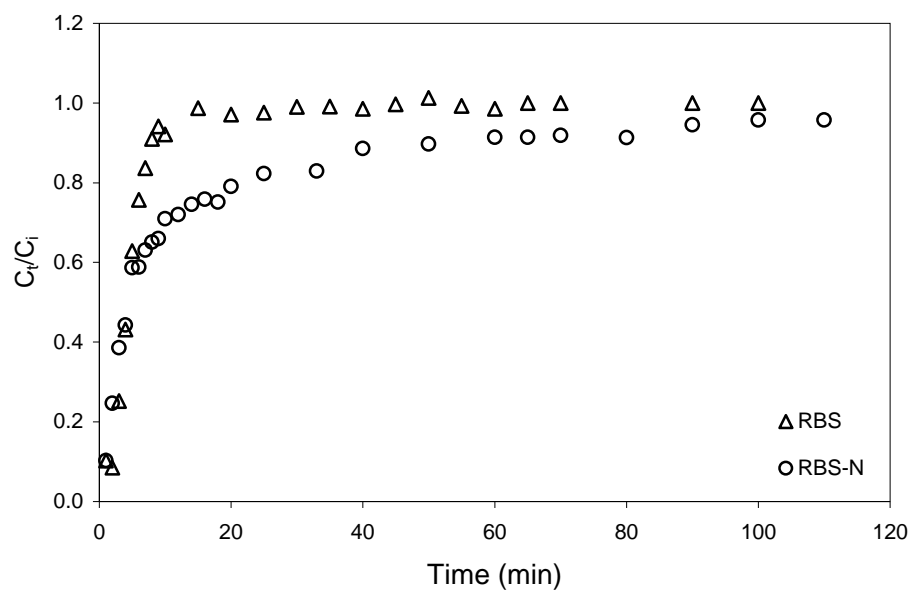


Figure 6.15a. Breakthrough plot of AB40 adsorption for RBS and RBS-N  
 ([AB40]:  $50 \text{ mgL}^{-1}$ ,  $H = 8.0 \text{ cm}$ ;  $m = 5.0 \text{ g}$ ;  $Q = 10.0 \text{ mL min}^{-1}$ )

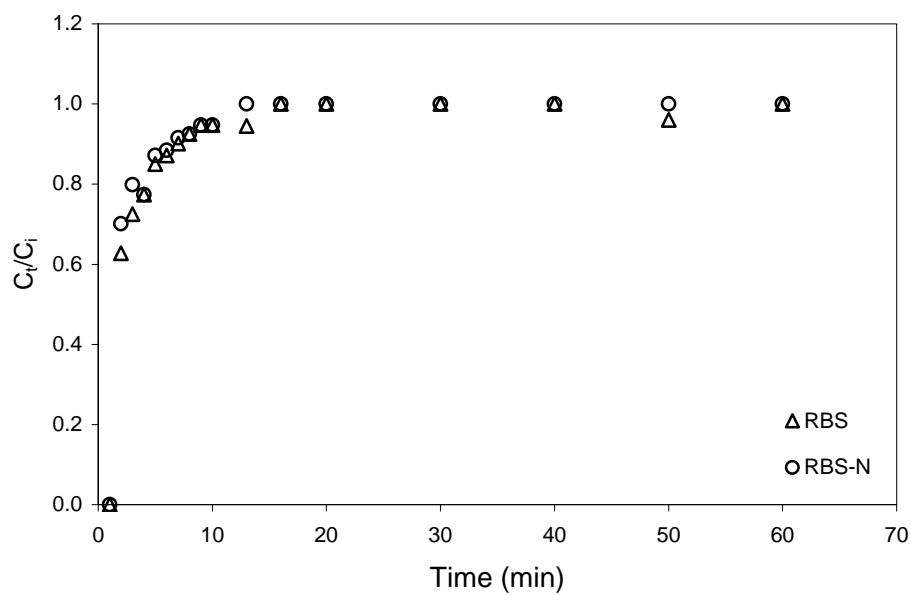


Figure 6.15b. Breakthrough plot of RB5 adsorption for RBS and RBS-N  
 ([RB5]:  $50 \text{ mgL}^{-1}$ ,  $H = 8.0 \text{ cm}$ ;  $m = 5.0 \text{ g}$ ;  $Q = 10.0 \text{ mL min}^{-1}$ )

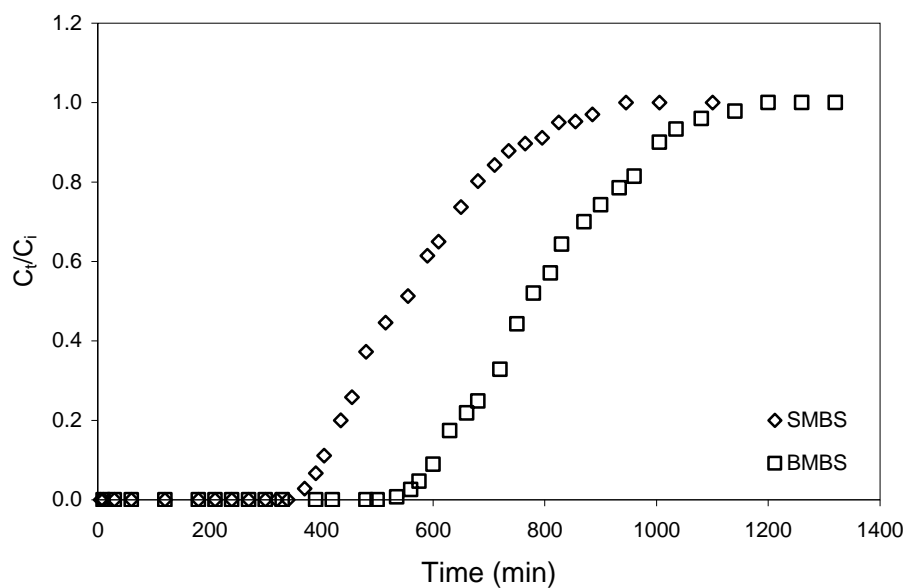


Figure 6.15c. Breakthrough plot of AB40 adsorption for SMBS and BMBS ([AB40]:  $50 \text{ mgL}^{-1}$ ,  $H = 8.0 \text{ cm}$ ;  $m = 5.0 \text{ g}$ ;  $Q = 10.0 \text{ mL min}^{-1}$ )

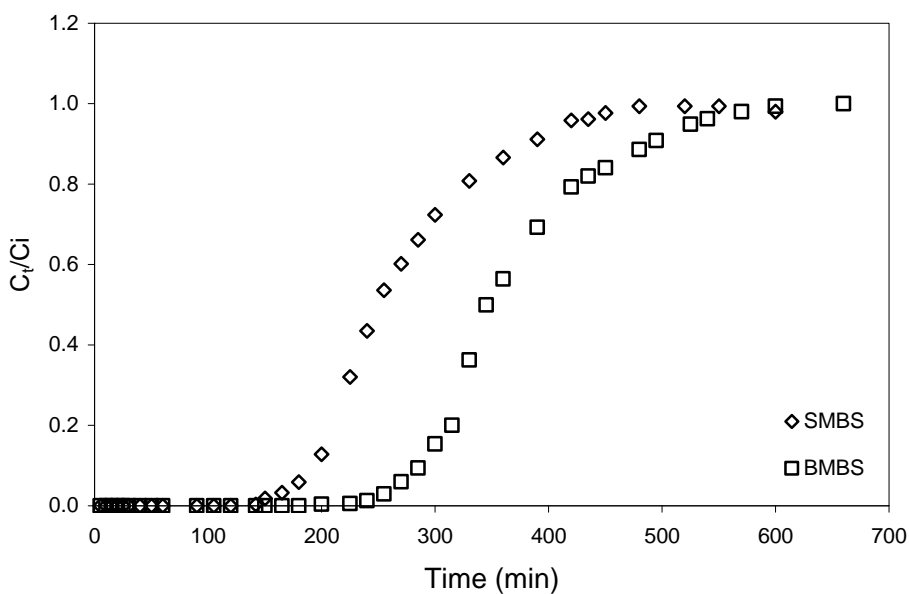


Figure 6.15d. Breakthrough plot of RB5 adsorption for SMBS and BMBS ([RB5]:  $50 \text{ mgL}^{-1}$ ,  $H = 8.0 \text{ cm}$ ;  $m = 5.0 \text{ g}$ ;  $Q = 10.0 \text{ mL min}^{-1}$ )

Table 6.5 summarizes the important data in the column studies. Similar to the fixed bed column studies for removal of oils that was discussed in section 5.10, the

breakthrough concentration for this study was also set at 5% of the inlet concentration. Hydraulic residence time, HRT, total effluent volume,  $V_{\text{eff}}$  and breakthrough capacity,  $q_b$  can be calculated from Eqs. 5.1, 5.2 and 5.3, respectively.

Data in Table 6.5 show that SMBS gave shorter breakthrough time than BMBS for both dyes, AB40 and RB5. The breakthrough time for SMBS and BMBS was 382 and 576 min (AB40); 176 and 265 min (RB5), respectively. The total volume of the dyes ( $V_b$ ) to be treated by 5 g of SMBS and BMBS was estimated as 3280 and 5760 mL for AB40; and 1760 and 2650 mL for RB5, respectively. These volumes are equivalent to column breakthrough capacities of 38.2 and 57.60  $\text{mg g}^{-1}$  for AB40; 17.60 and 26.50  $\text{mg g}^{-1}$  for RB5 respectively. Overall, BMBS showed a greater efficiency compared to SMBS as it exhibited longer column breakthrough time ( $t_b$ ), thus higher amount of dyes that could be treated at breakthrough time which leads to greater adsorption capacity. This however was expected and consistent with the finding obtained in batch adsorption study of AB40 and RB5 (section 6.4)

Table 6.5. Adsorption breakthrough data for column experiments for the adsorption of AB40 and RB5 on SMBS and BMBS

Dye	Adsorbent	HRT (min)	$t_b$ (min)	$V_b$ (mL)	$q_b$ ( $\text{mg g}^{-1}$ )	$t_{\text{exh}}$ (min)	$V_{\text{exh}}$ (mL)
AB40	SMBS	5.29	382	3280	38.20	825	8250
	BMBS	5.29	576	5760	57.60	1060	10600
RB5	SMBS	5.29	176	1760	17.60	414	4140
	BMBS	5.29	265	2650	26.50	526	5260

([AB40]: 50  $\text{mg L}^{-1}$ , [RB5]: 50  $\text{mg L}^{-1}$ ,  $H = 8.0$  cm;  $m = 5.0$  g;  $Q = 10.0$   $\text{mL min}^{-1}$ )

## 6.10 Modeling of Fixed Bed Column Breakthrough

To describe the adsorption behavior of column tests better, the results from fixed bed column tests were fitted to two column models such as the Thomas and Yoon-Nelson models. The nonlinear equations of these models listed in Eqs. 3.13 and 3.14 (section 3.8) were curve fitted for adsorption of AB40 and RB5 by employing the trial and error method using Polymath software.

### 6.10.1 Thomas Model

The Thomas model, which was formulated by Thomas [20], determines the maximum solid phase concentration of solute on the adsorbent and the adsorption rate constant for an adsorption column [264]. Higher  $R^2$  values of 0.99 shown in Table 6.6 for all the column system simulation of whole breakthrough curves were predicted well by the Thomas model for all the plots (Figs. 6.16a and 6.16b). The Thomas model is applicable as the packing of glass beads in column did assist in fairly distribution of the dye solution thus minimize the phenomenon of axial dispersion as what has been discussed in section 2.9.

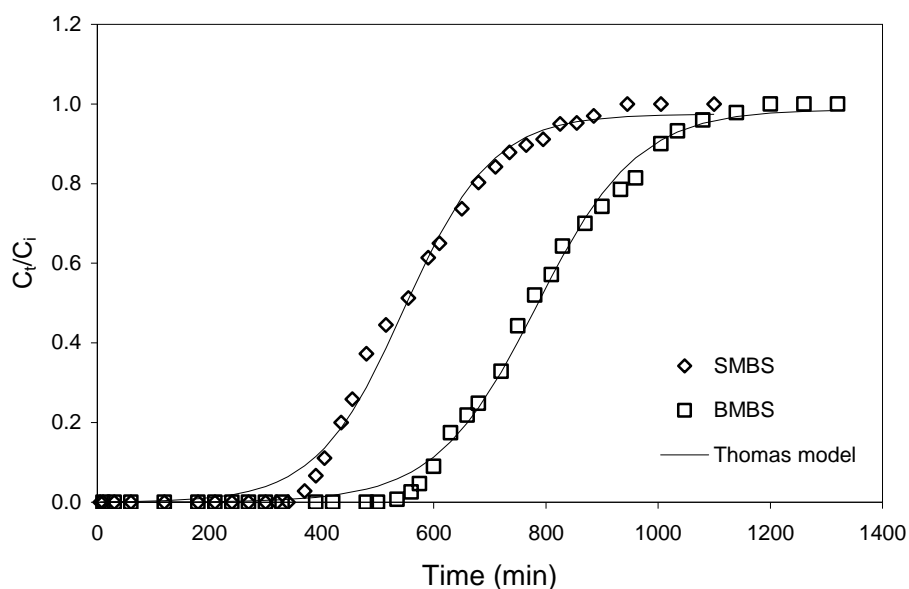


Figure 6.16a. Nonlinear Thomas plots for adsorption of AB40 onto SMBS and BMBS

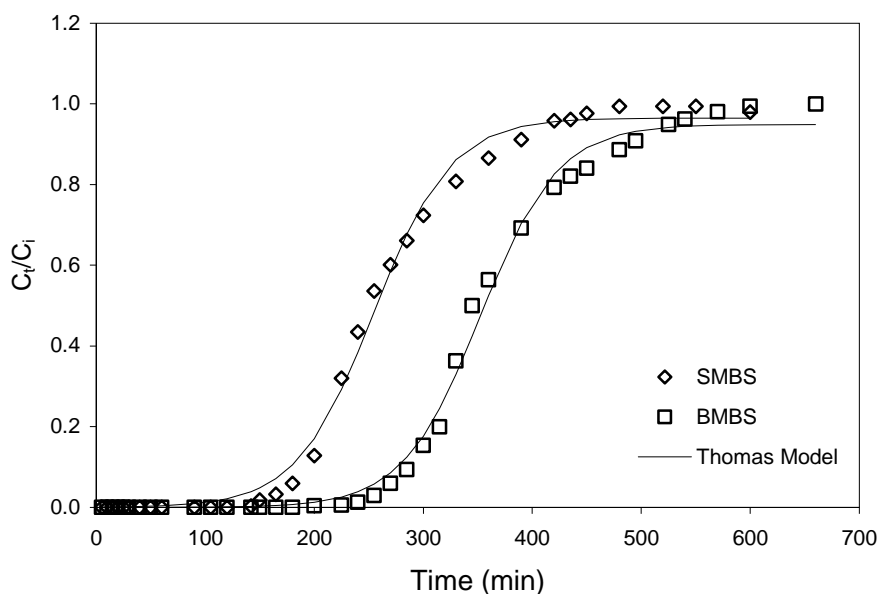


Figure 6.16b. Nonlinear Thomas plots for adsorption of RB5 onto SMBS and BMBS

Important information obtained from the Thomas model is presented in Table 6.6. The adsorption capacities,  $q_0$ , calculated from the Thomas model for SMBS and BMBS were 53.39 and 77.29  $\text{mg g}^{-1}$  for AB40; and 24.57 and 33.46  $\text{mg g}^{-1}$  for RB5 respectively. Meanwhile, the capacities from batch adsorption for AB40 and RB5 were 45.4 and 24.92  $\text{mg g}^{-1}$  for SMBS; 51.95 and 39.88  $\text{mg g}^{-1}$  for BMBS respectively. For AB40, the adsorption capacity of SMBS and BMBS from fixed bed column was higher, whereas, for RB5 the adsorption capacity of SMBS and BMBS was slightly lower in fixed bed column. The relatively higher adsorption capacity for fixed bed column for AB40 was suggested to be due to the relatively low molecular weight thus allowing greater penetration of AB40 molecules to the available adsorbent pores, even though its residence column time of about 5.29 min is much lower than the equilibrium contact time obtained from batch study (section 6.3). Meanwhile for RB5, relatively higher molecular weight resulted in higher liquid channelling thus lowered the interaction of RB5 molecule with SMBS and BMBS. Consistent with the finding made in fixed bed column of CO and SMO removal discussed in section 5.11.1, the adsorption capacity of BMBS was found greater than

SMBS for both of AB40 and RB5 column system. This was also consistent with the finding obtained in batch adsorption study of AB40 and RB5 in section 6.4.

Table 6.6. Thomas model parameters for fixed-bed adsorption of AB40 and RB5

Dye	Adsorbent	$k_{Th}$ (mL mg <sup>-1</sup> min <sup>-1</sup> )	$q_0$ (mg g <sup>-1</sup> )	R <sup>2</sup>
AB40	SMBS	0.261	53.392	0.99
	BMBS	0.225	77.29	0.99
RB5	SMBS	0.583	24.570	0.99
	BMBS	0.592	33.456	0.99

### 6.10.2 Yoon-Nelson model

The relatively high R<sup>2</sup> values obtained from the Yoon-Nelson breakthrough model as shown in Figs. 6.17a and 6.17b prove the suitability of this model to simulate the column experimental data. The time required to achieve 50% of adsorbate breakthrough ( $\tau$ ) for SMBS and BMBS was 578.4 and 783.47 min for AB40; and 254.4 and 353.38 min for RB5 respectively (Table 6.7). The relatively longer ' $\tau$ ' for BMBS for the column systems compared to SMBS showed the better applicability of BMBS to treat the studied dyes. It was found that, the time required to achieve 50% of adsorbate breakthrough ( $\tau$ ) from the Yoon-Nelson model seemed to agree well with the experimental data ( $t_{50\%,exp}$ ) in the entire column adsorption system, thus indicating a high applicability of this model in column operations.

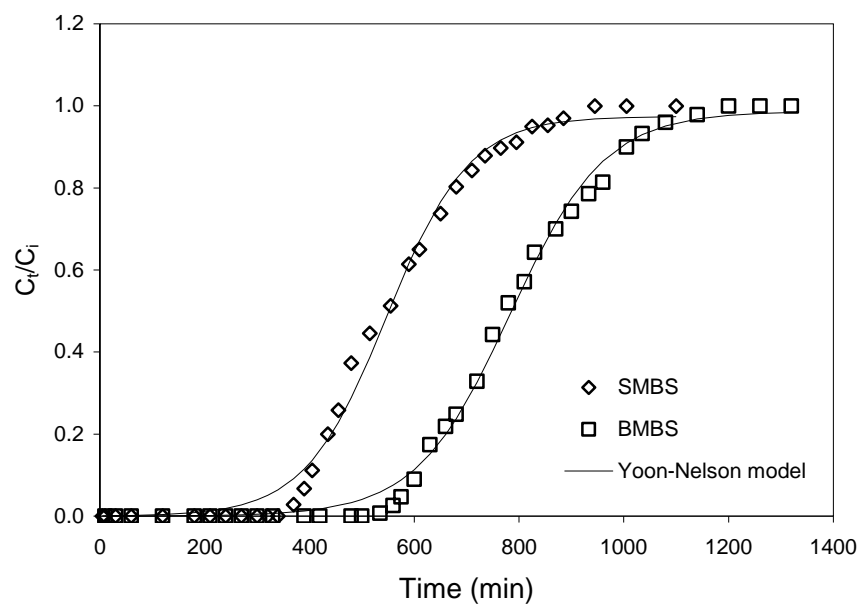


Figure 6.17a. Nonlinear Yoon-Nelson plots for adsorption of AB40 onto SMBS and BMBS

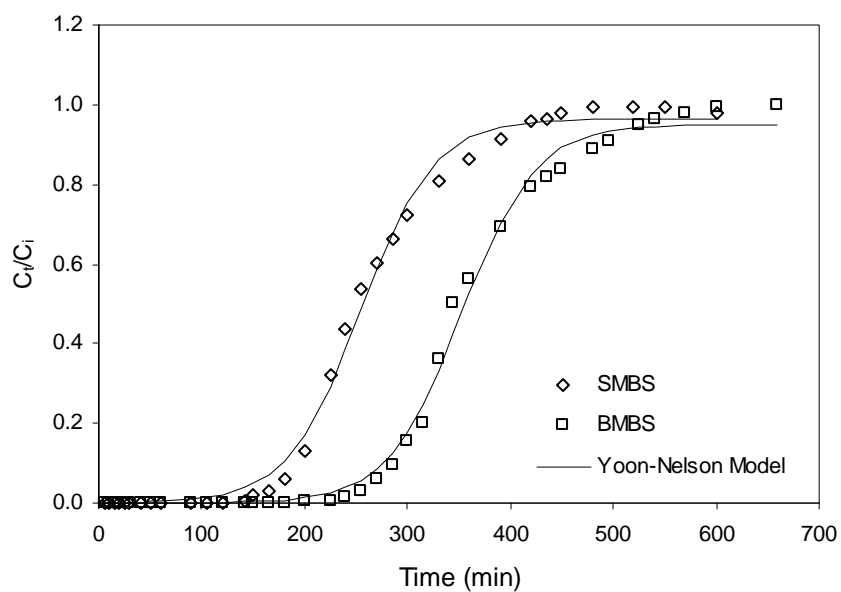


Figure 6.17b. Nonlinear Yoon-Nelson plots for adsorption of RB5 onto SMBS and BMBS

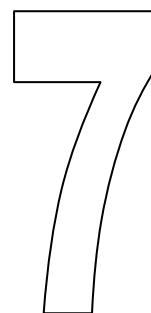
Table 6.7. Yoon-Nelsons model parameters for fixed-bed adsorption of AB40 and RB5

Dye	Adsorbent	$k_{YN}$ ( $\text{min}^{-1}$ )	$\tau$ (min)	$t_{50\%, \text{exp}}$ (min)	$R^2$ ( $\text{mg g}^{-1}$ )
AB40	SMBS	0.013	547.84	549	0.99
	BMBS	0.011	783.47	771	0.99
RB5	SMBS	0.028	254.54	249	0.99
	BMBS	0.028	353.38	345	0.99

### 6.11 Section Summary

In this study, the effectiveness of surfactant modified barley straws, SMBS and BMBS were tested for removal of anionic dyes, AB40, RB4 and RB5. In batch study, the kinetic experiments revealed that adsorption of dyes was rapid at initial stage followed by a slower phase where equilibrium uptake was achieved. The kinetic studies revealed that kinetic equilibrium adsorption of AB40, RB4 and RB5 was below 240 min depending on the initial dye concentration. Based on batch kinetic study of adsorption of AB40, RB4 and RB5 on SMBS and BMBS, the pseudo-second-order model fitted well to the kinetic data. Meanwhile kinetic diffusion study indicated that film diffusion controlled the adsorption of AB40, RB5 and RB5 onto SMBS and BMBS. The batch study also revealed that the adsorption was a function of dye concentration, pH and temperature. Adsorption capacity was found higher at pH about neutrality for AB40, but at acidic condition (pH 3) for the other dyes. The temperature influenced AB40 adsorption capacity, showing higher value as the temperature increased. However, for RB4 and RB5, the variation of temperature provided insignificant effect on the adsorption efficiency. The Langmuir isotherm provided the best correlation for the equilibrium adsorption data of AB40, RB4 and RB5 for both SMBS and BMBS. The Langmuir adsorption capacity of AB40, RB4 and RB5 were 45.4, 29.16 and 24.92  $\text{mg g}^{-1}$  for SMBS and 51.95, 31.50 and 39.88  $\text{mg g}^{-1}$  for BMBS respectively. Desorption experiments also showed that the dye loaded straw was stable at acidic condition but desorption increased as the pH increased (i.e pH 11).

In the fixed bed column study, SMBS and BMBS gave the favorable and normal column adsorption process for AB40 and RB5. However, for RBS and RBS-N, the column adsorption performance was poor. For both dyes, the duration of zero dye concentration in effluent was found shorter on SMBS compared to BMBS. The models of the Thomas and Yoon-Nelson show their suitability in the simulation of the column experimental data on SMBS and BMBS with  $R^2$  of 0.99 for all the plots. The adsorption capacities from the Thomas model for SMBS and BMBS were 53.39 and 77.29 mg g<sup>-1</sup> for AB40; and 24.57 and 33.46 mg g<sup>-1</sup> for RB5 respectively. It was observed that the time required to achieve 50% of adsorbate breakthrough ( $\tau$ ) from the Yoon-Nelson model agreed well with the experimental data ( $t_{50\%,exp}$ ) in all column adsorption system. The time required to achieve 50% adsorbate breakthrough ( $\tau$ ) for SMBS and BMBS was 578.4 and 783.47 min for AB40; and 254.4 and 353.38 min for RB5 respectively. BMBS showed better applicability to treat dye wastewater as the ' $\tau$ ' was relatively longer than SMBS for all the column system.



# CONCLUSIONS AND FUTURE DIRECTIONS

## 7.1 Introduction

This chapter summarizes the overall findings and presents some recommendations for future work. Batch and column studies show the effectiveness of oil and dye removal using the prepared adsorbents. The influences of parameters on the adsorption capacity were reported as well. Future directions generally suggest the possibilities of conducting further experiments either by using new materials and/or by another experimental procedure in order to complement the existing data.

## 7.2 Conclusions

This report investigates the feasibility of using an agricultural byproduct, barley straw, as a low cost adsorbent to remediate emulsified oil and dye contaminated wastewater. Due to the several issues associated with utilizing raw barley straw, such as the relatively low adsorption efficiency and the possibility of releasing soluble organic matters, raw barley straw was modified with a base solution and a cationic surfactant. In this study, surfactant modified barley straw samples were prepared, characterized and tested for removal of emulsified oil and dyes from aqueous solution. Thus the summary is based on the results of, i) Characterization of prepared adsorbents, ii) Batch adsorption study of the prepared adsorbents for emulsified oil and dye removal and iii) suggestions for the future research.

The main aim of characterization was to understand the properties of raw and modified straws. This is important, as these will help in understanding of adsorption behavior and mechanisms associated with the materials. Some of the important findings drawn from the characterization studies are listed below:

- The contents of cellulose, hemicelluloses, and lignin were 51.31, 30.80 and 5.99% for raw straw (RBS) and 56.88, 28.70 and 6.54% for base treated straw (RBS-N). The existence of higher cellulose, hemicelluloses and lignin in straw samples indicates the suitability of barley straw to be used as adsorbents.
- FT-IR spectra of RBS, RBS-N, SMBS, BMBS and pure CPC showed that the CPC was successfully retained on the straw surface. This can be proven by the two new peaks matching with CPC peaks at about 2922 and 2853  $\text{cm}^{-1}$  on both SMBS and BMBS. The existence of CPC on SMBS and BMBS was further supported by other evidences as well. The surface area for the modified straws (SMBS and BMBS) was found to remarkably decrease compared to the unmodified ones (RBS and RBS-N).
- Carbon and Nitrogen contents (C and N) were also higher in the modified straws (SMBS and BMBS) compared to RBS and RBS-N, due to cationic surfactant impregnation, hexadecylpyridinium chloride, CPC. Based on carbon

and nitrogen values, the impregnated CPC on SMBS and BMBS were calculated as 0.086 and 0.109 mmol g<sup>-1</sup>, respectively.

- Acidic groups were higher on RBS-N than RBS due to the base treatment increasing the negatively charged surface binding sites on RBS-N. This is important, as these binding sites will be responsible for attracting cationic surfactant molecules to bind onto them. More active binding sites could attract more cationic surfactant. The amount of acidic surface groups was observed lower in the modified straws (SMBS and BMBS) compared to RBS and RBS-N.
- Surface area was also higher for base treated straw (RBS-N) compared to RBS due to dissolution of some organic matters. Higher surface area means greater access/contact of cationic surfactant with the straw surface. However, the surface area was found to significantly decrease on SMBS and BMBS due to the existence of CPC on modified straws. The reduction percentage of surface area for BMBS and SMBS was 56.0% and 21.0%, respectively.
- The desorption of CPC from modified straws in deionized water was lower at 2.67 and 1.94% for SMBS and BMBS, respectively. However, desorption percentage was increased in aqueous acid solutions, where the desorption percentages of CPC in 0.0001, 0.001 and 0.01 N HCl were 0.37, 34.97 and 41.45% for SMBS; and 4.15, 20.94 and 26.37% for BMBS, respectively. This indicates a strong bonding between the CPC and straw surface with the ion exchange dominating the major mechanism of CPC adsorption on barley straw.

Utilization of prepared adsorbents for removal of emulsified oil and dyes was conducted in batch and fixed bed column reactors. In batch studies, influences of several significant experimental parameters were tested to determine the suitability of prepared adsorbents at different environment. The experimental data were later fitted to kinetic models and isotherm models to determine the best models that can represent the data obtained. The batch study for removing canola oil (CO) and standard mineral

oil (SMO) was tested only with the modified straw as a preliminary study using raw straw, RBS and RBS-N gave less than satisfactory removal efficiencies. The outcome drawn from the batch adsorption study of oil removal could be concluded as follows:

- The dynamic studies revealed that oil adsorption on SMBS and BMBS was rapid and equilibrium could be reached within 40 min. The equilibrium time at lower concentration of CO ( $1040 \text{ mg L}^{-1}$ ) was 15 min for both SMBS and BMBS. The equilibrium would however take a relatively longer at 45 and 35 min, for SMBS and BMBS, respectively at higher concentration of CO ( $3450 \text{ mg L}^{-1}$ ). For SMO, the equilibrium time for both SMBS and BMBS at lower concentration of  $1580 \text{ mg L}^{-1}$  was 20 min and the equilibrium time increased to 45 and 35 min for SMBS and BMBS, respectively at a relatively higher concentration of  $4315 \text{ mg L}^{-1}$ . The equilibrium was quicker for lower oil concentration. Kinetic experiments showed that the pseudo first order model fitted the kinetic data better.
- Kinetic diffusion study showed that film diffusion controlled the adsorption of CO and SMO onto SMBS and BMBS. The effective diffusion rates,  $D_i$  for initial CO concentration of 1040 and  $3450 \text{ mg L}^{-1}$  are  $6.89 \times 10^{-6}$  -  $3.84 \times 10^{-5}$  and  $1.82 \times 10^{-5}$  -  $1.01 \times 10^{-4} \text{ cm}^2 \text{ s}^{-1}$  (SMBS); and  $1.33 \times 10^{-5}$  -  $7.40 \times 10^{-5}$  and  $2.01 \times 10^{-5}$  -  $1.12 \times 10^{-4} \text{ cm}^2 \text{ s}^{-1}$  (BMBS), respectively. In the case of SMO,  $D_i$  values for the concentration of 1680 and  $4315 \text{ mg L}^{-1}$  are  $6.33 \times 10^{-6}$  -  $3.52 \times 10^{-5}$  and  $8.13 \times 10^{-6}$  -  $4.53 \times 10^{-5} \text{ cm}^2 \text{ s}^{-1}$  (SMBS); and  $5.30 \times 10^{-6}$  -  $2.95 \times 10^{-5}$  and  $7.53 \times 10^{-6}$  -  $4.19 \times 10^{-5} \text{ cm}^2 \text{ s}^{-1}$  (BMBS), respectively
- For isotherm experiments, CO and SMO adsorption on SMBS and BMBS were better represented by the Langmuir isotherm other than the Freundlich model. The Langmuir batch adsorption capacities of CO and SMO were  $576.00$  and  $518.63 \text{ mg g}^{-1}$  for SMBS; and  $613.29$  and  $584.22 \text{ mg g}^{-1}$  for BMBS, respectively.

- The oil adsorption was observed as a function of straw particle size. Adsorption was higher at smaller particle size. Adsorption capacity on SMBS at the particle size ( $< 0.50$  mm) was  $92.0$  and  $93.1 \text{ mg g}^{-1}$  for CO and SMO respectively. Meanwhile, for the same particle size of BMBS, the corresponding adsorption capacities of CO and SMO were  $111.0$  and  $110.5 \text{ mg g}^{-1}$ , respectively.
- For both CO and SMO, the maximum removal was observed at pH around neutrality (6 and 8). For SMBS, adsorption capacities at pH 6 and 8 were  $72.4$ ,  $72.7 \text{ mg g}^{-1}$ (CO) and  $77.4$ ,  $78.7 \text{ mg g}^{-1}$  (SMO) respectively. For BMBS, the corresponding values were  $77.4$ ,  $74.7 \text{ mg g}^{-1}$  (CO) and  $79.1$ ,  $78.5 \text{ mg g}^{-1}$  (SMO).
- Little effect on adsorption capacity at lower range of experimental temperature ( $23$  and  $33$  °C) was observed for both SMBS and BMBS. However, adsorption was found to slightly increase at relatively higher temperature ( $43$  °C). For SMBS, adsorption capacity at experimental temperature of  $43$  °C was  $109.2$  and  $105.6 \text{ mg g}^{-1}$  for CO and SMO respectively. For BMBS, experimental temperature of  $43$  °C gave their corresponding adsorption values at  $110.8$  and  $107.2 \text{ mg g}^{-1}$  for CO and SMO.
- The oil adsorbed on the straw was stable as desorption experiments showed less than  $4.0\%$  of oil washed out upon exposure to the desorption agent. The percentages of oil leached out at the exposure time of 1, 5 and 24 h were  $4.13$ ,  $3.67$  and  $3.67\%$  for CO and  $1.50$ ,  $2.80$  and  $2.20\%$  for SMO, respectively. Oil desorption was even less at 1, 5 and 24 h, which was  $2.30$ ,  $2.30$  and  $1.84\%$  for CO and  $1.70$ ,  $1.95$  and  $2.10\%$  for SMO, respectively.

In the fixed bed column for removing canola oil (CO) and standard mineral oil (SMO), the evaluation was only made for column breakthrough performance. The outcome drawn from the fixed bed column breakthrough for oil removal could be concluded as follows:

- RBS and RBS-N were found to give very poor adsorption performance in column breakthrough curves, however, favorable adsorption was observed on SMBS and BMBS. The breakthrough time of SMBS and BMBS was 223 and 274 min for CO; 192 and 225 min for SMO, respectively.
- The simulation of whole breakthrough curves predicted by the Thomas model for SMBS and BMBS showed high  $R^2$  values of above 0.99 for the column system. The Thomas column adsorption capacities of CO and SMO were 368.82 and 310.16 mg g<sup>-1</sup> for SMBS; and 440.74 and 336.31 mg g<sup>-1</sup> for BMBS respectively. This was lower compared to the batch adsorption capacity obtained from the Langmuir model.
- The Yoon-Nelson model also exhibited good fit to the experimental data with  $R^2$  values above 0.99 for the column system. The time required to achieve 50% of adsorbate breakthrough ( $\tau$ ) seemed to agree well with the time ( $t_{50\%,\text{exp}}$ ) from experimental data. The time required to achieve 50% of adsorbate breakthrough ( $\tau$ ) for CO and SMO was 265 and 227.7 min for SMBS; and 314.7 and 250.9 min for BMBS respectively

Three types of dyes, namely acid blue 40 (AB40), reactive blue 4 (RB4) and reactive black 5 (RB5) were tested with SMBS and BMBS as the adsorbents. RBS and RBS-N were found to give significantly lower dye removal. The outcome drawn from the batch adsorption study of dye removal could be concluded as follows:

- Dye adsorption on SMBS and BMBS could reach equilibrium within 240 min. For a lower concentration of dye solution of 50 mg L<sup>-1</sup>, the equilibrium time of SMBS and BMBS was 90 and 60 min for AB40; 90 and 60 min for RB4; 180 and 210 min for RB5 respectively. For a higher concentration of dye solution of 100 mg L<sup>-1</sup>, the equilibrium time of SMBS and BMBS was 120 and 90 min for AB40; and 120 and 240 min for RB4 and RB5 for both of the SMBS and BMBS. Kinetic experiment showed that the pseudo second order represented the kinetic data better.

- Kinetic diffusion study showed that film diffusion was the rate limiting step for adsorption of AB40, RB4 and RB5 onto SMBS and BMBS. For AB40,  $D_i$  for the concentration of 50 and 100 mg L<sup>-1</sup> were  $3.72 \times 10^{-6}$ - $2.07 \times 10^{-5}$  and  $1.40 \times 10^{-6}$  -  $7.79 \times 10^{-6}$  (SMBS); and  $2.04 \times 10^{-6}$  -  $1.14 \times 10^{-5}$  cm<sup>2</sup> s<sup>-1</sup> (BMBS), respectively. For RB4 the  $D_i$  values for the concentration of 50 and 100 mg L<sup>-1</sup> are  $4.00 \times 10^{-6}$  -  $2.23 \times 10^{-5}$  and  $1.04 \times 10^{-6}$  -  $5.82 \times 10^{-6}$  cm<sup>2</sup> s<sup>-1</sup> (SMBS); and  $3.06 \times 10^{-6}$  -  $1.71 \times 10^{-6}$  and  $6.90 \times 10^{-7}$  -  $3.84 \times 10^{-6}$  cm<sup>2</sup> s<sup>-1</sup> (BMBS), respectively. Meanwhile, for RB5, the  $D_i$  for the concentration of 50 and 100 mg L<sup>-1</sup> are  $8.36 \times 10^{-7}$  -  $4.66 \times 10^{-6}$  and  $6.90 \times 10^{-7}$  -  $3.84 \times 10^{-6}$  cm<sup>2</sup> s<sup>-1</sup> (SMBS); and  $9.56 \times 10^{-7}$  -  $5.33 \times 10^{-6}$  and  $6.40 \times 10^{-7}$  -  $3.56 \times 10^{-6}$  cm<sup>2</sup> s<sup>-1</sup> (BMBS), respectively.
- For isotherm experiments, adsorption of AB40, RB4 and RB5 on SMBS and BMBS was better represented by the Langmuir isotherm rather than the Freundlich model. The Langmuir adsorption capacities of AB40, RB4 and RB5 were 45.4, 29.16 and 24.92 mg g<sup>-1</sup> for SMBS; and 51.95, 31.50 and 39.88 mg g<sup>-1</sup> for BMBS respectively.
- Adsorption capacity was found higher at about neutral pH for AB40, and at acidic condition (pH 3) for the other dyes. The maximum adsorption capacity of AB40 of SMBS was 43.4 mg g<sup>-1</sup> (at pH 8) and 48.7 mg g<sup>-1</sup> (at pH 5) for BMBS. Meanwhile full removal was observed at pH 3 for RB4 and RB5 for both SMBS and BMBS.
- Adsorption capacity of AB40 was found to increase with increasing experimental temperature whereas no significant change was observed for both RB4 and RB5. For AB40, sorption capacity at the highest temperature was 58.0 mg g<sup>-1</sup> (SMBS) and 70.6 mg g<sup>-1</sup>(BMBS) respectively. For RB4 and RB5, the influence of temperature on sorption capacity was small. Average sorption capacity for RB4 was about 20 mg g<sup>-1</sup> (SMBS) and 22 mg g<sup>-1</sup> (BMBS). For RB5, the sorption capacity was 23.0 mg g<sup>-1</sup> (SMBS) and 30.0 mg g<sup>-1</sup> (BMBS).

- Desorption experiments also showed that the dye loaded on straw is stable at acidic condition but desorption will increase as the pH increases (i.e pH 11). The percentages of dye leached out at pH buffer solution of 3, 5, 8 and 11 for SMBS were 0, 13.86, 16.14 and 17.27% for AB40; 0, 10.09, 12.66 and 26.78% for RB4; 0, 16.85, 23.96 and 26.80% for RB5, respectively. For BMBS's case, the dye desorption was 0, 6.61, 8.82 and 13.84% for AB40; 0, 9.64, 15.07 and 27.77% for RB4; 0, 4.96, 13.51 and 22.13% for RB5, respectively

For the fixed bed column in removing acid blue (AB40) and reactive black (RB5), the evaluation was only made for column breakthrough performance. The outcome drawn from the fixed bed column breakthrough for dye removal could be concluded as follows:

- The fixed bed column breakthrough curves on SMBS and BMBS were observed to give the favorable and normal column adsorption process, however, column adsorption performance for RBS and RBS-N was poor. The breakthrough time for SMBS and BMBS was 382 and 576 min (AB40); 176 and 265 min (RB5), respectively
- The whole breakthrough curve was well predicted by the Thomas model for SMBS and BMBS with high  $R^2$  values of above 0.99 for all the column systems. The adsorption capacity was found to be higher on BMBS. The adsorption capacities from the Thomas model for SMBS and BMBS were 53.39 and 77.29 mg g<sup>-1</sup> for AB40; and 24.57 and 33.46 mg g<sup>-1</sup> for RB5 respectively. For AB40, the Thomas model adsorption capacity of SMBS and BMBS was higher than batch adsorption capacity obtained from the Langmuir model. However, a different result was observed for RB5, where the Thomas adsorption capacity was slightly lower compared to the Langmuir model batch adsorption capacity
- The Yoon-Nelson model also simulated the experimental data well with  $R^2$  values of above 0.99 for all the column systems. The time required to achieve

50% adsorbate breakthrough( $\tau$ ) agreed well with the time ( $t_{50\%,\text{exp}}$ ) from experimental data. The time required to achieve 50% adsorbate breakthrough( $\tau$ ) for SMBS and BMBS was 578.4 and 783.47 min for AB40; and 254.4 and 353.38 min for RB5 respectively. BMBS shows better applicability to treat dye wastewater as the ' $\tau$ ' was relatively longer than SMBS for all the column systems.

### 7.3 Future Directions

The applicability of barley straw for remediation of emulsified oil and dye wastewater was thoroughly presented in this report. The results showed the effectiveness of modified agricultural product/biomass as an adsorbent material for emulsified oil as well as dye wastewater cleaning. However, several issues need to be addressed in an effort to improve and compliment the present data before considering the real applications. Among the issues are:

- The potential of using other biomass materials need to be evaluated. Alternative cheap materials such as oat straw, grass, wheat straw etc should be explored and tested. Other cationic surfactants, i.e cetyltrimethylammonium bromide CTAB and others could also be used. It is interesting to further explore the potential of utilizing different types of biomass as well as other types of surfactant.
- Synthetic wastewater of emulsified oil from canola (CO) and standard mineral oil (SMO) and three anionic dyes of AB40, RB4 and RB5 were studied in this work. For better description of the effectiveness and applicability of the prepared adsorbents, evaluation with other types of emulsified oil wastewater, i.e animal originated oil (Fats), petroleum based oil etc, is also necessary. The synthetic dyes also need to be expanded to the other types of anionic dyes as well. As real dye wastewater always consists of more than a type of dye and probably mixed with other category of dyes such as cationic and non ionic, the mixture of more than one type of dye and different category of dyes seem to be sensible to be tested in order to obtain the realistic data.

- The ultimate goal is always to apply the prepared adsorbents in the real field, since the environmental conditions cannot be simulated by pure laboratory testing. For scale-up design purposes, column testing may be the most applicable method. However, in this study, the performance of column experiment only evaluated for limited column breakthrough parameter. To obtain comprehensive data, effects of the significant operation parameters in a fixed bed column such as variation in column height, column diameter, feeding solution volumetric flowrate and variation in feeding solution concentration need to be evaluated
- The option of disposing the used straw need to be established in order to address another pollutant in the form of oil and dye loaded straw. Finally, a Life Cycle Analysis (LCA) should be performed in an effort to investigate and evaluate the environmental impacts of a given product.

## REFERENCES

1. NAS, *National Academy of Sciences. Oil in the Sea: Inputs, Fates and Effects*. 1985, Washington DC: National Academy Press.
2. Demirbas, E. and M.Z. Nas, *Batch kinetic and equilibrium studies of adsorption of Reactive Blue 21 by fly ash and sepiolite*. *Desalination*, 2009. **243**(1-3): p. 8-21.
3. Robinson, T., G. McMullan, R. Marchant, and P. Nigam, *Remediation of dyes in textile effluent: a critical review on current treatment technologies with a proposed alternative*. *Bioresource Technology*, 2001. **77**(3): p. 247-255.
4. Ncibi, M.C., B. Mahjoub, and M. Seffen, *Kinetic and equilibrium studies of methylene blue biosorption by Posidonia oceanica (L.) fibres*. *Journal of hazardous materials*, 2007. **139**(2): p. 280-285.
5. Zhou, Y.-B., X.-Y. Tang, X.-M. Hu, S. Fritschi, and J. Lu, *Emulsified oily wastewater treatment using a hybrid-modified resin and activated carbon system*. *Separation and Purification Technology*, 2008. **63**(2): p. 400-406.
6. Rajakovic, V., G. Aleksic, M. Radetic, and L. Rajakovic, *Efficiency of oil removal from real wastewater with different sorbent materials*. *Journal of Hazardous Materials*, 2007. **143**(1-2): p. 494-499.
7. Crini, G., *Non-conventional low-cost adsorbents for dye removal: A review*. *Bioresource Technology*, 2006. **97**(9): p. 1061-1085.
8. Allen, S.J. and B. Koumanova, *Decolourisation of water/wastewater using adsorption*. *Journal of the University of Chemical Technology and Metallurgy*, 2005. **40**(3): p. 175-192.
9. Gupta, V.K. and Suhas, *Application of low-cost adsorbents for dye removal - A review*. *Journal of Environmental Management*, 2009. **90**(8): p. 2313-2342.
10. Birhanli, A. and M. Ozmen, *Evaluation of the toxicity and teratogenicity of six commercial textile dyes using the frog embryo teratogenesis assay-Xenopus*. *Drug and Chemical Toxicology*, 2005. **28**(1): p. 51-65.
11. Gottlieb, A., C. Shaw, A. Smith, A. Wheatley, and S. Forsythe, *The toxicity of textile reactive azo dyes after hydrolysis and decolourisation*. *Journal of Biotechnology*, 2003. **101**(1): p. 49-56.

12. Benito, J.M., G. Rios, C. Pasoz, and J. Coca, *Methods for the separation of emulsified oil from water: a state-of-the-art review*. Trends Chemical Engineering, 1998. **4** p. 203-231.
13. Delee, W., C. O'Neill, F.R. Hawkes, and H.M. Pinheiro, *Anaerobic treatment of textile effluents: A review*. Journal of Chemical Technology and Biotechnology, 1998. **73**(4): p. 323-335.
14. Rai, H.S., M.S. Bhattacharyya, J. Singh, T.K. Bansal, P. Vats, and U.C. Banerjee, *Removal of dyes from the effluent of textile and dyestuff manufacturing industry: A review of emerging techniques with reference to biological treatment*. Critical Reviews in Environmental Science and Technology, 2005. **35**(3): p. 219-238.
15. van der Zee, F.P. and S. Villaverde, *Combined anaerobic-aerobic treatment of azo dyes - A short review of bioreactor studies*. Water Research, 2005. **39**(8): p. 1425-1440.
16. Mondal, S., *Methods of dye removal from dye house effluent - An overview*. Environmental Engineering Science, 2008. **25**(3): p. 383-396.
17. Oei, B.C., S. Ibrahim, S. Wang, and H.M. Ang, *Surfactant modified barley straw for removal of acid and reactive dyes from aqueous solution*. Bioresource Technology, 2009. **100**(18): p. 4292-4295.
18. Kumar, A., N.N. Rao, and S.N. Kaul, *Alkali-treated straw and insoluble straw xanthate as low cost adsorbents for heavy metal removal - preparation, characterization and application*. Bioresource Technology, 2000. **71**(2): p. 133-142.
19. Moazed, H. and T. Viraraghavan, *Use of Organo-Clay/Anthracite Mixture in the Separation of Oil from Oily Waters*. Energy Sources, Part A: Recovery, Utilization, and Environmental Effects, 2005. **27**(1): p. 101 - 112.
20. Wang, S., Y. Boyjoo, A. Choueib, and Z.H. Zhu, *Removal of dyes from aqueous solution using fly ash and red mud*. Water Research, 2005. **39**(1): p. 129-138.
21. Alther, G.R., *Removing oils from water with organoclays*. Journal / American Water Works Association, 2002. **94**(7): p. 115-121.
22. Moazed, H. and T. Viraraghavan, *Removal of oil from water by bentonite organoclay*. Practice Periodical of Hazardous, Toxic, and Radioactive Waste Management, 2005. **9**(2): p. 130-134.

23. Wan Ngah, W.S. and M.A.K.M. Hanafiah, *Biosorption of copper ions from dilute aqueous solutions on base treated rubber (Hevea brasiliensis) leaves powder: kinetics, isotherm, and biosorption mechanisms*. Journal of Environmental Sciences, 2008. **20**(10): p. 1168-1176.
24. Larsen, V.J.V.J., *Use of straw for removal of heavy metals from waste water*. Journal of Environmental Quality, 1981. **10**(2): p. 188-193.
25. Pehlivan, E., T. Altun, and S. Parlayici, *Utilization of barley straws as biosorbents for  $Cu^{2+}$  and  $Pb^{2+}$  ions*. Journal of Hazardous Materials, 2009. **164**(2-3): p. 982-986.
26. Amer, A.A., A. El-Maghraby, G.F. Malash, N.A. Taha, T. Applications, and E. Alexandria, *Extensive Characterization of Raw Barley Straw and Study the Effect of Steam Pretreatment*. Journal of Applied Sciences Research, 2007. **3**(11): p. 1336-1342.
27. Šćiban, M., M. Klačnja, and B. Škrbi, *Adsorption of copper ions from water by modified agricultural by-products*. Desalination, 2008. **229**(1-3): p. 170-180.
28. Ibrahim, S., H.M. Ang, and S. Wang, *Removal of emulsified food and mineral oils from wastewater using surfactant modified barley straw*. Bioresource Technology, 2009. **100**(23): p. 5744-5749.
29. Fanta, G.F., T.P. Abbott, R.C. Burr, and W.M. Doane, *Ion exchange reactions of quaternary ammonium halides with wheat straw. Preparation of oil-absorbents*. Carbohydrate Polymers, 1987. **7**(2): p. 97-109.
30. Ozcan, A., C. Omeroglu, Y. Erdogan, and A.S. Ozcan, *Modification of bentonite with a cationic surfactant: An adsorption study of textile dye Reactive Blue 19*. Journal of Hazardous Materials, 2007. **140**(1-2): p. 173-179.
31. Zohra, B., K. Aicha, S. Fatima, B. Nourredine, and D. Zoubir, *Adsorption of Direct Red 2 on bentonite modified by cetyltrimethylammonium bromide*. Chemical Engineering Journal, 2008. **136**(2-3): p. 295-305.
32. Mohamed, M.M., *Acid dye removal: comparison of surfactant-modified mesoporous FSM-16 with activated carbon derived from rice husk*. Journal of Colloid and Interface Science, 2004. **272**(1): p. 28-34.
33. Kuleyin, A., *Removal of phenol and 4-chlorophenol by surfactant-modified natural zeolite*. Journal of Hazardous Materials, 2007. **144**(1-2): p. 307-315.

34. Anirudhan, T.S. and M. Ramachandran, *Adsorptive removal of tannin from aqueous solutions by cationic surfactant-modified bentonite clay*. Journal of Colloid and Interface Science, 2006. **299**(1): p. 116-124.
35. Adak, A., A. Pal, and M. Bandyopadhyay, *Removal of phenol from water environment by surfactant-modified alumina through adsolubilization*. Colloids and Surfaces A: Physicochemical and Engineering Aspects, 2006. **277**(1-3): p. 63-68.
36. Namasivayam, C. and M.V. Sureshkumar, *Removal of chromium(VI) from water and wastewater using surfactant modified coconut coir pith as a biosorbent*. Bioresource Technology, 2008. **99**(7): p. 2218-2225.
37. Farhat, A.L.I., *Edible Oils, Fats, and Waxes*, in *Handbook of industrial chemistry: Organic chemicals*, A.L.I. Farhat, E. Bassam, and J.G. Speight, Editors. 2005, McGraw-Hill. p. 86-121.
38. Pushkarev, V.V., A.G. Yuzhaninov, and S.K. Men, *Treatment of oil-containing wastewater*. 1983: Allerton Press.
39. Patterson, J., *Industrial Wastes Reduction*. Environmental Science & Technology, 1989. **23**(9): p. 1032-1038.
40. Liu, D.H.F. and B.G. Liptak, *Wastewater treatment*. 2000: CRC Press, Boca Raton, FL (US).
41. Fakhru'l-Razi, A., A. Pendashteh, L.C. Abdullah, D.R.A. Biak, S.S. Madaeni, and Z.Z. Abidin, *Review of technologies for oil and gas produced water treatment*. Journal of Hazardous Materials, 2009. **170**(2-3): p. 530-551.
42. Zhu, X., B.E. Reed, W. Lin, P.E. Carriere, and G. Roark, *Investigation of Emulsified Oil Wastewater Treatment with Polymers*. Separation Science and Technology, 1997. **32**(13): p. 2173 - 2187.
43. World Bank Group, *Pollution Prevention and Abatement Handbook: Vegetable Oil Processing*. 1998, Washington, DC: World Bank Group.
44. Chen, X., G. Chen, and P.L. Yue, *Separation of pollutants from restaurant wastewater by electrocoagulation*. Separation and Purification Technology, 2000. **19**(1-2): p. 65-76.
45. Ahmad, A.L., S. Sumathi, and B.H. Hameed, *Adsorption of residue oil from palm oil mill effluent using powder and flake chitosan: Equilibrium and kinetic studies*. Water Research, 2005. **39**(12): p. 2483-2494.

46. Jeganathan, J., A. Bassi, and G. Nakhla, *Pre-treatment of high oil and grease pet food industrial wastewaters using immobilized lipase hydrolyzation*. Journal of Hazardous Materials, 2006. **137**(1): p. 121-128.
47. Kobya, M., E. Senturk, and M. Bayramoglu, *Treatment of poultry slaughterhouse wastewaters by electrocoagulation*. Journal of Hazardous Materials, 2006. **133**(1-3): p. 172-176.
48. Tabakin, R.B., R. Trattner, and P.N. Cheremisinoff, *Oil water separation technology: the available options available*. Water and Sewage Works, 1978. **125**(8): p. 72-75.
49. Alther, G.R., *How to remove emulsified oil from wastewater with organoclays*. Water/Engineering & Management 2001. **148**(7): p. 27-28.
50. Bratskaya, S., V. Avramenko, S. Schwarz, and I. Philippova, *Enhanced flocculation of oil-in-water emulsions by hydrophobically modified chitosan derivatives*. Colloids and Surfaces A: Physicochemical and Engineering Aspects, 2006. **275**(1-3): p. 168-176.
51. Nag, A., *Utilization of charred sawdust as an adsorbent of dyes, toxic salts and oil from water*. Process Safety and Environmental Protection: Transactions of the Institution of Chemical Engineers, Part B, 1995. **73**(4): p. 299-306.
52. Alther, G., *Using organoclays to enhance carbon filtration*. Waste Management, 2002. **22**(5): p. 507-513.
53. Baig, M.A., M. Mir, and Z.I. Bhatti, *Removal of Oil and Grease from Industrial Effluents*. Electronic Journal of Environmental, Agricultural and Food Chemistry, 2003. **2**(5): p. 577-585.
54. King, S., *Small quantity generator oily wastewater management study, final report.*, in 1999, Local Hazardous Waste Management Program in King County: Seattle, WA.
55. Oil Spill Program Update, *The U.S. EPA's Oil Program Center Report*. 1998, United States Environmental Protection Agency: Cincinnati, OH.
56. Zollinger, H., *Color chemistry: syntheses, properties, and applications of organic dyes and pigments*. 2003: Wiley-VCH.
57. Clarke, E.A. and R. Anliker, *Organic dyes and pigments*. The handbook of environmental chemistry, 1980. **3**(Part A): p. 181-215.

58. Hunger, K., *Industrial dyes: chemistry, properties, applications*. 2003: Wiley-VCH.
59. Mishra, G. and M. Tripathy, *A critical review of the treatments for decolourization of textile effluent*. Colourage, 1993. **40**(10): p. 35-38.
60. Purkait, M.K., S. DasGupta, and S. De, *Adsorption of eosin dye on activated carbon and its surfactant based desorption*. Journal of environmental management, 2005. **76**(2): p. 135-142.
61. Lynch, D.G., *Estimating the properties of synthetic organic dyes*, in *Handbook of property estimation methods for chemicals: environmental and health sciences*, R.S. Boethling and D. Mackay, Editors. 2000, CRC Press: Boca Raton.
62. Ong, S.T., C.K. Lee, and Z. Zainal, *Removal of basic and reactive dyes using ethylenediamine modified rice hull*. Bioresource technology, 2007. **98**(15): p. 2792-2799.
63. Forgacs, E., T. Cserháti, and G. Oros, *Removal of synthetic dyes from wastewaters: a review*. Environment International, 2004. **30**(7): p. 953-971.
64. Muthukumar, M. and N. Selvakumar, *Studies on the effect of inorganic salts on decolouration of acid dye effluents by ozonation*. Dyes and Pigments, 2004. **62**(3): p. 221-228.
65. Øllgaard, H., L. Frost, J. Galster, and O.C. Hansen, *Survey of azo-colorants in Denmark: Consumption, use, health and environmental aspects*. 1998.
66. Easton, J.R., *The dye maker's view*, in *Colour in dyehouse effluent*, P. Cooper, Editor. 1995, Society of Dyers and Colourists Bradford. p. 9-21.
67. Banat, F., S. Al-Asheh, and L. Al-Makhadmeh, *Evaluation of the use of raw and activated date pits as potential adsorbents for dye containing waters*. Process Biochemistry, 2003. **39**(2): p. 193-202.
68. O'Neill, C., F.R. Hawkes, D.L. Hawkes, N.D. Lourenco, H.M. Pinheiro, and W. Delee, *Colour in textile effluents- sources, measurement, discharge consents and simulation: a review*. Journal of Chemical Technology and Biotechnology, 1999. **74**(11): p. 1009-1018.
69. Robinson, T., B. Chandran, and P. Nigam, *Removal of dyes from an artificial textile dye effluent by two agricultural waste residues, corncob and barley husk*. Environment International, 2002. **28**(1-2): p. 29-33.

70. Aksu, Z. and I.A. Isoglu, *Use of agricultural waste sugar beet pulp for the removal of Gemazol turquoise blue-G reactive dye from aqueous solution*. Journal of Hazardous Materials, 2006. **137**(1): p. 418-430.
71. Hao, O.J., H. Kim, and P.C. Chiang, *Decolorization of wastewater*. Critical Reviews in Environmental Science and Technology, 1999. **30**(4): p. 449-505.
72. Farah, J.Y., N.S. El-Gendy, and L.A. Farahat, *Biosorption of Astrazone Blue basic dye from an aqueous solution using dried biomass of Baker's yeast*. Journal of Hazardous Materials, 2007. **148**(1-2): p. 402-408.
73. Baughman, G.L. and E.J. Weber, *Transformation of dyes and related compounds in anoxic sediment: kinetics and products*. Environmental Science & Technology, 1994. **28**(2): p. 267-276.
74. Moussavi, G. and M. Mahmoudi, *Removal of azo and anthraquinone reactive dyes from industrial wastewaters using MgO nanoparticles*. Journal of Hazardous Materials, 2009. **168**(2-3): p. 806-812.
75. Brown, M.A. and S.C. DeVito, *Predicting azo dye toxicity*. Critical Reviews in Environmental Science and Technology, 1993. **23**(3): p. 249-324.
76. Fu, Y. and T. Viraraghavan, *Fungal decolorization of dye wastewaters: a review*. Bioresource Technology, 2001. **79**(3): p. 251-262.
77. Leechart, P., W. Nakbanpote, and P. Thiravetyan, *Application of 'waste' wood-shaving bottom ash for adsorption of azo reactive dye*. Journal of Environmental Management, 2009. **90**(2): p. 912-920.
78. Deng, D., J. Guo, G. Zeng, and G. Sun, *Decolorization of anthraquinone, triphenylmethane and azo dyes by a new isolated Bacillus cereus strain DC 11*. International Biodeterioration & Biodegradation, 2008. **62**(3): p. 263-269.
79. Novotný, N. Dias, A. Kapanen, K. Malachová, M. Vándrovcová, M. Itävaara, and N. Lima, *Comparative use of bacterial, algal and protozoan tests to study toxicity of azo-and anthraquinone dyes*. Chemosphere, 2006. **63**(9): p. 1436-1442.
80. Peters, R.W., M.P. Sharma, and T. Williams. *Oil/water separation: A review of the historical development and the evolution of new treatment techniques*. 2007. Houston, TX, United states: American Institute of Chemical Engineers.
81. Williams, T., R.W. Peters, and M.P. Sharma. *Oil/water separation: Examination of various treatment techniques*. 2007. Salt Lake City, UT, United states: American Institute of Chemical Engineers.

82. Gregory, J., *Particles in water: properties and processes*. 2006: CRC.
83. Dafnepatidou, E.K. and N.K. Lazaridis, *Dyes removal from simulated and industrial textile effluents by dissolved-air and dispersed-air flotation techniques*. Industrial and Engineering Chemistry Research, 2008. **47**(15): p. 5594-5601.
84. Burns, S.E., S. Yiacoumi, and C. Tsouris, *Microbubble generation for environmental and industrial separations*. Separation and Purification Technology, 1997. **11**(3): p. 221-232.
85. Rubio, J., M.L. Souza, and R.W. Smith, *Overview of flotation as a wastewater treatment technique*. Minerals Engineering, 2002. **15**(3): p. 139-155.
86. Li, X.b., J.t. Liu, Y.t. Wang, C.y. Wang, and X.h. Zhou, *Separation of Oil from Wastewater by Column Flotation*. Journal of China University of Mining and Technology, 2007. **17**(4): p. 546-551,577.
87. Mavros, P., A.C. Daniilidou, N.K. Lazaridis, and L. Stergiou, *Colour removal from aqueous solutions. Part I. Flotation*. Environmental Technology, 1994. **15**(7): p. 601-616.
88. Dafnopatidou, E.K., G.P. Gallios, E.G. Tsatsaroni, and N.K. Lazaridis, *Reactive dyestuffs removal from aqueous solutions by flotation, possibility of water reuse, and dyestuff degradation*. Industrial and Engineering Chemistry Research, 2007. **46**(7): p. 2125-2132.
89. Metcalf and I. Eddy, *Wastewater engineering, treatment, disposal and reuse*. 4th ed. 2003, Boston, MA.: McGraw-Hill.
90. Chang, I.S., C.M. Chung, and S.H. Han, *Treatment of oily wastewater by ultrafiltration and ozone*. Desalination, 2001. **133**(3): p. 225-232.
91. Matos, M., A. Lobo, E. Fernández, J.M. Benito, C. Pazos, and J. Coca, *Recycling of oily ultrafiltration permeates to reformulate O/W emulsions*. Colloids and Surfaces A: Physicochemical and Engineering Aspects, 2008. **331**(1-2): p. 8-15.
92. Manuele, M., C. Ingrid, M. Alessandro, and V. Guido, *Membrane technologies applied to textile wastewater treatment*. Annals of the New York Academy of Sciences, 2003. **984**: p. 53-64.
93. Van Der Bruggen, B., C. Vandecasteele, T. Van Gestel, W. Doyen, and R. Leysen, *A review of pressure-driven membrane processes in wastewater*

*treatment and drinking water production*. Environmental progress, 2003. **22**(1): p. 45-56.

94. Xu, Y., R.E. Lebrun, P.J. Gallo, and P. Blond, *Treatment of textile dye plant effluent by nanofiltration membrane*. Separation Science and Technology, 1999. **34**(13): p. 2501-2519.
95. Ahmad, A.L., S. Sumathi, and B.H. Hameed, *Residual oil and suspended solid removal using natural adsorbents chitosan, bentonite and activated carbon: A comparative study*. Chemical Engineering Journal, 2005. **108**(1-2): p. 179-185.
96. Alther, G.R., *Organically modified clay removes oil from water*. Waste Management, 1995. **15**(8): p. 623-628.
97. Ribeiro, T.H., J. Rubio, and R.W. Smith, *A dried hydrophobic aquaphyte as an oil filter for oil/water emulsions*. Spill Science and Technology Bulletin, 2003. **8**(5-6): p. 483-489.
98. Mysore, D., T. Viraraghavan, and Y.-C. Jin, *Treatment of oily waters using vermiculite*. Water Research, 2005. **39**(12): p. 2643-2653.
99. Solisio, C., A. Lodi, A. Converti, and M.D. Borghi, *Removal of exhausted oils by adsorption on mixed Ca and Mg oxides*. Water Research, 2002. **36**(4): p. 899-904.
100. Ahmad, A.L., S. Bhatia, N. Ibrahim, and S. Sumathi, *Adsorption of residual oil from palm oil mill effluent using rubber powder*. Brazillian Journal of Chemical Engineering, 2005. **22**(3): p. 371-379.
101. Alther, G., *Organoclay cost effectively removes oil from produced water*. Oil and Gas Journal, 1997. **95**(15): p. 54-55.
102. Guibal, E., P. McCarrick, and J.M. Tobin, *Comparison of the Sorption of Anionic Dyes on Activated Carbon and Chitosan Derivatives from Dilute Solutions*. Separation Science and Technology, 2003. **38**(12): p. 3049 - 3073.
103. Rashmi, S. and B. Bani, *Review on decolorisation of aqueous dye solutions by low cost adsorbents*. Coloration Technology, 2002. **118**(5): p. 256-269.
104. Alessandro, A., J.K. Bewtra, and I.A. Hambdy, *Physical and chemical treatment of wastewaters*, in *Encyclopedia of Environmental Science and Engineering*, J.R. Pfafflin and E.N. Ziegler, Editors. 2006, CRC. p. 972-989.

105. Drinan, J. and N.E. Whiting, *Water & wastewater treatment: a guide for the nonengineering professional*. 2000: CRC.
106. Randtke, S.J., *Organic contaminant removal by coagulation and related process combinations*. Journal American Water Works Association, 1988. **88**(5): p. 40-56.
107. Ahmad, A.L., S. Sumathi, and B.H. Hameed, *Coagulation of residue oil and suspended solid in palm oil mill effluent by chitosan, alum and PAC*. Chemical Engineering Journal, 2006. **118**(1-2): p. 99-105.
108. Suzuki, Y. and T. Maruyama, *Removal of emulsified oil from water by coagulation and foam separation*. Separation Science and Technology, 2005. **40**(16): p. 3407-3418.
109. Zouboulis, A.I. and A. Avranas, *Treatment of oil-in-water emulsions by coagulation and dissolved-air flotation*. Colloids and Surfaces A: Physicochemical and Engineering Aspects, 2000. **172**(1-3): p. 153-161.
110. Hanafy, M. and H.I. Nabih, *Treatment of oily wastewater using dissolved air flotation technique*. Energy Sources-Part A Recovery Utilization and Environmental Effects, 2007. **29**(1-3): p. 143-160.
111. Cañizares, P., F. Martínez, C. Jiménez, C. Sáez, and M.A. Rodrigo, *Coagulation and electrocoagulation of oil-in-water emulsions*. Journal of Hazardous Materials, 2008. **151**(1): p. 44-51.
112. Yoshida, H., S. Fukuda, A. Okamoto, and T. Kataoka, *Recovery of direct dye and acid dye by adsorption on chitosan fiber- equilibria*. Water Science & Technology, 1991. **23**(7): p. 1667-1676.
113. Lee, J.W., S.P. Choi, R. Thiruvengkatachari, W.G. Shim, and H. Moon, *Evaluation of the performance of adsorption and coagulation processes for the maximum removal of reactive dyes*. Dyes and Pigments, 2006. **69**(3): p. 196-203.
114. Sarasa, J., M.P. Roche, M.P. Ormad, E. Gimeno, A. Puig, and J.L. Ovelleiro, *Treatment of a wastewater resulting from dyes manufacturing with ozone and chemical coagulation*. Water Research, 1998. **32**(9): p. 2721-2727.
115. Southern, T.G., *Technical solutions to the colour problem: a critical review*, in *Colour in dyehouse effluent*, P. Cooper, Editor. 1995, Society of Dyers and Colourists Bradford. p. 73-91.

116. Lazarova, V., *Wastewater Treatment for Water Recycling*, in *Water reuse for irrigation: agriculture, landscapes, and turf grass*, V. Lazarova and A. Bahri, Editors. 2005, CRC Press, Boca Raton, Fla. p. 164-231.
117. Chu, W. and C.W. Ma, *Quantitative prediction of direct and indirect dye ozonation kinetics*. Water Research, 2000. **34**(12): p. 3153-3160.
118. Aplin, R. and T.D. Waite, *Comparison of three advanced oxidation processes for degradation of textile dyes*. Waste Minimisation and End of Pipe Treatment in Chemical and Petrochemical Industries, 2000. **42**(5-6): p. 345-354.
119. Rice, R.G., *Handbook of ozone technology and applications*. 1982, Ann Harbor: Science Publishers. 360-371.
120. Gunukula, R.V.B. and M.E. Tittlebaum, *Industrial wastewater treatment by an advanced oxidation process*. Journal of Environmental Science and Health - Part A Toxic/Hazardous Substances and Environmental Engineering, 2001. **36**(3): p. 307-320.
121. Karageorgos, P., A. Coz, M. Charalabaki, N. Kalogerakis, N.P. Xekoukoulotakis, and D. Mantzavinos, *Ozonation of weathered olive mill wastewaters*. Journal of Chemical Technology and Biotechnology, 2006. **81**(9): p. 1570-1576.
122. Andreozzi, R., V. Caprio, A. Insola, R. Marotta, and R. Sanchirico, *Advanced oxidation processes for the treatment of mineral oil-contaminated wastewaters*. Water Research, 2000. **34**(2): p. 620-628.
123. Majcen-Le Marechal, A., Y.M. Slokar, and T. Taufer, *Decoloration of chlorotriazine reactive azo dyes with H<sub>2</sub>O<sub>2</sub>/UV*. Dyes and Pigments, 1997. **33**(4): p. 281-298.
124. Marmagne, O. and C. Coste, *Color removal from textile plant effluents*. American Dyestuff Reporter, 1996. **85**(4): p. 15-21.
125. Gähr, F., F. Hermanutz, and W. Oppermann, *Ozonation- An important technique to comply with new German laws for textile wastewater treatment*. Water Science & Technology, 1994. **30**(3): p. 255-263.
126. Vandevivere, P.C., R. Bianchi, and W. Verstraete, *Review: Treatment and reuse of wastewater from the textile wet-processing industry: Review of emerging technologies*. Journal of Chemical Technology & Biotechnology, 1998. **72**(4): p. 289-302.

127. Bewtra, K. and N. Biswas, *Biological treatment of wastewater*, in *Encyclopedia of Environmental Science and Engineering*, J.R. Pfafflin and E.N. Ziegler, Editors. 2006, CRC: . p. 137-158.
128. El-Masry, M.H., E. El-Bestawy, and N.I. El-Adl, *Bioremediation of vegetable oil and grease from polluted wastewater using a sand biofilm system*. World Journal of Microbiology and Biotechnology, 2004. **20**(6): p. 551-557.
129. Chavan, A. and S. Mukherji, *Treatment of hydrocarbon-rich wastewater using oil degrading bacteria and phototrophic microorganisms in rotating biological contactor: Effect of N: P ratio*. Journal of Hazardous Materials, 2008. **154**(1-3): p. 63-72.
130. Lemmer, H. and M. Baumann, *Scum actinomycetes in sewage treatment plants. II: The effect of hydrophobic substrate*. Water research, 1988. **22**(6): p. 761-763.
131. Chao, A.C. and W. Yang, *Biological treatment of wool scouring wastewater*. Water Environment Federation, 1981. **53**(3): p. 311-317.
132. Eckenfelder, W.W., *Industrial Water Pollution*. 2000, McGraw-Hill, Singapore.
133. Cammarota, M.C. and D.M.G. Freire, *A review on hydrolytic enzymes in the treatment of wastewater with high oil and grease content*. Bioresource Technology, 2006. **97**(17): p. 2195-2210.
134. Manahan, S.E., *Fundamentals of environmental chemistry*. 2001: CRC Press.
135. Petruy, R. and G. Lettinga, *Digestion of a milk-fat emulsion*. Bioresource Technology, 1997. **61**(2): p. 141-149.
136. Rinzema, A., A. Alphenaar, and G. Lettinga, *Anaerobic digestion of long-chain fatty acids in UASB and expanded granular sludge bed reactors*. Process Biochemistry, 1993. **28**(8): p. 527-37.
137. Gizgis, N., M. Georgiou, and E. Diamadopoulos, *Sequential anaerobic/aerobic biological treatment of olive mill wastewater and municipal wastewater*. Journal of Chemical Technology and Biotechnology, 2006. **81**(9): p. 1563-1569.
138. Wahaab, R.A. and M.H. El-Awady, *Anaerobic/aerobic treatment of meat processing wastewater*. The Environmentalist, 1999. **19**(1): p. 61-65.

139. Lu, M., Z. Zhang, W. Yu, and W. Zhu, *Biological treatment of oilfield-produced water: A field pilot study*. International Biodeterioration & Biodegradation, 2009. **63**(3): p. 316-321.
140. Pagga, U. and D. Brown, *The degradation of dyestuffs: Part II. Behaviour of dyestuffs in aerobic biodegradation tests*. Chemosphere, 1986. **15**(4): p. 479-491.
141. Shaul, G.M., T.J. Holdsworth, C.R. Dempsey, and K.A. Dostal, *Fate of water soluble azo dyes in the activated sludge process*. Chemosphere, 1991. **22**(1): p. 107-119.
142. Pagga, U. and K. Taeger, *Development of a method for adsorption of dyestuffs on activated sludge*. Water Research, 1994. **28**(5): p. 1051-1057.
143. O'Neill, C., A. Lopez, S. Esteves, F.R. Hawkes, D.L. Hawkes, and S. Wilcox, *Azo-dye degradation in an anaerobic-aerobic treatment system operating on simulated textile effluent*. Applied Microbiology and Biotechnology, 2000. **53**(2): p. 249-254.
144. Tony, B.D., D. Goyal, and S. Khanna, *Decolorization of textile azo dyes by aerobic bacterial consortium*. International Biodeterioration and Biodegradation, 2009. **63**(4): p. 462-469.
145. Khehra, M.S., H.S. Saini, D.K. Sharma, B.S. Chadha, and S.S. Chimni, *Biodegradation of azo dye C.I. Acid Red 88 by an anoxic - Aerobic sequential bioreactor*. Dyes and Pigments, 2006. **70**(1): p. 1-7.
146. dos Santos, A.B., I.A.E. Bisschops, F.J. Cervantes, and J.B. van Lier, *The transformation and toxicity of anthraquinone dyes during thermophilic (55 C) and mesophilic (30 C) anaerobic treatments*. Journal of Biotechnology, 2005. **115**(4): p. 345-353.
147. Field, J.A., A.J.M. Stams, M. Kato, and G. Schraa, *Enhanced biodegradation of aromatic pollutants in cocultures of anaerobic and aerobic bacterial consortia*. Antonie van Leeuwenhoek, 1995. **67**(1): p. 47-77.
148. Rajaguru, P., K. Kalaiselvi, M. Palanivel, and V. Subburam, *Biodegradation of azo dyes in a sequential anaerobic-aerobic system*. Applied microbiology and biotechnology, 2000. **54**(2): p. 268-273.
149. Lourenço, N.D., J.M. Novais, and H.M. Pinheiro, *Effect of some operational parameters on textile dye biodegradation in a sequential batch reactor*. Journal of biotechnology, 2001. **89**(2-3): p. 163-174.

150. Lee, Y.H. and S.G. Pavlostathis, *Decolorization and toxicity of reactive anthraquinone textile dyes under methanogenic conditions*. Water Research, 2004. **38**(7): p. 1838-1852.
151. Weber, W.J., *Physicochemical processes for water quality control*. 1972: Wiley Interscience.
152. Cooney, D.O., *Adsorption design for wastewater treatment*. 1999, Boca Raton: Lewis Publisher, CRC Press.
153. D browski, A., *Adsorption—from theory to practice*. Advances in Colloid and Interface Science, 2001. **93**(1-3): p. 135-224.
154. Leij, F.J. and M.T. van Genuchten, *Solute Transport*, in *Soil physics companion* A.W. Warrick, Editor. 2002, CRC Press: Boca Raton, Fl. p. 189-244.
155. Delgado, J., *A critical review of dispersion in packed beds*. Heat and mass transfer, 2006. **42**(4): p. 279-310.
156. Naiya, T.K., A.K. Bhattacharya, S. Mandal, and S.K. Das, *The sorption of lead (II) ions on rice husk ash*. Journal of Hazardous Materials, 2009. **163**(2-3): p. 1254-1264.
157. Kirwan, D.J., *Mass Transfer principles*, in *Handbook of separation process technology*, R.W. R, Editor. 1987, Wiley-Interscience New York. p. 60-128.
158. Gunn, D.J., *Axial and radial dispersion in fixed beds*. Chemical Engineering Science, 1987. **42**(2): p. 363-373.
159. Bailey, S.E., T.J. Olin, R.M. Bricka, and D.D. Adrian, *A review of potentially low-cost sorbents for heavy metals*. Water Research, 1999. **33**(11): p. 2469-2479.
160. Rocha, C.G., D.A.M. Zaia, R.V.S. Alfaya, and A.A.S. Alfaya, *Use of rice straw as biosorbent for removal of Cu (II), Zn (II), Cd (II) and Hg (II) ions in industrial effluents*. Journal of Hazardous Materials, 2009. **166**(1): p. 383-388.
161. Garg, U., M.P. Kaur, G.K. Jawa, D. Sud, and V.K. Garg, *Removal of cadmium (II) from aqueous solutions by adsorption on agricultural waste biomass*. Journal of Hazardous Materials, 2008. **154**(1-3): p. 1149-1157.
162. Sureshkumar, M.V. and C. Namasivayam, *Adsorption behavior of Direct Red 12B and Rhodamine B from water onto surfactant-modified coconut coir pith*.

Colloids and Surfaces A: Physicochemical and Engineering Aspects, 2008. **317**(1-3): p. 277-283.

163. Gong, R., Y. Jin, F. Chen, J. Chen, and Z. Liu, *Enhanced malachite green removal from aqueous solution by citric acid modified rice straw*. Journal of hazardous materials, 2006. **137**(2): p. 865-870.
164. Gaballah, I., D. Goy, E. Allain, G. Kilbertus, and J. Thauront, *Recovery of copper through decontamination of synthetic solutions using modified barks*. Metallurgical and Materials Transactions B, 1997. **28**(1): p. 13-23.
165. Wan Ngah, W.S. and M.A.K.M. Hanafiah, *Removal of heavy metal ions from wastewater by chemically modified plant wastes as adsorbents: A review*. Bioresource Technology, 2008. **99**(10): p. 3935-3948.
166. Robinson, T., B. Chandran, and P. Nigam, *Effect of pretreatments of three waste residues, wheat straw, corncobs and barley husks on dye adsorption*. Bioresource technology, 2002. **85**(2): p. 119-124.
167. Zhu, B., T. Fan, and D. Zhang, *Adsorption of copper ions from aqueous solution by citric acid modified soybean straw*. Journal of Hazardous Materials, 2008. **153**(1-2): p. 300-308.
168. Altundogan, H.S., N.E. Arslan, and F. Tumen, *Copper removal from aqueous solutions by sugar beet pulp treated by NaOH and citric acid*. Journal of Hazardous Materials, 2007. **149**(2): p. 432-439.
169. Lu, D., Q. Cao, X. Cao, and F. Luo, *Removal of Pb (II) using the modified lawny grass: Mechanism, kinetics, equilibrium and thermodynamic studies*. Journal of Hazardous Materials, 2009. **166**(1): p. 239-247.
170. Min, S.H., J.S. Han, E.W. Shin, and J.K. Park, *Improvement of cadmium ion removal by base treatment of juniper fiber*. Water Research, 2004. **38**(5): p. 1289-1295.
171. Tiemann, K.J., G. Gamez, K. Dokken, J.G. Parsons, and J.L. Gardea-Torresdey, *Chemical modification and X-ray absorption studies for lead (II) binding by Medicago sativa (alfalfa) biomass*. Microchemical Journal, 2002. **71**(2-3): p. 287-293.
172. Xie, J.Z., H.L. Chang, and J.J. Kilbane, *Removal and recovery of metal ions from wastewater using biosorbents and chemically modified biosorbents*. Bioresource Technology, 1996. **57**(2): p. 127-136.

173. Huang, L., H. Xiao, and Y. Ni, *Cationic MCM-41: synthesis, characterization and sorption behavior towards aromatic compounds*. Colloids and Surfaces A: Physicochemical and Engineering Aspects, 2004. **247**(1-3): p. 129-136.
174. Barnes, G. and I. Gentle, *Interfacial science*. 2005: Oxford University Press.
175. Farn, R.J., *Chemistry and technology of surfactants*. 2006: Wiley-Blackwell.
176. Atkin, R., V.S.J. Craig, E.J. Wanless, and S. Biggs, *Mechanism of cationic surfactant adsorption at the solid-aqueous interface*. Advances in Colloid and Interface Science, 2003. **103**(3): p. 219-304.
177. Rangel-Yagui, C.O., A. Pessoa Jr, and L.C. Tavares, *Micellar solubilization of drugs*. Journal of Pharmacy & Pharmaceutical Sciences, 2005. **8**(2): p. 147-165.
178. Paria, S. and K.C. Khilar, *A review on experimental studies of surfactant adsorption at the hydrophilic solid-water interface*. Advances in Colloid and Interface Science, 2004. **110**(3): p. 75-95.
179. Praus, P., M. Turicová, S. Študentová, and M. Ritz, *Study of cetyltrimethylammonium and cetylpyridinium adsorption on montmorillonite*. Journal of colloid and interface science, 2006. **304**(1): p. 29-36.
180. Majdan, M., S. Pikus, Z. Rzaczyńska, M. Iwan, O. Maryuk, R. Kwiatkowski, and H. Skrzypek, *Characteristics of chabazite modified by hexadecyltrimethylammonium bromide and of its affinity toward chromates*. Journal of Molecular Structure, 2006. **791**(1-3): p. 53-60.
181. Li, Z. and R.S. Bowman, *Sorption of Perchloroethylene by Surfactant-Modified Zeolite as Controlled by Surfactant Loading*. Environmental Science and Technology, 1998. **32**(15): p. 2278-2282.
182. Choi, H.D., J.M. Cho, K. Baek, J.S. Yang, and J.Y. Lee, *Influence of cationic surfactant on adsorption of Cr (VI) onto activated carbon*. Journal of Hazardous Materials, 2009. **161**(2-3): p. 1565-1568.
183. Wesson, L.L. and J.H. Harwell, *Surfactant Adsorption in Porous Media*, in *Surfactants: Fundamentals and Applications in the Petroleum Industry*, L.L. Schramm, Editor. 2000, Cambridge University Press. p. 121-158.
184. Alkan, M., M. Karadas, M. Dogan, and Ö. Demirbas, *Adsorption of CTAB onto perlite samples from aqueous solutions*. Journal of Colloid and Interface Science, 2005. **291**(2): p. 309-318.

185. Kung, K.H.S. and K.F. Hayes, *Fourier transform infrared spectroscopic study of the adsorption of cetyltrimethylammonium bromide and cetylpyridinium chloride on silica*. Langmuir, 1993. **9**(1): p. 263-267.
186. Wisniewska, S.K., J. Nalaskowski, E. Witka-Jezewska, J. Hupka, and J.D. Miller, *Surface properties of barley straw*. Colloids and Surfaces B: Biointerfaces, 2003. **29**(2-3): p. 131-142.
187. Widiastuti, N., H. Wu, M. Ang, and D. Zhang, *The potential application of natural zeolite for greywater treatment*. Desalination, 2008. **218**(1-3): p. 271-280.
188. Rawajfih, Z. and N. Nsour, *Characteristics of phenol and chlorinated phenols sorption onto surfactant-modified bentonite*. Journal of Colloid and Interface Science, 2006. **298**(1): p. 39-49.
189. Hanna, K., R. Denoyel, I. Beurroies, and J.P. Dubès, *Solubilization of pentachlorophenol in micelles and confined surfactant phases*. Colloids and Surfaces A: Physicochemical and Engineering Aspects, 2005. **254**(1-3): p. 231-239.
190. Treiner, C., *Adsolubilization and related phenomena*, in *Structure-performance relationships in surfactants*, K. Esumi and M. Ueno, Editors. 2003, CRC.
191. Juang, R.S., S.H. Lin, and K.H. Tsao, *Mechanism of sorption of phenols from aqueous solutions onto surfactant-modified montmorillonite*. Journal of colloid and interface science, 2002. **254**(2): p. 234-241.
192. Wang, L. and A. Wang, *Adsorption properties of Congo Red from aqueous solution onto surfactant-modified montmorillonite*. Journal of Hazardous Materials, 2008. **160**(1): p. 173-180.
193. Jin, X., M. Jiang, X. Shan, Z. Pei, and Z. Chen, *Adsorption of methylene blue and orange II onto unmodified and surfactant-modified zeolite*. Journal of Colloid and Interface Science, 2008. **328**(2): p. 243-247.
194. Torres-Pérez, J., M. Solache-Rios, and A. Colín-Cruz, *Sorption and desorption of dye remazol yellow onto a Mexican surfactant-modified clinoptilolite-rich tuff and a carbonaceous material from pyrolysis of sewage sludge* Water, Air, & Soil Pollution, 2008. **187**(1): p. 303-313.
195. Namasivayam, C., R. Radhika, and S. Suba, *Uptake of dyes by a promising locally available agricultural solid waste: coir pith*. Waste Management, 2001. **21**(4): p. 381-387.

196. Choi, H.D., M.C. Shin, D.H. Kim, C.S. Jeon, and K. Baek, *Removal characteristics of Reactive Black 5 using surfactant-modified activated carbon*. Desalination, 2008. **223**(1-3): p. 290-298.
197. Özcan, A.S., B. Erdem, and A. Özcan, *Adsorption of Acid Blue 193 from aqueous solutions onto Na-bentonite and DTMA-bentonite*. Journal of Colloid and Interface Science, 2004. **280**(1): p. 44-54.
198. Jovic-Jovicic, N., A. Milutinovic-Nikolic, I. Grzetic, and D. Jovanovic, *Organobentonite as efficient textile dye sorbent*. Chemical Engineering & Technology, 2008. **31**(4): p. 567-574.
199. Ersoy, B. and M.S. Çelik, *Effect of hydrocarbon chain length on adsorption of cationic surfactants onto clinoptilolite*. Clays and Clay Minerals, 2003. **51**(2): p. 172-180.
200. Lee, S.Y., S.J. Kim, S.Y. Chung, and C.H. Jeong, *Sorption of hydrophobic organic compounds onto organoclays*. Chemosphere, 2004. **55**(5): p. 781-785.
201. Gao, B., X. Wang, J. Zhao, and G. Sheng, *Sorption and cosorption of organic contaminant on surfactant-modified soils*. Chemosphere, 2001. **43**(8): p. 1095-1102.
202. Akbal, F., *Sorption of phenol and 4-chlorophenol onto pumice treated with cationic surfactant*. Journal of Environmental Management, 2005. **74**(3): p. 239-244.
203. Gecol, H., *The basic theory*, in *Chemistry and technology of surfactants*, R.J. Farn, Editor. 2006, Wiley-Blackwell. p. 24-43.
204. Ghiaci, M., R. Kia, A. Abbaspur, and F. Seyedeyn-Azad, *Adsorption of chromate by surfactant-modified zeolites and MCM-41 molecular sieve*. Separation and Purification Technology, 2004. **40**(3): p. 285-295.
205. Widiastuti, N., H. Wu, M. Ang, and D. Zhang. *Preparation and FTIR study of organo-zeolite for the removal of phosphate in greywater*. in *CHEMECA*. 2007. Melbourne, Australia.
206. Zhu, L. and R. Zhu, *Surface structure of CTMA<sup>+</sup> modified bentonite and their sorptive characteristics towards organic compounds*. Colloids and Surfaces A: Physicochemical and Engineering Aspects, 2008. **320**(1-3): p. 19-24.
207. Zhu, R., L. Zhu, and L. Xu, *Sorption characteristics of CTMA<sup>+</sup>-bentonite complexes as controlled by surfactant packing density*. Colloids and Surfaces A: Physicochemical and Engineering Aspects, 2007. **294**(1-3): p. 221-227.

208. Ahmedna, M., M.M. Johns, S.J. Clarke, W.E. Marshall, and R.M. Rao, *Potential of agricultural by-product-based activated carbons for use in raw sugar decolourisation*. Journal of the Science of Food and Agriculture, 1997. **75**(1): p. 117-124.
209. APHA, *Standard Methods for the Examination of Water and Wastewater*. 20th ed. 1999: American Public Health Association/American Water Works Association/Water Environment Federation, Washington, DC, USA.
210. Cheng, C.H., J. Lehmann, J.E. Thies, S.D. Burton, and M.H. Engelhard, *Oxidation of black carbon by biotic and abiotic processes*. Organic Geochemistry, 2006. **37**(11): p. 1477-1488.
211. McQueen, R.E. and J.W.G. Nicholson, *Modification of the neutral-detergent fiber procedure for cereals and vegetables by using alpha-amylase*. Journal of the Association of Official Analytical Chemists (USA), 1979.
212. van Soest, P.J. and J.B. Robinson, *The detergent system of analysis and its application to human foods*, in *The analysis of dietary fibre in foods*, W.P.T. James and O. Theander, Editors. 1981, Marcel Dekker: New York. p. 123.
213. AOAC, *Official methods of analysis of AOAC International*, ed. K. Helrich. 1990, Arlington, Virginia: AOAC Inc. 965–35.
214. AOAC, *Official Methods of Analysis of AOAC International*. AOAC International, ed. P. Cunniff. 1995, Arlington, Virginia.
215. Ho, Y.S. and G. McKay, *Comparison of chemisorption kinetic models applied to pollutant removal on various sorbents*. Process Safety and Environmental Protection: Transactions of the Institution of Chemical Engineers, Part B, 1998. **76**(4): p. 332-340.
216. Ho, Y.S. and G. McKay, *The kinetics of sorption of divalent metal ions onto sphagnum moss peat*. Water Research, 2000. **34**(3): p. 735-742.
217. Lei, L., X. Li, and X. Zhang, *Ammonium removal from aqueous solutions using microwave-treated natural Chinese zeolite*. Separation and Purification Technology, 2008. **58**(3): p. 359-366.
218. Ncibi, M.C., B. Mahjoub, and M. Seffen, *Investigation of the sorption mechanisms of metal-complexed dye onto Posidonia oceanica (L.) fibres through kinetic modelling analysis*. Bioresource Technology, 2008. **99**(13): p. 5582-5589.

219. Boyd, G.E., J. Schubert, and A.W. Adamson, *The exchange adsorption of ions from aqueous solutions by organic zeolites. I. Ion-exchange equilibria*. Journal of the American Chemical Society, 1947. **69**(11): p. 2818-2829.
220. Reichenberg, D., *Properties of ion-exchange resins in relation to their structure. III. Kinetics of exchange*. Journal of the American Chemical Society, 1953. **75**(3): p. 589-597.
221. El-Kamash, A.M., A.A. Zaki, and M.A. El Geleel, *Modeling batch kinetics and thermodynamics of zinc and cadmium ions removal from waste solutions using synthetic zeolite A*. Journal of hazardous materials, 2005. **127**(1-3): p. 211-220.
222. Gupta, V.K. and I. Ali, *Removal of lead and chromium from wastewater using bagasse fly ash—a sugar industry waste*. Journal of colloid and interface science, 2004. **271**(2): p. 321-328.
223. Langmuir, I., *The constitution and fundamental properties of solids and liquids. part i. Solids*. Journal of the American Chemical Society, 1916. **38**(11): p. 2221-2295.
224. Freundlich, H.M.F., *Over the adsorption in solution*. Journal of Physical Chemistry 1906. **57**: p. 385–470.
225. Baral, S.S., N. Das, T.S. Ramulu, S.K. Sahoo, S.N. Das, and G.R. Chaudhury, *Removal of Cr (VI) by thermally activated weed Salvinia cucullata in a fixed-bed column*. Journal of Hazardous Materials, 2009. **161**(2-3): p. 1427-1435.
226. Aksu, Z., a. Ça, and F. Gönen, *Continuous fixed bed biosorption of reactive dyes by dried Rhizopus arrhizus: Determination of column capacity*. Journal of hazardous materials, 2007. **143**(1-2): p. 362-371.
227. Hawari, A., *Biosorption of lead, copper, cadmium and nickel by anaerobic biomass*, in *Department of Civil Engineering*. 2004, Concordia University Montreal, Canada. p. 173.
228. Thomas, H.C., *Heterogeneous ion exchange in a flowing system*. Journal of the American Chemical Society, 1944. **66**(10): p. 1664-1666.
229. Suksabye, P., P. Thiravetyan, and W. Nakbanpote, *Column study of chromium (VI) adsorption from electroplating industry by coconut coir pith*. Journal of Hazardous Materials, 2008. **160**(1): p. 56-62.

230. Yoon, Y.H. and J.H. Nelson, *Application of gas adsorption kinetics. Part I. A theoretical model for respirator cartridge service time*. American Industrial Hygiene Association Journal, 1984. **45** p. 509-516.
231. Öztürk, N. and D. Kavak, *Boron removal from aqueous solutions by adsorption on waste sepiolite and activated waste sepiolite using full factorial design*. Adsorption, 2004. **10**(3): p. 245-257.
232. Aksu, Z. and F. Gönen, *Biosorption of phenol by immobilized activated sludge in a continuous packed bed: prediction of breakthrough curves*. Process Biochemistry, 2004. **39**(5): p. 599-613.
233. Marquardt, D., *An algorithm for least-squares estimation of nonlinear parameters*. SIAM Journal on Applied Mathematics, 1963. **11**(2): p. 431-441.
234. David, M.L. *HyperStat Online Statistics Textbook Sampling Distributions* 2007 [cited 2010 25 February]; Available from: <http://davidmlane.com/hyperstat/A103735.html>.
235. Tan, G. and D. Xiao, *Adsorption of cadmium ion from aqueous solution by ground wheat stems*. Journal of Hazardous Materials, 2009. **164**(2-3): p. 1359-1363.
236. Low, K.S., C.K. Lee, and S.C. Liew, *Sorption of cadmium and lead from aqueous solutions by spent grain*. Process Biochemistry, 2000. **36**(1-2): p. 59-64.
237. O'Haver, J.H. and J.H. Harwell, *Adsolubilization: some expected and unexpected results*, in *Surfactant adsorption and surface solubilization*, R. Sharma, Editor. 1995, American Chemical Society Washington, DC. p. 49-66.
238. Somasundaran, P. and L. Huang, *Adsorption/aggregation of surfactants and their mixtures at solid-liquid interfaces*. Advances in Colloid and Interface Science, 2000. **88**(1-2): p. 179-208.
239. Hendriks, A. and G. Zeeman, *Pretreatments to enhance the digestibility of lignocellulosic biomass*. Bioresource Technology, 2009. **100**(1): p. 10-18.
240. Arisoy, M., *The effect of sodium hydroxide treatment on chemical composition and digestibility of straw*. Turkish Journal of Veterinary and Animal Sciences, 1998. **22**: p. 165-170.
241. Brígida, A.I.S., V.M.A. Calado, L.R.B. Gonçalves, and M.A.Z. Coelho, *Effect of chemical treatments on properties of green coconut fiber*. Carbohydrate Polymers, 2010. **79**(4): p. 832-838.

242. Pettersen, R.C., *The chemical composition of wood*, in *The chemistry of solid wood*, *Advances in Chemistry Series*, R.M. Rowell, Editor. 1984, American Chemical Society Washington, DC. p. 984.
243. Wartelle, L.H. and W.E. Marshall, *Citric acid modified agricultural by-products as copper ion adsorbents*. *Advances in Environmental Research*, 2000. **4**(1): p. 1-7.
244. Wan Ngah, W.S. and M.A.K.M. Hanafiah, *Adsorption of copper on rubber (Hevea brasiliensis) leaf powder: Kinetic, equilibrium and thermodynamic studies*. *Biochemical Engineering Journal*, 2008. **39**(3): p. 521-530.
245. Krishna, B.S., D.S.R. Murty, and B.S. Jai Prakash, *Thermodynamics of Chromium(VI) Anionic Species Sorption onto Surfactant-Modified Montmorillonite Clay*. *Journal of Colloid and Interface Science*, 2000. **229**(1): p. 230-236.
246. Kenkel, J., *Analytical chemistry for technicians*. 3rd ed. 2002, Boca Raton, FL: CRC Press. 205-243.
247. Arief, V.O., K. Trilestari, J. Sunarso, N. Indraswati, and S. Ismadji, *Recent progress on biosorption of heavy metals from liquids using low cost biosorbents: characterization, biosorption parameters and mechanism studies*. *CLEAN-Soil, Air, Water*, 2008. **36**(12): p. 937-962.
248. Achak, M., A. Hafidi, N. Ouazzani, S. Sayadi, and L. Mandi, *Low cost biosorbent "banana peel" for the removal of phenolic compounds from olive mill wastewater: Kinetic and equilibrium studies*. *Journal of Hazardous Materials*, 2009. **166**(1): p. 117-125.
249. Nishikida, K. and R.W. Hannah, *Selected applications of modern FT-IR techniques*. 1996, Tokyo: Kodansha Ltd. 3-17.
250. Thermo Nicolet Corp., *Introduction to Fourier Transform Infrared Spectrometry*. 2001, Madison, Wisconsin.
251. Majdan, M., O. Maryuk, S. Pikus, E. Olszewska, R. Kwiatkowski, and H. Skrzypek, *Equilibrium, FTIR, scanning electron microscopy and small wide angle X-ray scattering studies of chromates adsorption on modified bentonite*. *Journal of Molecular Structure*, 2005. **740**(1-3): p. 203-211.
252. Bhattacharyya, K.G. and S. Sen Gupta, *Pb(II) uptake by kaolinite and montmorillonite in aqueous medium: Influence of acid activation of the clays*. *Colloids and Surfaces A: Physicochemical and Engineering Aspects*, 2006. **277**(1-3): p. 191-200.

253. Noeline, B.F., D.M. Manohar, and T.S. Anirudhan, *Kinetic and equilibrium modelling of lead(II) sorption from water and wastewater by polymerized banana stem in a batch reactor*. Separation and Purification Technology, 2005. **45**(2): p. 131-140.
254. Babel, S. and T.A. Kurniawan, *Cr(VI) removal from synthetic wastewater using coconut shell charcoal and commercial activated carbon modified with oxidizing agents and/or chitosan*. Chemosphere, 2004. **54**(7): p. 951-967.
255. Pérez-Marín, A.B., V.M. Zapata, J.F. Ortuño, M. Aguilar, J. Sáez, and M. Lloréns, *Removal of cadmium from aqueous solutions by adsorption onto orange waste*. Journal of Hazardous Materials, 2007. **139**(1): p. 122-131.
256. Srinivasan, A. and T. Viraraghavan, *Removal of oil by walnut shell media*. Bioresource Technology, 2008. **99**(17): p. 8217-8220.
257. Sun, X.-F., SunSun, and J.-X. Sun, *Acetylation of rice straw with or without catalysts and Its characterization as a natural sorbent in oil spill cleanup*. Journal of Agricultural and Food Chemistry, 2002. **50**(22): p. 6428-6433.
258. Sun, X.-F., R.C. Sun, and J.X. Sun, *A convenient acetylation of sugarcane bagasse using NBS as a catalyst for the preparation of oil sorption-active materials*. Journal of Materials Science, 2003. **38**(19): p. 3915-3923.
259. Argun, M.E., S. Dursun, C. Ozdemir, and M. Karatas, *Heavy metal adsorption by modified oak sawdust: Thermodynamics and kinetics*. Journal of Hazardous Materials, 2007. **141**(1): p. 77-85.
260. Rajakovic-Ognjanovic, V., G. Aleksic, and L. Rajakovic, *Governing factors for motor oil removal from water with different sorption materials*. Journal of Hazardous Materials, 2008. **154**(1-3): p. 558-563.
261. Shukla, S.R. and R.S. Pai, *Adsorption of Cu(II), Ni(II) and Zn(II) on modified jute fibres*. Bioresource Technology, 2005. **96**(13): p. 1430-1438.
262. Al-Degs, Y.S., M.A.M. Khraisheh, S.J. Allen, and M.N. Ahmad, *Adsorption characteristics of reactive dyes in columns of activated carbon*. Journal of Hazardous Materials, 2009. **165**(1-3): p. 944-949.
263. Chen, J.P. and L. Wang, *Characterization of metal adsorption kinetic properties in batch and fixed-bed reactors*. Chemosphere, 2004. **54**(3): p. 397-404.

264. Yin, C.Y., M.K. Aroua, and W. Daud, *Fixed-bed adsorption of metal ions from aqueous solution on polyethyleneimine-impregnated palm shell activated carbon*. Chemical Engineering Journal, 2009. **148**(1): p. 8-14.
265. Amarasinghe, B. and R.A. Williams, *Tea waste as a low cost adsorbent for the removal of Cu and Pb from wastewater*. Chemical Engineering Journal, 2007. **132**(1-3): p. 299-309.
266. Bayramoglu, G., G. Çelik, and M.Y. Arica, *Biosorption of reactive blue 4 dye by native and treated fungus Phanerocheate chrysosporium: Batch and continuous flow system studies*. Journal of Hazardous Materials, 2006. **137**(3): p. 1689-1697.
267. Özacar, M. and A. Şengil, *Adsorption of acid dyes from aqueous solutions by calcined alunite and granular activated carbon*. Adsorption, 2002. **8**(4): p. 301-308.
268. Akar, T., A.S. Ozcan, S. Tunalı, and A. Ozcan, *Biosorption of a textile dye (Acid Blue 40) by cone biomass of Thuja orientalis: Estimation of equilibrium, thermodynamic and kinetic parameters*. Bioresource Technology, 2008. **99**(8): p. 3057-3065.
269. Teker, M., M. Imamoglu, and N. Bocek, *Adsorption of some textile dyes on activated carbon prepared from rice hulls*. Fresenius Environmental Bulletin, 2009. **18**(5 A): p. 709-714.
270. Fetterolf, M.L., H.V. Patel, and J.M. Jennings, *Adsorption of methylene blue and acid blue 40 on titania from aqueous solution*. Journal of Chemical & Engineering Data, 2003. **48**(4): p. 831-835.
271. Ip, A.W.M., J.P. Barford, and G. McKay, *Reactive Black dye adsorption/desorption onto different adsorbents: Effect of salt, surface chemistry, pore size and surface area*. Journal of Colloid and Interface Science, 2009. **337**(1): p. 32-38.
272. Won, S.W., H.-J. Kim, S.-H. Choi, B.-W. Chung, K.-J. Kim, and Y.-S. Yun, *Performance, kinetics and equilibrium in biosorption of anionic dye Reactive Black 5 by the waste biomass of Corynebacterium glutamicum as a low-cost biosorbent*. Chemical Engineering Journal, 2006. **121**(1): p. 37-43.
273. Ozdemir, O., B. Armagan, M. Turan, and M.S. Çelik, *Comparison of the adsorption characteristics of azo-reactive dyes on mezoporous minerals*. Dyes and Pigments, 2004. **62**(1): p. 49-60.

274. Xue, Y., H. Hou, and S. Zhu, *Adsorption removal of reactive dyes from aqueous solution by modified basic oxygen furnace slag: Isotherm and kinetic study*. Chemical Engineering Journal, 2009. **147**(2-3): p. 272-279.
275. Patel, R. and S. Suresh, *Kinetic and equilibrium studies on the biosorption of reactive black 5 dye by Aspergillus foetidus*. Bioresource Technology, 2008. **99**(1): p. 51-58.
276. Vijayaraghavan, K. and Y.-S. Yun, *Biosorption of C.I. Reactive Black 5 from aqueous solution using acid-treated biomass of brown seaweed Laminaria sp.* Dyes and Pigments, 2008. **76**(3): p. 726-732.
277. Eren, Z. and F.N. Acar, *Adsorption of Reactive Black 5 from an aqueous solution: equilibrium and kinetic studies*. Desalination, 2006. **194**(1-3): p. 1-10.
278. Eren, Z. and F.N. Acar, *Equilibrium and kinetic mechanism for Reactive Black 5 sorption onto high lime Soma fly ash*. Journal of Hazardous Materials, 2007. **143**(1-2): p. 226-232.
279. Pengthamkeerati, P., T. Satapanajaru, and O. Singchan, *Sorption of reactive dye from aqueous solution on biomass fly ash*. Journal of Hazardous Materials, 2008. **153**(3): p. 1149-1156.
280. Osma, J.F., V. Saravia, J.L. Toca-Herrera, and S.R. Couto, *Sunflower seed shells: A novel and effective low-cost adsorbent for the removal of the diazo dye Reactive Black 5 from aqueous solutions*. Journal of Hazardous Materials, 2007. **147**(3): p. 900-905.
281. Santhy, K. and P. Selvapathy, *Removal of reactive dyes from wastewater by adsorption on coir pith activated carbon*. Bioresource technology, 2006. **97**(11): p. 1329-1336.
282. Malik, P.K., *Dye removal from wastewater using activated carbon developed from sawdust: adsorption equilibrium and kinetics*. Journal of Hazardous Materials, 2004. **113**(1-3): p. 81-88.
283. Akkaya, G. and A. Özer, *Biosorption of Acid Red 274 (AR 274) on Dicranella varia: determination of equilibrium and kinetic model parameters*. Process Biochemistry, 2005. **40**(11): p. 3559-3568.
284. Gibbs, G., J.M. Tobin, and E. Guibal, *Sorption of Acid Green 25 on chitosan: Influence of experimental parameters on uptake kinetics and sorption isotherms*. Journal of Applied Polymer Science, 2003. **90**(4): p. 1073-1080.

285. Atia, A.A., A.M. Donia, and W.A. Al-Amrani, *Adsorption/desorption behavior of Acid Orange 10 on magnetic silica modified with amine groups*. Chemical Engineering Journal, 2009. **150**(1): p. 55-62.
286. Banat, I.M., P. Nigam, D. Singh, and R. Marchant, *Microbial decolorization of textile-dye-containing effluents: a review*. Bioresource Technology, 1996. **58**(3): p. 217-227.
287. Tsai, W.-T., K.-J. Hsien, H.-C. Hsu, C.-M. Lin, K.-Y. Lin, and C.-H. Chiu, *Utilization of ground eggshell waste as an adsorbent for the removal of dyes from aqueous solution*. Bioresource Technology, 2008. **99**(6): p. 1623-1629.
288. Dizge, N., C. Aydiner, E. Demirbas, M. Kobya, and S. Kara, *Adsorption of reactive dyes from aqueous solutions by fly ash: Kinetic and equilibrium studies*. Journal of Hazardous Materials, 2008. **150**(3): p. 737-746.
289. Tunç, Ö., H. Tanacı, and Z. Aksu, *Potential use of cotton plant wastes for the removal of remazol black B reactive dye*. Journal of Hazardous Materials, 2009. **163**(1): p. 187-198.
290. Li, Q., Q.Y. Yue, Y. Su, B.Y. Gao, and J. Li, *Two-step kinetic study on the adsorption and desorption of reactive dyes at cationic polymer/bentonite*. Journal of Hazardous Materials, 2009. **165**(1-3): p. 1170-1178.

# APPENDIX A

RAW DATA AND STANDARD ERROR MEASUREMENT FOR  
ADSORBENT CHARACTERIZATION

## Appendix A-1

## Analysis of Cellulose, Hemicellulose and Lignin

	Cellulose (%)				Hemicellulose (%)			
	Analysis No.		Error Analysis		Analysis No.		Error Analysis	
	1	2	Mean	$\sigma_m$	1	2	Mean	$\sigma_m$
RBS	53.04	49.58	51.31	1.73	28.18	33.42	30.80	2.62
RBS-N	55.30	58.46	56.88	1.58	30.17	27.23	28.70	1.47

	Lignin (%)			
	Analysis No.		Error Analysis	
	1	2	Mean	$\sigma_m$
RBS	6.56	5.42	5.99	0.57
RBS-N	6.54	6.54	6.54	0.00

Experimental condition:

Straw size: 0.5-1.18 mm

Appendix A-6      Analysis of surface area (BET) and Pore Volume

	sBET				Po			
	Analysis No.		Error Analysis		Analysis No.		Error Analysis	
	1	2	Mean	$\sigma_m$	1	2	Mean	$\sigma_m$
RBS	98	93.580	95.79	2.210	0.083	0.037	0.06	0.023
RBS-N	148.4	138.600	143.5	4.900	0.101	0.071	0.086	0.015
SBS	78.99	72.404	75.697	3.293	0.084	0.004	0.044	0.040
BBS	70.24	56.146	63.193	7.047	0.028	0.066	0.047	0.019

Experimental condition:

Straw size: 0.5-1.18 mm

Appendix A-7      Analysis of water soluble mineral content

	Water soluble mineral ( (us/cm)			
	Analysis No.		Error Analysis	
	1	2	Mean	$\sigma_m$
RBS	192.43	199.77	196.10	3.67
RBS-N	191.33	199.07	195.20	3.87
SBS	35.31	33.89	34.60	0.71
BBS	17.74	15.97	16.86	0.89

Experimental condition:

Straw size: 0.5-1.18 mm

	Surface acidic groups (mmol/g)				Surface basic groups (mmol/g)			
	Analysis No.		Error Analysis		Analysis No.		Error Analysis	
	1	2	Mean	$\sigma_m$	1	2	Mean	$\sigma_m$
RBS	3.55	3.15	3.35	0.20	0.47	0.43	0.45	0.02
RBS-N	3.89	4.01	3.95	0.06	0.42	0.24	0.33	0.09
SBS	3.33	3.02	3.18	0.16	0.51	0.43	0.47	0.04
BBS	3.28	3.07	3.18	0.10	0.48	0.52	0.50	0.02

Experimental condition:

Straw size: 0.5-1.18 mm

Appendix A-9 Analysis of Bulk Density

	Bulk Density (g/mL)			
	Analysis No.		Error Analysis	
	1	2	Mean	$\sigma_m$
RBS	0.08	0.08	0.08	0.00
RBS-N	0.08	0.08	0.08	0.00
SBS	0.09	0.08	0.08	0.01
BBS	0.09	0.09	0.09	0.00

Experimental condition:

Straw size: 0.5-1.18 mm

Appendix A-10      Analysis Carbon and Nitrogen content

	Carbon (%)				Nitrogen(%)			
	Analysis No.		Error Analysis		Analysis No.		Error Analysis	
	1	2	Mean	$\sigma_m$	1	2	Mean	$\sigma_m$
RBS	44.61	44.89	44.75	0.14	0.26	0.23	0.24	0.01
RBS-N	44.69	44.69	44.69	0.00	0.18	0.16	0.17	0.01
SBS	46.95	46.95	46.95	0.00	0.34	0.38	0.36	0.02
BBS	48.57	46.02	47.30	1.28	0.35	0.31	0.33	0.02

Experimental condition:

Straw size: 0.5-1.18 mm

# APPENDIX B

RAW DATA AND STANDARD ERROR MEASUREMENT FOR  
EMULSIFIED OIL REMOVAL

# Appendix B-1: Screening experiments of CO and SMO adsorption

	CO Removal (%)				SMO Removal (%)			
	run 1	run 2	Mean	$\sigma_m$	run 1	run 2	Mean	$\sigma_m$
RBS	2.93	2.71	2.82	0.11	1.37	1.54	1.45	0.08
RBS-N	2.47	2.66	2.56	0.09	9.05	6.22	7.64	1.41
SBS	89.86	91.68	90.77	0.91	88.06	90.12	89.09	1.03
BBS	92.02	93.11	92.56	0.54	91.07	90.75	90.91	0.16

## Experimental Conditions

Initial oil concentration

CO 2750 mg/L  
SMO 3900 mg/L

Contact time 5 h

Shaking speed 170 rpm

Adsorbent dosage 10 g/L

Experimental temperature 25 C

Adsorbent size 0.5-1.18 mm

Solution pH

CO 7.5  
SMO 7.3

Appendix B-2      Effect of contact time on adsorption of CO onto SMBS at initial oil concentration of 1040.0 mg/L

Time (min)	Concentration ( mg/L)			Adsorption capacity ( mg/g)			$\sigma_m$
	run 1	run 2	mean	run1	run2	mean	
0	1040.0	1040.0	1040.0	0.0	0.0	0.0	0.0
1	750.0	990.0	870.0	29.0	5.0	17.0	12.0
3	650.0	490.0	570.0	39.0	55.0	47.0	8.0
6	460.0	260.0	360.0	58.0	78.0	68.0	10.0
9	230.0	50.0	140.0	81.0	99.0	90.0	9.0
12	160.0	100.0	130.0	88.0	94.0	91.0	3.0
15	85.0	125.0	105.0	95.5	91.5	93.5	2.0
20	110.0	82.0	96.0	93.0	95.8	94.4	1.4
60	95.0	103.0	99.0	94.5	93.7	94.1	0.4
120	95.0	105.0	100.0	94.5	93.5	94.0	0.5

Experimental Conditions

Shaking speed	170 rpm
Adsorbent dosage	10 g/L
Experimental temperature	25 C
Solution pH	7.5
Adsorbent size	0.5-1.18 mm

Appendix B-3      Effect of contact time on adsorption of CO onto SMBS at initial oil concentration of 3450.0 mg/L

Time (min)	Concentration ( mg/L)			Adsorption capacity ( mg/g)			$\sigma_m$
	run 1	run 2	mean	run1	run2	mean	
0	3450.0	3450.0	3450.0	0.0	0.0	0.0	0.0
5	2200.0	2580.0	2390.0	125.0	87.0	106.0	19.0
10	1420.0	1640.0	1530.0	203.0	181.0	192.0	11.0
15	800.0	660.0	730.0	265.0	279.0	272.0	7.0
20	650.0	770.0	710.0	280.0	268.0	274.0	6.0
25	500.0	600.0	550.0	295.0	285.0	290.0	5.0
30	500.0	520.0	510.0	295.0	293.0	294.0	1.0
35	480.0	330.0	405.0	297.0	312.0	304.5	7.5
45	350.0	390.0	370.0	310.0	306.0	308.0	2.0
60	430.0	350.0	390.0	302.0	310.0	306.0	4.0
120	400.0	270.0	335.0	305.0	318.0	311.5	6.5

Experimental Conditions

Shaking speed	170 rpm
Adsorbent dosage	10 g/L
Experimental temperature	25 C
Solution pH	7.5
Adsorbent size	0.5-1.18 mm

Appendix B-4      Effect of contact time on adsorption of CO onto BMBS at initial oil concentration of 1040.0 mg/L

Time (min)	Concentration ( mg/L)			Adsorption capacity ( mg/g)			$\sigma_m$
	run 1	run 2	mean	run1	run2	mean	
0	1040.00	1040.00	1040.00	0.00	0.00	0.00	0.00
1	760.00	840.00	800.00	28.00	20.00	24.00	4.00
3	600.00	610.00	605.00	44.00	43.00	43.50	0.50
6	210.00	330.00	270.00	83.00	71.00	77.00	6.00
9	130.00	130.00	130.00	91.00	91.00	91.00	0.00
12	95.00	125.00	110.00	94.50	91.50	93.00	1.50
15	90.00	86.00	88.00	95.00	95.40	95.20	0.20
20	92.00	88.00	90.00	94.80	95.20	95.00	0.20
60	89.00	97.00	93.00	95.10	94.30	94.70	0.40
120	93.00	87.00	90.00	94.70	95.30	95.00	0.30

Experimental Conditions

Shaking speed	170 rpm
Adsorbent dosage	10 g/L
Experimental temperature	25 C
Solution pH	7.5
Adsorbent size	0.5-1.18 mm

## Appendix B-5

Effect of contact time on adsorption of CO onto BMBS at  
initial oil concentration of 3450.0 mg/L

Time (min)	Concentration ( mg/L)			Adsorption capacity ( mg/g)			$\sigma_m$
	run 1	run 2	mean	run1	run2	mean	
0	3450.00	3450.00	3450.00	0.00	0.00	0.00	0.00
5	2400.00	2420.00	2410.00	105.00	103.00	104.00	1.00
10	1370.00	1130.00	1250.00	208.00	232.00	220.00	12.00
15	550.00	630.00	590.00	290.00	282.00	286.00	4.00
20	400.00	380.00	390.00	305.00	307.00	306.00	1.00
25	320.00	360.00	340.00	313.00	309.00	311.00	2.00
30	210.00	260.00	235.00	324.00	319.00	321.50	2.50
35	215.00	245.00	230.00	323.50	320.50	322.00	1.50
45	230.00	220.00	225.00	322.00	323.00	322.50	0.50
60	220.00	270.00	245.00	323.00	318.00	320.50	2.50
120	190.00	250.00	220.00	326.00	320.00	323.00	3.00

## Experimental Conditions

Shaking speed	170 rpm
Adsorbent dosage	10 g/L
Experimental temperature	25 C
Solution pH	7.5
Adsorbent size	0.5-1.18 mm

Appendix B-6      Effect of contact time on adsorption of SMO onto SMBS at initial oil concentration of 1680.0 mg/L

Time (min)	Concentration ( mg/L)			Adsorption capacity ( mg/g)			$\sigma_m$
	run 1	run 2	mean	run1	run2	mean	
0	1680.0	1680.0	1680	0.00	0.00	0.0	0.0
1	1300.0	1540.0	1420	38.00	14.00	26.0	12.0
3	1280.0	1120.0	1200	40.00	56.00	48.0	8.0
6	450.0	540.0	495	123.00	114.00	118.5	4.5
9	530.0	410.0	470	115.00	127.00	121.0	6.0
15	310.0	410.0	360	137.00	127.00	132.0	5.0
20	60.0	88.0	74	162.00	159.20	160.6	1.4
45	70.0	64.0	67	161.00	161.60	161.3	0.3
60	66.0	94.0	80	161.40	158.60	160.0	1.4
120	85.0	75.0	80.0	159.50	160.50	160.0	0.5

Appendix B-7      Effect of contact time on adsorption of SMO onto SMBS at initial oil concentration of 4315.0 mg/L

Time	Concentration ( mg/L)			Adsorption capacity ( mg/g)			
(min)	run 1	run 2	mean	run1	run2	mean	$\sigma_m$
0	4315.0	4315.0	4315	0.00	0.00	0.00	0.0
5	3500.0	3120.0	3310	81.50	119.50	100.50	19.0
10	1220.0	1420.0	1320	309.50	289.50	299.50	10.0
15	890.0	930.0	910	342.50	338.50	340.50	2.0
25	550.0	650.0	600	376.50	366.50	371.50	5.0
35	340.0	284.0	312	397.50	403.10	400.30	2.8
45	280.0	380.0	330	403.50	393.50	398.50	5.0
60	320.0	260.0	290	399.50	405.50	402.50	3.0
120	310.0	410.0	360	400.50	390.50	395.50	5.0

Experimental Conditions

Shaking speed	170 rpm
Adsorbent dosage	10 g/L
Experimental temperature	25 C
Solution pH	7.3
Adsorbent size	0.5-1.18 mm

Appendix B-8      Effect of contact time on adsorption of SMO onto BMBS at initial oil concentration of 1680.0 mg/L

Time (min)	Concentration ( mg/L)			Adsorption capacity ( mg/g)			$\sigma_m$
	run 1	run 2	mean	run1	run2	mean	
0	1680.0	1680.0	1680	0.00	0.00	0.0	0.0
1	1200.0	1340.0	1270	48.00	34.00	41.0	7.0
3	950.0	1150.0	1050	73.00	53.00	63.0	10.0
6	670.0	710.0	690	101.00	97.00	99.0	2.0
9	400.0	300.0	350	128.00	138.00	133.0	5.0
15	190.0	350.0	270	149.00	133.00	141.0	8.0
20	50.0	90.0	70	163.00	159.00	161.0	2.0
45	76.0	94.0	85	160.40	158.60	159.5	0.9
60	55.0	91.0	73	162.50	158.90	160.7	1.8
120	65.0	69.0	67.0	161.50	161.10	161.3	0.2

Experimental Conditions

Shaking speed	170 rpm
Adsorbent dosage	10 g/L
Experimental temperature	25 C
Solution pH	7.3
Adsorbent size	0.5-1.18 mm

Appendix B-9      Effect of contact time on adsorption of SMO onto BMBS at initial oil concentration of 4315.0 mg/L

Time (min)	Concentration ( mg/L)			Adsorption capacity ( mg/g)			$\sigma_m$
	run 1	run 2	mean	run1	run2	mean	
0	4315	4315.0	4315	0.00	0.00	0.00	0.0
5	3280	3520.0	3400	103.50	79.50	91.50	12.0
10	1370	1210.0	1290	294.50	310.50	302.50	8.0
15	1020	940.0	980	329.50	337.50	333.50	4.0
25	650	750.0	700	366.50	356.50	361.50	5.0
35	370	250.0	310	394.50	406.50	400.50	6.0
45	110	186.0	148	420.50	412.90	416.70	3.8
60	90	138.0	114	422.50	417.70	420.10	2.4
120	130	140.0	135	418.50	417.50	418.00	0.5

Experimental Conditions

Shaking speed	170 rpm
Adsorbent dosage	10 g/L
Experimental temperature	25 C
Solution pH	7.3
Adsorbent size	0.5-1.18 mm

## Appendix B-10

## Adsorption of CO onto different dosage of SMBS

Dosage	Concentration ( mg/L)				Adsorption capacity ( mg/g)			
mg	Initial	run 1	run 2	mean	run1	run2	mean	$\sigma_m$
0.10	3400.00	2887.00	2913.00	2900.00	513.00	487.00	500.00	13.00
0.40	3400.00	1310.00	1370.00	1340.00	522.50	507.50	515.00	7.50
0.55	3400.00	885.00	935.00	910.00	457.27	448.18	452.73	4.55
0.70	3400.00	565.00	535.00	550.00	405.00	409.29	407.14	2.14
1.00	3400.00	315.00	365.00	340.00	308.50	303.50	306.00	2.50
1.30	3400.00	220.00	176.00	198.00	244.62	248.00	246.31	1.69

## Experimental Conditions

Shaking speed	170 rpm
Contact time	1 h
Experimental temperature	25 C
Solution pH	7.5
Adsorbent size	0.5-1.18 mm

Dosage	Concentration ( mg/L)				Adsorption capacity ( mg/g)			
mg	Initial	run 1	run 2	mean	run1	run2	mean	$\sigma_m$
0.10	3400.00	2890.00	2850.00	2870.00	510.00	550.00	530.00	20.00
0.40	3400.00	1090.00	1150.00	1120.00	577.50	562.50	570.00	7.50
0.55	3400.00	760.00	680.00	720.00	480.00	494.55	487.27	7.27
0.70	3400.00	330.00	394.00	362.00	438.57	429.43	434.00	4.57
1.00	3400.00	200.00	240.00	220.00	320.00	316.00	318.00	2.00
1.30	3400.00	190.00	140.00	165.00	246.92	250.77	248.85	1.92

## Experimental Conditions

Shaking speed	170 rpm
Contact time	1 h
Experimental temperature	25 C
Solution pH	7.5
Adsorbent size	0.5-1.18 mm

Dosage	Concentration ( mg/L)				Adsorption capacity ( mg/g)			
mg	Initial	run 1	run 2	mean	run1	run2	mean	$\sigma_m$
0.40	4250.00	2250.00	2150.00	2200.00	500.00	525.00	512.50	12.50
0.55	4250.00	1530.00	1430.00	1480.00	494.55	512.73	503.64	9.09
0.70	4250.00	780.00	960.00	870.00	495.71	470.00	482.86	12.86
1.00	4250.00	200.00	280.00	240.00	405.00	397.00	401.00	4.00
1.30	4250.00	70.00	100.00	85.00	321.54	319.23	320.38	1.15

## Experimental Conditions

Shaking speed	170 rpm
Contact time	1 h
Experimental temperature	25 C
Solution pH	7.3
Adsorbent size	0.5-1.18 mm

Appendix B-13      Adsorption of SMO onto different dosage of BMBS

Dosage	Concentration ( mg/L)				Adsorption capacity ( mg/g)			
mg	Initial	run 1	run 2	mean	run1	run2	mean	$\sigma_m$
0.40	4250.00	1870.00	1930.00	1900.00	595.00	580.00	587.50	7.50
0.55	4250.00	1290.00	1410.00	1350.00	538.18	516.36	527.27	10.91
0.70	4250.00	530.00	590.00	560.00	531.43	522.86	527.14	4.29
1.00	4250.00	180.00	206.00	193.00	407.00	404.40	405.70	1.30
1.30	4250.00	150.00	12.00	81.00	315.38	326.00	320.69	5.31

Experimental Conditions

Shaking speed                      170 rpm  
Contact time                        1 h  
Experimental temperature        25 C  
Solution pH                         7.3  
Adsorbent size                      0.5-1.18 mm

pH	Concentration ( mg/L)				Adsorption capacity ( mg/g)			$\sigma_m$
	Initial	run 1	run 2	mean	run1	run2	mean	
2	860.00	660.00	700.00	680.00	20.00	16.00	18.00	2.00
4	860.00	205.00	231.59	218.29	65.50	62.84	64.17	1.33
6	860.00	150.00	122.09	136.05	71.00	73.79	72.40	1.40
8	860.00	110.00	155.88	132.94	75.00	70.41	72.71	2.29
10	860.00	140.00	172.94	156.47	72.00	68.71	70.35	1.65

## Experimental Conditions

Shaking speed	170 rpm
Adsorbent dosage	10 g/L
Experimental temperature	25 C
Adsorbent size	0.5-1.18 mm
Contact time	1 h

pH	Concentration ( mg/L)				Adsorption capacity ( mg/g)			$\sigma_m$
	Initial	run 1	run 2	mean	run1	run2	mean	
2	860.00	570.00	630.00	600.00	29.00	23.00	26.00	3.00
4	860.00	90.00	150.00	120.00	77.00	71.00	74.00	3.00
6	860.00	95.00	76.43	85.71	76.50	78.36	77.43	0.93
8	860.00	100.00	125.88	112.94	76.00	73.41	74.71	1.29
10	860.00	85.00	110.35	97.67	77.50	74.97	76.23	1.27

## Experimental Conditions

Shaking speed                      170 rpm  
 Adsorbent dosage                  10 g/L  
 Experimental temperature        25 C  
 Adsorbent size                    0.5-1.18 mm  
 Contact time                        1 h

pH	Concentration ( mg/L)				Adsorption capacity ( mg/g)			$\sigma_m$
	Initial	run 1	run 2	mean	run1	run2	mean	
2	820.67	700.00	633.33	666.67	12.07	18.73	15.40	3.33
4	820.67	350.00	341.27	345.63	47.07	47.94	47.50	0.44
6	820.67	55.00	39.00	47.00	76.57	78.17	77.37	0.80
8	820.67	25.00	38.33	31.67	79.57	78.23	78.90	0.67
10	820.67	30.00	36.67	33.33	79.07	78.40	78.73	0.33

## Experimental Conditions

Shaking speed                      170 rpm  
 Adsorbent dosage                  10 g/L  
 Experimental temperature        25 C  
 Adsorbent size                    0.5-1.18 mm  
 Contact time                        1 h

Appendix B-17      Effect of pH on adsorption of SMO onto BMBS

pH	Concentration ( mg/L)				Adsorption capacity ( mg/g)			$\sigma_m$
	Initial	run 1	run 2	mean	run1	run2	mean	
2	820.67	660.00	696.67	678.33	16.07	12.40	14.23	1.83
4	820.67	310.00	265.53	287.77	51.07	55.51	53.29	2.22
6	820.67	25.00	33.67	29.33	79.57	78.70	79.13	0.43
8	820.67	40.00	31.33	35.67	78.07	78.93	78.50	0.43
10	820.67	20.00	36.67	28.33	80.07	78.40	79.23	0.83

Experimental Conditions

Shaking speed                      170 rpm  
 Adsorbent dosage                10 g/L  
 Experimental temperature      25 C  
 Adsorbent size                    0.5-1.18 mm  
 Contact time                        1 h

## Appendix B-18

## Effect of size on adsorption of CO onto SMBS

pH	Concentration ( mg/L)				Adsorption capacity ( mg/g)			
	Initial	run 1	run 2	mean	run1	run2	mean	$\sigma_m$
< 0.5	1020.00	120.00	80.00	100.00	90.00	94.00	92.00	2.00
0.5-1.18	1020.00	170.00	206.20	188.10	85.00	81.38	83.19	1.81
1.18-1.4	1020.00	220.00	209.00	214.50	80.00	81.10	80.55	0.55

## Experimental Conditions

Shaking speed	170 rpm
Adsorbent dosage	10 g/L
Contact time	1 h
Solution pH	7.5
Experimental temperature	25 C

pH	Concentration ( mg/L)				Adsorption capacity ( mg/g)			$\sigma_m$
	Initial	run 1	run 2	mean	run1	run2	mean	
< 0.5	1020.00	95.00	82.80	88.90	92.50	93.72	93.11	0.61
0.5-1.18	1020.00	120.00	145.80	132.90	90.00	87.42	88.71	1.29
1.18-1.4	1020.00	150.00	140.20	145.10	87.00	87.98	87.49	0.49

## Experimental Conditions

Shaking speed	170 rpm
Adsorbent dosage	10 g/L
Contact time	1 h
Solution pH	7.5
Experimental temperature	25 C

Size	Concentration ( mg/L)				Adsorption capacity ( mg/g)			
mm	Initial	run 1	run 2	mean	run1	run2	mean	$\sigma_m$
< 0.5	1180.00	75.00	65.00	70.00	110.50	111.50	111.00	0.50
0.5-1.18	1180.00	105.00	85.00	95.00	107.50	109.50	108.50	1.00
1.18-1.4	1180.00	170.00	150.00	160.00	101.00	103.00	102.00	1.00

## Experimental Conditions

Shaking speed	170 rpm
Adsorbent dosage	10 g/L
Contact time	1 h
Solution pH	7.3
Experimental temperature	25 C

Size	Concentration ( mg/L)				Adsorption capacity ( mg/g)			
mm	Initial	run 1	run 2	mean	run1	run2	mean	$\sigma_m$
< 0.5	1180.00	65.00	85.00	75.00	111.50	109.50	110.50	1.00
0.5-1.18	1180.00	91.00	75.00	83.00	108.90	110.50	109.70	0.80
1.18-1.4	1180.00	135.00	145.00	140.00	104.50	103.50	104.00	0.50

## Experimental Conditions

Shaking speed	170 rpm
Adsorbent dosage	10 g/L
Contact time	1 h
Solution pH	7.3
Experimental temperature	25 C

Time	oil loaded straw (mg/g)	Desorption capacity mg/g			Desorption percentage %			
		run 1	run 2	$\sigma_m$	run1	run2	mean	
h								
1	21.80	1.10	0.70	0.90	5.05	3.21	4.13	0.92
2	21.80	0.70	0.90	0.80	3.21	4.13	3.67	0.46
5	21.80	0.70	0.90	0.80	3.21	4.13	3.67	0.46

## Experimental Conditions

Shaking speed	170 rpm
Adsorbent dosage	10 g/L
Experimental temperature	25 C
Adsorbent size	0.5-1.18 mm

Appendix B-23 Desorption of CO loaded BMBS in deionized water

Time	oil loaded straw (mg/g)	Desorption capacity mg/g			Desorption percentage %			
		run 1	run 2	$\sigma_m$	run1	run2	mean	
h								
1	21.70	0.70	0.30	0.50	3.23	1.38	2.30	0.92
2	21.70	0.40	0.60	0.50	1.84	2.76	2.30	0.46
5	21.70	0.40	0.40	0.40	1.84	1.84	1.84	0.00

Experimental Conditions

Shaking speed 170 rpm  
 Adsorbent dosage 10 g/L  
 Experimental temperature 25 C  
 Adsorbent size 0.5-1.18 mm

Time	oil loaded straw (mg/g)	Desorption capacity mg/g			Desorption percentage %			
hr		run 1	run 2	$\sigma_m$	run1	run2	mean	$\sigma_m$
1	20.00	0.40	0.20	0.30	2.00	1.00	1.50	0.50
2	20.00	0.50	0.50	0.50	2.50	2.50	2.50	0.00
5	20.00	0.40	0.40	0.40	2.00	2.00	2.00	0.00

## Experimental Conditions

Shaking speed                      170 rpm  
 Adsorbent dosage                  10 g/L  
 Experimental temperature        25 C  
 Adsorbent size                      0.5-1.18 mm

Time h	oil loaded straw (mg/g)	Desorption capacity mg/g			Desorption percentage %			$\sigma_m$
		run 1	run 2	$\sigma_m$	run1	run2	mean	
1	23.10	0.50	0.30	0.40	2.16	1.30	1.73	0.43
2	23.10	0.40	0.40	0.40	1.73	1.73	1.73	0.00
5	23.10	0.60	0.40	0.50	2.60	1.73	2.16	0.43

## Experimental Conditions

Shaking speed	170 rpm
Adsorbent dosage	10 g/L
Experimental temperature	25 C
Adsorbent size	0.5-1.18 mm

time(min)	Experimental		
	volume L	Ct (mg/L)	Ct/Ci
14	0.10	900	0.87
43	0.30	980	0.95
71	0.50	980	0.95
114	0.80	1000	0.97
143	1.00	970	0.94

## Experimental condition

Adsorbate                      CO  
initial conc (Ci)            1030 mg/L  
Adsorbent                     RBS  
Column Bed Height        8 cm  
Adsorbent Weight          5 g  
Flowrate                      7 ml/min

time(min)	Experimental		
	volume L	Ct (mg/L)	Ct/Ci
14	0.10	950	0.92
43	0.30	900	0.87
71	0.50	1000	0.97
114	0.80	900	0.87
143	1.00	990	0.96

## Experimental condition

initial conc (Ci)      1030 mg/L

Adsorbent              RBS-N

Column Bed Height   8 cm

Adsorbent Weight     5 g

Flowrate                7 ml/min

time(min)	Experimental			Column Model			
	volume L	Ct (mg/L)	Ct/Ci	Thomas Ct (mg/L)	Yoon Ct (mg/L)	Thomas Ct/Ci	Yoon Ct/Ci
14	0.10	0.00	0.00	0.00	0.00	0.00	0.00
29	0.20	0.00	0.00	0.00	0.00	0.00	0.00
43	0.30	0.00	0.00	0.00	0.00	0.00	0.00
57	0.40	0.00	0.00	0.00	0.00	0.00	0.00
71	0.50	0.00	0.00	0.00	0.00	0.00	0.00
86	0.60	0.00	0.00	0.00	0.00	0.00	0.00
100	0.70	17.00	0.02	0.00	0.00	0.00	0.00
114	0.80	10.00	0.01	0.00	0.00	0.00	0.00
129	0.90	25.00	0.02	0.00	0.00	0.00	0.00
143	1.00	25.00	0.02	0.00	0.00	0.00	0.00
157	1.10	20.00	0.02	0.00	0.00	0.00	0.00
171	1.20	15.00	0.01	0.00	0.00	0.00	0.00
186	1.30	35.00	0.03	0.02	0.02	0.00	0.00
200	1.40	29.00	0.03	0.13	0.13	0.00	0.00
214	1.50	25.00	0.02	0.92	0.93	0.00	0.00
229	1.60	67.00	0.07	6.40	6.43	0.01	0.01
243	1.70	114.00	0.11	43.07	43.16	0.04	0.04
257	1.80	200.00	0.19	238.87	238.76	0.23	0.23
271	1.90	700.00	0.68	683.53	682.98	0.66	0.66
286	2.00	930.00	0.90	931.74	931.75	0.90	0.90
300	2.10	1000.00	0.97	982.82	983.13	0.95	0.95
314	2.20	970.00	0.94	990.59	990.97	0.96	0.96
329	2.30	989.00	0.96	990.59	990.97	0.96	0.96

Experimental condition

Adsorbate                    CO  
 initial conc (Ci)        1030 mg/L  
 Adsorbent                SMBS  
 Column Bed Height    8 cm  
 Adsorbent Weight     5 g  
 Flowrate                 7 ml/min

time(min)	Experimental			Column Model			
	volume L	Ct (mg/L)	Ct/Ci	Thomas Ct (mg/L)	Yoon Ct (mg/L)	Thomas Ct/Ci	Yoon Ct/Ci
14	0.10	0.00	0.00	0.00	0.00	0.00	0.00
29	0.20	0.00	0.00	0.00	0.00	0.00	0.00
43	0.30	0.00	0.00	0.00	0.00	0.00	0.00
57	0.40	0.00	0.00	0.00	0.00	0.00	0.00
71	0.50	0.00	0.00	0.00	0.00	0.00	0.00
86	0.60	0.00	0.00	0.00	0.00	0.00	0.00
100	0.70	0.00	0.00	0.00	0.00	0.00	0.00
114	0.80	0.00	0.00	0.00	0.00	0.00	0.00
129	0.90	15.00	0.01	0.00	0.00	0.00	0.00
143	1.00	25.00	0.02	0.00	0.00	0.00	0.00
157	1.10	33.00	0.03	0.00	0.00	0.00	0.00
171	1.20	30.00	0.03	0.00	0.00	0.00	0.00
186	1.30	37.00	0.04	0.00	0.00	0.00	0.00
200	1.40	35.00	0.03	0.00	0.00	0.00	0.00
214	1.50	30.00	0.03	0.02	0.02	0.00	0.00
229	1.60	25.00	0.02	0.08	0.08	0.00	0.00
243	1.70	38.00	0.04	0.36	0.37	0.00	0.00
257	1.80	35.00	0.03	1.75	1.77	0.00	0.00
271	1.90	40.00	0.04	8.36	8.44	0.01	0.01
286	2.00	95.00	0.09	38.98	39.30	0.04	0.04
300	2.10	150.00	0.15	163.31	164.31	0.16	0.16
314	2.20	470.00	0.46	484.30	485.87	0.47	0.47
329	2.30	850.00	0.83	818.79	819.58	0.79	0.80
343	2.40	950.00	0.92	956.02	956.21	0.93	0.93
357	2.50	970.00	0.94	990.53	990.56	0.96	0.96
371	2.60	1010.00	0.98	998.02	998.02	0.97	0.97
386	2.70	1000.00	0.97	999.59	999.59	0.97	0.97

Experimental condition

Adsorbate                    CO  
 initial conc (Ci)        1030 mg/L  
 Adsorbent                BMBS  
 Column Bed Height    8 cm  
 Adsorbent Weight     5 g  
 Flowrate                 7 ml/min

time(min)	Experimental		
	volume L	Ct (mg/L)	Ct/Ci
14	0.10	900	0.91
43	0.30	800	0.81
71	0.50	800	0.81
114	0.80	970	0.98
143	1.00	950	0.96

## Experimental condition

Adsorbate	SMO
initial conc (Ci)	990 mg/L
Adsorbent	RBS
Column Bed Height	8 cm
Adsorbent Weight	5 g
Flowrate	7 ml/min

time(min)	Experimental		
	volume L	Ct (mg/L)	Ct/Ci
14	0.10	780	0.79
43	0.30	900	0.91
71	0.50	850	0.86
114	0.80	900	0.91
143	1.00	900	0.91

Adsorbate                    SMO  
initial conc (Ci)        990 mg/L  
Adsorbent                RBS-N  
Column Bed Height    8 cm  
Adsorbent Weight      5 g  
Flowrate                 7 ml/min

time(min)	Experimental			Column Model			
	volume L	Ct (mg/L)	Ct/Ci	Thomas Ct (mg/L)	Yoon Ct (mg/L)	Thomas Ct/Ci	Yoon Ct/Ci
14	0.10	0.00	0.00	0.00	0.00	0.00	0.00
29	0.20	0.00	0.00	0.00	0.00	0.00	0.00
43	0.30	0.00	0.00	0.00	0.00	0.00	0.00
57	0.40	0.00	0.00	0.00	0.00	0.00	0.00
71	0.50	0.00	0.00	0.00	0.00	0.00	0.00
86	0.60	0.00	0.00	0.00	0.00	0.00	0.00
100	0.70	0.00	0.00	0.00	0.00	0.00	0.00
114	0.80	0.00	0.00	0.01	0.01	0.00	0.00
129	0.90	9.00	0.01	0.04	0.04	0.00	0.00
143	1.00	10.00	0.01	0.16	0.16	0.00	0.00
157	1.10	10.00	0.01	0.71	0.71	0.00	0.00
171	1.20	11.00	0.01	3.05	3.05	0.00	0.00
186	1.30	13.00	0.01	13.02	13.03	0.01	0.01
200	1.40	90.00	0.09	53.83	53.89	0.05	0.05
214	1.50	189.00	0.19	196.33	196.58	0.20	0.20
229	1.60	500.00	0.51	507.69	508.19	0.51	0.51
243	1.70	800.00	0.81	802.58	802.93	0.81	0.81
257	1.80	970.00	0.98	927.38	927.51	0.94	0.94
271	1.90	950.00	0.96	962.04	962.07	0.97	0.97
286	2.00	940.00	0.95	970.44	970.45	0.98	0.98
300	2.10	980.00	0.99	972.41	972.41	0.98	0.98

Adsorbate                    SMO  
 initial conc (Ci)        990 mg/L  
 Adsorbent                SMBS  
 Column Bed Height    8 cm  
 Adsorbent Weight     5 g  
 Flowrate                 7 ml/min

time(min)	Experimental			Column Model			
	volume L	Ct (mg/L)	Ct/Ci	Thomas Ct (mg/L)	Yoon Ct (mg/L)	Thomas Ct/Ci	Yoon Ct/Ci
14	0.10	0.00	0.00	0.00	0.00	0.00	0.00
29	0.20	0.00	0.00	0.00	0.00	0.00	0.00
43	0.30	0.00	0.00	0.00	0.00	0.00	0.00
57	0.40	0.00	0.00	0.00	0.00	0.00	0.00
71	0.50	0.00	0.00	0.00	0.00	0.00	0.00
86	0.60	0.00	0.00	0.00	0.00	0.00	0.00
100	0.70	0.00	0.00	0.00	0.00	0.00	0.00
114	0.80	10.00	0.01	0.00	0.00	0.00	0.00
129	0.90	20.00	0.02	0.00	0.00	0.00	0.00
143	1.00	9.00	0.01	0.00	0.00	0.00	0.00
157	1.10	10.00	0.01	0.00	0.00	0.00	0.00
171	1.20	15.00	0.02	0.00	0.00	0.00	0.00
186	1.30	10.00	0.01	0.00	0.00	0.00	0.00
200	1.40	25.00	0.03	0.03	0.03	0.00	0.00
214	1.50	20.00	0.02	0.51	0.52	0.00	0.00
229	1.60	60.00	0.06	9.60	9.64	0.01	0.01
243	1.70	150.00	0.15	153.30	153.91	0.15	0.16
257	1.80	750.00	0.76	748.86	749.75	0.76	0.76
271	1.90	970.00	0.98	943.63	943.71	0.95	0.95
286	2.00	950.00	0.96	956.85	956.85	0.97	0.97
300	2.10	940.00	0.95	957.56	957.56	0.97	0.97

Adsorbate                      SMO  
 initial conc (Ci)            990 mg/L  
 Adsorbent                      SMBS  
 Column Bed Height        8 cm  
 Adsorbent Weight          5 g  
 Flowrate                        7 ml/min

# APPENDIX C

RAW DATA AND STANDARD ERROR MEASUREMENT FOR DYE  
WASTEWATER REMOVAL

## Appendix C-1

## Preliminary screening of dye onto unmodified and modified straw

	AB40 Removal (%)				RB4 Removal (%)			
	run 1	run 2	Mean	$\sigma_m$	run 1	run 2	Mean	$\sigma_m$
RBS	9.53	5.70	7.61	1.92	2.05	0.96	1.51	0.54
RBS-N	14.44	10.71	12.57	1.87	0.93	1.75	1.34	0.41
SMBS	93.75	97.50	95.63	1.88	53.43	56.68	55.05	1.62
BMBS	96.37	98.52	97.44	1.07	63.65	61.18	62.42	1.23

	RB5 Removal (%)			
	run 1	run 2	Mean	$\sigma_m$
RBS	1.24	0.60	0.92	0.32
RBS-N	0.95	0.65	0.80	0.15
SMBS	54.97	55.51	55.24	0.27
BMBS	65.05	64.31	64.68	0.37

## Experimental Conditions

Initial dye concentration	100 mg/L
Contact time	8 h
Shaking speed	170 rpm
Adsorbent dosage	2 g/L
Experimental temperature	25 C
Adsorbent size	0.5-1.18 mm
Solution pH	
AB40	5.8
RB4	5.6
RB5	5

## Appendix C-2

## Kinetic adsorption of AB40 onto modified straw

Time (min)	SMBS				BMBS			
	Adsorption capacity ( mg/g)			SEM	Adsorption capacity ( mg/g)			$\sigma_m$
0	run1	run2	mean		run1	run2	mean	
0	0.00	0.00	0.00	0.00	0.00	0.00	0.00	0.00
2	18.02	16.67	17.34	0.68	20.03	19.34	19.69	0.34
5	18.50	18.07	18.29	0.21	22.07	23.10	22.59	0.52
10	21.96	22.94	22.45	0.49	29.15	28.26	28.71	0.44
20	28.35	27.10	27.73	0.62	35.08	36.11	35.59	0.51
30	32.10	30.07	31.08	1.02	39.13	39.75	39.44	0.31
45	35.10	35.04	35.07	0.03	43.17	41.86	42.52	0.65
60	37.30	36.69	36.99	0.31	44.50	44.17	44.34	0.16
90	39.65	41.61	40.63	0.98	48.32	47.34	47.83	0.49
120	44.20	43.44	43.82	0.38	49.53	47.04	48.29	1.24
180	44.05	44.58	44.31	0.26	48.25	48.35	48.30	0.05

## Experimental conditions

Initial dye concentration	100 mg/L
Shaking speed	170 rpm
Adsorbent dosage	2 g/L
Experimental temperature	25 C
Solution pH	5.8
Adsorbent size	0.5-1.18 mm

## Appendix C-3

## Kinetic adsorption of AB40 onto modified straw

Time (min)	SMBS				BMBS			
	Adsorption capacity ( mg/g)			SEM	Adsorption capacity ( mg/g)			$\sigma_m$
	run1	run2	mean		run1	run2	mean	
0	0.00	0.00	0.00	0.00	0.00	0.00	0.00	0.00
5	11.95	12.88	12.41	0.46	14.15	16.41	15.28	1.13
10	13.58	15.65	14.62	1.04	19.97	21.08	20.52	0.55
20	20.15	20.41	20.28	0.13	23.05	22.54	22.80	0.25
30	26.10	24.39	25.24	0.86	26.00	25.00	25.50	0.50
45	26.05	24.72	25.38	0.67	25.80	25.16	25.48	0.32
60	26.99	25.93	26.46	0.53	27.01	27.02	27.01	0.00
90	27.01	27.02	27.01	0.00	27.01	27.02	27.01	0.00
180	27.01	27.02	27.01	0.00	27.01	27.02	27.01	0.00

## Experimental conditions:

Initial dye concentration	50 mg/L
Shaking speed	170 rpm
Adsorbent dosage	2 g/L
Experimental temperature	25 C
Solution pH	5.8
Adsorbent size	0.5-1.18 mm

## Appendix C-4

## Kinetic adsorption of RB4 onto modified straw

Time (min)	SMBS				BMBS			
	Adsorption capacity ( mg/g)			SEM	Adsorption capacity ( mg/g)			$\sigma_m$
	run1	run2	mean		run1	run2	mean	
0	0.00	0.00	0.00	0.00	0.00	0.00	0.00	0.00
5	20.10	18.87	19.48	0.62	16.90	18.27	17.59	0.69
10	19.50	18.60	19.05	0.45	18.81	18.60	18.71	0.10
15	21.00	19.86	20.43	0.57	20.50	19.36	19.93	0.57
20	20.90	20.13	20.52	0.38	20.93	19.04	19.98	0.95
25	21.50	20.36	20.93	0.57	20.30	20.56	20.43	0.13
30	21.80	20.44	21.12	0.68	23.30	21.53	22.41	0.89
45	23.00	22.69	22.84	0.16	23.45	23.10	23.28	0.17
60	23.20	20.94	22.07	1.13	22.94	21.20	22.07	0.87
90	23.40	21.77	22.59	0.81	22.40	22.60	22.50	0.10
120	24.50	23.26	23.88	0.62	25.35	26.13	25.74	0.39
180	23.90	22.96	23.43	0.47	28.00	26.86	27.43	0.57
240	24.15	23.71	23.93	0.22	26.70	25.20	25.95	0.75
300	24.50	24.36	24.43	0.07	25.80	25.06	25.43	0.37

## Experimental Conditions

Initial dye concentration	100 mg/L
Shaking speed	170 rpm
Adsorbent dosage	2 g/L
Experimental temperature	25 C
Solution pH	5.6
Adsorbent size	0.5-1.18 mm

## Appendix C-5

## Kinetic adsorption of RB4 onto modified straw

Time (min)	SMBS				BMBS			
	Adsorption capacity ( mg/g)			SEM	Adsorption capacity ( mg/g)			$\sigma_m$
	run1	run2	mean		run1	run2	mean	
0	0.00	0.00	0.00	0.00	0.00	0.00	0.00	0.00
5	14.15	15.16	14.66	0.51	16.00	15.72	15.86	0.14
10	16.00	15.38	15.69	0.31	17.48	16.14	16.81	0.67
15	16.55	16.97	16.76	0.21	17.45	16.77	17.11	0.34
20	18.75	18.84	18.79	0.04	19.05	17.33	18.19	0.86
25	19.50	18.32	18.91	0.59	18.10	19.42	18.76	0.66
30	19.95	18.33	19.14	0.81	19.25	18.77	19.01	0.24
45	19.90	19.27	19.59	0.31	18.54	19.22	18.88	0.34
60	19.52	17.20	18.36	1.16	21.05	19.81	20.43	0.62
90	20.30	19.87	20.09	0.21	20.10	21.28	20.69	0.59
120	20.55	21.00	20.78	0.23	20.90	21.10	21.00	0.10
240	19.90	21.12	20.51	0.61	21.20	21.32	21.26	0.06
300	20.35	20.37	20.36	0.01	20.60	19.92	20.26	0.34

## Experimental Conditions

Initial dye concentration	50 mg/L
Shaking speed	170 rpm
Adsorbent dosage	2 g/L
Experimental temperature	25 C
Solution pH	5.6
Adsorbent size	0.5-1.18 mm

## Appendix C-6

## Kinetic adsorption of RB5 onto modified straw

Time (min)	SMBS				BMBS			
	Adsorption capacity ( mg/g)			SEM	Adsorption capacity ( mg/g)			$\sigma_m$
	run1	run2	mean		run1	run2	mean	
0	0.00	0.00	0.00	0.00	0.00	0.00	0.00	0.00
5	11.00	10.66	10.83	0.17	9.10	8.16	8.63	0.47
10	12.90	13.02	12.96	0.06	14.10	12.27	13.18	0.92
20	18.35	16.81	17.58	0.77	16.15	15.24	15.70	0.45
30	18.90	19.22	19.06	0.16	19.45	17.77	18.61	0.84
45	21.05	19.98	20.52	0.53	20.50	20.76	20.63	0.13
60	21.80	22.06	21.93	0.13	22.10	22.20	22.15	0.05
90	23.45	22.83	23.14	0.31	25.15	23.95	24.55	0.60
120	24.90	24.11	24.51	0.39	25.95	26.61	26.28	0.33
150	25.00	25.31	25.16	0.16	27.20	27.33	27.26	0.06
180	25.70	26.23	25.96	0.26	29.00	27.77	28.39	0.61
210	27.15	25.59	26.37	0.78	28.85	29.76	29.30	0.45
240	27.10	28.20	27.65	0.55	30.50	31.83	31.16	0.66
300	27.50	26.40	26.95	0.55	31.74	30.10	30.92	0.82
360	27.00	28.11	27.56	0.56	31.85	31.87	31.86	0.01

## Experimental Conditions

Initial dye concentration	100 mg/L
Shaking speed	170 rpm
Adsorbent dosage	2 g/L
Experimental temperature	25 C
Solution pH	5
Adsorbent size	0.5-1.18 mm

Time (min)	SMBS				BMBS			
	Adsorption capacity ( mg/g)			SEM	Adsorption capacity ( mg/g)			$\sigma_m$
	run1	run2	mean		run1	run2	mean	
0	0.00	0.00	0.00	0.00	0.00	0.00	0.00	0.00
5	9.20	7.84	8.52	0.68	7.50	8.55	8.03	0.53
10	10.55	11.38	10.96	0.41	10.95	11.74	11.35	0.40
20	12.90	13.24	13.07	0.17	13.85	12.83	13.34	0.51
30	15.00	13.65	14.33	0.67	16.50	15.02	15.76	0.74
45	15.98	16.89	16.43	0.45	17.57	18.30	17.94	0.37
60	16.70	17.38	17.04	0.34	18.95	19.21	19.08	0.13
90	17.53	19.20	18.36	0.83	19.75	20.83	20.29	0.54
120	18.97	19.28	19.13	0.16	21.50	21.86	21.68	0.18
150	20.06	19.94	20.00	0.06	23.05	21.93	22.49	0.56
180	22.00	20.71	21.36	0.64	24.45	23.04	23.74	0.71
210	19.70	20.39	20.04	0.34	24.55	23.39	23.97	0.58
240	21.45	21.51	21.48	0.03	24.17	24.31	24.24	0.07
300	22.07	22.01	22.04	0.03	24.60	24.59	24.60	0.00
360	20.90	22.78	21.84	0.94	24.25	25.21	24.73	0.48

## Experimental Conditions

Initial dye concentration	50 mg/L
Shaking speed	170 rpm
Adsorbent dosage	2 g/L
Experimental temperature	25 C
Solution pH	5
Adsorbent size	0.5-1.18 mm

## Appendix C-8

## Adsorption of AB40 onto various dosage of SMBS

Dosage	Concentration ( mg/L)				Concentration ( mg/L)			
mg	Initial	run 1	run 2	$\sigma_m$	run1	run2	mean	$\sigma_m$
1.00	215.00	0.70	0.30	0.50	21.43	21.47	21.45	0.02
0.70	215.00	2.31	2.69	2.50	30.38	30.33	30.36	0.03
0.50	215.00	12.54	7.46	10.00	40.49	41.51	41.00	0.51
0.30	215.00	71.45	68.55	70.00	47.85	48.82	48.33	0.48
0.10	215.00	168.00	172.00	170.00	47.00	43.00	45.00	2.00

## Experimental Conditions

Initial dye concentration	50 mg/L
Shaking speed	170 rpm
Contact time	5 h
Experimental temperature	25 C
Solution pH	5.8
Adsorbent size	0.5-1.18 mm

Dosage	Concentration ( mg/L)				Concentration ( mg/L)			
mg	Initial	run 1	run 2	$\sigma_m$	run1	run2	mean	$\sigma_m$
1.00	215.00	0.20	0.40	0.30	21.48	21.46	21.47	0.01
0.70	215.00	1.10	0.86	0.98	30.56	30.59	30.57	0.02
0.50	215.00	1.89	2.03	1.96	42.62	42.59	42.61	0.01
0.30	215.00	61.15	58.85	60.00	51.28	52.05	51.67	0.38
0.10	215.00	162.24	163.98	163.11	52.76	51.02	51.89	0.87

## Experimental Conditions

Initial dye concentration	50 mg/L
Shaking speed	170 rpm
Contact time	5 h
Experimental temperature	25 C
Solution pH	5.8
Adsorbent size	0.5-1.18 mm

Appendix C-10      Adsorption of RB4 onto various dosage of SMBS

Dosage	Concentration ( mg/L)				Concentration ( mg/L)			
mg	Initial	run 1	run 2	$\sigma_m$	run1	run2	mean	$\sigma_m$
1.00	223.00	1.90	0.70	1.30	22.11	22.23	22.17	0.06
0.70	223.00	22.00	18.00	20.00	28.71	29.29	29.00	0.29
0.50	223.00	93.57	91.46	92.52	25.89	26.31	26.10	0.21
0.30	223.00	137.40	142.60	140.00	28.53	26.80	27.67	0.87
0.10	223.00	193.50	186.50	190.00	29.50	36.50	33.00	3.50

Experimental Conditions

Initial dye concentration      50 mg/L  
Shaking speed                    170 rpm  
Contact time                        5 h  
Experimental temperature      25 C  
Solution pH                         5.6  
Adsorbent size                    0.5-1.18 mm

Appendix C-11      Adsorption of RB4 onto various dosage of BMBS

Dosage	Concentration ( mg/L)				Concentration ( mg/L)			
mg	Initial	run 1	run 2	$\sigma_m$	run1	run2	mean	$\sigma_m$
1.00	223.00	2.00	1.00	1.50	22.10	22.20	22.15	0.05
0.70	223.00	14.53	16.02	15.28	29.78	29.57	29.67	0.11
0.50	223.00	89.17	85.86	87.52	26.77	27.43	27.10	0.33
0.30	223.00	135.53	128.81	132.17	29.16	31.40	30.28	1.12
0.10	223.00	185.28	186.72	186.00	37.72	36.28	37.00	0.72

Experimental Conditions

Initial dye concentration      50 mg/L  
 Shaking speed                    170 rpm  
 Contact time                        5 h  
 Experimental temperature      25 C  
 Solution pH                         5.6  
 Adsorbent size                    0.5-1.18 mm

Appendix C-12      Adsorption of RB5 onto various dosage of SMBS

Dosage	Concentration ( mg/L)				Concentration ( mg/L)			
mg	Initial	run 1	run 2	$\sigma_m$	run1	run2	mean	$\sigma_m$
1.00	212.00	14.95	17.05	16.00	19.71	19.50	19.60	0.11
0.70	212.00	51.34	48.66	50.00	22.95	23.33	23.14	0.19
0.50	212.00	98.68	100.45	99.57	22.66	22.31	22.49	0.18
0.30	212.00	137.50	132.50	135.00	24.83	26.50	25.67	0.83
0.10	212.00	186.90	189.10	188.00	25.10	22.90	24.00	1.10

Experimental Conditions

Initial dye concentration	50 mg/L
Shaking speed	170 rpm
Contact time	5 h
Experimental temperature	25 C
Solution pH	5
Adsorbent size	0.5-1.18 mm

Dosage mg	Concentration ( mg/L)				Concentration ( mg/L)			
	Initial	run 1	run 2	$\sigma_m$	run1	run2	mean	$\sigma_m$
1.00	212.00	0.40	0.20	0.30	21.16	21.18	21.17	0.01
0.70	212.00	1.15	0.81	0.98	30.12	30.17	30.15	0.02
0.50	212.00	2.20	1.72	1.96	41.96	42.06	42.01	0.05
0.30	212.00	58.65	61.35	60.00	51.12	50.22	50.67	0.45
0.10	212.00	162.35	163.87	163.11	49.65	48.13	48.89	0.76

## Experimental Conditions

Initial dye concentration	50 mg/L
Shaking speed	170 rpm
Contact time	5 h
Experimental temperature	25 C
Solution pH	5
Adsorbent size	0.5-1.18 mm

Appendix C-14      Effect of pH on adsorption of AB40 onto SMBS

pH	Concentration ( mg/L)				Concentration ( mg/L)			$\sigma_m$
	Initial	run 1	run 2	mean	run1	run2	mean	
3	93.85	31.05	30.91	30.98	31.40	31.47	31.43	0.04
5	99.09	11.97	12.51	12.24	43.56	43.29	43.43	0.13
8	99.02	16.85	17.84	17.34	41.09	40.59	40.84	0.25
11	98.60	41.03	38.27	39.65	28.79	30.17	29.48	0.69

Experimental Conditions

Shaking speed	170 rpm
Contact time	5 h
Experimental temperature	25 C
Adsorbent dosage	2 g/L
Adsorbent size	0.5-1.18 mm

Appendix C-15      Effect of pH on adsorption of AB40 onto BMBS

pH	Concentration ( mg/L)				Concentration ( mg/L)			$\sigma_m$
	Initial	run 1	run 2	mean	run1	run2	mean	
3	93.85	33.17	33.96	33.57	30.34	29.94	30.14	0.20
5	99.09	1.59	1.63	1.61	48.75	48.73	48.74	0.01
8	99.02	4.33	4.62	4.48	47.35	47.20	47.27	0.07
11	98.60	19.79	19.93	19.86	39.41	39.34	39.37	0.04

Experimental Conditions

Shaking speed                      170 rpm  
Contact time                        5 h  
Experimental temperature        25 C  
Adsorbent dosage                 2 g/L  
Adsorbent size                      0.5-1.18 mm

Appendix C-16      Effect of pH on adsorption of RB4 onto SMBS

pH	Concentration ( mg/L)				Concentration ( mg/L)			$\sigma_m$
	Initial	run 1	run 2	mean	run1	run2	mean	
3	99.92	0.00	0.00	0.00	49.96	49.96	49.96	0.00
5	97.52	50.09	52.19	51.14	23.71	22.67	23.19	0.52
8	98.72	57.24	55.04	56.14	20.74	21.84	21.29	0.55
11	105.79	83.43	86.43	84.93	11.18	9.68	10.43	0.75

Experimental Conditions

Shaking speed                      170 rpm  
Contact time                         5 h  
Experimental temperature        25 C  
Adsorbent dosage                  2 g/L  
Adsorbent size                      0.5-1.18 mm

Appendix C-17      Effect of pH on adsorption of RB4 onto BMBS

pH	Concentration ( mg/L)				Concentration ( mg/L)			$\sigma_m$
	Initial	run 1	run 2	mean	run1	run2	mean	
3	99.92	0.00	0.00	0.00	49.96	49.96	49.96	0.00
5	97.52	44.90	58.71	51.81	26.31	19.40	22.86	3.45
8	98.72	54.05	51.45	52.75	22.34	23.64	22.99	0.65
11	105.79	31.87	33.81	32.84	36.96	35.99	36.48	0.48

Experimental Conditions

Shaking speed                      170 rpm  
Contact time                         5 h  
Experimental temperature        25 C  
Adsorbent dosage                  2 g/L  
Adsorbent size                      0.5-1.18 mm

Appendix C-18      Effect of pH on adsorption of RB5 onto SMBS

pH	Concentration ( mg/L)				Concentration ( mg/L)			$\sigma_m$
	Initial	run 1	run 2	mean	run1	run2	mean	
3	99.92	0.00	0.00	0.00	49.96	49.96	49.96	0.00
5	100.78	65.74	62.72	64.23	17.52	19.03	18.27	0.76
8	100.96	68.98	70.15	69.57	15.99	15.40	15.70	0.29
11	99.39	64.49	66.57	65.53	17.45	16.41	16.93	0.52

Experimental Conditions

Shaking speed                      170 rpm  
Contact time                         5 h  
Experimental temperature        25 C  
Adsorbent dosage                  2 g/L  
Adsorbent size                      0.5-1.18 mm

Appendix C-19      Effect of pH on adsorption of RB5 onto BMBS

pH	Concentration ( mg/L)				Concentration ( mg/L)			$\sigma_m$
	Initial	run 1	run 2	mean	run1	run2	mean	
3	99.92	0.00	0.00	0.00	49.96	49.96	49.96	0.00
5	100.78	52.89	50.72	51.81	23.94	25.03	24.48	0.54
8	100.96	51.67	53.83	52.75	24.64	23.56	24.10	0.54
11	99.39	33.06	32.62	32.84	33.16	33.38	33.27	0.11

Experimental Conditions

Shaking speed                      170 rpm  
Contact time                        5 h  
Experimental temperature       25 C  
Adsorbent dosage                 2 g/L  
Adsorbent size                      0.5-1.18 mm

time(min)	Experimental		
	volume L	Ct (mg/L)	Ct/Ci
1	0.01	5.14	0.10
2	0.02	4.28	0.09
3	0.03	12.64	0.25
4	0.04	21.56	0.43
5	0.05	31.42	0.63
6	0.06	37.85	0.76
7	0.07	41.85	0.84
8	0.08	45.49	0.91
9	0.09	47.06	0.94
10	0.10	46.06	0.92
15	0.15	49.35	0.99
20	0.20	48.56	0.97
25	0.25	48.78	0.98
30	0.30	49.49	0.99
35	0.35	49.56	0.99
40	0.40	49.28	0.99
45	0.45	49.85	1.00
50	0.50	50.64	1.01
55	0.55	49.64	0.99
60	0.60	49.28	0.99
65	0.65	49.99	1.00
70	0.70	50.00	1.00
90	0.90	50.00	1.00
100	1.00	49.99	1.00

## Experimental conditions

Adsorbate	AB40
initial conc (Ci)	50 mg/L
Adsorbent	RBS
Column Bed Height	8 cm
Adsorbent Weight	5 g
Flowrate	10 ml/min

time(min)	Experimental		
	volume L	Ct (mg/L)	Ct/Ci
1	0.01	5.14	0.10
2	0.02	12.35	0.25
3	0.03	19.28	0.39
4	0.04	22.14	0.44
5	0.05	29.35	0.59
6	0.06	29.42	0.59
7	0.07	31.56	0.63
8	0.08	32.56	0.65
9	0.09	32.99	0.66
10	0.10	35.49	0.71
12	0.12	35.99	0.72
14	0.14	37.28	0.75
16	0.16	37.92	0.76
18	0.18	37.56	0.75
20	0.20	39.56	0.79
25	0.25	41.14	0.82
33	0.33	41.49	0.83
40	0.40	44.28	0.89
50	0.50	44.85	0.90
60	0.60	45.71	0.91
65	0.65	45.71	0.91
70	0.70	45.92	0.92
80	0.80	45.64	0.91
90	0.90	47.28	0.95

## Experimental conditions

Adsorbate	AB40
initial conc (Ci)	50 mg/L
Adsorbent	RBS
Column Bed Height	8 cm
Adsorbent Weight	5 g
Flowrate	10 ml/min

	Experimental			Column Model			
		Ct		Thomas	Yoon	Thomas	Yoon
time(min)	volume L	(mg/L)	Ct/Ci	Ct (mg/L)	Ct (mg/L)	Ct/Ci	Ct/Ci
5	0.05	0.00	0.00	0.05	0.05	0.00	0.00
10	0.10	0.00	0.00	0.05	0.05	0.00	0.00
30	0.30	0.00	0.00	0.07	0.07	0.00	0.00
60	0.60	0.00	0.00	0.10	0.10	0.00	0.00
120	1.20	0.00	0.00	0.21	0.21	0.00	0.00
180	1.80	0.00	0.00	0.44	0.44	0.01	0.01
210	2.10	0.00	0.00	0.65	0.65	0.01	0.01
240	2.40	0.00	0.00	0.94	0.94	0.02	0.02
270	2.70	0.00	0.00	1.37	1.37	0.03	0.03
300	3.00	0.00	0.00	1.98	1.98	0.04	0.04
320	3.20	0.00	0.00	2.53	2.53	0.05	0.05
340	3.40	0.00	0.00	3.21	3.22	0.06	0.06
370	3.70	1.42	0.03	4.57	4.58	0.09	0.09
390	3.90	3.35	0.07	5.74	5.75	0.11	0.11
405	4.05	5.56	0.11	6.78	6.79	0.14	0.14
435	4.35	9.99	0.20	9.34	9.35	0.19	0.19
455	4.55	12.92	0.26	11.41	11.43	0.23	0.23
480	4.80	18.64	0.37	14.43	14.44	0.29	0.29
515	5.15	22.28	0.45	19.33	19.34	0.39	0.39
555	5.55	25.64	0.51	25.46	25.48	0.51	0.51
590	5.90	30.71	0.61	30.75	30.77	0.61	0.62
610	6.10	32.49	0.65	33.53	33.55	0.67	0.67
650	6.50	36.85	0.74	38.30	38.32	0.77	0.77
680	6.80	40.14	0.80	41.10	41.11	0.82	0.82
710	7.10	42.14	0.84	43.25	43.26	0.87	0.87
735	7.35	43.92	0.88	44.62	44.63	0.89	0.89
765	7.65	44.85	0.90	45.85	45.85	0.92	0.92
795	7.95	45.56	0.91	46.73	46.73	0.93	0.93
825	8.25	47.49	0.95	47.35	47.35	0.95	0.95
855	8.55	47.64	0.95	47.78	47.78	0.96	0.96
885	8.85	48.49	0.97	48.08	48.08	0.96	0.96
945	9.45	49.99	1.00	48.42	48.42	0.97	0.97
1005	10.05	49.99	1.00	48.59	48.59	0.97	0.97
1100	11.00	49.99	1.00	48.69	48.69	0.97	0.97

## Experimental conditions

Adsorbate	AB40
initial conc (Ci)	50 mg/L
Adsorbent	SMBS
Column Bed Height	8 cm
Adsorbent Weight	5 g
Flowrate	10 ml/min

## Appendix C-22

## Adsorption of AB40 onto BMBS (Packed Bed Column)

time(min)	Experimental			Column Model			
	volume L	Ct (mg/L)	Ct/Ci	Thomas Ct (mg/L)	Yoon Ct (mg/L)	Thomas Ct/Ci	Yoon Ct/Ci
10	0.10	0.00	0.00	0.01	0.01	0.00	0.00
30	0.30	0.00	0.00	0.01	0.01	0.00	0.00
60	0.60	0.00	0.00	0.02	0.02	0.00	0.00
120	1.20	0.00	0.00	0.03	0.03	0.00	0.00
180	1.80	0.00	0.00	0.06	0.06	0.00	0.00
210	2.10	0.00	0.00	0.08	0.08	0.00	0.00
240	2.40	0.00	0.00	0.12	0.12	0.00	0.00
270	2.70	0.00	0.00	0.16	0.16	0.00	0.00
300	3.00	0.00	0.00	0.23	0.23	0.00	0.00
330	3.30	0.00	0.00	0.32	0.32	0.01	0.01
390	3.90	0.00	0.00	0.61	0.61	0.01	0.01
420	4.20	0.00	0.00	0.85	0.85	0.02	0.02
480	4.80	0.00	0.00	1.63	1.63	0.03	0.03
500	5.00	0.00	0.00	2.02	2.02	0.04	0.04
535	5.35	0.35	0.01	2.93	2.93	0.06	0.06
560	5.60	1.28	0.03	3.79	3.79	0.08	0.08
575	5.75	2.35	0.05	4.42	4.42	0.09	0.09
600	6.00	4.49	0.09	5.67	5.67	0.11	0.11
630	6.30	8.71	0.17	7.58	7.57	0.15	0.15
660	6.60	10.92	0.22	9.97	9.97	0.20	0.20
680	6.80	12.42	0.25	11.86	11.85	0.24	0.24
720	7.20	16.42	0.33	16.30	16.30	0.33	0.33
750	7.50	22.14	0.44	20.12	20.12	0.40	0.40
780	7.80	25.99	0.52	24.19	24.18	0.48	0.48
810	8.10	28.56	0.57	28.27	28.27	0.57	0.57
830	8.30	32.16	0.64	30.90	30.90	0.62	0.62
870	8.70	34.99	0.70	35.69	35.68	0.71	0.71
900	9.00	37.14	0.74	38.73	38.72	0.77	0.77
933	9.33	39.28	0.79	41.46	41.46	0.83	0.83
960	9.60	40.71	0.81	43.25	43.24	0.87	0.86
1005	10.05	44.99	0.90	45.46	45.45	0.91	0.91
1035	10.35	46.64	0.93	46.49	46.48	0.93	0.93
1080	10.80	47.99	0.96	47.57	47.56	0.95	0.95
1140	11.40	48.92	0.98	48.41	48.40	0.97	0.97
1200	12.00	49.99	1.00	48.85	48.84	0.98	0.98
1260	12.60	49.99	1.00	49.08	49.07	0.98	0.98
1320	13.20	49.99	1.00	49.20	49.19	0.98	0.98

## Experimental conditions

Adsorbate	AB40
initial conc (Ci)	50 mg/L
Adsorbent	BMBS
Column Bed Height	8 cm
Adsorbent Weight	5 g
Flowrate	10 ml/min

time(min)	Experimental		
	volume L	Ct (mg/L)	Ct/Ci
1	0.01	0.00	0.00
2	0.02	31.39	0.63
3	0.03	36.27	0.73
4	0.04	38.71	0.77
5	0.05	42.49	0.85
6	0.06	43.59	0.87
7	0.07	45.05	0.90
8	0.08	46.27	0.93
9	0.09	47.37	0.95
10	0.1	47.37	0.95
13	0.13	47.24	0.94
16	0.16	50.00	1.00
20	0.2	50.00	1.00
30	0.3	50.00	1.00
40	0.4	50.00	1.00
50	0.5	48.00	0.96
60	0.6	50.00	1.00

## Experimental conditions

Adsorbate	RB5
initial conc (Ci)	50 mg/L
Adsorbent	RBS
Column Bed Height	8 cm
Adsorbent Weight	5 g
Flowrate	10 ml/min



Appendix C-23 Adsorption of RB5 onto RBS-N (Packed Bed Column)

time(min)	Experimental		
	volume L	Ct (mg/L)	Ct/Ci
1	0.01	0.00	0.00
2	0.02	35.05	0.70
3	0.03	39.93	0.80
4	0.04	38.71	0.77
5	0.05	43.59	0.87
6	0.06	44.20	0.88
7	0.07	45.78	0.92
8	0.08	46.27	0.93
9	0.09	47.37	0.95
10	0.1	47.37	0.95
13	0.13	50.00	1.00
16	0.16	50.00	1.00
20	0.2	50.00	1.00
30	0.3	50.00	1.00
40	0.4	50.00	1.00
50	0.5	50.00	1.00
60	0.6	50.00	1.00

Experimental conditions

Adsorbate	RB5
initial conc (Ci)	50 mg/L
Adsorbent	RBS-N
Column Bed Height	8 cm
Adsorbent Weight	5 g
Flowrate	10 ml/min

time(min)	Experimental			Column Model			
	volume L	Ct (mg/L)	Ct/Ci	Thomas Ct (mg/L)	Yoon Ct (mg/L)	Thomas Ct/Ci	Yoon Ct/Ci
5	0.05	0.00	0.00	0.04	0.04	0.00	0.00
10	0.10	0.00	0.00	0.05	0.05	0.00	0.00
15	0.15	0.00	0.00	0.06	0.06	0.00	0.00
20	0.20	0.00	0.00	0.07	0.07	0.00	0.00
25	0.25	0.00	0.00	0.07	0.08	0.00	0.00
30	0.30	0.00	0.00	0.09	0.09	0.00	0.00
40	0.40	0.00	0.00	0.11	0.11	0.00	0.00
50	0.50	0.00	0.00	0.15	0.15	0.00	0.00
60	0.60	0.00	0.00	0.20	0.20	0.00	0.00
90	0.90	0.00	0.00	0.46	0.47	0.01	0.01
105	1.05	0.00	0.00	0.70	0.71	0.01	0.01
120	1.20	0.00	0.00	1.06	1.07	0.02	0.02
142	1.42	0.14	0.00	1.94	1.95	0.04	0.04
150	1.50	0.93	0.02	2.41	2.42	0.05	0.05
165	1.65	1.62	0.03	3.58	3.59	0.07	0.07
180	1.80	2.97	0.06	5.25	5.27	0.11	0.11
200	2.00	6.42	0.13	8.52	8.56	0.17	0.17
225	2.25	16.02	0.32	14.60	14.65	0.29	0.29
240	2.40	21.73	0.43	19.22	19.27	0.38	0.39
255	2.55	26.80	0.54	24.24	24.30	0.48	0.49
270	2.70	30.07	0.60	29.26	29.31	0.59	0.59
285	2.85	33.06	0.66	33.85	33.90	0.68	0.68
300	3.00	36.20	0.72	37.73	37.77	0.75	0.76
330	3.30	40.39	0.81	43.09	43.12	0.86	0.86
360	3.60	43.30	0.87	45.90	45.91	0.92	0.92
390	3.90	45.59	0.91	47.22	47.22	0.94	0.94
420	4.20	47.92	0.96	47.81	47.81	0.96	0.96
435	4.35	48.08	0.96	47.96	47.96	0.96	0.96
450	4.50	48.84	0.98	48.06	48.06	0.96	0.96
480	4.80	49.69	0.99	48.18	48.18	0.96	0.96
520	5.20	49.69	0.99	48.23	48.23	0.96	0.96
550	5.50	49.69	0.99	48.25	48.25	0.96	0.96
600	6.00	49.00	0.98	48.26	48.26	0.97	0.97

## Experimental conditions

Adsorbate                RB5  
 initial conc (Ci)        50 mg/L  
 Adsorbent                SMBS  
 Column Bed Height    8 cm  
 Adsorbent Weight      5 g  
 Flowrate                 10 ml/min

time(min)	Experimental			Column Model			
	volume L	Ct (mg/L)	Ct/Ci	Thomas Ct (mg/L)	Yoon Ct (mg/L)	Thomas Ct/Ci	Yoon Ct/Ci
5	0.05	0.00	0.00	0.00	0.00	0.00	0.00
10	0.10	0.00	0.00	0.00	0.00	0.00	0.00
15	0.15	0.00	0.00	0.00	0.00	0.00	0.00
20	0.20	0.00	0.00	0.00	0.00	0.00	0.00
25	0.25	0.00	0.00	0.00	0.00	0.00	0.00
30	0.30	0.00	0.00	0.01	0.01	0.00	0.00
40	0.40	0.00	0.00	0.01	0.01	0.00	0.00
50	0.50	0.00	0.00	0.01	0.01	0.00	0.00
60	0.60	0.00	0.00	0.01	0.01	0.00	0.00
90	0.90	0.00	0.00	0.03	0.03	0.00	0.00
105	1.05	0.00	0.00	0.05	0.05	0.00	0.00
120	1.20	0.00	0.00	0.07	0.07	0.00	0.00
142	1.42	0.00	0.00	0.13	0.13	0.00	0.00
150	1.50	0.00	0.00	0.16	0.16	0.00	0.00
165	1.65	0.00	0.00	0.24	0.24	0.00	0.00
180	1.80	0.00	0.00	0.37	0.37	0.01	0.01
200	2.00	0.19	0.00	0.64	0.65	0.01	0.01
225	2.25	0.28	0.01	1.28	1.29	0.03	0.03
240	2.40	0.63	0.01	1.93	1.93	0.04	0.04
255	2.55	1.46	0.03	2.88	2.88	0.06	0.06
270	2.70	2.99	0.06	4.26	4.26	0.09	0.09
285	2.85	4.69	0.09	6.20	6.21	0.12	0.12
300	3.00	7.67	0.15	8.85	8.85	0.18	0.18
315	3.15	10.00	0.20	12.28	12.29	0.25	0.25
330	3.30	18.12	0.36	16.49	16.50	0.33	0.33
345	3.45	25.00	0.50	21.26	21.28	0.43	0.43
360	3.60	28.21	0.56	26.25	26.26	0.52	0.53
390	3.90	34.60	0.69	35.22	35.23	0.70	0.70
420	4.20	39.63	0.79	41.29	41.30	0.83	0.83
435	4.35	41.02	0.82	43.23	43.23	0.86	0.86
450	4.50	42.02	0.84	44.60	44.60	0.89	0.89
480	4.80	44.31	0.89	46.19	46.19	0.92	0.92
495	4.95	45.43	0.91	46.62	46.62	0.93	0.93
525	5.25	47.45	0.95	47.10	47.10	0.94	0.94
540	5.40	48.12	0.96	47.23	47.23	0.94	0.94
570	5.70	49.01	0.98	47.37	47.37	0.95	0.95
600	6.00	49.69	0.99	47.42	47.42	0.95	0.95
660	6.60	50.00	1.00	47.46	47.46	0.95	0.95

Experimental conditions

Adsorbate                RB5  
 initial conc (Ci)        50 mg/L  
 Adsorbent                BMBS  
 Column Bed Height    8 cm  
 Adsorbent Weight      5 g  
 Flowrate                 10 ml/min

